Department of Biomedical Engineering

University of Strathclyde

Investigation into the relationship between blunt impacts and bruising

By

Heather Ilona Black

A thesis presented in fulfilment of the requirements for the degree of Doctor of Philosophy

2017

Declaration

This thesis is the result of the author's original research. It has been composed by the author and has not been previously submitted for examination which has led to the award of a degree.

Signed:

Date:

Acknowledgements

Firstly, thank you to my supervisors Dr Philip Riches and Dr Sylvie Coupaud for their encouragement and support, who when I had a problem would send me on my way with a new-found enthusiasm (even if I didn't show it). Thanks also to Prof Niamh Nic Daéid, who's input helped shape my PhD.

I would also like to acknowledge the EPSRC equipment grant support which allowed for the purchase of the high speed camera which was used in this research.

To the all the PhD and EngD folk, thanks for sharing all the ups and downs and telling me whenever they had a new bruise. Shout out to Olivia and Lindsay for the fun filled tea breaks and to Kayleigh, for reminding me how to talk about something other than my work!

Thank you to Fraser, my parents and the rest of my family for all the support and encouragement. I guess it really is time for me to get a haircut and get a real job!

Finally, a huge thank you to those who volunteered to take part in this research.

Abstract

Bruising is an injury commonly observed within suspect cases of assault or abuse, however their interpretation is purely visual. Although the biology of bruising is known, how a blunt impact initiates bruising and influences its severity is not understood. Furthermore, the standard method of documenting bruising with colour photography is known to have limitations which in turn influence the already subjective analysis of bruise age and severity.

Following ethical approval, this research aimed to address these problems through characterisation of a standardised blunt impact which was delivered to 18 volunteers. The resulting bruise was then imaged using 3 different photography techniques (colour, cross polarised (CP) and infrared (IR)) to determine if colour photography could be improved upon, whilst colour patterns using the L*a*b* colour model were taken from both colour and CP images to determine whether a measured colour timeline could be created to aid bruise age determination.

Results showed that although no photography technique held any significant advantage over any other, CP provided greater image contrast than colour photography whilst IR imaging produced a clearer image of bruising over the initial stages of bruise formation. Although a general trend was seen for the measured colour patterns, they could not be characteristically attributed to any group of people, thus no colour timeline could be produced. Impact results demonstrated a characteristic tissue response which was strongly influenced by anthropometric features. These features also appeared to influence the severity of resultant bruising observed.

It was concluded that both the photography and colour pattern methods assessed may not be the most appropriate for future research, whilst the potential variability of bruise severity between individuals was successfully visualised Therefore to gain a complete understanding of bruising, a detailed approach which combines impact, tissue response and the resulting bruise appearance is required.

Presentations

Oral Presentations

The influence of biomechanics on bruise formation. *British Association for Human Identification Conference*, Dundee, Scotland, June 2016

The influence of biomechanics on bruise formation. *University of Strathclyde Research Day*, Glasgow, Scotland, June 2016

Investigation into the biomechanics surrounding bruise formation. *Scottish Student Forensic Research Symposium*, Glasgow, Scotland, April 2016

Investigation into the biomechanics of contusion formation. *European Academy of Forensic Science Conference*, Prague, Czech Republic, September 2015

Poster Presentations

Black, H. I., Rynn, C., Coupaud, S., Nic Daéd, N., Riches, P. Investigation of the biomechanics of bruising. *International Society of Biomechanics Conference*, Glasgow, Scotland, July 2015

Black, H. I., Coupaud, S., Nic Daéd, N., Riches, P. The biomechanics of bruising. *University of Strathclyde Research Day*, Glasgow, Scotland, June 2015

Black, H. I., Coupaud, S., Nic Daéd, N., Riches, P. The biomechanics of bruising. *Scottish Student Forensic Research Symposium*, Dundee, Scotland, March 2015

Contents

List of figures

List of tables

Chapter 1

Introduction

1.1 The problem

With regards to physical assault, bruising is the most commonly observable injury. Though not all bruises result from malicious acts (e.g., sports and falls), there is a distinct lack of information which can be ascertained from their presence. This is problematic within a legal context, as experts such as medical doctors or pathologists will subjectively comment on the size, shape and age of a bruise and how this relates to the force likely to have caused it. Therefore, it is not uncommon for there to be differences in opinion on the information which a bruise can provide during a court case.

The biology of a bruise is known in terms of blood vessel rupture, repair and blood breakdown. It is widely acknowledged that due to the individuality of each person, many other factors can be involved in influencing the bruising process, for example in age, adiposity and diet – thus making no two bruises exactly the same.

To improve the interpretation of bruising, greater knowledge of this type of injury is required. Currently, how bruise size and colour relates to the level of force which caused it, is based on the concept that a harder hit causes greater damage. Although not necessarily a false conclusion, greater understanding is required as to how impact force, in combination with each person's individual characteristics, influences bruise formation. Furthermore, the subjectivity surrounding bruise age also requires addressing. At the moment, age estimation is based on colour perception and whether or not a bruise appears to be recent or older. Therefore, the relationship between how bruise colour development varies between individuals must also be considered in greater detail.

1.2 Literature overview

A recent review (Byard and Langlois, 2015), discussed the state of bruise interpretation and the approaches considered thus far in an attempt to improve the bruise analysis process.

Their primary focus, like the majority of research in this area, was on the aging of bruises. With colour perception being the fundamental part of bruise age determination, there is a commonly accepted colour pattern of red, blue, green yellow and it used to be that each colour and various other tones would be expected to be seen within certain timeframes. For example, red is commonly seen in the first 2 days, green between 4 and 7 days while yellow appears last from 7 to 10 days.

Currently, bruise age is completely dependent on human interpretation. As pointed out by Hughes et al. 2004, colour perception can vary significantly between individuals, particularly of the colour yellow – considered one of the most important colours in bruising as it indicates an older bruise. As a result, there have been numerous studies attempting to improve bruise interpretation and remove subjectivity. Such attempts include colour charts as a visual aid (Nuzzolese and Di Vella, 2012), utilising specific colour measurement tools (Mimasaka et al., 2010; Scafide et al., 2016, 2013; Thavarajah et al., 2012), histology and measuring the chemical components of a bruise via hyperspectral imaging (Payne et al., 2007; Randeberg et al., 2006). More invasive approaches have also been considered such as taking bruise biopsies (Fronczek et al., 2015), yet given varied approaches, there is yet to be a proven and practical improvement to visual analysis.

As is also mentioned by Byard & Langlois, 2015, this colour analysis problem is further complicated as how a bruise in perceived *in vivo* will vary from that in an image. Standard colour photography can either add or remove details if exposure is incorrect. Furthermore, varying lighting conditions can strongly influence the depth of colour which you see in the resultant images. Thus, research into improving the documentation (and in some cases detection), of bruising is also common. The common approach to this (when not combined with improving colour interpretation), is to look at alternative photography techniques. These include ultraviolet, infrared, cross polarised and alternate light source photography (Baker et al., 2013; Lawson et al., 2011; Lombardi et al., 2015; Rowan et al., 2010; Tetley, 2005).

However, despite these studies, there is yet to be an accepted appropriate photography protocol developed to replace the standard colour photography used.

One important factor rarely considered is the causation of injury. Generally bruising will result from a blunt impact; however, how the mechanics of such an impact influence the extent of bruising seen is currently unknown. There is currently only one study which primarily focuses on bruise mechanics (Desmoulin and Anderson, 2011), with only one subject however, their study provided more of a proof of concept rather than conclusive results. In another study, the influence of tissue biomechanics was briefly considered by delivering blunt impacts to volunteers (Black, 2013b; MSc thesis)). Their findings indicated that the individual can influence bruise appearance as much as the impact, however to what extent is still unknown. How the body responds to blunt impact is more likely to be investigated, from specific tissues (e.g. skin, muscle and bone), to whole body impacts. However, the focus is on response and finding the failure limits of the body and ultimately preventing major trauma. Unfortunately, this means that how a bruise formed (beyond a basic explanation), is overlooked.

1.3 Research aims and objectives

The overall aim of this research is to significantly improve the validity of bruising as a piece of evidence to a court. To do this, bruise analysis would have to be able to accurately determine with a known confidence if a bruise was made at a certain time under certain conditions. With a current lack of understanding of the fundamentals of bruising and accurate method of analysis and documentation, this is not possible. Therefore, the objectives of this research were:

1. To characterise bruising mechanics using a controlled method of blunt impact generation.
2. To assess the suitability of colour, cross polarised and infrared photography techniques for imaging bruising, in terms of the extent of information which can be extracted (e.g. bruise size and colour range).

3. Investigate the use of a colour model for pattern identification within a healing bruise, which could allow for a more accurate age estimation for bruising.
4. Determine if the information extracted from each image type (bruise characteristics and colour model values), can be statistically associated with the bruising mechanics and physiological and anthropometric measures.

1.4 Structure of thesis

Chapter 2 provides an overview of the current understanding of bruising from a biological and medico-legal viewpoint, whilst chapter 3 discusses the approaches taken to study bruise forming blunt impacts, visual interpretation of bruising and methods to improve bruise imaging.

Chapter 4 reiterates the justification and aims of this thesis and the development of an appropriate blunt impact generating methodology to generate bruising. This chapter also presents the development of the photography and colour analysis methods. Chapter 5 outlines the final methodology used.

Chapter 6 presents the results relative to the bruising seen, impact characterisation, bruise colour patterns, photography techniques and how, if at all, impact relates to injury. Chapter 7 provides discussion for these results.

The final discussions and conclusions are presented in Chapter 8, alongside considerations for future work.

Chapter 2

Bruising: Current Biological and Medico-Legal Opinion

2.1 Wounds and injuries

2.1.1 Legal and medical aspect

From a medical viewpoint alone, if any of the body's tissues sustain damage, then it will be defined as a wound. However, it is more common for wounds to be referred to as injuries (Cowan and Hunt, 2008). Either wound or injury may be defined as any damage which the human body has sustained as the result of the application of mechanical force (Saukko and Knight, 2004). Some legal systems have called for a distinction between wound and injury and thus have stated that for an injury to be specifically termed a wound, there must be a breech to the skin surface or a mucous membrane (Saukko and Knight, 2004; Watson, 1989).

2.1.2 Skin Structure

Skin is considered to be the largest organ of the human body, covering the majority of the human body (surface area of approximately 1.5 – 2 m^2), with a body weight contribution of approximately 14 - 16 % (Martini, 2004; Venus et al., 2011; Xu et al., 2008). It is a multi-layered structure (Figure 2-1), which acts as a defensive barrier to protect the body's internal tissues and organs from damage (Martini, 2004; Sanders et al., 1995; Silver et al., 2001).

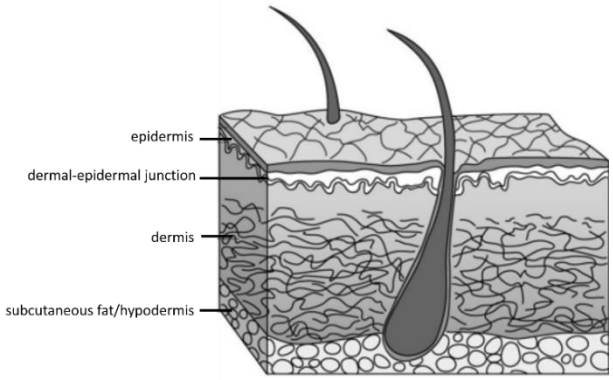

Figure 2-1 Schematic showing multi-layered structure of the skin (Adapted from Geerlings 2010)

Such damage could be caused by ultraviolet light, foreign chemicals, microbial attack and mechanical forces (Martini, 2004; Sanders et al., 1995; Silver et al., 2001).

Skin also has a part in some of the body's regulation processes, including temperature control, nutrient storage and molecule excretion (Geerligs, 2010; Martini, 2004).

2.1.3 Types of skin injury

Throughout everyday life, the human body is subjected to a range of mechanical forces, ranging from the gravitational pull of the planet, to larger impacts encountered during sporting activities (Saukko and Knight, 2004). These forces are normally absorbed by the body via soft tissue (skin, subcutaneous fat and the underlying musculature) and/or skeletal structures, yet if the threshold for these structures to resist or adapt is exceeded, the tissues are damaged and an injury is produced (Saukko and Knight, 2004). The first injuries to be observed are those which affect the skin, and can be categorised into four groups: abrasions, lacerations, incised wounds and bruises (Saukko and Knight, 2004).

2.1.3.1 Abrasions

Commonly referred to as scratches or grazes (Saukko and Knight, 2004), an abrasion is a wound caused by the skin being scrapped, by fingernails for example (Figure 2-2).

Figure 2-2 Abrasion to the hand (Cox 2011)

As a result, the uppermost (epidermal) layers of skin are removed, with either minimal or no bleeding observed. In more severe cases abrasions may involve removal of deeper layers of skin, or even the underlying tissues and muscles, thus bleeding is more likely to be observed (Cox, 2011).

Such wounds can give an indication of shape or direction of the object responsible. For example, tangential abrasions indicate directionality as the epidermis may be collected at one end of the wound, whereas patterned abrasions may represent a bite mark or tyre tread (Cox, 2011). However, if an object hits perpendicularly to the skin producing an abrasion (termed crushing abrasions), the wound is likely to be accompanied with bruising (Cox, 2011).

2.1.3.2 Lacerations

Also known as tears or cuts (Saukko and Knight, 2004), lacerations are caused by stretching or crushing of tissues resulting from blunt impacts (Figure 2-3) (Gooch and Williams, 2007). Although also found internally, skin lacerations are the result of underlying tissues being stretched over bone and tearing. These types of wounds will usually follow cleave lines or Langer's Lines - the tension lines of the skin as its stretched and moves with the underlying muscle and bone (Carmichael, 2014; Cox, 2011; Martini and Nath, 2009). Therefore, this injury is influenced by the properties of the skin itself, which vary anatomically (Cox, 2011).

Figure 2-3 Example of a laceration to the back of the hand (Cox, 2011)

2.1.3.3 Incised wounds

These wounds, which can be referred to as cuts, slashes or stabs (Saukko and Knight, 2004), are commonly observed as knife (or other sharp instrument) wounds (Gooch and Williams, 2007). Such wounds do not necessarily follow skin tension lines,

and have much cleaner edges (Figure 2-4), i.e. the skin is not rough or torn (Cox, 2011).

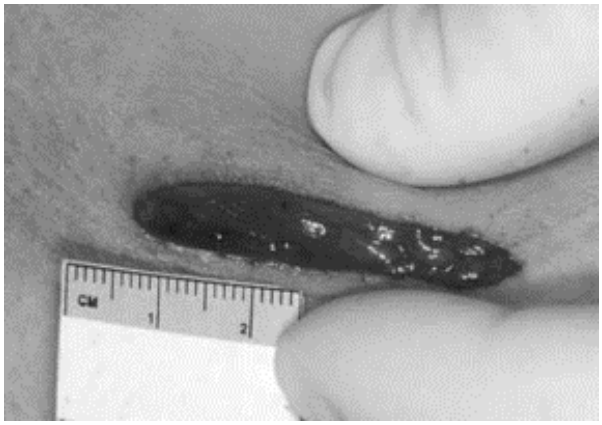

Figure 2-4 Example of an incised wound, edges manually apposed (Adapted from Shkrum & Ramsay 2007)

2.1.3.4 Bruises

Bruises are injuries normally resulting from a mechanical force being applied to the skin, damaging the underlying small arteries, venules and veins. Such injuries appear as discoloured areas of skin (Figure 2-5), where blood has escaped into the surrounding tissues (Gooch and Williams, 2007; Saukko and Knight, 2004; Watson, 1989). These injuries are explained in detail in the following section.

Figure 2-5 Example of a bruise (Cox, 2011)

2.2 Bruising

2.2.1 Terminology

There are different terms used when discussing bruising however, there are contrasting views on which should be used and when. There is general agreement

that bruising itself is an injury which results from a blunt impact to the skin, causing underlying blood vessels to rupture and blood to pool in the surrounding tissues. Confusion comes when the terms including ecchymosis, haematoma and contusion are used.

Ecchymosis, one of the oldest terms to be used, is less common today. Originally it was the term used when bruising was discussed within a medical or professional context (Lewis, 1984), though has been used when referring to small bruises (Saukko and Knight, 2004). Ecchymosis is generally used interchangeably with bruising (Buttaravoli and Leffler, 2012; Cox, 2011; Pounder, 2009; Saukko and Knight, 2004; Stephenson, 1995; Vanezis, 2001) but alternatively, has been used specifically to refer to blood which has migrated through tissue planes, becoming visible on the skin surface (Kaczor et al., 2006). Furthermore, it can simply be used to describe a large bruise (Gooch and Williams, 2007). This is in contrast to the definitions for contusions and haematomas (Buttaravoli and Leffler, 2012; Harris and Flaherty, 2011; Kaczor et al., 2006; Payne-James et al., 2005). The use of ecchymosis may also be determined by the conditions under which the injury was sustained. For example, it has been suggested that ecchymosis refers to bruises which have not resulted directly from a blunt force impact but from other injury types. These would include surgical incisions or needle punctures (Carson, 2010; Cox, 2011; Harris and Flaherty, 2011; Nash and Sheridan, 2009; Saukko and Knight, 2004).

Like ecchymosis, the term contusion may be symonymous to bruising (Gooch and Williams, 2007; Nash and Sheridan, 2009; Pounder, 2009; Scafide, 2012; Stephenson, 1995), or used to describe such skin injuries specifically, i.e. bruising is a form of contusion (Bohnert et al., 2000). In some cases contusion is used to specifically refer to bruising which is present internally, for example present on organs, muscles or bone (Aggrawal, 2016; Saukko and Knight, 2004; Vanezis, 2001). An alternative approach has been to use the term contusion when referring to a bruise injury which is suspected or known to have resulted from a blunt impact (Carson, 2010; Harris and Flaherty, 2011; Kaczor et al., 2006).

Haematoma is another term which can be defined as the same as a bruise (Gooch and Williams, 2007; Vanezis, 2001), however it is less common to do so. Haematoma is more generally defined as a collection of blood which forms an unstable mass beneath the skin, normally associated with cases of more severe trauma (Bilo et al., 2013a; Harris and Flaherty, 2011; Payne-James et al., 2005). If swelling is observed as well as bruising, the injury may be referred to as a haematoma (Stephenson, 1995).

Generally bruising involves the rupture of small arteries, veins and venules however, if capillaries are ruptured petechiae, or petechial haemorrhages, may be observed (Cox, 2011; Gooch and Williams, 2007). This type of haemorrhage refers to the smallest of bruising, where small red or purple marks are present on the skin. They are approximately the size of a pin head (between 1 and 3 mm) and do not necessarily result from blunt impacts (Cox, 2011; Gooch and Williams, 2007; Scafide, 2012; Stephenson, 1995).

Purpura is another term used, again with the same definition as bruising (Bilo et al., 2013a). However, it is more likely to be used when describing such injuries which have appeared spontaneously or did not resulted from a blunt impact (Nash and Sheridan, 2009; Payne-James et al., 2005).

When discussing bruising, a distinction needs to be made between intracutaneous and subcutaneous injury (Bohnert et al., 2000). Subcutaneous bruising is the most common of the two, and involves not only the dermal layer of the skin, but the subcutaneous tissues (Cox, 2011). Sometimes even the underlying muscle can also be included in this category, however this can also be referred to simply as deep bruising (Aggrawal, 2016; Cox, 2011). Such bruising is not restricted to the site of impact and can be observed elsewhere if the released blood is able to migrate through the tissues (Bohnert et al., 2000; Kim et al., 2012). Intracutaneous or intradermal bruising, involves only the dermal layer of the skin and involves a smaller amount of blood than found in subcutaneous bruising (Cox, 2011; Saukko and Knight, 2004). Such bruising will be clearly defined and punctiform (pin/dot like),

often in the form of a pattern representative of the impacting object and is regarded as a sign of severe impact (Bohnert et al., 2000; Cox, 2011; Kim et al., 2012; Saukko and Knight, 2004).

In forensic assessment of such injuries, it has been stated that while bruise and petechiae are appropriate terms, purpura, ecchymosis and contusion should be avoided (Bilo et al., 2013a). Others quoting Stedman's Medical Dictionary of 2005, state that that the term bruise should not be used when describing non blunt impact injuries (Nash and Sheridan, 2009). Unfortunately, there does not appear to be a clear rule for which terms should be used and when. However, 'bruise' appears the most commonly used of the terminology, both in published work and by pathologists (Turner, 2016), thus will be the term used within this research.

2.2.2 Bruising process

For bruising to occur, mechanical forces applied externally to the body result in internal forces (e.g. shear, tension and compression), causing damage to the underlying vessels (Viano et al., 1989). Figure 2-6, demonstrates bruise formation from a blunt impact in its simplest form (this will be expanded on throughout this thesis). A 'pure' bruise is found beneath an intact epidermis (Saukko and Knight, 2004).

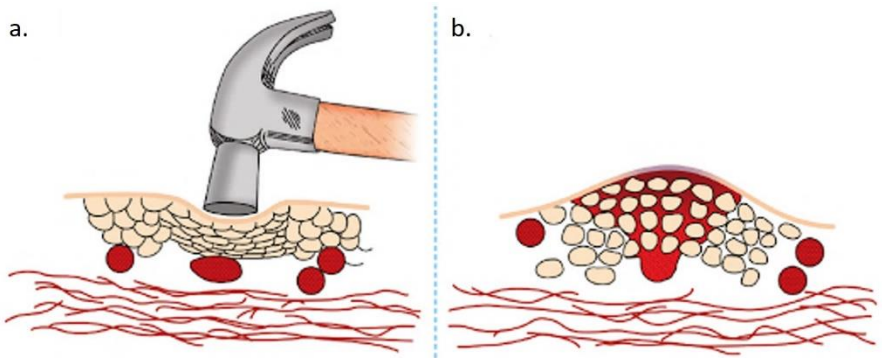

Figure 2-6 Example of bruise formation a. blunt impact from an object (e.g. a hammer) b. damaged vessel releasing blood into the surrounding tissues beneath an intact epidermis (Adapted from Aggrawal, 2016)

2.2.3 Healing of ruptured vessels

When the vessels are ruptured, the body responds by initiating haemostasis. This process is responsible for forming blood clots to stop further bleeding and repair the damaged vessels (Martini, 2004; Ogedegbe, 2002), and results from both biochemical and cellular actions (Ogedegbe, 2002). Haemostasis is composed of three main phases; the vascular phase, platelet phase and coagulation phase (Martini, 2004; Ogedegbe, 2002). The vascular phase is responsible for causing the damaged vessel walls to contract, sealing off the wounded area, reducing blood loss (Martini, 2004; Ogedegbe, 2002). The endothelial cells of the inner wall of vessels secrete hormones and chemical factors, for example the von Willebrand factor, which are required to promote platelet attachment via turning local cell membranes sticky (Martini, 2004; Ogedegbe, 2002).

The platelet phase involves platelets within the circulatory system to migrate to the damaged site, attaching to the sticky cells of the vessel wall (Martini, 2004). As the number of platelets increases at the injury site, they join with each other (platelet adhesion), ultimately forming a platelet plug (Martini, 2004).

During the coagulation phase, coagulation factors (or clotting factors) are released and act to convert fibrinogen to fibrin, which acts as a scaffold, reinforcing the platelet plug at the injury site (Martini, 2004; Ogedegbe, 2002). Red blood cells attach to this scaffold to form a blood clot, which in turn stops the bleeding into the tissues and also provides the scaffold for vessel repair (Martini, 2004). The fibrin fibres which have attached to the vessel then contract during the healing process, closing the rupture (Martini, 2004). As endothelial and smooth muscle cells proliferate to complete vessel repair, fibrinolysis occurs removing the fibrin scaffold through enzyme degradation, ending the healing process (Martini, 2004; Ogedegbe, 2002).

2.2.4 Degradation of extravasated blood

As well as vessel repair, the damaged blood cells must be degraded and removed. For extravasated blood, the break-down process is performed by macrophages. This type of white blood cell engulfs the red blood cells (RBCs) and begins the process of degradation, releasing haemoglobin and converting that into its component parts (Kim et al., 2013; McKinley and O'Loughlin, 2006)

The globular protein of haemoglobin is reduced to amino acids, which the body either recycles for new protein production, or metabolises (McKinley and O'Loughlin, 2006). The haeme component requires further breakdown, where iron is released, forming haemoserdin and also biliverdin (Kim et al., 2013; McKinley and O'Loughlin, 2006). Transferrin (iron binding protein), transports the released iron round the body, either to the bone marrow to be used in the production of new haemoglobin, or to body tissues for storage (McKinley and O'Loughlin, 2006). Biliverdin can then be converted to bilirubin, which the body can then excrete (Kim et al., 2013; McKinley and O'Loughlin, 2006). For the red blood cells damaged during trauma, the haemoglobin released within the bloodstream is degraded in the liver before excretion (Kim et al., 2013).

Extravasated blood degradation can be linked the colour changes observed on the skin when it is bruised. Although there is uncertainty about the specific timings relating to colour appearance, it is accepted that the colours are linked to blood components and their subsequent breakdown. Thus, a general colour pattern is also accepted.

As haemoglobin is what gives blood its red colour, when bruises first develop, red is the first colour to be observed. As haemoglobin begins to degrade, blue tones begin to be observed. Approximately two days after bruise formation, purple tones can begin to be seen while after three days black can be seen. These colours (blue, purple and black), are associated with the oxygen removal from haemoglobin. By four or five days, any brown tones observed can be linked to haemoserdin, while from five to seven days any green pigmentation is associated with the process of biliverdin. The

final colour found in bruising, yellow, is associated with bilirubin and generally presents between 7 and 10 days after bruise formation (Dimitrova et al., 2006; Wilson, 1977).

2.2.5 Bruise patterns

Bruises generally reflect whatever object is responsible for causing the injury. A typical pattern observed is known as tramline or railway line bruising (shown in Figure 2-7). Observed as a clear central area between two parallel lines of bruising (Bilo et al., 2013a; Kaczor et al., 2006; Saukko and Knight, 2004; Stam et al., 2012), they are commonly observed after blunt impacts from rod-like objects such as sticks, batons, belts and even fingers (Bilo et al., 2013a; Saukko and Knight, 2004; Stam et al., 2012). This is because the vessels around the impact site are subject to tensile and shear stress, causing them to rupture away from the impacting area (both types of vessel rupture shown in Figure 2-8) (Kaczor et al., 2006; Stam et al., 2012). Similarly, doughnut shaped bruising (circular bruise with clear centre), form in a similar way to tramline bruising, with the difference being the impacting object being circular in shape, e.g. a ball.

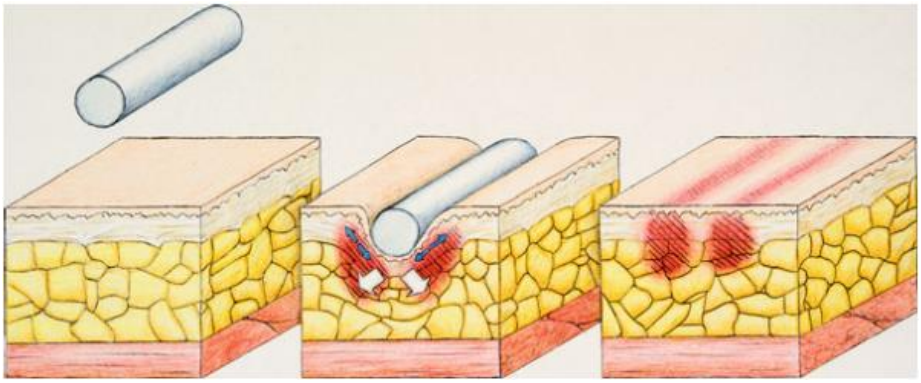

Figure 2-7 Cylindrical object impacting soft tissues to form a tramline bruise (Bilo et al., 2013a)

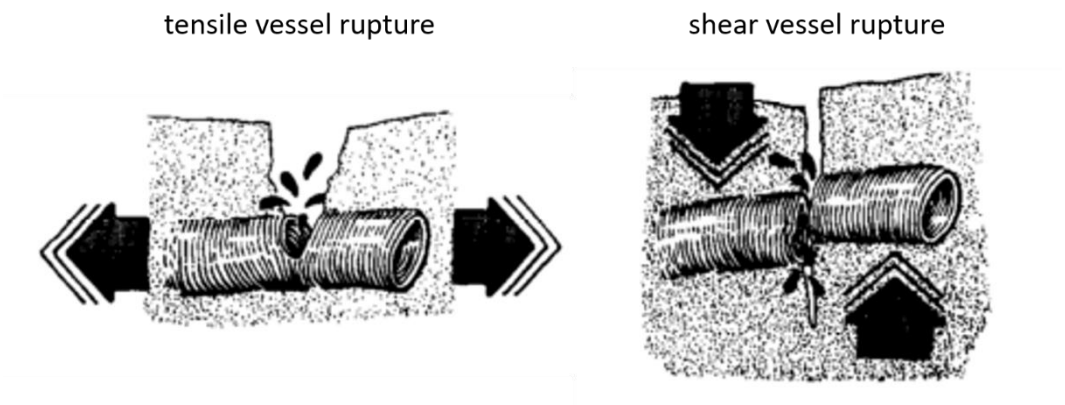

Figure 2-8 Schematic of tensile and shear vessel rupture (Adapted from Viano et al., 1989)

In other cases, bruising may not present with a clear zone. Where a blunt impact is absent (i.e. a dead weight is applied), such as when a person is forcefully restrained/gripped by another, their fingers may leave behind oval shaped marks of where they were gripping – known as finger-pad or fingertip bruising. These appear slightly larger than the fingers which caused them, though generally expected to be approximately 1 centimetre in diameter (Gooch and Williams, 2007; Palmer et al., 2013; Saukko and Knight, 2004).

However not all bruising presents with a pattern which indicates the impacting object or applied pressure. For example, falls could produce bruising of a non-descript pattern or shape, while more severe injury or surgery could produce extensive bruising which does not relate to the injury site. An example of this is shown in Figure 2-9, where an individual has undergone surgery following a broken tibia and fibula, resulting from a fall. Without context, this bruise would indicate a large impact, whilst suggesting the impact site would have likely been to the thigh. Therefore, patterns are not always useful at interpreting causation. Furthermore, anatomical location has to be considered as this can be influential.

Figure 2-9 Example of bruising following surgery. Image produced with permission of the individual.

2.2.6 Bruise location

Bruise patterns can also be associated with the location they are found, for example a 'black eye' is characteristic of being located around the eye. However, it should be noted that this does not necessarily mean that an impact was directed at the eye itself– head injuries can be the source as the extravasated blood travels downwards around the eye, where the tissues are naturally looser and blood can easily pool (Saukko and Knight, 2004). The effects of gravity (unless assessing someone who is in a different environment, e.g. an astronaut in microgravity), should also be considered as where the tissues allow it (see Section 2.3.1), extravasated blood will migrate (i.e. follow the path of least resistance).

2.2.7 Bruise mimicking marks

It is possible for bruise injuries to be confused with other forms of dermal injury or discolouration. Therefore, it is important that a distinction is made between true bruising and mimicking marks (Ward et al., 2013).

Birthmarks are the most likely to appear bruise-like, in particular Mongolian blue spots. These marks usually fade over time, though are known to persist (Ashrafi et al., 2006; Hospital, 2013). They range in colour from a light grey to a dark blue and are flat on the skin (Figure 2-10) (Hospital, 2013; Ward et al., 2013). Where bruising can appear as a mix of colours, Mongolian spots will appear consistent across the whole mark (Hospital, 2013).

Figure 2-10 Example of mongolian sports on the back of an infant (Adapted from Ashrafi et al. 2006)

Striae are another form of mark which can mimic bruising (Elshimy and Gandhi, 2013; Ward et al., 2013). Commonly known as stretch marks, they can present as a red discolouration and could be misinterpreted as bruising (Figure 2-11). Unlike bruising which will heal over an approximate 3 week period, striae will remain for much longer and not demonstrate the stereotypical colour changes associated with bruising.

Figure 2-11 Example of stiae to the lower back (Elshimy and Gandhi, 2013)

Traditional eastern medical practices such as cupping where a vacuum is applied to specific areas of skin, consequently generate circular bruising (Crawford, 2010; Heath and Byard, 2015; Li et al., 2015; Tham et al., 2006). Although this process does cause bruising (Figure 2-12), they are not formed in the traditional sense of a blunt impact.

Figure 2-12 Example of cupping marks (Adapted from Chirali, 2014)

2.3 Influential factors

Although the process of bruising is the same for everyone, the tendency for such injuries to occur and the extent of the injury can vary from person to person, based on their individuality. Furthermore, many of the factors which make us individual, for example age, build or gender, can be interlinked when referring to their influence on bruising.

2.3.1 Effect of skin structure

The skins ability to deform and not tear during a blunt impact is linked to its elastic properties (see Section 3.1.2). This elasticity varies depending on anatomical location, age, an individual's physical build and environmental factors.

Skin structure and its underlying tissues change with age, as their function changes. In young children, the subcutaneous tissues are greater all over the body (Martini, 2004; Vij, 2011). This is to act as a cushioning system while they develop mobility, and as a result they have much softer skin. Thus, children can be found to have a greater tendency to bruise as the softer tissues provide less protection to the vasculature (Martini, 2004; Vij, 2011). During development from child to adult, the subcutaneous tissues redistribute around the body, becoming more prominent in some locations compared to others (Martini, 2004; Mueller, 1982). This redistribution is linked to gender, with females retaining a larger volume (Vanezis, 2001; Vij, 2011). Within men, these tissues become more prominent in areas such as

the arms lower back and neck, whereas in females the hips and thighs (Martini, 2004). The softer areas of tissue on the body have a greater likelihood of bruising. Consequently, the anatomical location of a blunt impact can dictate the extent of injury observed (Vij, 2011). This leads onto a person's physical build. The greater adiposity an individual has, the greater their tendency to bruise (Vij, 2011).

Along with the degree of injury being dictated by the extent of softer subcutaneous tissues across the body, anatomical location also allows for some areas to be looser than others. This can be measured through the use of tensiometers (Paul et al., 2016). Common examples of loose tissue locations are the eyelids and genitalia and if subjected to a blunt impact, larger bruises are likely to be observed as a consequence of there being more space for extravasated blood to travel and pool within (Kaczor et al., 2006; Vanezis, 2001; Vij, 2011). Where the skin has a greater support, due to underlying musculature, the vasculature has greater protection and any extravasated blood has less area to travel into (Kaczor et al., 2006; Vanezis, 2001; Vij, 2011). Thus, there is a lesser tendency to bruise and any injury sustained may appear much smaller than expected (Kaczor et al., 2006; Vanezis, 2001; Vij, 2011). Although underlying bony structures can add support to the skin, they do increase the likelihood of bruising. For example, there is an increased tendency to bruise over the shins and hips, where there is little subcutaneous tissue present (Kaczor et al., 2006). The level of vascularisation to an area is also important in bruise development (Kaczor et al., 2006; Vij, 2011). For example, the face contains a large vascular network and so if subject to a blunt impact, it is more likely that vessels will be damaged and a bruise will be produced (Langlois, 2007; Vij, 2011).

As we get older, the supporting subcutaneous adipose tissues is lost and supportive collagen network is subject to degradation, thus skin loses its elasticity and the vasculature beneath the skin becomes more vulnerable to rupture (Diridollou et al., 2001; Escoffier et al., 1989; Pounder, 2009; Vanezis, 2001). In younger skin, the fibril network is found in abundance composed of continuous strands, with crosslinking in between, providing skin with its strength and stability (Kruger et al.,

2010). As we age, these fibrils become more sparse but densely packed, leaving open spaces within the skin structure, reducing its strength (Kruger et al., 2010). This degradation of the skin's supportive structure can be influenced by environmental factors, with excessive sun exposure over a long period accelerating skin degradation (Ono, 2011; Rawlings, 2006). An example of how this natural aging process affects skin structure/appearance is shown in Figure 2-13.

Figure 2-13 Example of natural skin aging (Ono, 2011)

Medication can influence the skins protective properties. Steroids are a popular anti-inflammatory medication, which can be prescribed to treat various conditions including eczema, asthma and hay fever (Whitehall and Kenny, 2012). However, the side effects of their use include thinning of the skin and consequently, the underlying vasculature will become vulnerable to rupture (Whitehall and Kenny, 2012).

Ethnicity has also been investigated as an influential factor in the skin's response to blunt impact. Skin colour is the most apparent difference, which does not necessarily affect bruise formation itself, but rather influences the visibility of such injuries (Angelopoulou, 1999; Rawlings, 2006). Melanin present within the skin dictates the degree of skin colour observed through the level and distribution of synthesising organelles (melanosomes) through the epidermis (Angelopoulou, 1999). Therefore, the higher the melanin content, the darker the skin and, as a result, the less defined bruising becomes (Angelopoulou, 1999; Pounder, 2009). Although ethnicity does not directly influence bruise formation, different skin types are

affected by sun exposure causing them to age at varying rates (Rawlings, 2006). It is known that caucasian skin will show signs of aging earlier than other, darker pigmented, skin types (Rawlings, 2006). This should be taken into consideration, including if there has been any significant use of sun protection creams (Rawlings, 2006), when comparing bruising tendency across various skin types.

2.3.2 Effect of Bleeding Tendency

Together with skin specific properties, blood coagulation is important in bruise formation. Aging is predominantly responsible for the elderly bruising more easily than other age groups, due to the influence of medications. Along with the skin's decreased protection and support of the vasculature, if the elderly are in poor health they are likely to be taking any number of prescribed medications. Anticoagulants are commonly prescribed to prevent clotting from occurring within blood vessels, preventing health problems such as deep vein thrombosis and strokes (Whitehall and Kenny, 2013). As a consequence, bleeding will occur more readily (Spinks, 2007) and can be more difficult to control and stop. Warfarin is the most well-known of this type of medication, though there are various others including apixaban and dabigatran (Whitehall and Kenny, 2013). Another type of medication likely to be taken by the elderly is antiplatelet drugs, to lower the risk of stroke and heart attack (Kenny, 2012). These drugs act by reducing the stickiness of platelets, reducing their ability to form a clot (Kenny, 2012). Aspirin is the commonly used antiplatelet drug but alternatives such as clopidogrel and dipyridamole can be used (Kenny, 2012). The use of such medications are not restricted to the elderly, but can also be prescribed to those who have received medical implants such as mechanical heart valves and replacement joints (Whitehall and Kenny, 2013).

Like medications, health conditions and disease can also increase bleeding tendency and/or effect the coagulation of the blood (Vanezis, 2001). One such condition is a vitamin K deficiency, which can result in the development of a bleeding disorder (Vanezis, 2001). Vitamin K is involved in the synthesis of blood clotting factors II, VII, IX and X (Tidy, 2014a). If these factors are unable to be produced then

an individual may bleed much more excessively than someone without this deficiency (Tidy, 2014b). This deficiency is most commonly observed in newborn children, while being rarely observed in adults (Tidy, 2014a).

There are many conditions which effect blood coagulation, for example von Willebrand disease (vWBD), (deficiency of von Willebrand and VIII coagulation factors) (Jackson et al., 2012; Kaczor et al., 2006; Pasi et al., 2004; Vanezis, 2001; Vij, 2011) and haemophilia (Jackson et al., 2012; Vanezis, 2001; Vij, 2011). This condition often develops at birth (Jackson et al., 2012) and can be one of two types, haemophilia A or haemophilia B. Haemophilia A is the more common form resulting from a clotting factor VIII deficiency (Knott, 2014a), whereas haemophilia B is a deficiency of clotting factor IX and is less severe (Knott, 2014b). Like haemophilia B, the Leyden variation of the condition is a deficiency of factor IX; however, factor levels rise once an individual reaches puberty to between 40 % and 60 % of what would normally be expected (Knott, 2014b). Generally clotting factor deficiencies, whilst also being responsible for increased bruising, have more severe consequences when an individual is injured as haematoma formation is likely (Knott, 2014b). Platelet disorders, while also causing increased bleeding, are more likely to result in an increased likelihood of bruising being observed (Knott, 2014b).

Platelet disorders, also known as thrombocytopathy, can be either inherited or acquired. They effect the initial (primary) stages of haemostasis (formation of a platelet plug), resulting in extended bleeding times and thus the formation of bruising (Tidy, 2012). There are many different types of disorders, for example Bernard-Soulier syndrome (BSS) and Glanzmann's thrombasthenia (GT). Both BSS and GT are severe disorders which result from the deficiency of the glycoprotein 1b and glycoprotein IIb/IIIa complex respectively, compromising platelet migration and attachment to an injury site (Tidy, 2012). In comparison grey platelet syndrome is a disorder of platelet structure itself, causing them to be large and appear grey in colour (Tidy, 2012). Chemical signals and receptor disorders (e.g. ADP receptor defect or platelet cyclo-oxygenase deficiency), also reduce platelet response, whereas the

clotting disorder vWD also affects platelets by limiting their adhesion ability (Tidy, 2012).

A source for acquired platelet disorders is diet and the use of food supplements. For example, garlic, ginger, fish oil, ginseng and ginkgo biloba have been found to have platelet-inhibiting effects (Konkle, 2011; Spinks, 2007; Tidy, 2012). Alcohol can also reduce platelet function, not only in those who suffer from alcoholism, but even moderate alcohol intake can have a temporary effect (Konkle, 2011; Mukamal et al., 2005; Spinks, 2007; Tidy, 2012).With diet also being linked to the composition of soft tissues, the full extent of influence that these factors can have is currently unknown (Konkle, 2011; Spinks, 2007).

2.4 Medico-legal significance

2.4.1 The field of forensic biomechanics

Forensic biomechanics is the combination of both forensic and biomechanical work. Biomechanics can be defined as mechanical principles being applied to the understanding of biology often, but not restricted to, the human body. This ranges from the large scale workings of organs and the skeletal system, to the microscopic properties of individual cells (Engin, 2014). Forensics relates to the application any field of knowledge to attempt to solve of civil or criminal legal questions, thus forensic biomechanics specifically uses biomechanical knowledge and understanding to answer questions concerning injury causation (Engin, 2014; Hannon and Knapp, 2008; Hayes et al., 2007; Zioupos, 2014). This is most likely to be within a criminal context, for example to support or refute injury causation claims, yet it can also be applied to understanding trips, slips and falls, sporting injuries or investigations into safety standards within workplaces (Engin, 2014; Hayes et al., 2007).

2.4.2 Injury biomechanics

Injury biomechanics is a branch of forensic biomechanics, which specifically aims to explain the physiological and anatomical response to an impact which has resulted in injury, through use of mechanical principles (Hannon and Knapp, 2008;

Viano et al., 1989). Non-penetrating (e.g. bruising) and penetrating injuries (e.g. stab wounds) are both investigated by this field, however the former are more complicated as they are difficult to understand (Viano et al., 1989). It is more common for injury biomechanics to be used in understanding the serious injuries which can be sustained in vehicle accidents, allowing for design of new driver and passenger safety features (King, 2004).

When investigating injury causation, there are some fundamental questions which are aimed to be answered. The questions in quotes below, which were first developed by Watson (1989), are still highly relevant and applicable to current legal investigation. They have not been superseded.

The first of which is, 'how was an injury caused?'. For example, did the injury result from a fall or a deliberate attack? This question may not always have a definite answer. However, if causation can be identified, the information can aid police investigations.

The next question is, 'when was an injury sustained?'. The timing and dating of injuries is not always easy. There are no precise methods of aging an injury, yet some general rules can be used to gain a rough idea, for example, examination of the level of tissue repair surrounding penetrative skin wounds or bone fractures. As found when trying to identify injury causation, this question can sometimes be difficult to answer.

'How much force was used?'. The precise figures or calculations for identifying the level of force are not available. Estimations could be made, however the answer is largely dependent upon the area of the impacting object, as the same degree of force will generate greater impacting pressures if focused on a smaller area that it would over a larger area. Thus, the severity of observed injuries will vary dramatically. This question must also consider the level of resistance offered by the impacted tissues, as the level of force absorption varies between soft and hard tissues. It is normal for a general scale is used to describe applied force composed of four degrees of force, minor, moderate, considerable and severe.

Where a victim is deceased, 'has the injury contributed to the death?' is asked. In some cases, multiple injuries can be present. Therefore, identifying (if possible), if one or more injuries were responsible for death is important when investigating criminal cases.

Forensic biomechanics, whilst applicable in answering all of the above, specifically targets answering questions 1 and 3. It aims to do so through an understanding of the tolerance levels of body tissues and utilising concepts found in both material and structural engineering (Zioupos, 2014). It should be noted that a biomechanical interpretation of injuries is different from a medical diagnosis of injury. An assessment from a medical viewpoint will look at symptoms to make a diagnosis of injury type, while a biomechanical assessment will not necessarily argue with the medical opinion, but focuses on the mechanisms which caused the injury to occur (Hannon and Knapp, 2008).

2.4.3 Medico-legal significance of bruising

Skin bruising is rarely considered a fatal injury. As a result it is unlikely that bruising will be given much attention, particularly if more severe injuries are present, for example those observed as a result of stabbing or high speed vehicle collisions (Kaczor et al., 2006; Langlois and Gresham, 1991; Spilsbury, 1939). However, their importance is becoming more recognisable as they can indicate a possible time of injury (although subjective, see Section 2.2.4) or can be an early indicator of cases of physical abuse (Crawford, 2010; Kaczor et al., 2006; Langlois and Gresham, 1991; Nuzzolese and Di Vella, 2012; Pounder, 2009). In addition, if bruising is in the form of a pattern, then information about the impacting object can be obtained, for example its approximate size and shape (see Section 2.2.5).

As a result, during legal cases of physical assault, forensic examination of bruising can prove an important factor in supporting or refuting a claim. Unfortunately, the mechanics of bruise formation and whether bruising can be accurately aged are currently poorly understood. Research within this field is limited, yet it is accepted that visual assessment of bruising alone is highly subjective, thus a

more reliable method of bruise interpretation is required (Desmoulin and Anderson, 2011; Grossman et al., 2011; Hughes et al., 2004).

2.4.4 Important questions when assessing bruising

During forensic assessment of bruising, several key questions need to be addressed. As in Section 2.4.2, the questions below developed by Watson (1989), are still highly relevant and applicable to current legal investigation and have not been superseded.

The first of which is, 'does the bruise indicate the level of violence sustained?'. This is likely to be the most important question to be asked, yet the most difficult to answer. Before any estimation of force or pressure can be made, individual physiological factors must be considered (see Section 2.3). Their effect on bruise formation can highly influence their appearance, e.g. a relatively minor impact may generate a small bruise on one individual, but a much large bruise on another.

Another question can be 'is the bruise located at the point of injury?'. As bruising can occur are relatively close to the skin surface, or much deeper within the dermal or subcutaneous layers, the extravasated blood may be able to migrate along tissue planes (see Section 2.2.6), causing bruising to appear in a different location from where the impact occurred. Generally there is close bruise location-impact site relationship.

Next, 'does the bruise exhibit a pattern?'. If the bruise exhibits a pattern, this can be used to indicate a possible impacting object (see Section 2.2.5) and may even aid identification of the degree of violence sustained. However, if bruising has occurred deep within the tissues, any pattern may be lost once the blood has become visible on the skin surface sometime later.

In cases when the victim of an assault in deceased, 'is bruising ante-mortem or post-mortem?'. It is important to make this distinction so bruises can be described within context. Bruise formation is dependent on blood being able to flow out of a damaged vessel. Once deceased, there is no blood flow and thus theoretically no

bruise can be formed. However, as blood remains fluid for a period of time after death, some blood may be released from damaged vessels. However, the extent of this bleeding is small in comparison to that observed in a living person. Therefore, when distinguishing between ante- and post-mortem bruising, larger bruising is associated with having occurred before death.

Finally, 'is the discolouration a result of post-mortem hypostasis?'. Post-mortem hypostasis refers to the settling of blood within the body after death, becoming visible through the skin as an area of discolouration. In this case, to distinguish from bruising, a visible observation is made by dissecting the affected tissues.

2.4.5 Unreliable interpretations

Due to the subjective nature of bruise assessment, it is inevitable that these injuries can be mistaken for signs of assault or abuse. Bruising is most likely to be misinterpreted in cases involving children; and with abuse being such a serious crime, any accusation must be taken seriously. Consequently, the observation of any bruise-like mark can cause a rushed assumption of child abuse. Such an assumption was made in 2012 in Colorado, when the police had been alerted by nursery staff that one of the children in its care had bruising on her back and suspected that the child was being abused at home (Meredith, 2012). As a result the child's mother was questioned until it was later found that the child had not been harmed and the marks were in fact Mongolian Spots (Meredith, 2012). Another example of a rushed decision was made in the UK, when a Judge ordered that 3 children were to be removed from their parents (Doughty, 2011). This judgement was made in just 15 minutes, based on one of the children having bruising present on their ear, which doctors had stated (as an opinion), resulted from pinching. This decision was later overturned as it was made far too quickly, based on a subjective opinion and almost tearing apart a family needlessly (Doughty, 2011).

Along with the possibility of false accusations, a misinterpretation of bruising can also lead to wrongful convictions. In Mississippi, 1990, Sabrina Butler was

convicted of child abuse and the murder of her 9 month old son and given the death penalty (Innocence, 2014; Possley, 2012). This was based on the bruising alongside the internal injuries observed. It was not until an appeal declared that the prosecution had not provided sufficient evidence that the injuries were not the result of Butler's attempted CPR and thus accidental, that a retrial took place (Innocence, 2014; Possley, 2012). During this retrial, evidence from a neighbour corroborated that CPR had been attempted and the medical examiner changed their opinion, acknowledging that the CPR could have caused the bruising and injuries observed. In this case, the accused was exonerated (Innocence, 2014; Possley, 2012).

Dr Charles Smith, a paediatric pathologist, was well respected until his work was called into question in 2005 (Cromwell, 2011). The following review found many problems, particularly with him "overstating his knowledge" and discussing evidence "outside his area of expertise" (Cromwell, 2011). With bruising only capable of being interpreted speculatively, his comments on such injuries did lead to wrongful convictions. One such case was that of William Mullins-Johnson, where the accused was convicted of the murder of his niece who he had been looking after the night before she had been found deceased (Cromwell, 2011). The basis for this conviction was that according to Dr Smith, bruising suggested that she had suffered a sexual assault and abdominal or chest compression causing asphyxia (Cromwell, 2011). Once the aforementioned's work came into question, six other pathologists assessed his findings in this case, all coming to the conclusion that the bruising did not support the original claim, but were in fact the result of the normal biological changes which occur after death (Cromwell, 2011).

2.4.6 Description of bruising

Given the significance this type of injury can have, it is surprising that when referring to any physical injury, there is no accurate method of stating how severe an injury is. For example in an appeal by George Donald Smith against Her Majesty's Advocate (Carloway et al., 2016), the following description is given referring to blunt injuries observed on the deceased:

"The force used was in the mild to moderate range and caused by blows with hands or feet or an impact with a hard surface, such as a floor … The deceased had bruising to his abdomen, which was older than the facial injuries. He had relatively recent bruising of his arms, wrists and hands, which could have occurred at the time of the incident or some hours earlier. The bruises to the hands and arms could have been defensive or indicative of being gripped or held … He also had old bruising or abrasions of the left knee."

The language does not portray exact timeframes, just old, older and recent. Although acknowledged that the exact impacting object is unknown, the force level is described as mild to moderate, again with no reference to what that level of force is equivalent to. Currently this vague terminology is the norm, with only three terms being used to describe bruise/impact severity: mild, moderate and severe (Turner, 2016).

Another problem with the reporting of bruise injuries is that in some cases their presence alone is all that is noted. For example, during the appeal case of Rachel Trelfa (or Fee) in 2017, the evidence discussed referred to injuries sustained by a child including bruising to various locations (Turnbull et al., 2017). These observations were made at post mortem and although not necessarily the most severe injuries observed, the bruising was part of conclusion that the child sustained blunt force trauma immediately and sometime prior, to death. The issue here was that although bruising was mentioned, there was little to no detail on size or colour of these injuries. Given they were considered non-fatal, this is not a surprise, however as an injury considered worthy of being noted as evidence, it is this author's opinion that a greater description (both of appearance and causation), would have been beneficial.

As with any appeal judgement, the full details may not always be included as would be found in an original trial case; nevertheless, even from the summary of a legal case the lack of detail is apparent. Unsurprisingly this leads to disagreement between experts about bruise causation. An example is from 2015, where during the original examination the two pathologists described facial and head bruising (and other injuries) as likely being caused by 'finger pressure'. However, another pathologist challenged this by suggesting that such injuries were likely caused by falls or impacts (Carloway et al., 2015). In this case, the disagreement did not influence the outcome of the appeal as there were other factors taken into consideration, however it does show how causation uncertainty can become problematic.

Chapter 3

Bruising: Blunt Impacts, Photography and Visual Interpretation

3.1 Impact theory

As previously mentioned in Section 2.2.2 bruising results from a blunt impact which has ruptured the skin's underlying blood vessels. On impact the soft tissues respond by dissipating force away from the impact site. Although force is an important factor (and for bruising is often used to explain the extent of bruising seen on an individual), the mechanism of injury needs to be considered in more detail.

It should be noted that force is the mechanical parameter referred to throughout this research as it is that which is used throughout other published research in this field and quoted within this thesis. It is acknowledged that other parameters, specifically energy, may be more appropriate. An explanation of why can be found in Section 8.4 of this thesis.

3.1.1 Force transfer during impact

Blunt impacts to the body can occur as part of general everyday movement, for example during heel strike while walking, to injuries occurring during physical assault (Gooch and Williams, 2007). They occur when a person struck by a blunt object such as a foot, fist or ball; or if they were to come into contact with a stationary object such as the floor or wall (Gooch and Williams, 2007).

The different tissues of the human body have different characteristics in terms of both strength and stiffness (Bahr and Krosshaug, 2005). During blunt impacts the soft tissues are seen to move independently of the skeletal structures, resulting in the theory that they are responsible for dissipation of the associated force (Pain and Challis, 2002).

For blunt impacts the impulse of an applied force is equal to the change in momentum of an object. This change is dependent upon both the level of force and the time which this force is applied (Hannon and Knapp, 2008). Therefore, for soft tissues, the greater their stiffness, the shorter the impact time and thus the greater the applied force (Hannon and Knapp, 2008).

The ability of soft tissues to protect themselves and the body as a whole, is not strictly due to their stiffness, but also due to their own anisotropic and viscoelastic properties.

3.1.2 Tissue properties

3.1.2.1 Anisotropic properties

Soft tissues are composed of different materials with different properties and as such demonstrate anisotropic properties i.e. they will respond differently dependent on loading direction (Hannon and Knapp, 2008; Özkaya et al., 2012). These properties explain why soft tissues can adapt during loading and therefore reduce the overall damage sustained not just by that specific tissue, but to the body as a whole.

The most common component of soft tissues are the collagen fibres. The anisotropic nature of soft tissues is the result of such fibres having a preferred alignment within the tissue (Holzapfel, 2000). As shown in Figure 3-1, when no load is applied the fibres appear unorganised. As a load is applied, the low stress will cause a large deformation in tissues (Phase I). Moving into Phase II, as loads are increased the collagen fibres begin to align and stretch. At this point tissues will begin to increase in stiffness. By Phase III the fibres are at their most linear becoming fully aligned. If loading is increased beyond this point, the fibres will begin to break resulting in injury (Holzapfel, 2000; Kieser et al., 2008).

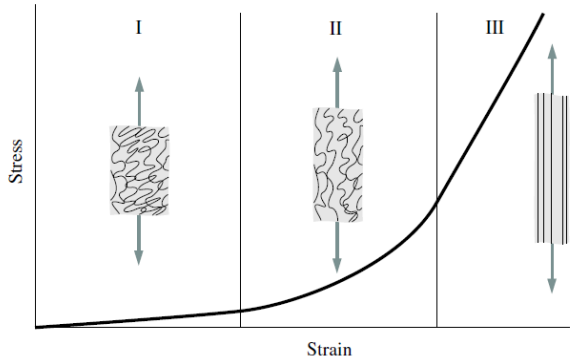

Figure 3-1 Schematic diagram showing the three phases of collagen fibre realignment associated with a typical (tensile), stress-strain curve (Adapted from (Holzapfel, 2000)

Combined with elastin, soft tissues are able to not only stretch but return to their original state (Hannon and Knapp, 2008). Regarding the soft tissues most likely to be subject to a blunt impact (muscle and skin), the arrangement of fibres in their natural state differs. For skeletal muscle, the fibres run from their origin to insertion and are generally aligned in the direction of pull. Whilst for skin, the fibres are less organised but do exhibit a natural alignment with cleavage lines, thus skin can adjust to loading from multiple directions compared to muscle (Carmichael, 2014; Hannon and Knapp, 2008). This property explains why skin is considered to be the primary tissue responsible for injury prevention in response to mechanical loading.

3.1.2.2 Viscoelastic properties

Viscoelasticity relates to both the viscous and elastic properties of a material. Conventionally viscosity is a property of liquids while elasticity is a solid property, thus a viscoelastic material exhibits both solid and fluid properties (Burgin and Aspden, 2007; Hannon and Knapp, 2008; Kieser et al., 2008; Özkaya et al., 2012). When such a material is subject to a form of loading, the extent of deformation is linked to the rate at which the load is either applied or removed (Burgin and Aspden, 2007; Hannon and Knapp, 2008; Kieser et al., 2008; Özkaya et al., 2012). Therefore, the material response is time dependent (Burgin and Aspden, 2007; Hannon and Knapp, 2008; Kieser et al., 2008; Özkaya et al., 2012; Purslow et al., 1998; Silver et al., 2001).

A common example of this property is found with non-Newtonian fluids (fluids which behave as a liquid, but under specific conditions will behave as a solid) (Miodownik, 2013), such as Oobleck (mixture of cornflour and water) or custard. For these fluids, you can easily move your hand through them however, if you were to punch or hit them with an object, their surface would act as a solid (shown in Figure 3-2).

The body's soft tissues exhibit viscoelasticity and as a result when subject to rapid loading they will appear much stiffer whereas, if loading is slower, the response will be much more fluid-like (Hannon and Knapp, 2008; Holzapfel, 2000; Özkaya et

al., 2012; Sharkey et al., 2012). The viscoelastic and anisotropic properties are the basic principles which explain how, when subject to a blunt impact, tissues can adapt to loading rather than sustaining damage. When major and minor trauma occurs, the tissues fail to absorb and dissipate all of the energy transferred during loading (Bilo et al., 2013b).

Figure 3-2 Example of Oobleck acting as a solid when being rolled between hands but as a liquid when external forces are removed (Miodownik, 2013)

3.1.3 Tissue response

The movement when soft tissues sustain a blunt impact can also be referred to as tissue wobble, originating at the site of impact (Pain and Challis, 2002). As the tissues are deformed, they act to return to their original state as the applied force is removed, producing the characteristic wave-like deformation associated with blunt impacts (Challis and Pain, 2008; Pain and Challis, 2002). This deformation explains why not all falls or impacts result in open wounds. Tissues deform and dissipate force, preventing the tissue reaching its failure point and rupturing (Hannon and Knapp, 2008).

The rate at which this tissue response occurs is based on the anisotropic and viscoelastic properties of the tissue. Furthermore, the distribution of these tissues, which can vary across the body and between individuals, can also influence the rate at which the tissues respond to impact (Challis and Pain, 2008).

3.1.4 The subcutaneous tissues

The components of the human body include bone, muscle, adipose tissue and skin from which skin is the initial tissue to undergo deformation during a blunt impact

(Challis and Pain, 2008). However, impacts can also cause the underlying fatty tissues and musculature to deform, thus transmitting the applied force away from the initial impact area through the surrounding tissues (Challis and Pain, 2008; Tanaka and Kaneko, 2006). It is at this point where damage to the underlying vasculature can occur.

The subcutaneous adipose tissues (sometimes referred to as the 3rd layer of skin, behind the epidermis and dermis), is deformable and like skin and muscle, can also sustain bruising (Harris and Flaherty, 2011; Randeberg et al., 2011). This tissue has viscoelastic properties, however its role and response during blunt impact is less understood. There is an argument that this layer can provide some cushioning, absorbing impact and protecting underlying tissues (Kent et al., 2010). Nonetheless, depending upon the extent of adiposity (i.e. if someone is considered obese), this could contribute to injury being increased when the body is subjected to large impacts (e.g. from a car crash) (Kent et al., 2010). It is thought that the stiffness of subcutaneous fat varies with anatomical location, for example, the fatty tissue within the heel would be expected to be stiffer compared to that found elsewhere, as it is continually subject to loading during walking (Kassab and Sacks, 2016).

3.1.5 Biomechanics, blunt impacts and bruising

Although research investigating blunt impact injury causation and prevention is common, there is less focus on the specific mechanics involved in the tissue response. When mechanical processes are discussed, they are relative to more significant impacts/trauma such as car impacts or stabbing injuries. This thesis will go on to consider comparatively minor blunt impacts and injuries to those commonly investigated, specifically focusing on impacts to the thigh. Evidence as to how tissues respond with respect to minor or non-penetrating blunt impacts is currently lacking.

One study (Desmoulin and Anderson, 2011), has studied bruise generating blunt impacts to the lower leg, the only one known to the author which considered the mechanics of impact within this context. Their aim was to create a method which

could be used to experimentally identify how an impact can influence bruise formation across different anatomical locations.

Their study was limited in that it tested only one male participant, however it did involve him being subject to 12 drop mass impacts (split equally between two weights – 1.9 kg and 2.6 kg). Through use of a force plate and a potentiometer, a list of impact characteristics including peak force and energy absorbed, were produced for each of the 12 impacts. The extent of bruising observed was not discussed in depth, but only whether bruising was observed or not.

As this study investigated the link between impact and bruise, they concluded that as when tissue stiffness increased, the peak pressure of each impact increased ($r = 0.728$, $p < 0.01$) and therefore claimed bruising was more likely to occur where tissue was stiffest. The problem with this conclusion was that the range of tissue stiffness observed (12.8 to 89.3 kN/m), did not have a clear correlation with bruise formation (i.e bruised and non-bruised areas were observed for this stiffness range).

Limitations aside, this study did provide a starting point for this research and tried to bridge the gap between impact and injury, which for bruising had not to this author's knowledge, been previously considered.

3.1.5.1 Practical studies

As previously stated, studies which considered blunt impacts focused on injuries of greater severity, with their aim tending to focus on prevention, such as reducing injuries associated with a specific sport. The problem being that there are a wide variety of injuries which an individual can sustain under multiple circumstances (Bahr and Krosshaug, 2005).

Injury prevention is a common topic for blunt impact research. This is based on the idea that if the deceleration time of an impact can be prolonged, the potential for injury will be reduced (Crawford, 2003; Viano and King, 2000).

For example, assessment of a wrist brace to be used by individuals who take part in snow sports (e.g. skiing or snowboarding). A study of a cadaveric forearm drop

mass system indicated that injuries sustained by individuals, despite wearing this support, were as a result of the support itself not altering loading conditions (i.e. providing support, reducing loading) (Greenwald et al., 1998). In fact, impacting force was seen to increase from unbraced to braced wrists. However, although they looked at impact forces, the specific response of the tissues and how they react under this type of loading were not specifically addressed.

Another example reviewed the impact forces which the human body could sustain and survive when constrained by a full-body harness (Crawford, 2003). If the decelerations applied to the body from the harness are excessive, then injuries ranging from skin surface to internal damage across the torso (e.g. internal organ damage) could occur. As in the previous example this review considered impact forces, with the focus being on what level of force could cause injury to occur, with no consideration given as to how tissues responded to this type of restraint.

An alternative approach to the investigation of blunt impacts is to look at those which can commonly occur during an assault. One such study compared whether empty and full beer bottles shatter during a blunt impact alongside investigating whether the impact generated would be enough to fracture a skull (Bolliger et al., 2009). Their conclusion was simply that beer bottles can be dangerous instruments when used as a weapon. This approach is consistent with many blunt impact studies which consider whether the measured force (or in this case energy), matched or exceed that known to cause significant damage. How this type of impact produces the fracture was not addressed.

Another study which considered the force associated with skull fracture, delivered blunt impacts from different objects (wooden flooring, shoe, hammer and broom handle), to a porcine head (Sharkey et al., 2012). Each method resulted in varying injury patterns and although they did not necessarily comment on how different objects interact with tissues and thus cause damage, they do acknowledge that for skull fracture and any associated soft tissue lacerations, individuality was influential (i.e. shape of skull, thickness of soft tissue, impact area, angle and velocity). This hint in acknowledging that impact mechanics can influence tissue response and

that this in turn influences injury, is something which is commonly assumed as true but rarely discussed in detail.

However, such factors have also been shown to be of no significance. Such an example was in a study which considered the tolerance of the nasal bone when subject to a blunt impact. In this case a drop mass system was used to determine the force required to fracture the bone (Cormier et al., 2010). Their results indicated that the anthropometric factors considered (nose length and bone length, width and thickness), did not influence the force required to break the bone. There was a relationship between age and risk of fracture found, suggesting bone composition rather than shape was influential but again, how the impact produced the injury was not addressed.

The punch from a boxer to the face has been investigated via punches being delivered to a dummy with accelerometers located on both the boxer's glove and the dummy's head (Walilko et al., 2005). This study focussed purely on the impact and showed that punch force for various boxers increased with boxer weight and that the resultant head accelerations also increased (i.e. energy transfer relative to impact conditions). Once more, how tissues move in response to impact is not covered, but the approach was more detailed than others with respect to the impacted surface.

The limitation to the existing practical studies of blunt impact, is that the impact itself was not always taken into consideration more the injury. When it is considered however, it is expressed in terms of the magnitude of force it generates.

Specifically for blunt impacts and bruising, there is also an ethical factor to consider, particularly where research makes use of volunteers. Unlike conventional studies, bruising by blunt impact involves deliberately harming an individual. With pain being subjective, no accurate description of the discomfort that an individual would experience can be provided prior to recruitment. Furthermore, the extent of injury cannot necessarily be predicted and thus there is always a chance that one person's bruise could be much larger compared to another. While this could be avoided through the use of animal models, this has its own issues in the justification

of the deliberate injury and sacrifice of an animal for research. By fully informing volunteers of the risks involved and the pain and injury they would likely sustain (emphasising this cannot be quantified exactly for them), makes such experimental studies possible. It should be noted that given the nature of such work, the ability recruit large numbers of volunteers is also a limitation. Examples of such studies have been discussed elsewhere in this thesis as their focus was either to age bruising using various colour measurement techniques, or to investigate different documentation techniques (e.g. photography).

3.1.5.2 Computer simulation

Although computer simulations of blunt impacts are theory based and cannot currently truly represent the variability between people (e.g. parameters of tissue stiffness will always have to be applied), they do provide an insight into how tissue responds during an impact and how forces are being transferred in and across tissues. Furthermore, they can provide a more realistic representation of human tissue than an artificial dummy could provide during experimental testing (Mackay, 2007).

Another advantage of computer modelling is in that it is not restricted by composition i.e. it can be a single tissue type, whole limb or full body. However, the accuracy can then be limited by the level of detail of the model, such as containing different tissues with varying thickness and stiffness or a chest model including the internal organs and not just the skeletal structures.

For both blunt impact and general injury biomechanics research, computer modelling provides a way to visually reconstruct an event after the fact. Such an example is in using an existing human body model to analyse vehicle incidents or falls from height (Adamec et al., 2010; Číhalová and Hynčík, 2008; Crandall et al., 2011). However, although this approach has its uses, it does not necessarily provide specific information on the tissue response; at least not within the context of this research.

More focused blunt impact research can concentrate on larger impacts given their likelihood for severe trauma. This can include Finite Element (FE) modelling of the thoracic and abdominal regions of the body, comprised of bones, organs and soft

tissues (Shen et al., 2008). This particular study delivered blunt impacts to pigs, taking CT scans and then developing a computer model replicating the event. Overall, they obtained good results comparing modelled impact with resultant injury, showing that modelling can be used to demonstrate injury causation.

Another approach of FE modelling is to model specific anatomy (e.g. bone or soft tissue), mapping stresses under loading where injury to a localised area is of interest (Affagard et al., 2014; Iivarinen et al., 2011; Ionescu et al., 2006; Kassab and Sacks, 2016; Tham et al., 2006; Zhao and Narwani, 2007). However, as with the majority of research surrounding blunt impact, the focus is on the most severe injuries and how their occurrence can be explained.

When considering blunt impacts and bruising (specifically bruising seen on the skin, not to internal organs), studies using computer modelling are limited. One approach ignores the mechanics of a blunt impact altogether and focuses on blood pooling and its breakdown instead (Stam et al., 2012, 2010). Although proposing a method for categorising healing time based on the extent of bleeding present and how the blood pools (i.e. distribution within tissues), this provides no information on how the tissue responds to an impact, producing the bruise injury.

The closest study to showing an impact, the response of tissues in terms of stress and strain and how this influences the resultant injury is one by Huang et al., in 2012. In their study, they created a cross-sectional model of a human upper arm containing all main soft tissue layers (muscle, subcutaneous fat and skin), with a hollow area representing the bone. Capillaries were added to the muscle layer and each tissue type was given its own density, Poisson's ratio and Young's modulus.

The above simulation involved a pressure of 0.1 MPa being applied to an area of 648 mm^2 over a period of 0.06 s. Although bruising itself could not be specifically modelled, they assumed that it occurred where the applied stress level exceeded the ultimate tensile stress defined for capillary walls. Their model successfully demonstrated the level of deformation (Figure 3-3), that such an impact could produce, and how this moved not only across but through the modelled limb,

towards the bone. The stresses generated were not only present at point of impact, but also around the underlying bone (Figure 3-3). They also showed that skin and adipose tissue were the most compliant to the deformation with the musculature responding to reduce the depth of impact. As a result, high compressive forces applied to the outer soft tissue layers were not found to transfer to a level capable of rupturing underlying capillaries. However, tensile stresses applied to the capillaries were found to travel from impact site outwards, exceeding that which was expected to cause vessel rupture.

This approach was not perfect, in so far as it did not consider soft tissue to be viscoelastic and thus likely underestimated the transient stiffness of the tissues. Furthermore, they only considered failure to be due to tensile stress on the tissues and capillaries, not shear stress. However, it does provide an insight into how tissues respond to impact, not as single entities but in combination with other tissues (as found naturally within the body). Furthermore, they are presented in the form of a limb and not a 2D cross section thus making the model more realistic. Capillaries, however were not distributed throughout each tissue segment but positioned in one specific location. Therefore, the stress applied to them could vary more in real life, particularly if the volume of soft tissues surrounding them is also altered to reflect individuals of varying body type.

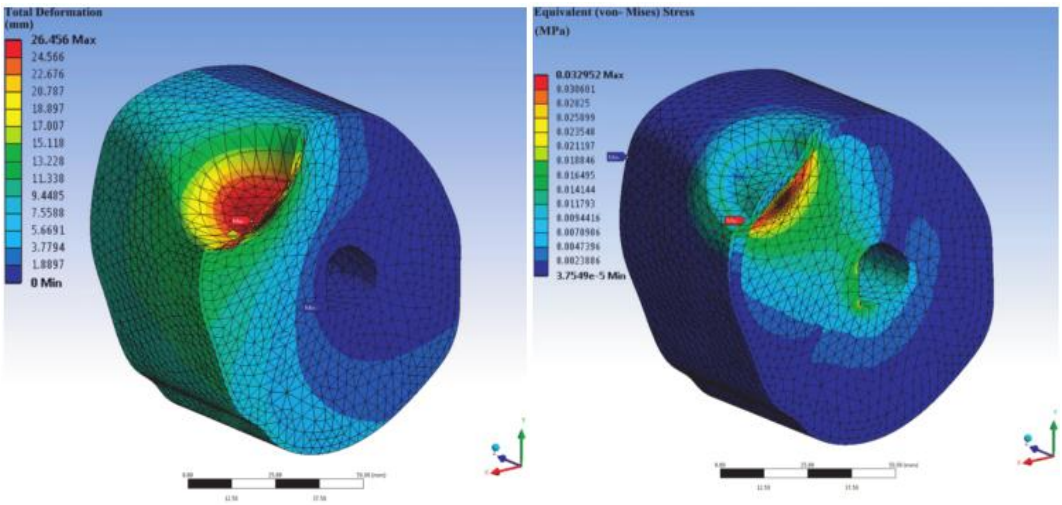

a. **b.**

Figure 3-3 Point of maximum deformation (a.) and respective stresses (b.) as seen in the model created by Huang et al., in 2012

The impact itself does not reflect a particular object, however if this could be altered within the model, it would be beneficial to forensic scientists in the understanding of how bruise formation occurs for different conditions.

Such models present potential for investigating stress response of tissues of larger magnitude without the dangers of testing human volunteers. This also provided a way of visualising internal response, which cannot be seen experimentally. However, without such models containing a more detailed map of vasculature and viscoelastic tissue character, predicting bruise occurrence and severity may not be accurate.

3.2 Visual interpretation of bruising

3.2.1 Electromagnetic spectrum

To recognise the problems associated with visibly interpreting bruising, an understanding of the basic principles of the human perception of light is required.

Like our hearing, our eyes work by detecting light waves. These waves move perpendicular to the direction of light and therefore explaining why a narrow beam of light will spread out from its source (Benson et al., 2008; Choudhury, 2014a). These waves are what our brains transform into what we perceive as sight. Our eyes can detect visible light, which is a small part of the wider electromagnetic spectrum (Choudhury, 2014b; de Mayo, 2015; Gibson, 1934; Rai and Kaur, 2013). There are no exact points for each part of the spectrum to begin and end, thus the different types can overlap (de Mayo, 2015; Gibson, 1934; Rai and Kaur, 2013).

3.2.2 Colour and colour perception

Visible light ranges from approximately 400-700 nm (Figure 3-4), representing different colours (Table 3-1), (Choudhury, 2014c; Kim et al., 2012; Pilling et al., 2010; Rai and Kaur, 2013). An object's colour is dictated by the ability of its surface to absorb all or some of the visible light which illuminates it (as shown in Figure 3-5). The wavelengths which are not absorbed but reflected back off the surface, are those

which the eye detect and perceive as a specific colour (Beeson and Mayer, 2008; Choudhury, 2014c).

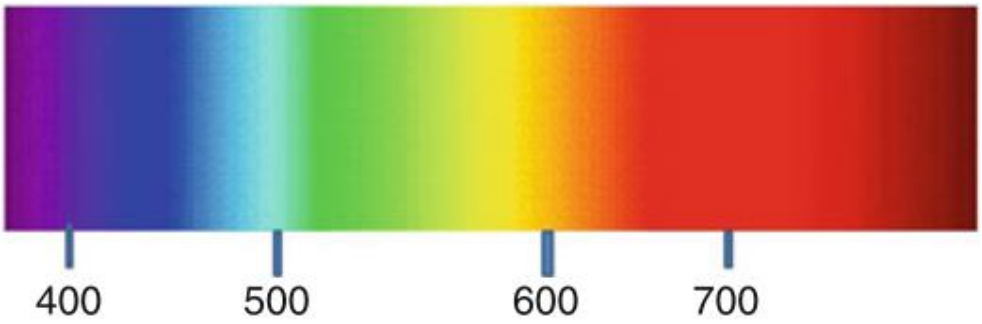

Figure 3-4 Spectrum of visible light (Rai and Kaur, 2013)

Table 3-1 List of colours and their associated wavelength range (Choudhury, 2014a; de Mayo, 2015; Rai and Kaur, 2013)

Colour	Wavelength (nm)
Violet	380 – 450
Blue	450 – 480
Blue/Green	480 – 510
Green	510 – 550
Yellow/Green	550 – 570
Yellow	570 – 590
Orange	590 – 630
Red	630 – 750

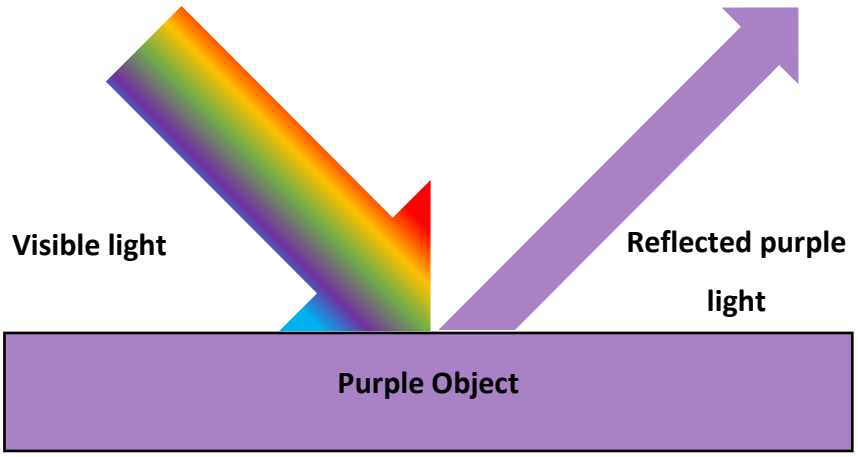

Figure 3-5 Visible light being directed onto a purple object, with only purple wavelengths being reflected off the object. Adapted from (Beeson and Mayer, 2008)

However, the specific colour detected it dictated by the eye's ability to detect and interpret these waves as colour, and so will vary in tone between observers

(Pilling et al., 2010). This is what makes colour perception itself a complex but inconsistent process, which can be generally categorised as normal, inherited defects or acquired defects (Gaudart and Pétrakian, 2005). It should be noted that in reality classification of vision is even more complicated (Gaudart and Pétrakian, 2005).

Although capable of detecting all colour wavelengths, the human eye is most sensitive to three primary colours – red, green and blue (RGB). For those considered to have normal vision, it is assumed there is no difference between them in their ability to perceive these colours (de Mayo, 2015; Georgieva et al., 2005a).

This assumption that we all perceive colour the same way is false however. Individuals, who are otherwise healthy may vary in their ability to detect colours (the example of yellow sensitivity is described in Section 3.2.3). Therefore, colour perception is very subjective, particularly as it is influenced by the lighting conditions of a particular environment and most importantly the individual's interpretation of the RGB signals which they are capable of detecting (Choudhury, 2014d; de Mayo, 2015; Georgieva et al., 2005a; Hughes and Langlois, 2011; Pilling et al., 2010).

In addition to the sensitivity variation between individuals, there are multiple factors which can further influence our colour perception. For example, inherited defects such as colour blindness or eye condition can inhibit the eyes ability to detect some or all colours (i.e. everything will be seen as either black or white) (de Mayo, 2015; Gaudart and Pétrakian, 2005). As for acquired defects which influence colour perception, the most common results from the ageing process (Gaudart and Pétrakian, 2005). Sustaining injury or intake of certain medications can also damage colour perception (Gaudart and Pétrakian, 2005).

Overall, colour perception an individual trait, hence what one person perceives will likely differ from another (Choudhury, 2014d; Pilling et al., 2010).

3.2.3 Visual perception of bruising

As colour perception differs between individuals, describing and aging bruising by visual analysis alone is not reliable (Harris and Flaherty, 2011; Hughes et al., 2004; Pilling et al., 2010). Several studies highlight the inconsistencies between

observer descriptions and how the level of experience in dealing with such injuries has no influence over description accuracy (Bariciak et al., 2003; Grossman et al., 2011; Munang et al., 2002).

One such study assessed observer variability by asking health professionals to describe a bruise whilst *in vivo* (excluding other factors such as swelling) and then again from a digital photograph at a later date (Munang et al., 2002). A total of 58 bruises were included in the study, assessed by nine nurses, four doctors and one medical student. The sample group was of caucasian children between the ages of 16 months and 14.25 years old. The majority of injuries documented were to the lower and upper limbs, with only four to the head and one bruise to the trunk. The results reported in the study seem to relate to only three observers (one doctor, nurse and medical student). In total, 174 inter-observer comparisons of the dominant colour described between doctor and nurse, doctor and medical student and nurse and medical student. When describing bruising in vivo, it was found that, out of 174, 47 observations were in complete agreement, 73 were in partial agreement and 54 were in complete disagreement between at least two observers. A total of 6 descriptions were in complete agreement between all three of the observers and in 30 of the 174 observation comparisons, yellow was described however, only on 14 occasions was this in agreement between observers. When assessing the bruises from photographs at a later date, the number of observations in complete agreement decreased to 41, partial agreement increased to 89 and those in disagreement decreased to 44. Yellow was observed on 52 occasions, with agreement on the presence of yellow in 16 cases. The number of descriptions between all three observers decreased to only 4 occasions. In only 1 instance was there complete agreement on the dominant colour present between all three observers both in vivo and from the photograph.

Another study investigated observer accuracy when assessing bruising in vivo, where other factors such as the presence of swelling or abrasions may influence opinion (Bariciak et al., 2003). Over a nine month period, children up to the age of 18 (mean age of 6.5 years old), who had obtained an accidental bruise took part in the study. A total of 42 bruises were used with known age, which ranged from 2 hours

up to 16 days old. Observers were categorised by their profession: emergency paediatricians, other physicians or trainees. The total number of bruises examined by each group was not consistent, with the emergency paediatricians examining all 42, physicians examining 17 and the trainees examining 38 bruises. A total of 13 bruises were observed by at least by one member of each group. For the study, each observer was asked to complete a standardised form detailing an estimated bruise age, presence of surrounding injury or swelling, bruise location, colours present and the factors which influenced estimation of bruise age. The results showed that for each group, the percentage of successful age estimation (within 24 hours) never exceeded 50 %. The emergency paediatricians showed the greatest accuracy of 47.6 %, trainees had an accuracy of 36.8 % and the other physicians had the lowest level of 29.4 %. There was no instance of an entire group agreeing on the colours which were present in any of the bruises.

Alternatively, a study specifically focused upon the accuracy of bruise interpretation by forensic experts (Grossman et al., 2011). A total of 23 experts participated in the study, recruited from one of three groups: qualified paramedics, clinicians and nurses; police and forensic medical examiners; members of the Essex Medical and Forensic Services. Bruises were assessed from photographs, where the observers were asked to complete a standardised form and also indicate which factors influenced their assessment (for example colours present and intensity, bruise size and swelling), ranking them in order of relevance. A total of 575 age estimations were made with only 4 being correct. Most of the results (320) were overestimates, with the rest (250) being underestimates. All observers stated that bruise colour was the basis for their age estimations.

All studies concluded that colour was the most important characteristic which participants based their findings on. With inconsistent observations, regardless of an individual's professional experience, it is clear that visual perception is not a reliable method of bruise estimation. It is generally accepted that of all the colours that can be observed in bruising, yellow is the most significant, as it indicates older bruises (> 48 hours) (Maguire et al., 2005).

Highlighting the variance in perception between individuals, research was conducted into the perception of the colour yellow specifically in bruises (Hughes et al., 2004). In this study, the effects of gender, colour vision impairment and age on yellow perception were assessed. They used a photograph of a fresh bruise (i.e. contained no yellow), and through the use of Photoshop, known levels of yellow were added to the bruise. An image of a bruise containing yellow was used as a reference, to ensure the digitally altered image appeared as realistic as possible. The levels of yellow added ranged from 0 % to 20 %, increasing in 2 % intervals. These images were then printed and shown, in order, to 52 observers aged between 21 and 53 years old. Each person was asked to indicate the image in which they first noticed the yellow colour. Their findings indicated that the threshold for yellow perception ranged between 4 % and 16 %, highlighting how inconsistent colour discrimination is by the human eye. They also found that gender had no effect on colour perception. Two subjects had a deficiency in their ability discriminate between red and green and as a result were able to perceive yellows at a lower threshold. Age was found to be an influential factor, with the threshold increasing by about 0.07 % each year, thus reinforcing how inappropriate visual analysis is of colour is and in turn, of bruising.

Assessing bruising based on colour alone is very subjective and with differences in skin tone influencing bruise appearance, it cannot be relied upon.

3.3 Photography of bruises

3.3.1 Colour photography

Photography is a vital tool within the forensic field, particularly when documenting injuries, including bruising, as visual data is unlikely to be disputed when presented as evidence in court (Özkalipci and Volpellier, 2010; Piva, 2013; Rai and Kaur, 2013). Generally speaking, physical injuries are photographed if they are relevant to serious crimes (for example rape, domestic violence or aggravated assault), but not cases of minor assault (Black, 2013a; personal communication). At the time of such serious crimes being reported, injuries can be temporarily photographed using an officer's camera phone before such time a scene of crime

officer is available to image injures to be part of official records (Black, 2013a; personal communication).

This type of photography is the standard method used to document all injuries. The problem, is that their interpretation is visual only and on what the interpreter sees as the most important characteristics of the bruise (Burgmüller et al., 2014; Gaudart and Pétrakian, 2005). They do capture the range of colours which may present however, colour photography is easily influenced by lighting conditions and reflection of light from the skin surface. This combined with the subjectivity of visual analysis makes colour photography unreliable and yet there is currently no appropriate alternative.s

3.3.2 Cross polarised photography

Cross polarised photography has been identified as a possible alternative to colour photography. It requires covering both light source and lens of the camera with filters, then taking images as you would for traditional colour photography (Witmer and Lebovitz, 2012). The use of linear polarisers blocks those waves which are not perpendicular to its surface (Benson et al., 2008). This is shown in Figure 3-6, where an unpolarised light beam passes through a filter (polariser 1), leaving only those waves in the plane aligned with the filter (i.e. the waves are only traveling in one direction) (Baker et al., 2013; Benson et al., 2008). For cross polarised photography, the filters covering the camera flash and lens are perpendicular (similar setup as shown by polariser 2 and 3). This restricts the volume of light reaching the camera lens and when combined with colour photography, unwanted reflections are removed and the depth of colour is enhanced (Benson et al., 2008; Hershberger, 2004; Witmer and Lebovitz, 2012).

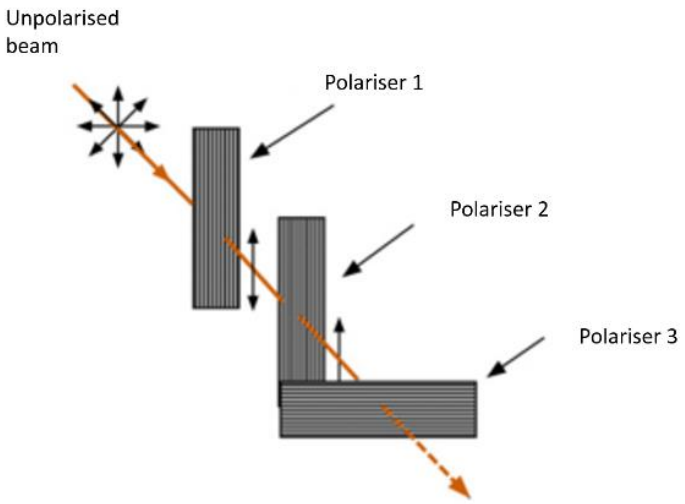

Figure 3-6 Light beam passing through polarising filters (Adapted from de Mayo, 2015)

Few studies have investigated the use of cross polarised light for bruise documentation and although it still generates images which would be subjectively interpreted, it has shown potential in imaging bruising in a more standardised and reliable manner (Baker et al., 2013).

3.3.3 IR photography

IR photography is one of the more common imaging techniques to have been investigated for bruise analysis. It has other uses in the forensic field such as analysis of questioned documents, bite marks and vein pattern analysis (Rai and Kaur, 2013). For imaging skin tissue the NIR (near infrared) wavelength range (700 – 1400 nm), can penetrate further into the skin (Cuper et al., 2013). Furthermore, the melanin which give skin its colour does not absorb as much IR as it does visible light, therefore the influence of skin tone on bruise visibility is reduced (Cuper et al., 2013; Mangold et al., 2013).

Deoxygenated blood has a unique property in that it absorbs NIR light. This allows it to be distinguished both from oxygenated blood and the skin which reflect NIR. As a result, superficial vein patterns can be identified and analysed as when imaged they appear darker than the surrounding tissue (Lingyu and Leedham, 2006; Shrotri et al., 2010; Strangman et al., 2002).

This same principle has been applied to bruising as in theory, the extravasated blood will absorb the light, causing the bruise to appear as a dark area (Rowan et al., 2010; Shrotri et al., 2010).

3.3.4 Photography techniques and bruising

Given there is no proven gold standard for bruise photography, there have been a few studies to directly assess different modalities and their influence on visual bruise assessment. Such studies tend to consider ultraviolet (UV), IR and standard colour photography (both standard and cross polarised). This is as the different wavelengths penetrate the skin to different lengths. Generally, UV light has a very low penetration, increasing with wavelength to the visible wavelengths. IR has the deepest penetration, hence its ability to enhance underlying vasculature (Figure 3-7).

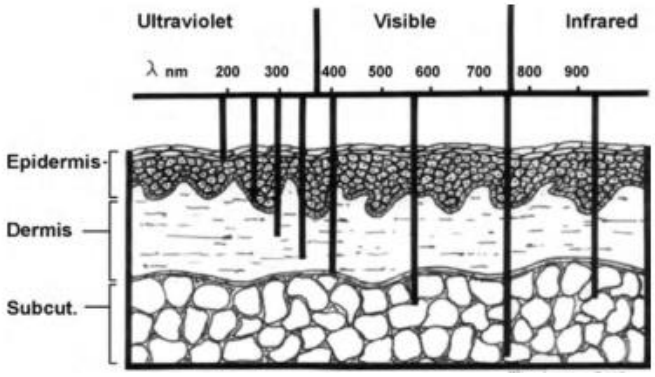

Figure 3-7 Penetration depths of UV, visible and IR light into skin (Wright and Golden, 2010)

When these four methods have been compared, it has been the finding that UV provided the least information. Although some studies have successfully used UV for identifying bruising (Rai and Kaur, 2013; Tetley, 2005), when compared to colour, CP and IR photography it is considered the least beneficial (Baker et al., 2013; Lawson et al., 2011).

Focusing on colour, CP and IR, the studies by Lawson et al. (2011), and Baker et al. (2013), both came to similar conclusions. Lawson et al., focused on determining the preferred photography technique of 9 paediatricians with child protection expertise, prior to commencing a larger study focused on bruise assessment. Four bruises were chosen from a 2 year old child with known bleeding disorder (i.e. the bruises were not purposefully made), from various locations on the body. Each was

photographed using five techniques: colour, colour (greyscale), IR and UV, generating a library of 20 images. Each paediatrician was asked to rank each image between 1 and 5, for the level of information is provided in terms of clarity of bruise border, shape and size. Their findings, although from a small sample, found that on average CP imagery was favoured by all observers, for all bruises. The other techniques were ranked in the order colour (greyscale), colour, IR and then UV. As for which method best represented the bruise colours, it was found that CP was best for the majority of assessments. However, colour photography was selected as the favoured technique for one of the bruises. Even so, this indicates that CP is of greater value to bruise analysis than colour, even with subjective interpretation. Although ranked below 3 of the 5 techniques, IR was also found to provide some useful information. Unfortunately, it was concluded that like colour photography, it was influenced by the reflected light from the skin – even though it was to a smaller extent. Given their findings, Lawson et al., went on to continue their work using CP photography.

Baker et al., also investigated colour, CP, IR and UV photography (finding UV to be of limited use). Their study involved visually assessing 75 bruises and scoring them based on bruise visibility and the measured contrast between bruise and non-bruised tissues (using Photoshop). For their assessment, the bruises were split based on their causation: 32 by recreational paintballing (images 1-3, 4-7 and 8-10 days post impact), 43 by accidental impacts. Individuals were also split based on their skin tone: 1 being pale skin, 2 for fair asian/tanned caucasian skin and 3 for dark asian or black skin tones. They found that in general, bruises would tend to increase in contrast before they began to fade and like Lawson et al., colour and CP images provided the greatest contrast, followed by IR photography. Excluding UV, colour and CP were significantly better at capturing bruising than IR, both having the highest contrast for all bruises. IR imaging did however appear to eliminate the effect of darker skin tones masking the appearance of bruising. However, their study also indicated that IR was not ideal for imaging faded bruising, suggesting that alternative imaging methods could be better suited. Overall, the concluded that CP scored highest for visual interpretation, i.e. bruises appeared larger with bolder colours.

Both these studies indicate that CP photography colour be a more beneficial tool in bruise documentation as it enhances colour, removes reflections and thus makes visual interpretation somewhat more reliable than with conventional colour photography. They do acknowledge the lighting conditions can cause problems and Baker et al., does comment on how darker skin tones reduced contrast between bruised and non-bruised tissue. However, they also imply that IR imaging is not particularly of use in comparison, contrary to some published work.

Published in 2013, a study by Bernstein et al., (2013) discussed IR imaging research carried out in 1986. A total of 28 injuries (fresh non-lacerated contusions and/or abrasions), were imaged from 9 victims of traumatic death. At the time, these images were taken using a film camera and appropriate lighting. Results found the IR imaging improved visibility of bruising, neutralising the effects of discolouration caused by lividity and also skin colour. Therefore, IR shows promise in allowing fair bruise analysis, out with the influence of skin tone, where the darkest skins can conceal the extent of injury and the lightest skin tones can make it appear much more severe.

In a study from 2010, digital IR photography was used with sunlight as the light source to identify bruising when no longer visible to the naked eye. Bruising were imaged on 10 healthy adult volunteers however, IR imaging managed to only detect 1 bruise when it appeared to be no longer visible (Rowan et al., 2010). The lack of positive results is thought to be due to their use of sunlight that a more reliable IR light source would improve the quality of results. Although they only obtained one positive result, their findings combined with those of Bernstein, Nichols and Blair in 2013, highlight the potential for the use of IR photography.

In summary colour, CP and IR imaging techniques are the most readily available for documenting bruising and yet, given all its faults, colour photography is used without question while CP photography could provide more reliable images. Although the ability of IR photography to detect non-visible bruising may be limited, when assessing at the causation of bruising, the level of bleeding which IR can detect could be of significant benefit.

3.3.5 Possible imaging alternatives

The following methods could be used as alternatives to the conventional photography techniques described above. However, each were deemed inappropriate for use in this research as the aim was to focus on readily available techniques already in use within forensic investigations.

3.3.5.1 Alternate light source

A potential alternative to the photography techniques which are assessed in this research, could be the use of an alternate light source, commonly referred to as an ALS. Unlike colour and CP photography which make use of the full visible spectrum, ALS can switch between specific ranges of wavelengths such as red or violet light (Lombardi et al., 2015). It is used within forensic investigations where detection of bodily fluids is required, as it causes them to fluoresce or where bruising is concerned, enhance the contrast from non-bruised skin (Lee and Khoo, 2010).

A simple, non-invasive method, ALS has shown success (Limmen et al., 2013; Lombardi et al., 2015; Olds et al., 2017, 2016a), however there are some problems with its use. All conclude that ALS can detect bruising, with the violet and blue wavelengths providing the greatest contrast (see Figure 3-8). Lombardi et al., (2015), found like all imaging techniques, that the ability of ALS imaging to detect older bruising was limited compared to younger bruising while Limmen et al., (2013), showed that what they had observed was in fact a bruise, by pressing the location to see if there was sensitivity compared to the surrounding areas. Therefore, there is a potential for false positives to occur, thus optimisation of methodology is required (Olds et al., 2016b).

Recent studies have aimed to address the problem of false positives (namely Olds et al., 2017, 2016a), by combining ALS imaging with histological analysis on both porcine and cadaver models. Their work confirmed that what ALS photography detected was in fact bruising and that not only did it detect, but also enhanced the size of bruising compared to colour photography (Olds et al., 2017, 2016a). Unfortunately, the false positives observed in earlier studies could not be removed

and they concluded that not only melanin within the skin, but also traces of sunscreen on the skin surface can be responsible for the false positives (Olds et al., 2016a). Therefore, ALS cannot be said to be a bruise specific method and has not been found to provide any extra information which can be used to age bruising (Hughes et al., 2006).

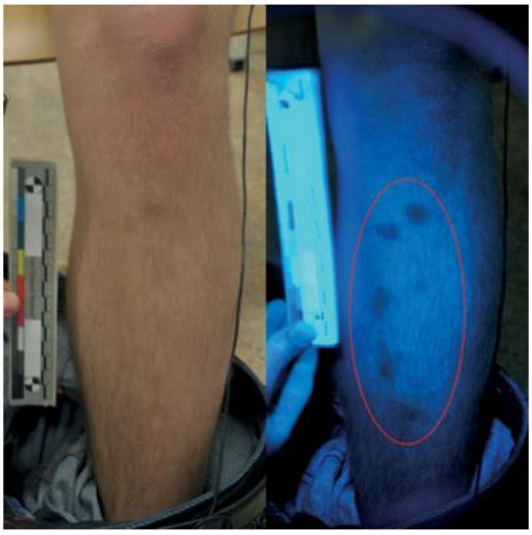

Figure 3-8 Example of the ability of ALS (violet wavelength), to detect bruising not clearly visible to the naked eye (Limmen et al., 2013)

3.3.5.2 Ultrasound

Ultrasound has been considered as an alternative method of documenting bruising as it can be used to characterise skin thickness (Kong et al., 2008; Quan et al., 1997; Randeberg et al., 2007). Therefore, to consider its use in characterising dermal/subcutaneous bruising is logical, as it could provide a more detailed observation of bruise depth and size. Such a method provides advantages in that it is non-invasive and is a widely available piece of medical equipment (Helm et al., 2016; Mimasaka et al., 2012). However, whether it can be used to provide a clear image of a bruise and in turn bruise size and possibly bruise age, is not fully understood.

Although the use of ultrasound to assess muscular bruising has become more common, the use of such technology for dermal and/or subcutaneous bruising has yet to be fully developed. This is largely due to a lack of published work supporting its use within this context, with studies by Helm et al., (2016) and Mimasaka et al., (2012), being the only ones known to the author.

Both studies ultimately came to the same conclusion that ultrasound has something to offer in the documenting of bruising which photography alone cannot offer: depth below skin surface and height of bruising. However, there is a lack of correlation between ultrasound results and that seen on individuals. For Mimasaka et al., they considered both bruises observed during autopsy (n = 10), and on living children (n = 16). Their approach had the advantage that they could compare ultrasound results to the bruise itself through histological analysis (for autopsy results), thus showing that ultrasound represented the bruising. For the bruising on living participants, they found that the height of bruise reduced with time, with its depth relative to skin surface remaining relatively consistent. This therefore highlighted a method of imaging bruising, providing more beneficial information which could be used to infer impact severity. It should be noted, that this study failed to link the internal bruise dimensions with those observed on the skin surface.

This failure was the focus of the study by Helm et al., in 2016. Colour photography, although the standard method of documenting bruising; inferring bruise extent and likely mechanism of impact, provides no information on the bruising within the tissue itself. If ultrasound results could be linked to that seen in photography, then this would provide a robust method for fully characterising bruising and therefore a more likely determination of severity and mechanism of formation.

Helm et al. (2016), studied 22 bruises from 18 participants and concluded that there was no correlation between ultrasound measurements and the size of bruising observed on the skin surface. Given the findings of Mimasaka et al., this emphasised the inaccuracies in current bruise analysis and how accurate representation of the extent of bruising present is not possible. With other photography methods being more likely to produce an image representative of bruising, there could be potential for linking it with ultrasound.

However, it should be noted that their conclusion was reached by combining both positive (bruise visible), and negative (no-visible bruise), ultrasound results, assuming a negative result was a bruise with a depth of zero. Negative results

accounted for nearly half of the bruises studied (10/22) and were older on average (approximately 120 hours compared to 17 hours old for negative and positive results respectively). However, for positive results (specifically bruising 48 hours old or younger), there was a correlation observed between bruise area and the ultrasound measured height. This indicated that ultrasound investigation may be more suited to early assessment and not for older bruising. Therefore, to use ultrasound successfully in documenting bruising, much greater research would be required.

3.3.5.3 Magnetic resonance imaging

Magnetic resonance imaging (MRI), has also been considered in the imaging of bruising, like many other studies with the aim to age such injuries. The concept behind this approach was that during intracranial scans, MRI had been shown to detect haemoserdin (blood component found within a healing bruise), thus in theory, if detected during whole body scans could identify and/or age bruising (Langlois et al., 2013). The two studies known to have investigated this (Langlois et al., 2013; Sherman et al., 2003), simulated bruising by either injecting blood under the skin of rats or delivering blunt impacts directly to rats. In the study by Sherman et al., (2003), it was proven that MRI could successfully identify bruising while the study by Langlois et al., (2013), successfully imaged bruising at various times post injection and corroborated 'bruise' presence and healing with histology.

At the moment MRI has greater potential in identifying and diagnosing bone bruising (Blankenbaker et al., 2008; Boks et al., 2007; Rangger et al., 1998) which unfortunately means the focus of MRI research is not to minor bruising. However, if this was taken further, MRI could be a non-invasive method of bruise identification and possibly ageing.

3.3.5.4 Thermal imaging

The use of IR thermal imaging to identify bruising is currently a common research area within the food industry, where the aim is to identify and/or prevent damaged produce reaching the consumer. This research area considers many of the

same techniques which more biological fields use for bruising, however thermal imaging is less common outwith the food injury.

Thermal imaging, like all other imaging methods, is non-invasive, requires no additional illumination and employs the use of IR light, but at higher wavelengths than that used for standard IR photography. For fruits such as apples, tomatoes or pears, thermal imaging has proven successful in identifying bruised areas (Baranowski et al., 2012; Kim et al., 2014; R. Vadivambal, 2014; Varith et al., 2003).

Such imaging has been considered for sporting injuries such and bone fracture or ligament damage (Hildebrandt et al., 2010), unfortunately this does not seem to have been explored within the context of subcutaneous bruising. There has also been limited use within the veterinary field for detecting equine injury (Gade and Moeslund, 2014). However, it has been reported that thermal imaging can detect bruising, as bruised tissue exhibits different thermal properties when compared to the surrounding tissue (Gade and Moeslund, 2014). Therefore, this should also be considered as a possible imaging alternative, as the thermal properties will change throughout the healing process and thus not only identify bruising, but potentially a thermal timeline for the healing process.

3.4 Improving bruise assessment

When investigating in more detail the alternatives to identifying colours and aging bruises, colour models appear to be the most successful overall. The simplest alternative has suggested using a colour scale as a visual comparison tool (Figure 3-9) (Nuzzolese and Di Vella, 2012; Pilling et al., 2010). This did not remove subjectivity, but aimed to provide observers with a standardised reference to relate their interpretation to, therefore limiting inter-observer variability. Unfortunately, although a simple idea, subjectivity and variability remained and furthermore, failed to consider darker skin tones (they only looked at caucasian skin).

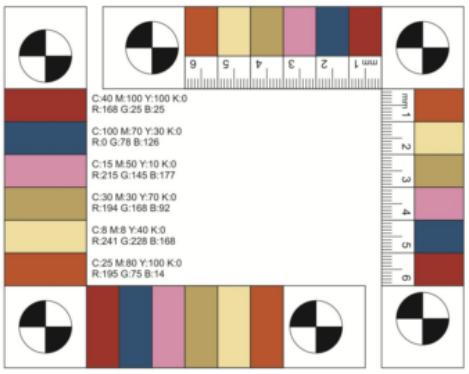

Figure 3-9 Example of a standardised colourimetric scales (Nuzzolese and Di Vella, 2012)

An alternative to a reference colour chart, is to use a colour reference chart to standardise images. A couple of studies have done this (Grossman et al., 2011; Lawson et al., 2011), and although they altered the colour levels within an image, it enhanced them all to the same level. This improved interpretation by removing variances in lighting. However, if a visual assessment is made, the problem still remains. This led to the approach of measuring the colour levels of an image once standardised, which has demonstrated greater promise.

3.4.1 Colour models

3.4.1.1 RBG, HSV and L*a*b*

In an attempt to remove subjectivity, an alternative approach to visually interpreting bruising has been to make use of colour measurements via computer software such as Photoshop. There are different colour value systems which have been used to measure bruise colours in a standardised manner. The RGB system, commonly used in televisions and computer screens, represents each of the three colours capable of being detected by the human eye present as a ratio, scaled between the numbers 0 and 255 (Georgieva et al., 2005a; Hughes and Langlois, 2011).

The HSV, HSB or HSI model defines colour in three components, hue, saturation and value/brightness/intensity (Georgieva et al., 2005a; Langlois, 2007). Hue refers to the type of colour present, i.e. yellow, green, red, magenta, blue or cyan, and can range from 0 degrees to 360 degrees (Georgieva et al., 2005a). Saturation reflects the intensity of the hue present and can range from 0 % to 100 %

(Georgieva et al., 2005a). Value related to the brightness of the colour being measured and again can range from 0 % to 100 % (Georgieva et al., 2005a).

Another model is the L*a*b* colour model. This model was specifically produced to specifically reflect the wavelength range detected by the eye and thus measure colour differences (Langlois, 2007). The L* value refers to the brightness or luminosity (negative values being dark, positive being light), a* refers to the level of green and red (negative being green, positive being red), and b* refers to the level of blue and yellow (negative being blue, positive being yellow) (Hughes and Langlois, 2011; Langlois, 2007).

3.4.2 Colour models and bruising

As visual perception of bruising is subjective by nature, several studies have attempted to use colour models to describe such injuries in more definitive terms and investigate if there is any consistency in colour levels observed between people.

The RGB model is the most common to have been used, and has shown some limited success when assessing digital images of bruising. A relationship between the RGB components of bruising over time have been previously identified (Black, 2013b; Georgieva et al., 2005b; Grossman et al., 2011), however these could not be applied to entire populations, with the strongest correlations only being visible between bruises intra-personally only (Black, 2013b; Grossman et al., 2011). Both Grossman et al. and Black reported little correlation between any colour patterns.

Difficulties have been found using the RGB colour model, in that it appears to be influenced by the level of image standardisation performed and skin tone (Black, 2013b; Grossman et al., 2011). Furthermore, the RGB model was found to be difficult to use when trying to distinguish between various shades on a set colour (Georgieva et al., 2005a). Despite the problems with the use of RGB model, it does show some potential for future use if appropriate methodology for image photography and standardisation can be developed.

The HSV colour model is only known to have been used once in the assessment of bruising. It was found to have the same level of success as the RGB

model used within the same study, although being most useful in measuring the set colours already known to be found in traumatic injuries (Georgieva et al., 2005a).

The L*a*b* model has shown more success identifying patterns between individuals. Studies carried out in 2010, 2012 and subsequently 2016 and 2013 all found that measurements for each part of the colour model followed a similar pattern across participants (Mimasaka et al., 2010; Scafide et al., 2016; Scafide, 2012; Thavarajah et al., 2012; Yajima et al., 2003; Yajima and Funayama, 2006). Furthermore, one of these studies (Thavarajah et al., 2012), was specifically focussed on dark-skinned individuals and Scafide et al., acknowledged that this particular approach does not appear to be influenced by skin tone. Each similar pattern is shown in Figure 3-10.

The findings of each of these studies would be expected, as bruises lighten as they fade, whilst becoming more green and yellow and the blood is broken down and the injury heals. However, each case has involved the use of a colourimeter or spectrophotometer to measure the colours directly from the skin. Given that photography is standard for documenting bruising, if the measurements could be made via computer software, then these measurements could be carried out with no need for extra equipment.

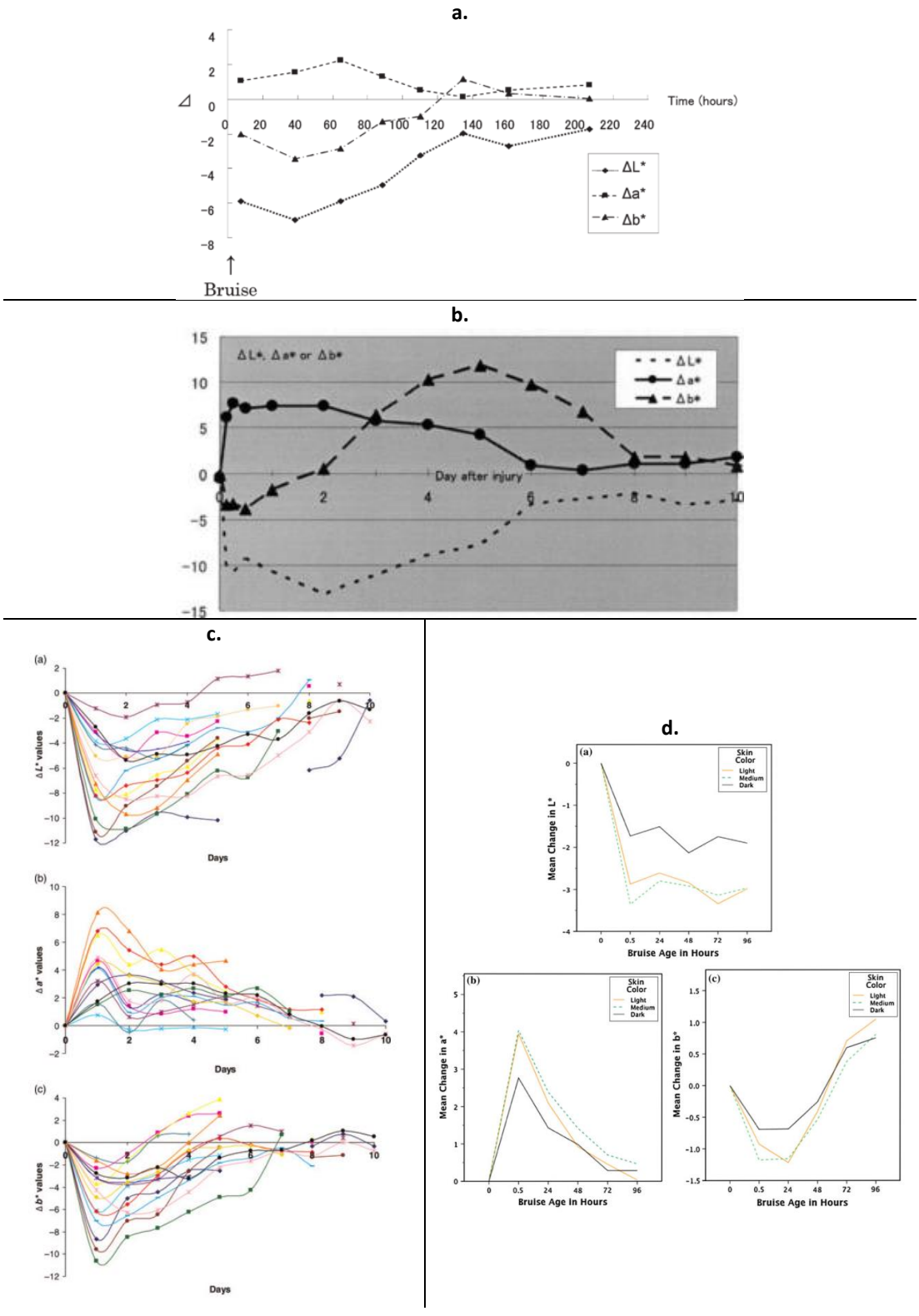

*Figure 3-10 Examples of similar L*a*b* colour patterns measured from bruises a. Mimasaka et al., 2010, pattern from one subject b. Yajima et al., 2003, pattern from one subject c. Thavarajah et al., 2012, patterns from each subject d. Scafide et al., 2013, average patterns of all subjects categorised by skin tone*

Chapter 4

Methodology Development

4.1 Experimental justification

The overall approach of blunt impact research in investigating whether force generates injury is not entirely wrong, as it does provide valuable information on impact tolerances. However, whether a specific level of force generates the same severity of injury for an entire population, is never considered. Furthermore, knowledge of the mechanics involved during the soft tissue response, could go a long way to explaining how the commonly seen variances between people occur, rather than being treated as just a natural phenomenon as is the case within the biological view of bruising.

The incomplete picture of how the mechanics of an impact generate bruising combined with the inaccuracies surrounding bruise photography and subsequent visual analysis, makes their use as evidence unreliable. Therefore, to gain a greater understanding of bruising this study:

1. Characterised bruising mechanics using a controlled method of blunt impact generation.
2. Assessed the suitability of colour, cross polarised and infrared photography techniques for imaging bruising.
3. Investigated the use of a colour model for pattern identification within a healing bruise.
4. Determined if the information extracted from each image type can be statistically associated with the bruising mechanics.

This research also aimed to propose a theory explaining how soft tissue deformation caused vessel rupture within the context of the methodology carried out. By taking into consideration individuals themselves (e.g. BMI, gender and age), it was hypothesised that a quantifiable link between an individual and the bruising they sustain would be identified. This would in turn provide a greater understanding of how the human body itself influences its own injury potential and protective efficacy.

4.2 Blunt impact generation

4.2.1 Bruises in research

Generally speaking, studies which focus on bruising tend to avoid purposefully generating such injuries, i.e. using animal models or individuals already bruised. As human participants are more appropriate for this area of research, it is common to recruit volunteers from places such as a nursery, a hospital accident and emergency department or after a sporting event (Baker et al., 2013; Kim et al., 2012; Mimasaka et al., 2010). However, in this approach the exact circumstances which initiated bruising is unknown. Therefore, the best approach to investigate the mechanics of bruise formation, is to initiate bruising under controlled conditions.

To date, there have been several different approaches to this, the first of which involved using a vacuum. When this method has been used, a vacuum pump has been held against the skin of the upper arm and held in place for either 10 or 15 minutes to generate a bruise (Grossman et al., 2011; Pilling et al., 2010). Although a simple method of bruise generation, it does not replicate a blunt impact, where applied forces are sudden, e.g. impacts from either a hand or foot in karate last approximately 5 to 20 milliseconds (Randeberg et al., 2007).

An alternative is the use of a drop mass system, (Black, 2013b; Desmoulin and Anderson, 2011). One particular study involved a single participant being subject to six 1.9kg mass and six 2.6kg mass impacts at various locations on their legs from unknown heights (Desmoulin and Anderson, 2011), while another involved 5 participants subject to impacts from a 3 kg mass from heights of 3, 4 and 5 cm (Black, 2013b). Both studies generated a force profile for each impact, from which mechanical parameters including pressure, tissue stiffness and absorbed energy could be inferred and any relationship between the parameters and bruise formation could be determined. The studies indicated that where tissue was the stiffest, there was a greater chance of bruise formation however, both studies involved a limited number of participants. It is unknown if Desmoulin's study had any issues with the drop mass system, but it was not ideal within Black's study. The drop mass system

was found to be unreliable, with drop heights unable to be kept consistent. Impact times of approximately 30-60 ms were recorded however, once the initial impact occurred, the mass came to rest on the arm until removed. This mass could not be removed fast enough to replicate a sudden blunt impact, so although a drop mass system is more realistic than using a vacuum, it is still not representative of a true blunt impact.

An alternative is to use a projectile based system. Examples within published work include a tennis ball machine (Hawkins, 2014) or more commonly, a paintball marker. In paintball tournaments, markers are used to fire paintballs at other players. Although a type of air weapon, these markers are classed as low powered and non-fatal, therefore no licence is required for their use. The most common injury seen from their use is bruising hence being ideal for studies investigating bruising.

Although easy to use, not all studies have specifically used paintball markers to generate bruises, i.e. they may recruit volunteers after they have been paintballing rather than recruiting people to be shot with a paintball. In terms of their reliability they are often considered inconsistent, however the extent of this inconsistency has yet to be proven. Few of the studies which have deemed a paintball marker suitable for blunt impact generation provide evidence on firing velocity, firing distance or repeatability. Therefore, there is a need for the use of a paintball marker to be validated prior to its use as a method of blunt impact generation.

Of 11 studies currently known to use bruising initiated via paintballs, only 4 provide information on firing velocity and 6 on firing distance. Not all studies used human volunteers, instead using porcine models (animals anesthetised for impact, sacrificed for analysis). Although the use of a porcine model could be useful, as it does not directly relate to bruising on human beings, their use is would be inappropriate for this research. The number of volunteers has ranged from 1 to 122 across the studies. A full list of the details provided in each study is shown in Table 4-1.

Table 4-1 List of studies which investigate bruising resulting from paintballing

UK Legal Requirements: Firing velocity should range between 76 – 85 ms^{-1}. Must not exceed 91 ms^{-1}.						
Author	Firing Distance (m)	Firing Velocity (ms^{-1})	Nature of Participants	Bruising Origin	Impact Location (s)	No. of Participants
Aboutalebi & Stetson, 2005	*	*	Human volunteers	Injuries sustained prior to study	Trunk	2
Randeberg, Baarstad, Løke, Kaspersen, & Svaasand, 2006	5	*	Human volunteers	Shot as part of study	Forearm	1
Ambay & Stratman, 2007	*	*	Human volunteers	Injuries sustained prior to study	Shoulder, back, chest and arm	2
Gundersen, 2007	*	*	Human volunteers	Injuries sustained prior to study	Elbow	2
	*	*	Porcine model	*	*	1
Randeberg et al., 2007	0.5	104	Porcine model	Shot as part of study	Shoulder and hip	-
Winnem et al., 2007	0.15 – 0.5	89	Porcine model	Shot as part of study	Hip, shoulder and chest	-
Randeberg, Larsen, & Svaasand, 2010	0.5	104	Porcine model	Shot as part of study	Shoulder and hip	-
Randeberg & Hernandez-Palacios, 2012	10	*	Human volunteers	Shot as part of study	Underarm	3
Randeberg & Hernandez-Palacios, 2012a	*	*	Human volunteers	*	Underarm	*
Baker, Marsh, & Quinones, 2013	*	*	Human volunteers	Injuries sustained prior to study	Variety of locations	16
Scafide, Sheridan, Campbell, Deleon, & Hayat, 2013	6.1	67	Human volunteers	Shot as part of study	Arm	122

Of the studies mentioned, only one author is known to have tested marker velocity at various distances prior to testing on volunteers (Scafide, 2012). As part of

their work, they used a high speed camera to record paintballs at distances of 15, 20, 25 and 30 ft (4.5, 6.1, 7.6 and 9.1 m respectively), with 3 shots being fired for each distance. They found that at distances of 20 ft, paintball velocity was around 220 fts^{-1} (67 ms^{-1}). The results for all distances is not stated, but they do state that they then used this firing distance during their investigations as it had slower velocities that at closer distances and had higher accuracy than the larger distances (Scafide, 2012; Scafide et al., 2013).

To investigate the mechanics of bruise formation, a paintball marker could be used to generate bruising on volunteers, with impacts being recorded so impact and bruise formation mechanics can be calculated. However, none of the reviewed studies have discussed the repeatability or accuracy of paintball markers in any detail. Therefore, appropriate firing conditions would have to be pre-determined before it could be used on human volunteers.

4.3 Paintball marker characterisation

4.3.1 Paintball

The Nelson Paint Company in the US was first to develop paintball in the 1970's as a method of marking objects within the ranching and forestry industries (Force, 2014; Paintball, 2014; Sbicca and Hatch, 2012). In 1981, paintball became a war-like sport and has since grown in popularity, played at designated sites worldwide (Force, 2014; Paintball, 2014). The sport uses a gas operated gun, filled with either carbon dioxide or air. This fires paint filled capsules or reusable rubber balls at other players (Force, 2014).

4.3.2 Paintball markers

Paintball markers are a type of air weapon. This class of weapon is defined as those which propel a chosen projectile through the use of compressed air or gas (Ceylan et al., 2002). The majority of air weapons are high velocity (exceeding 300 fps, approximately 91 ms^{-1}), with sustained injuries from such weapons being serious or fatal (Ceylan et al., 2002). The UK is known for having some of the strictest laws

surrounding air weapons and firearms. Yet, air weapons are the least controlled as licencing is not always required. The paintball marker is one such weapon which requires no licence and is readily available to buy. It should be noted that although their purchase and use is not tightly regulated, they are low velocity air weapons (fire below 91 ms^{-1}), so are considered to be less likely to produce serious or fatal injuries (Ceylan et al., 2002).

Paintball markers can be electronic or mechanical, automatic, semi-automatic or pump action. In the UK, since 2001, the United Kingdom Paintball Sports Federation will only recognise semi-automatic markers for tournament play and other events, thus making it the most readily available marker type. This study makes use of a mechanical, semi-automatic paintball marker. Unlike electronic markers, where the firing mechanism requires a battery to operate the marker's internal components, this type of marker operates through a series of mechanical processes initiated once the trigger is pulled (Muhlestein, 2014).

A paintball marker consists of three principal components – propellant gas, the hopper (paintball holder) and the gun itself (the trigger, barrel etc.) (Rodriguez, 2014). The firing mechanism is found primarily within the barrel and consists of the bolt, spring, hammer, sear, valve tube, valve and gas inlet (Rodriguez, 2014). The bolt and hammer and connected by a linking arm (Odin, 2010; Sosta, 2014), which allows them to move forward and back together. The hammer is powered by a drive spring and is held in place, prior to firing, by the sear (Odin, 2010; Rodriguez, 2014; Sosta, 2014). The valve and valve tube are the components which direct and store the gas prior and during firing (Figure 4-1and Figure 4-2) (Odin, 2010; Rodriguez, 2014; Sosta, 2014).

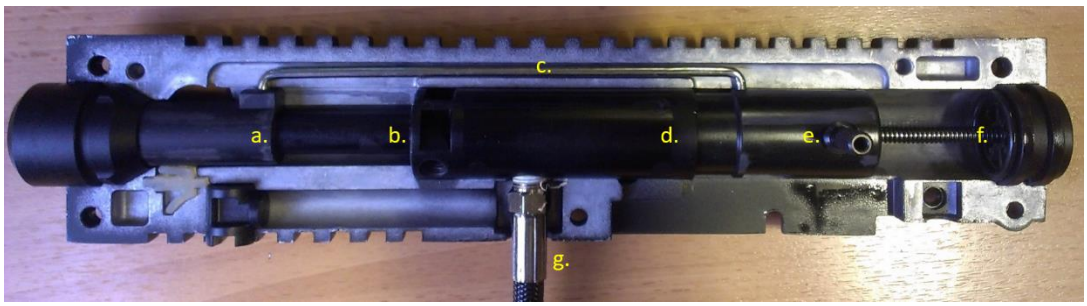

Figure 4-1 Interior components of the firing mechanism: a. bolt b. valve tube c. linking arm d. valve e. hammer f. drive spring g. gas inlet

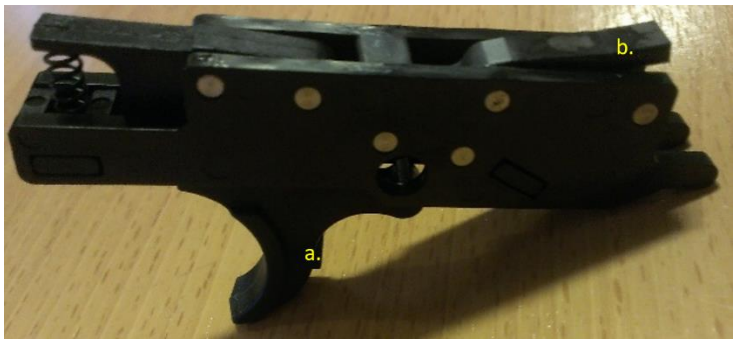

Figure 4-2 Trigger component: a. trigger b. sear

Initially, as part of marker set up, the shooter will manually pull back the bolt causing a paintball to fall from the hopper into the back of the barrel (Rodriguez, 2014). This also causes the hammer to move back, compressing the drive spring and the sear, located underneath the hammer, locks it into place (Odin, 2010; Rodriguez, 2014; Sosta, 2014). At this point, the marker is ready to fire (Figure 4-3).

Figure 4-3 Internal components when marker ready to fire: hammer (a) locked into place by the sear (b), compressing drive spring. Arrow indicates where the ball enters the back of the barrel (c)

When the trigger is pulled, the sear releases the hammer (Odin, 2010; Rodriguez, 2014; Sosta, 2014; UPT, 2014). The drive spring moves the hammer-bolt assembly forwards, coming into contact with the valve pin (Odin, 2010; Sosta, 2014;

UPT, 2014). This pin is what seals the valve containing the propellant gas (Figure 4-4) (Odin, 2010; Sosta, 2014).

Figure 4-4 Internal components during firing: a. hammer comes into contact with valve pin, releasing air down the valve tube b. side view of valve pin

At the same time, the bolt moves forwards, pushing the paintball into the barrel (Odin, 2010; Rodriguez, 2014; Sosta, 2014). As the hammer pushes the plunger, the valve is opened causing propellant gas to enter the valve tube (Odin, 2010; Sosta, 2014). This gas travels though the tube towards the bolt ultimately firing the paintball (Odin, 2010; Rodriguez, 2014; Sosta, 2014; UPT, 2014). In semi-automatic markers, some gas, termed blow-back gas, pushes against the hammer moving it backwards (Odin, 2010; Rodriguez, 2014; Sosta, 2014). This causes the pin to move back sealing the valve and blocking the gas supply (Odin, 2010; Sosta, 2014). The hammer continues to move back to its original position, compressing the drive spring and is locked back into place by the sear (Odin, 2010; Sosta, 2014). As this happens, the bolt moves back allowing another paintball to enter into the barrel, completing marker reset (Odin, 2010; Rodriguez, 2014; Sosta, 2014; UPT, 2014).

Marker velocity often needs to be adjusted. This is done through turning a screw located in front of the valve (Sosta, 2014). Turning this screw results in the volume of gas which can be released from the valve either being increased or decreased, altering paintball velocity (Sosta, 2014). However, through general use

this screw can loosen, altering the velocity setting, hence regular checks being required.

4.3.3 Chronograph

The CED M2 chronograph which was used to record firing velocity, works by calculating velocity based on the time taken for a projectile to pass over 2 sensors positioned at a set distance from each other (26 inches for the CED M2). In this case the IR screens were used to ensure that a consistent and equal level of light flooded each sensor (Dynamics, 2014).

There is no published data on the accuracy of this chronograph compared to other chronographs or instrumentation. However, the company do state that it has a 99.95 % accuracy rate when use with IR screens and that this was calculated during laboratory testing. Chronographs are not instruments which can be calibrated prior to use as they are reliant on the sensitivity of their components (Hardy, 2017). Chronographs themselves are the most common method of measuring projectile velocity and therefore it is considered the 'gold standard' within this research. Standard operating procedures for both the paintball marker and the chronograph can be found in Appendix A.

4.3.4 Experimental methods

As previously stated where studies have used a paintball marker for blunt impact generation, the repeatability and accuracy of their use is never discussed in any detail.

To assess these marker characteristics marker firing velocity and impact locations were recorded through use of the aforementioned chronograph and a purpose made target respectively. Results were then used to determine appropriate firing conditions which could be used for impacts to volunteers.

Statistical analysis (descriptive statistics and ANOVA), were performed using Microsoft Excel. Unless stated otherwise, a 5% significance level was used.

4.3.4.1 Repeatability and reliability

The paintball marker was secured within a purpose built table mount (University of Strathclyde, UK) behind the chronograph (Figure 4-5). The paintball marker was then fired repeatedly (using reusable paintballs (Just Paintball, UK), 1.6 cm diameter), until the air cylinder was almost empty (allowing safe dismantlement of the marker and prevention of damage to the cylinder). The velocity of each shot was recorded using the chronograph and the aim was to consistently fire approximately 74 ms^{-1}, as recommended by the marker supplier. This procedure was then repeated a further 5 times.

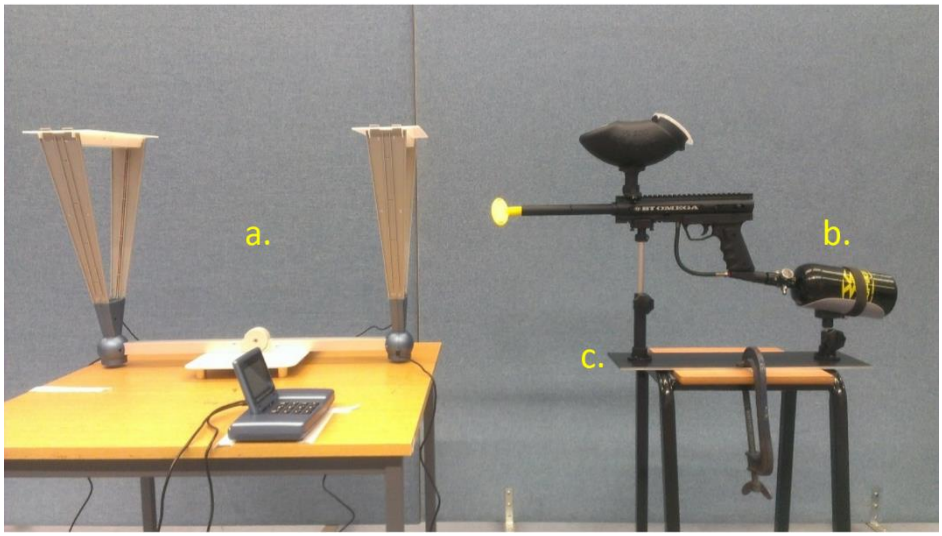

Figure 4-5 Experimental set up: a. chronograph b. paintball marker c. table mount

4.3.4.2 Accuracy and precision

Using the same experimental set up as used in Section 4.2.4.1, a target was placed at distances of 4, 5, 6, 7 and 8 m. Although future work is unlikely to occur as close as 4 or as far as 8 m, these distances were included to give a greater understanding of marker accuracy. The target was made by placing carbon paper between A4 pieces of paper. This target was later changed to card (still using carbon paper), as a more robust impacting surface.

Using a full cylinder of air, a total of 10 shots were fired at the target, firstly at the 8 m distance. The target was then moved closer by 1 m then another 10 shots

fired. This was repeated down to the 4 m distance. After this, the target was moved back to 8 m and the whole process was repeated. This accuracy test was then repeated for a second time on a different day. A total of 20 accuracy tests (4 at each distance) were performed, with a total of 200 shots being fired. A new target was used for each test. A laser pointer (RS Components, UK), was attached to the marker barrel via a purpose built clamp (University of Strathclyde, UK). This was used to mark on the target where the marker was aiming, whilst also providing a point of reference when assessing the spread of impacts.

4.3.5 Results

Overall, the marker was found to be easy to use and control, with the experimental set up allowing the marker to be easily moved and secured when required. The use of the table mount also prevented any sudden movement during testing, ensuring safety and reducing the likelihood of the air cylinder becoming loose. With the marker itself allowing for velocity adjustment, it was found to be a versatile piece of equipment.

However, there are some minor drawbacks with the air cylinder which should be noted. It was not able to be pressurised to exactly the same level for each test, with total levels ranging between approximately 2,600 and 3,100 psi. This was dependent on who supplied the compressed air. During the study, it was found that Aquatron Dive Store were able to consistently fill the cylinder to a higher level compared to the Strathclyde SubAqua club, so became the primary source for compressed air.

Cylinder pressurisation could not be recorded accurately. The cylinder came with a built in pressure gauge marked with 500 psi intervals (Figure 4-6), causing any pressure readings to be approximations only. Although the exact volume could not be measured, the marker appeared to use the same volume of compressed air for each shot. However, it was possible to calculate that cylinder pressurisation would drop by approximately 5 psi per shot. This was assumed to be true for all shots fired.

A full cylinder can produce up to 620 shots, however to prolong the life of the cylinder and to safely dismantle the marker, it should not be fully emptied during use.

Figure 4-6 Air cylinder pressure gauge

4.3.6 Repeatability and reliability

The velocity traces recorded followed the same pattern in all 6 tests (Figure 4-7). In each test, the first few hundred shots (where pressurisation is above 1500 psi), was where the marker was able to produce the most consistent velocities, close to the 74 ms^{-1} which was aimed for. As cylinder pressure dropped below this level, the velocities produced also began to drop, however remain fairly consistent. Once cylinder pressurisation drops below 1000 psi, the marker can no longer fire consistently and velocities decrease with each shot.

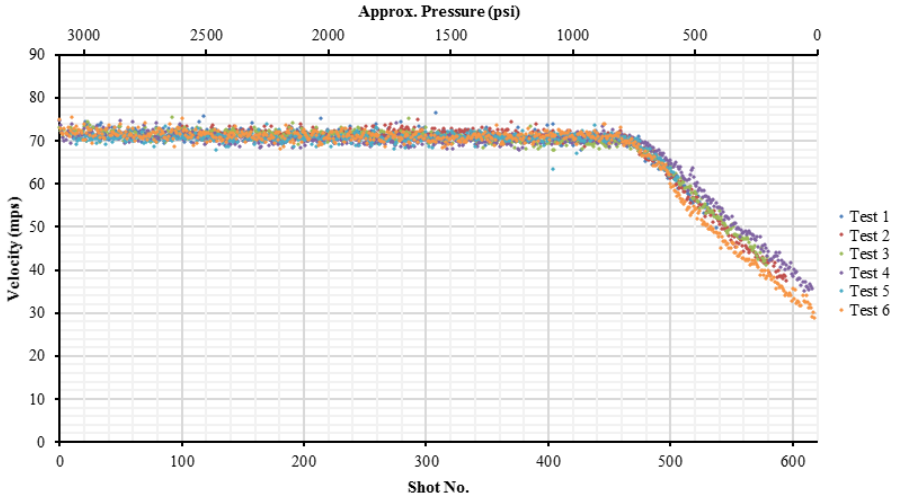

Figure 4-7 Measured velocities for all 6 tests

After the first 500 shots of test 6, the decreasing velocities appear to follow a slightly different pattern to the other tests, decreasing at a faster rate (as seen in Figure 4-7). This is due to a failure to successfully record data (approximately 20 shots), as a result of human error (chronograph storage space became full and was not noticed immediately). However, as the exact number of missing velocities is unknown, this could not be accounted for in the results.

Focusing on the recordings taken where cylinder pressure was above 1,500 psi, similar patterns were observed (shown in Figure 4-8) while statistical analysis (ANOVA, $p < 0.05$) did indicate that there was a significant difference between tests. However, with a range of 1 ms^{-1} and all mean velocities falling below the 74 ms^{-1} aimed for (shown in

Table 4-2), this difference was considered acceptable.

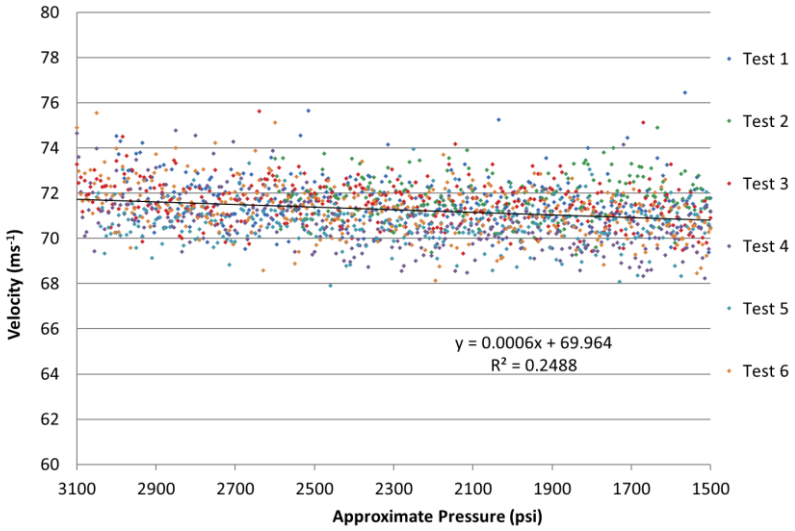

Figure 4-8 Velocities while cylinder pressurisation was above 1,500 psi, for all 6 tests, with average trendline

Table 4-2 Average velocities of each test while cylinder pressurisation was above 1,500 psi

Test Number	Average Velocity (ms^{-1})
1	71.65 ± 1.04
2	71.77 ± 0.94
3	71.57 ± 0.94
4	70.63 ± 1.11
5	70.72 ± 0.91
6	71.28 ± 1.13

4.3.7 Accuracy and precision

For the shots delivered to carbon paper, only 177 of the total 200 shots fired were visible on the targets. All shots were visibly observed impacting each target so initially it was thought that the use of a paper target, which sustained damage during use, was the cause for lost data (Figure 4-9). On changing the target to a sturdier material, the clarity of results improved (a list of the number of impacts visible for each target is shown in Table 4-3). Yet it was still not possible to identify 10 impacts for all targets (an example is shown in Figure 4-10). With all shots again visibly observed hitting the targets, it was concluded that impact overlap occurred (images of all recorded shots are shown in Appendix B).

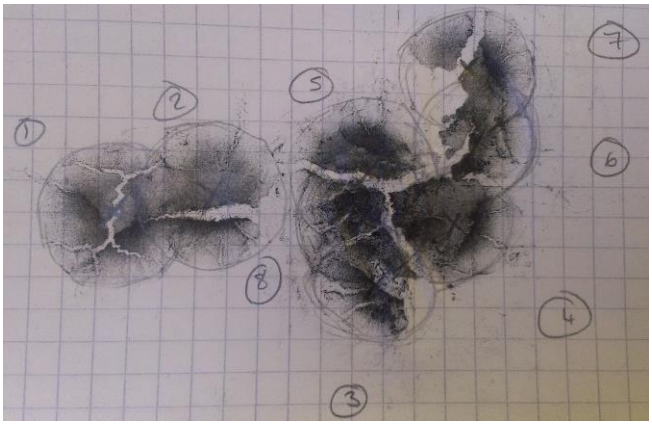

Figure 4-9 Example of where paper damage reduces clarity of results

Table 4-3 Breakdown of the number of impacts visible for each target

Target	Distance (m)				
	4	**5**	**6**	**7**	**8**
	Number of visible impacts per target from a total of 10				
Paper	9	9	9	8	7
	8	8	7	7	7
Card	10	10	10	10	10
	9	10	9	10	10
Total number of visible impacts: 177/200					

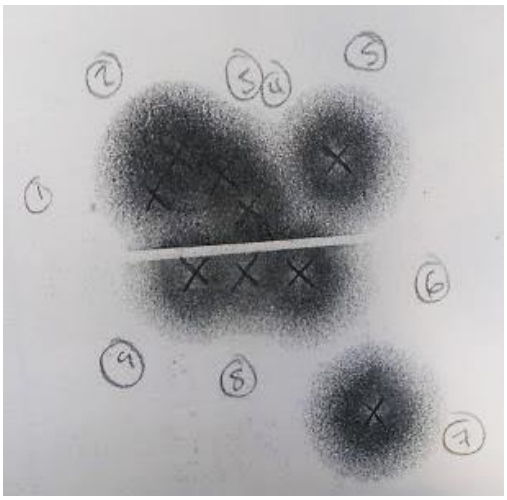

Figure 4-10 Results of 4 m test, where only 9 out of 10 impacts are observed

With the laser pointer taken as the origin, for each distance all impacts occurred within the same general area, however, as expected, the impact dispersion increased as target distance increased (Figure 4-11). Marker trajectory and laser sight were divergent causing predictable vertical error (~2 cm/m) and horizontal error (~1 cm/m) (Figure 4-12). The spread of shots around the mean impact location averaged at ~2 cm (Table 4-4). It should be noted that the laser site was not in alignment with the centre of the barrel, but parallel to the underside of the barrel. Therefore, the specific accuracy of the marker is difficult to assess.

It was concluded that for this setup, equipment was predictable, reducing accuracy and reducing precision with increasing target distance. However, with an approximate 2 cm deviation for each distance, the possible effect of gravity causing a sudden drop off in impact location can be excluded.

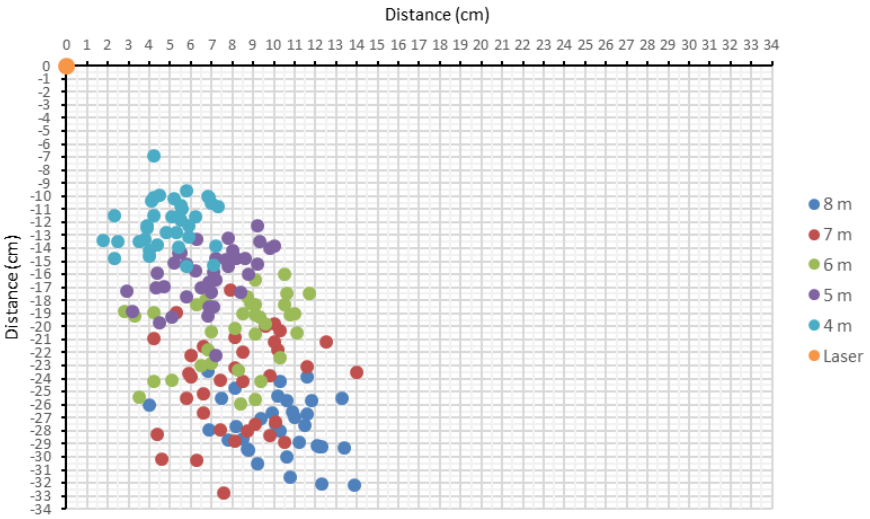

Figure 4-11 Plot of all impact locations for targets at 4, 5, 6, 7 and 8 m distances

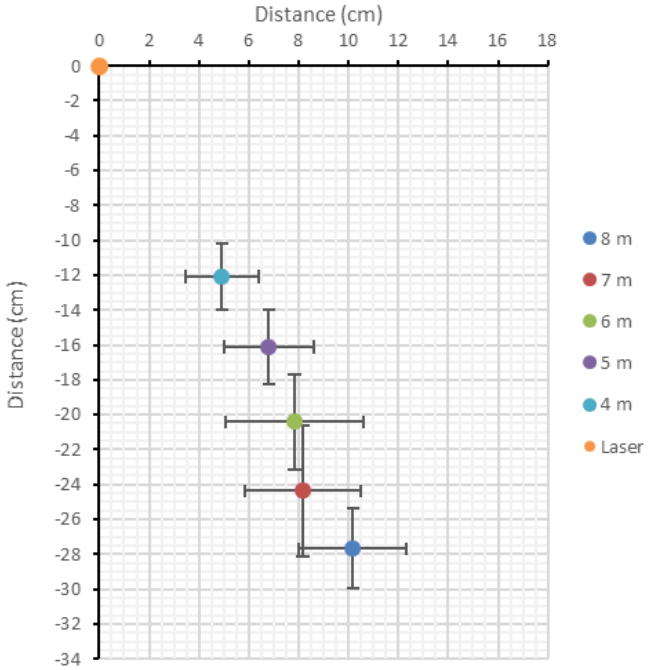

Figure 4-12 Average impact location ± x and y standard deviations for each target distance

Table 4-4 x and y standard deviations around the mean impact location

Distance (m)	x SD (cm)	y SD (cm)
4	1.45	1.87
5	1.49	2.15
6	2.77	2.72
7	2.31	3.74
8	2.15	2.28
Mean	2.09	2.55

4.3.8 Conclusions

Marker aim could not be determined by using a laser site to specifically predict projectile trajectory. This could have been a significant problem, however the proven repeatability and predictable impact location made the paintball marker an appropriate method for blunt impact generation.

From these findings, a firing distance of 6 m was chosen to be used in future work. This was based on both the above results and the conditions used in similar work (Scafide et al., 2013), where any closer was considered to be too close and had an increased probability of producing injuries of greater severity.

4.4 Additional equipment

Chronographs themselves are a standard piece of equipment hence its use during Section 4.2.2. However, for the determination of impact velocity, the use of a second chronograph was considered inappropriate as it would not be able to identify the ball's behaviour during impact, only before. Furthermore, the inaccuracies of paintballs as projectiles would increase the likelihood of damage to the equipment. Therefore, the chronograph remained in use for determining firing velocity – ensuring the marker fired within legally safe limits (<76 ms^{-1}).

With the need to record the behaviour of both the tissue and ball before, during and after impact, a high speed camera was identified as an appropriate method of recording impacts. Compared to conventional video recording equipment, high speed cameras are capable of recording events which happen much faster than the human eye is capable of seeing (Engineering360, 2015; Fuller, 2015; Imaging, 2015). A standard video camera records images at a rate of 30 frames per second (fps), while a high speed camera can record at frame rates in the thousands (Imaging, 2015). This allows for a detailed understanding of the events which have been recorded (Imaging, 2015).

Although the paintball marker was shown to be accurate, there would still be a risk that impact locations could vary. To ensure shots would hit a specific area and any wayward shots would not cause unintended injury to any volunteers, a purpose

built wooden target screen (University of Strathclyde, UK) with foam covering was constructed with an 8 cm diameter hole to be used as a target area based on the proven precision of the marker (i.e. for 95 % success, 2SD radius of 4 cm chosen. Dimensions shown in Figure 4-13). The foam was added to slow any shots which impacted it, reducing the likelihood of any accidental injuries from their rebound. The 8 cm area was chosen based on the range at which most shots fell within the same area for all distances.

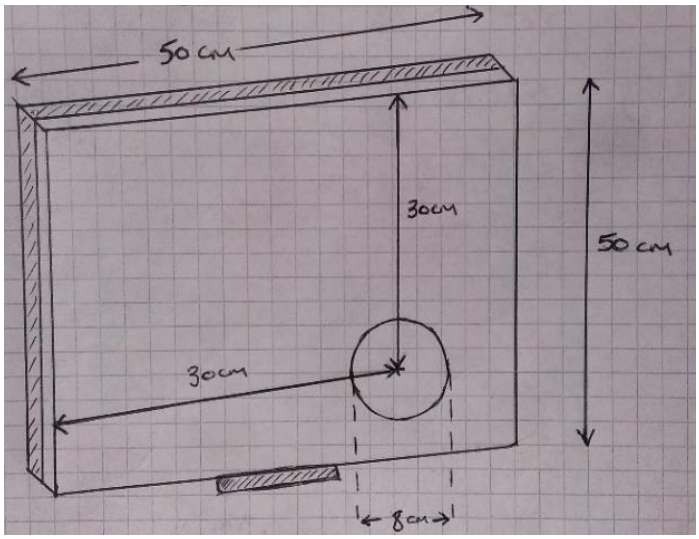

Figure 4-13 Screen dimensions

The screen was placed on top of a table and taped into place ensuring it was stable and sitting level. The screen was marked to provide a point of reference for the laser sight for each distance of 4 to 8 m, to ensure that shots would go through the hole. These guide-marks were pre-determined from the results presented in Section 4.2.7.

4.5 High speed camera settings

The high speed camera used in this research (Photron Fastcam SA4, Photron UK.(University of Strathclyde, UK)), fitted with a Nikkor 55-200 mm lens (University of Strathclyde, UK), has the ability to record at frame rates ranging from 3,600 fps up to 500,000 fps. However, for the camera to be able to record at higher rates, the camera's field of view (resolution), is reduced and thus increased illumination is

required. Therefore, a compromise had to be identified which would allow for clear impact recordings.

4.5.1 Frame rate testing

4.5.1.1 Methodology

Shots were fired from 6 m onto a wooden board with impacts recorded for a range of frame rates. Frame rate is chosen from the software's available list as it was not possible to manually input a frame rate. The specific frame rates tested were 1,000, 2,000, 3,000, 4,500 and 13,500 fps. An LED lamp was used as the light source whilst the purpose built screen was positioned 50 cm in front of the wooden board. This allowed for the camera to be focused on the area where the shots would be expected to hit. The chronograph was used to record firing velocities, using the methods described previously, ensuring testing conditions would be safe. Recordings were analysed using the high speed camera software (Photron FASTCAM Viewer).

4.5.1.2 Results

Generally, recordings from 1,000 to 4,500 fps were too low to record enough detail. The ball itself appeared blurry and impacts would be recorded by a limited number of frames (Table 4-5). The number of frames are, regardless of frame rate, approximations. This is due to the fact that the point at which the ball is no longer in contact with the wooden board is masked from the cameras field of view by the ball itself. However, this is not considered a significant issue as identification of the point at which the ball ceases its forward motion is the part which is most relevant to this research. The number of frames which captured this part of the impact (Table 4-5), was too small to allow for any clear indication of the velocities involved in the impacts.

Table 4-5 Approximate number of frames which categorise impacts for recording frame rates of 1,000 – 4,500 fps

Recording frame rate (fps)	Number of frames capturing complete impact	Number of frames capturing forward motion
1,000	1	1
2,000	2	1
3,000	3	2
4,500	4	3

In addition to the lack of frames capturing each impact, image quality was found to be a significant factor when identifying point of impact and where the ball's forward momentum ceases. This is shown in Figure 4-14, where a snapshot of the beginning of impact for each chosen frame rate. It is clear from these images the ball moved faster than the camera was able to capture clearly, causing the ball to appear either as a blur or missing the key events, i.e. exact point of impact. Thus, with both image clarity and a lack of frames to capture impacts, the frame rates of 1,000 to 4,500 fps were deemed inappropriate for use in this study.

The frame rate of 13,500 fps was the highest which could be achieved with the LED lighting. Impacts recorded at this rate appeared clear and the point at which the ball came into contact with the wooden board could be identified (Figure 4-15). Impacts could be characterised by approximately 10 frames, with 5 frames capturing the initial part of the impact.

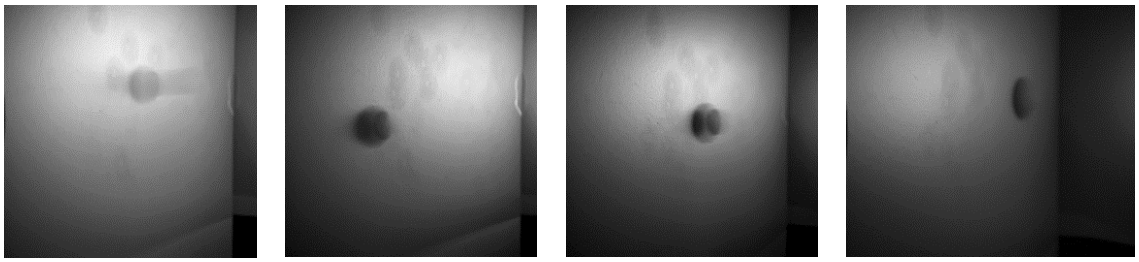

Figure 4-14 Point of impact image quality for 1,000 – 4,500 fps frame rates

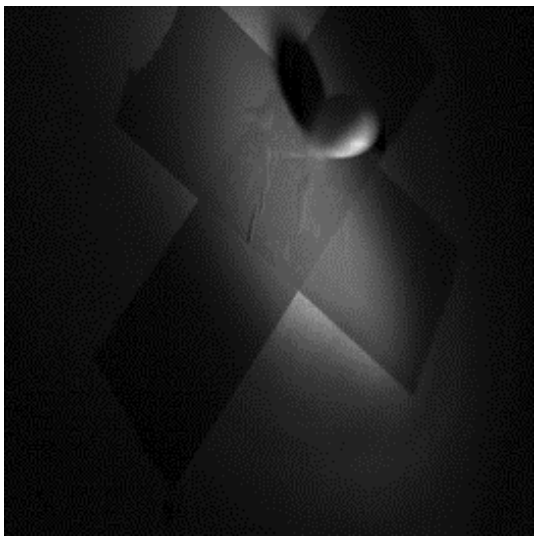

Figure 4-15 Point of impact image quality for 13,500 fps frame rate

4.6 Optical marker velocity determination

4.6.1 Methodology

Ideally, the high speed camera and chronograph would both record velocities as the same values. To determine if that was true in this case, both pieces of equipment were set up to record firing velocities of the paintball marker at the same time. The camera was set up to record the ball as it travelled between the two IR sensors of the chronograph, i.e. positioned perpendicular to the ball's path of travel.

The camera was set to record at 13,500 fps with a 1/frame second shutter speed (i.e. 7.407×10^{-5} s). An LED lamp was used to illuminate the area with a piece of tracing paper being used to diffuse the light (shown in Figure 4-16). A total of 10 shots were fired as part of this test.

Figure 4-16 LED light and tracing paper set up for high speed camera recordings of firing velocities

Using the high speed camera software, marker firing velocity was calculated. For each video, prior to calculations being made, the measurement scale within the function was calibrated based on the ball's vertical diameter (horizontal diameter had less defined edges). Once calibrated, the distance the ball travelled between each frame before, during and after impact was measured. This was done using the mid-base of the ball (shown in Figure 4-17). For each video, 20 distance measurements were made. These distances were then combined so a plot of the balls movement could be made.

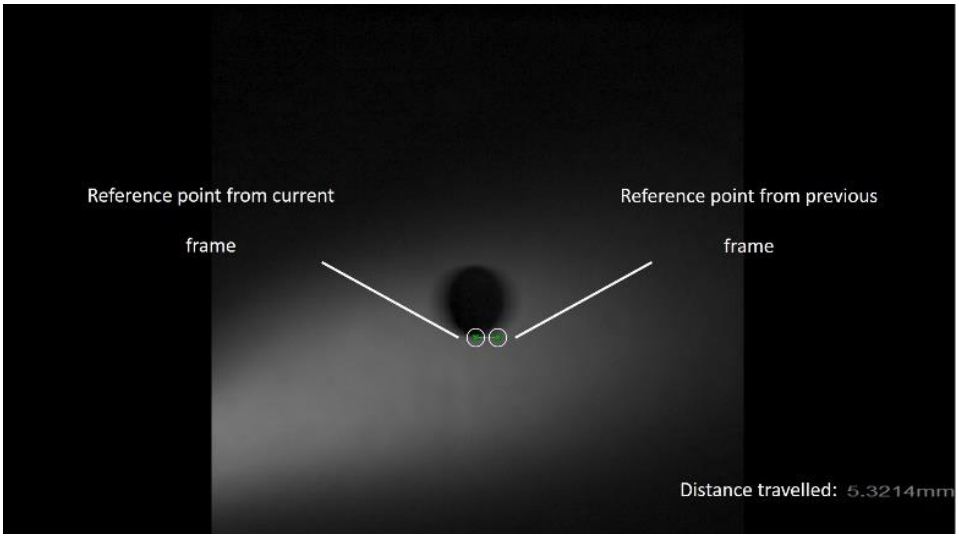

Figure 4-17 Measurement of distance ball travelled

Using the directional data, ball velocity was calculated using the equation:

Eqn. 1

$$v_n = \frac{\Delta d}{2 \times \Delta t}$$

where v_n is velocity, Δd is the change in distance between points d_{n+1} and d_{n-1} and Δt is 7.407x10^{-5} seconds.

Although the camera software allows for distance measurements up to 4 decimal places, there was still error involved. With measurements being restricted to whole pixels, measurement accuracy was good to ± a pixel. For a 13,500 fps frame rate, accuracy was good to approximately ± 0.127 mm. Furthermore, ball mass calculated to vary by ± 0.0099 g. However, the scale of each pixel would change with each video dependent upon the size of the ball within the image. Therefore, given the potential inaccuracy in measurements and how they are the basis for the velocity and force calculations which follow, all data will be reported to 3 significant figures to reflect this.

4.6.2 Results

For the majority of cases (9 out of 10), the high speed camera velocities were greater than those recorded by the chronograph (Table 4-6). There was a significant difference between the recordings of both pieces of equipment (t-test, $p < 0.001$), with the high speed camera tending to record a higher velocity.

Table 4-6 Results comparing chronograph and high speed camera velocity recordings

Test Number	Chronograph recording (ms^{-1})	Average high speed camera recording (ms^{-1})	Difference (m^{-1})
1	72.4	77.3 ± 10.1	4.92
2	75.1	77.6 ± 8.42	2.50
3	72.4	75.7 ± 6.83	3.34
4	73.0	76.4 ± 8.42	3.44
5	75.4	75.4 ± 8.14	0.02
6	72.4	72.6 ± 3.32	0.18
7	72.0	73.8 ± 8.31	1.82
8	73.0	73.3 ± 6.67	0.27
9	72.0	70.7 ± 8.06	-1.28
10	71.7	74.1 ± 5.00	2.43
Average potential error of camera		± 7.33	
Average difference			1.76 ± 1.92

However, differences between the recordings was to be expected. The chronograph records and calculates velocities itself – there is no human input and internal algorithms unknown. In comparison, for the video recordings, the point of reference which all calculations are based is chosen manually. Furthermore, the lighting set up resulted in the ball being dark (i.e. it was illuminated from behind). This therefore meant its edges were less defined than if lighting was directed to the side of the ball which the camera would capture.

As shown in Table 4-6, the average difference between the two methods of velocity measurement was 1.76 ms^{-1}. However, this does not consider the potential error surrounding each measurement made for the high speed camera velocities, only the average. Having considered all the uncertainties associated with the calculation of velocity based on the high speed camera recordings, the velocity values reported in Table 4-6 were found to vary by ± 7 ms^{-1} on average. And whereas the error associated with the chronograph for comparison was unknown, the uncertainties associated with the measurements made using the high speed camera setup were such that the latter measurement technique was able to record the velocity of the paintball accurately, within the bounds of uncertainty. Therefore, both pieces of equipment were considered to be suitable for use at this time.

4.7 Camera angle

Ideally, to determine impact velocity the camera should be perpendicular to the ball as was done in Section 4.5.1 However, to observe the tissue response to impact, the camera needs to be placed at an angle, to give a view of both the ball and the impact response (Figure 4-18). By measuring the distances at which the camera was positioned in relation to the impacted surface, the angle could be calculated after experimental work was performed.

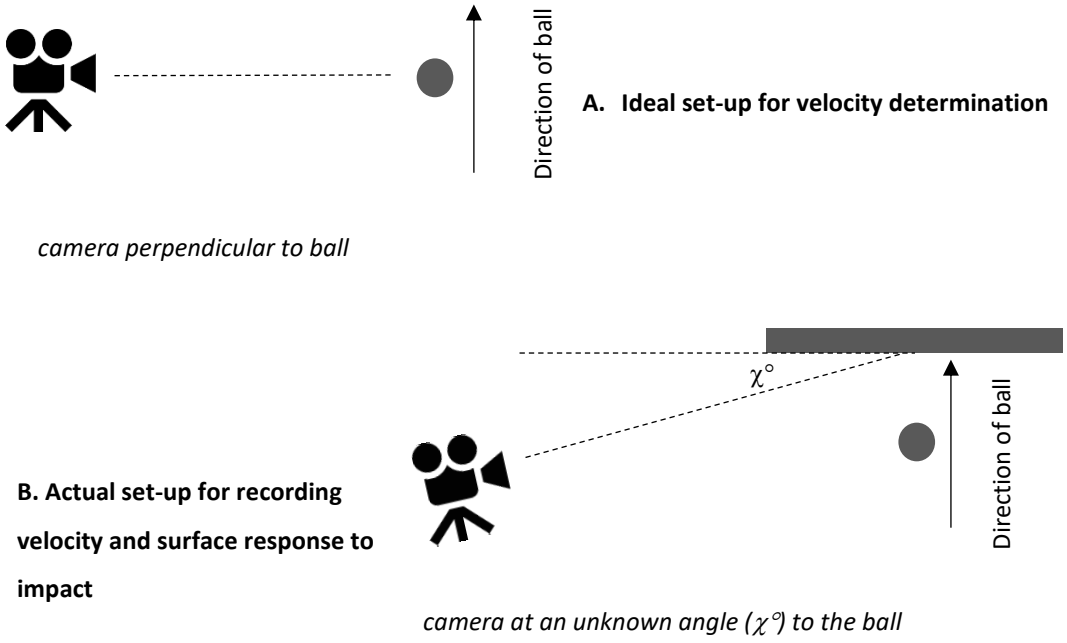

Figure 4-18 Camera set up

4.7.1 Testing camera collected data

Prior to pilot testing, generation of an impact profile was carried out to have a template to that we would expect participant data to follow. Using the directional data from an impact directed onto a wooden board (measured using the same method described in Section 4.4.1), recorded at 13,500 fps, impact velocity was calculated using Eqn. 1.

However, it should be noted that as the ball impacted the surface and changed direction, this had to be accounted for when combining the directional data. Therefore, once the ball's forward motion appeared to cease and change direction within the video, the distances were no longer added but subtracted from each other.

The camera angle was not perpendicular to the impacting surface, thus the directional data had to be corrected to account for this. This was done using the equation:

Eqn. 2

$$d_c = \frac{d_r}{\cos\theta}$$

where d_c is the corrected distance, d_r is the raw directional data and ϑ is the camera angle. The derivation for this equation is shown in Appendix C.

From this, a velocity profile was produced, shown in Figure 4-19. Acceleration was also calculated from the distance data, using Eqn. 3, the central difference formula:

Eqn. 3

$$a_i = \frac{d_{c,i+1} + d_{c,i-1} - 2d_{c,i}}{(\Delta t)^2}$$

where a_i is acceleration at time i, d_c is the horizontal position at time i and Δt is the change in time (7.407×10^{-5} seconds for a frame rate of 13,500 fps).

The force profile (Figure 4-20), of the impact was calculated based on the momentum of the ball, using the equation:

Eqn. 4

$$f_i = ma_i$$

where f_i is force, m is mass of the ball and a_i is acceleration. Vertical acceleration including gravity was ignored.

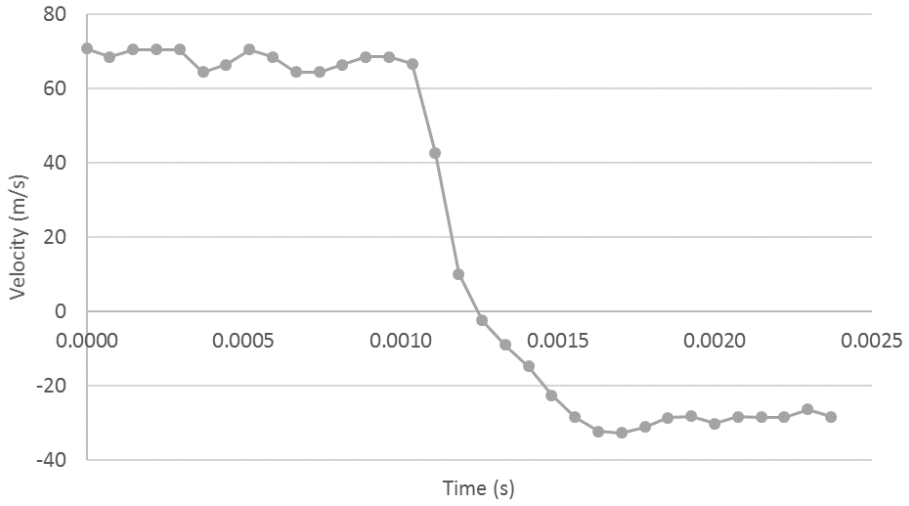

Figure 4-19 Velocity profile for an impact on a wooden board from 6 m, recorded at 13,500 fps

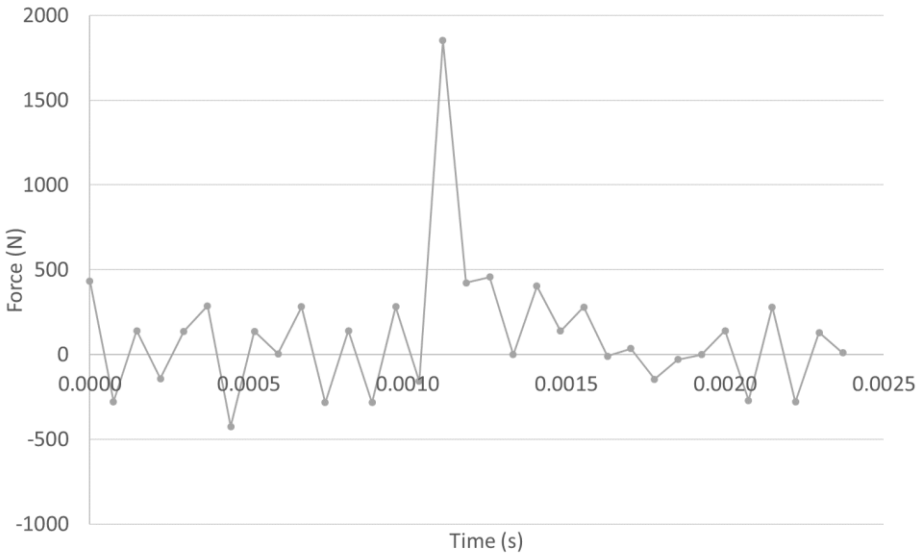

Figure 4-20 Force profile for an impact on a wooden board from 6 m, recorded at 13,500 fps

This analysis example indicated that the ball would impact with a force of approximately 1,850 N, when impacting a solid wooden surface. Peak force is represented by one data point due to the stiffness of the board and the fast rebound. Therefore, the peak was not well characterised. However, human tissue is much more compliant and thus a lower force will be observed and the peak will be better characterised. This is as there a greater number of data points will describe the force.

4.7.2 Uncertainty analysis

As was done in Section 4.6.2, when considering the error of the measurements for this test, velocity presented with an uncertainty of ± 8.26 ms^{-1}. This leads on to an uncertainty of ± 429.0 N for the force measurements. As shown in Figure 4-20, data points vary pre- and post-impact by approximately the ± 400 N, thus it is clear that the uncertainty in the measurements had some influence over the results.

As directional data was not consistent from frame to frame, the maximum and minimum measurements were considered when calculating velocity and force uncertainty. Combined with the uncertainties calculated in Section 4.6.2, it was concluded that although an accurate recording of paintball behaviour is achieved, this magnitude of uncertainty would present within all future high speed camera

recordings, Therefore, specific velocity and force values reported can only be considered approximations rather than specific values.

4.7.3 Impact force compared to other studies

Comparing the impact force to those used in other studies to establish suitability was not completely possible. As shown back in Table 4-1, not all studies which used a paintball marker provided details on impact characteristics as they were only interested in the appearance of bruising. Similar studies which use a drop mass system or another alternative (e.g. a tennis ball machine (Hawkins, 2014)), again did not always provide impact characteristics. Therefore, comparison with studies which considered much more severe trauma (e.g. skull fracture), or activities likely to cause bruising if inflicted to a person (e.g. foot stamping), was carried out.

Using 1,850 N as the expected impact force, this is much lower than would be required for bone fracture, for example 5-7 kN is typically required for tibia fracture (Hainsworth, 2013). Within similar studies (Table 4-7), the expected force was at the higher end of the examples.

Studies by Farrugia et al., (2012) and McBrier et al., (2009) compared impacts to different materials and demonstrated a change of impact force. Both studies measured impacts to a solid surface and then to a softer material. Of the two studies, McBrier et al., presents with the lowest impact forces, which is reflective of their small impacting mass (267 g) and use of a rat model, whilst Farrugia et al., used high density foam. Although neither tested human tissue, the reduction in material stiffness reduced the impact force. This was expected as softer materials are more compliant to an impact, increasing object deceleration times and in turn the resulting force (this is further explained within the findings of this thesis). Therefore, the force of 1,850 N measured from the wooden board tests would be expected to be lower for impacts to soft tissues.

The surprising difference is the comparison of impact force with those reported by Scafide, 2012, who's work this methodology was based upon. With both methods using a paintball marker and high speed camera, it would be expected the

impact force would be similar, even though impact surface differed. Scafide had calculated that impacts occurred with a force of 210 N however, as this thesis demonstrated in Section 4.4 their chosen frame rate of 1,000 fps was insufficient to accurately calculate any impact characteristics. Therefore, it can be concluded that the 210 N impact force was a vast underestimation.

Table 4-7 Published examples of forces generated as part of a controlled blunt impact

Author	Method of impact	Impacting surface	Impact force (N)
This research	Paintball marker	Wooden board	1,850
(Desmoulin and Anderson, 2011)	Drop mass system	Human	342 to 874
(Scafide, 2012)	Paintball marker	Human	210
(McBrier et al., 2009)	Drop mass system	Solid surface (unknown material)	718.9 to 1032.7
		Rat model	181.9 to 244.5
(Black, 2013b)	Drop mass system	Human	181.46 to 213.39
(Farrugia et al., 2012)	Stamping	Wood	2,996 (average)
		Foam	2,592.5 (average)
(Sharkey et al., 2012)	Drop mass system	Porcine model	3,200

It was concluded that although the peak force was high, it was not at a level likely to cause severe injury under the proposed methodology and the force transferred to human tissue would be much less. However, as testing had only used a wooden board, piloting work was required to determine the extent of injuries which could be produced and if they were appropriate to be applied to a larger study. Furthermore, with previous studies having applied their paintball impacts to the arm, pilot testing was required to determine if any other anatomical location would be more appropriate and to ensure the safety of the protocol.

4.8 Pilot Work

4.8.1 Ethical Approval and Volunteers

Prior to any pilot testing being carried out, due to the purposeful and injurious nature of the experiment, ethical approval was sought from the University of Strathclyde's University Ethics Committee (UEC). Approval was obtained for both a pilot study and a much larger study, on the proviso that a report of the pilot study was submitted to the UEC after completion of the pilot, stating which parameters had been selected for use within the main study (ethical approval is shown in Appendix D).

For the pilot study, the study supervisors were recruited. No detailed personal characteristics were taken except for gender and age.

4.8.2 Pilot Methodology

The paintball marker was set up as it was in Section 4.6 and the reusable paintballs were used for testing while the compressed air cylinder was pressurised to approximated 3,000 psi. The chronograph was again fitted with the IR screens and used to record the barrel exit velocity of each shot, ensuring it was operating within safe limits (i.e. below 74 ms^{-1}).

Single shots were delivered to the upper arm, lower back and lateral thigh of each participant (see Figure 4-21 for reference). Volunteers stood behind the purpose built screen and were provided with safety goggles to ensure that in the unlikely circumstance that a misfired shot struck the face, their eyes were protected (as per the safety requirements of a paintball game). Impacts were delivered to bare skin to gain an idea of the worst case scenario for injuries. Prior to shots being delivered to each participant, shots were initially directed onto a wooden board. This was to ensure a safe testing environment by confirming all equipment was working correctly before firing shots at the participant's body.

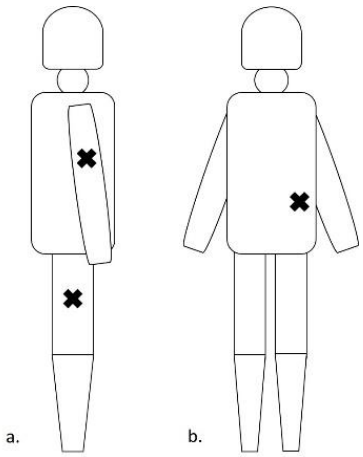

Figure 4-21 Illustration of pilot impact locations a. upper arm and lateral thigh b. lower back

The marker was secured within the purpose built table mount, at a 6 m distance from the participant and the laser guide was used to line up the marker with the appropriate guide-mark on the screen. While for greater distances the increased chance of variable impact locations implied that there could be a chance of the impacts occurring out with the high speed camera's field of view.

The high speed camera, fitted with the Nikkor 55-200 mm lens, was used to record each impact to the skin at a frame rate of 13,500 fps with the LED lamp being used to illuminate the impact site. The camera was at an angle to the skin to allow clear observation of the tissue response to the impact. This angle was later calculated to be approximately 37° for each participant. The camera was manually focussed and secured within a tripod. For data extraction from the high speed videos, the process described in Section 4.6 was used.

For the video snapshots presented, brightness and contrast were manually manipulated to increase image clarity.

4.8.3 Pilot work findings

4.8.3.1 Results from impacts to the arm and back

The arm and back impacts could not be directly compared with each other due to one impact at each location being a glancing blow (shown in Figure 4-22a and Figure 4-22b). This was due to the smaller target areas associated with each location (for the back impact the aim was to be off centre to avoid hitting the spine, hence the

smaller area), thus there was a greater chance of the ball not coming into direct contact with the chosen area.

Therefore, this meant that identifying the point at which the impacting ball's direction of motion changed was very difficult, hence the results are unreliable. This was particularly problematic for P.2's back shot (Figure 4-23b), as the deflection was masked by the tissue deformation and impact location was more towards the participant's side than back – thus not completely within the field of view of the camera. Data on velocity, impact time and impact force were calculated for both arm and back impacts (shown in Table 4-8), however given the problems of indirect impacts identifying the point at which the ball changes direction, the calculated velocity and force values presented, must be considered to have significant error attached.

a.

b.

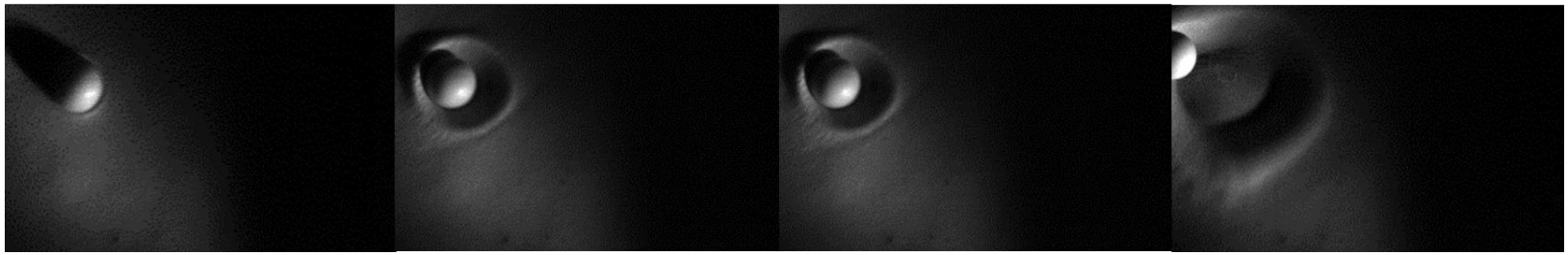

Figure 4-22 Snapshots of P.1 arm and back impacts: a. arm impact, glancing blow b. back impact, more direct impact

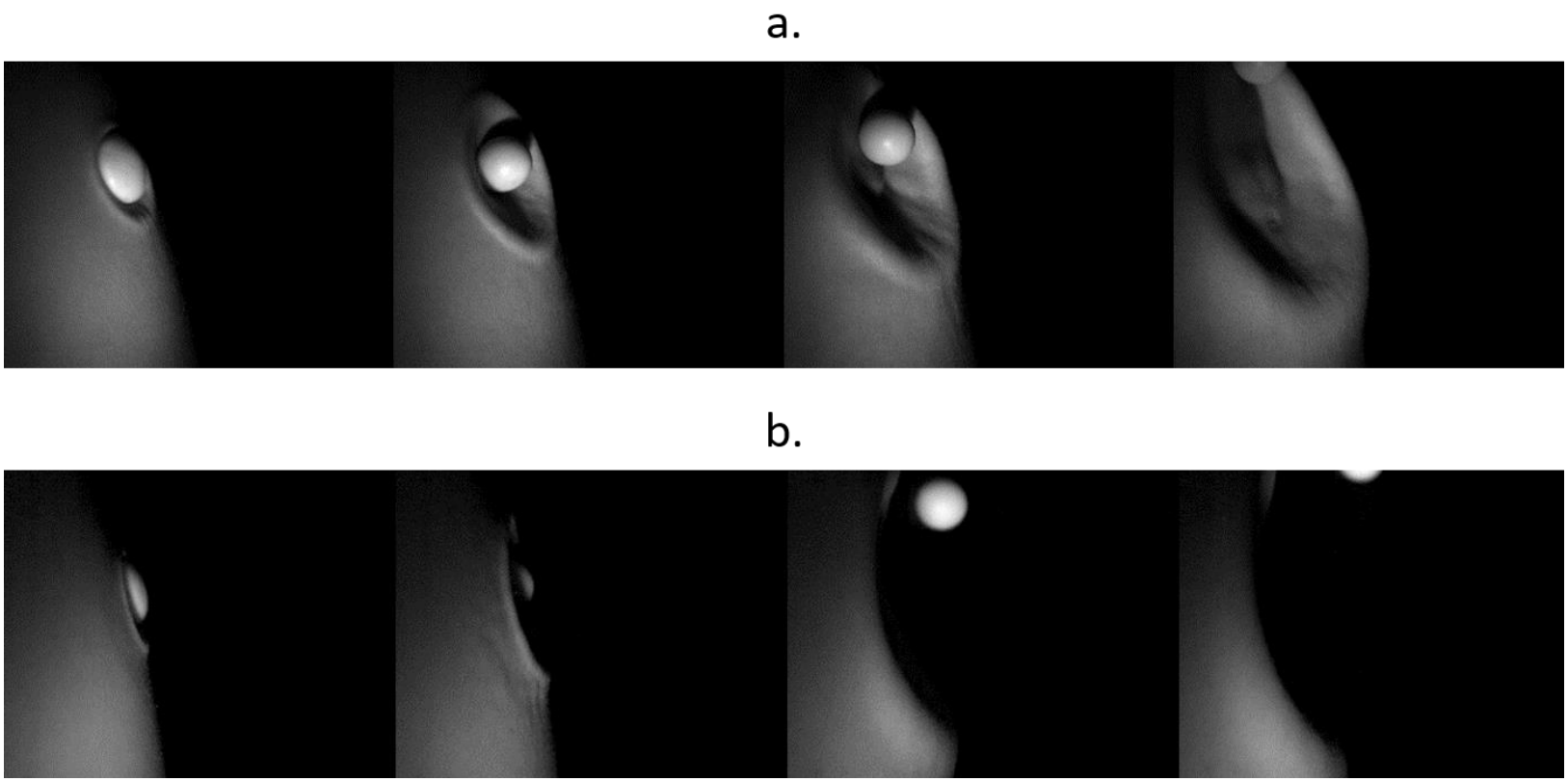

Figure 4-23 Snapshots of P.2 arm and back impacts: a. arm impact, more direct impact b. back impact, glancing blow

The two direct blunt impacts are highlighted in Table 4-8 (Figure 4-22b and Figure 4-23a). However, the impact to P.1's back was not ideal (the ball was seen to deflect off the back, still moving in a forwards direction). Of the four impacts, P.2's arm impact appeared ideal and the closest to what would be expected in a larger study.

For the velocity data collected, impacts can be said to have been made under the same conditions, with impact time, time to and peak force calculated to be different. With a limited number of tests carried out during the pilot, it cannot be said if this was due to the difference in gender and/or anatomical location.

Table 4-8 Impact characteristics from impacts to the arm and back or both participants

Participant	**P.1**		**P.2**	
Gender	Male		Female	
Age	43		36	
Impact location	Arm	Back	Arm	Back
Impact velocity (m/s)	63.5	66.5	67.00	70.0
Impact time (ms)	0.889	0.815	1.63	1.04
Time to peak force (ms)	0.0741	0.148	0.222	0.0741
Peak impact force (N)	1,880	1,410	1,050	1,250

Visually, the extent of deformation differs between individuals, but as no measurements were taken it cannot be concluded if this was due to the muscle to fat ratio of each participant.

Comparing both arm impacts (as they were the clearest compared to the back impacts, the differing impact force and impact time indicate that the differences in tissue composition influence impact characteristics. However, the inaccuracies in the data extraction from the videos combined with the lack of participant specific information made it impossible to form any conclusive conclusions.

4.8.3.2 Results from impacts to the thigh

With the impacts to the thigh being direct for both participants, their results could be compared. There was a difference in impact velocities observed (Table 4-9).

Based on the previous findings (Section 4.2) although velocities may be different, they can be compared and assumed not significantly different.

Table 4-9 Participant characteristics and impact parameters

Participant	P.1	P.2
Gender	Male	Female
Age	43	36
Impact location	Thigh	Thigh
Impact velocity (m/s)	63.8	66.0
Impact time (ms)	0.815	1.04
Time to peak force (ms)	0.148	0.148
Peak impact force (N)	1,110	1,310

To confirm this, all shots fired across the 2 days of the pilot study were compared using ANOVA. For each day, there were 5 shots – 2 onto the wooden surface and the 3 onto each participant (one at each body segment). With the *p*-value calculated to be greater than 0.05, it was confirmed that there was no significant difference between impacting velocities.

There are however differing impact times, but matching time to peak force. There is also a difference in peak forces. The difference observed in impact time and peak force can be said to be due to the tissue properties of the participants themselves. However, with no quantifiable tissue measurements and only two observations, the level of experimental error cannot be ascertained.

The force profiles generated using the video data (Figure 4-24), show a consistent pattern of 2 distinct peaks with both impacts. Seven data points characterised the impact with the first peak found to occur at the point at which the ball first came into contact with the thigh, as seen in Figure 4-24a. At this point the ball itself has not visibly deformed. Therefore, differences in initial force and the time over which this force was delivered can be attributed to the tissue stiffness of the participants themselves. Although no measurements were taken (skin fold thickness for example), it was visibly clear that P.1's thigh had a higher muscle-to-fat ratio than that of P.2. Therefore, P.1 had a greater tissue stiffness, explaining the sharper

impact force. For P.2, the initial force is shallower, indicating that the greater fat ratio cushions the initial impact. For the second peak (Figure 4-24b), this relates to the point at which the ball's forward momentum has ceased, delivering the peak impact force. This force is similar for both participants and takes place over the same period of time, thus is dictated by the ball itself. Force varied ± 200 N after impact, when the ball was no longer in contact. This could be considered an experimental error or relating to the movement of the ball as it changes shape, returning to its original spherical shape. Therefore, it should be considered when interpreting results using this method.

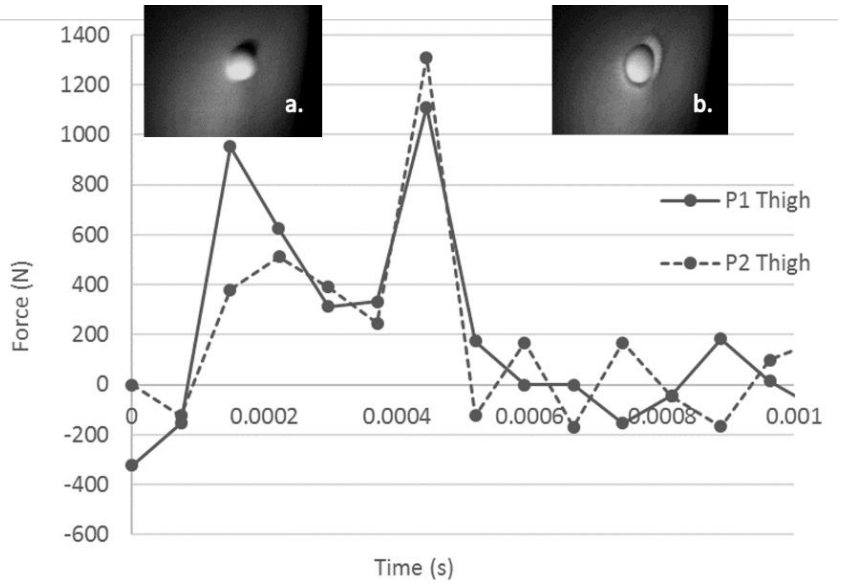

Figure 4-24 Force profiles for thigh impacts

With each impact being made under the same conditions, the tissue deformations which they produced over time were visually different. This is shown in Figure 4-25, where each image is 4 frames apart (1 image every 0.296 ms). For P.1, a shallow deformation was generated with a smooth wave dissipating out from the impact origin. In comparison, the impact on P.2 generated a visually larger deformation, however this variance was unable to be quantified. This variance was most likely a result of the differences in fat content within each thigh, but as previously stated, this cannot be confirmed.

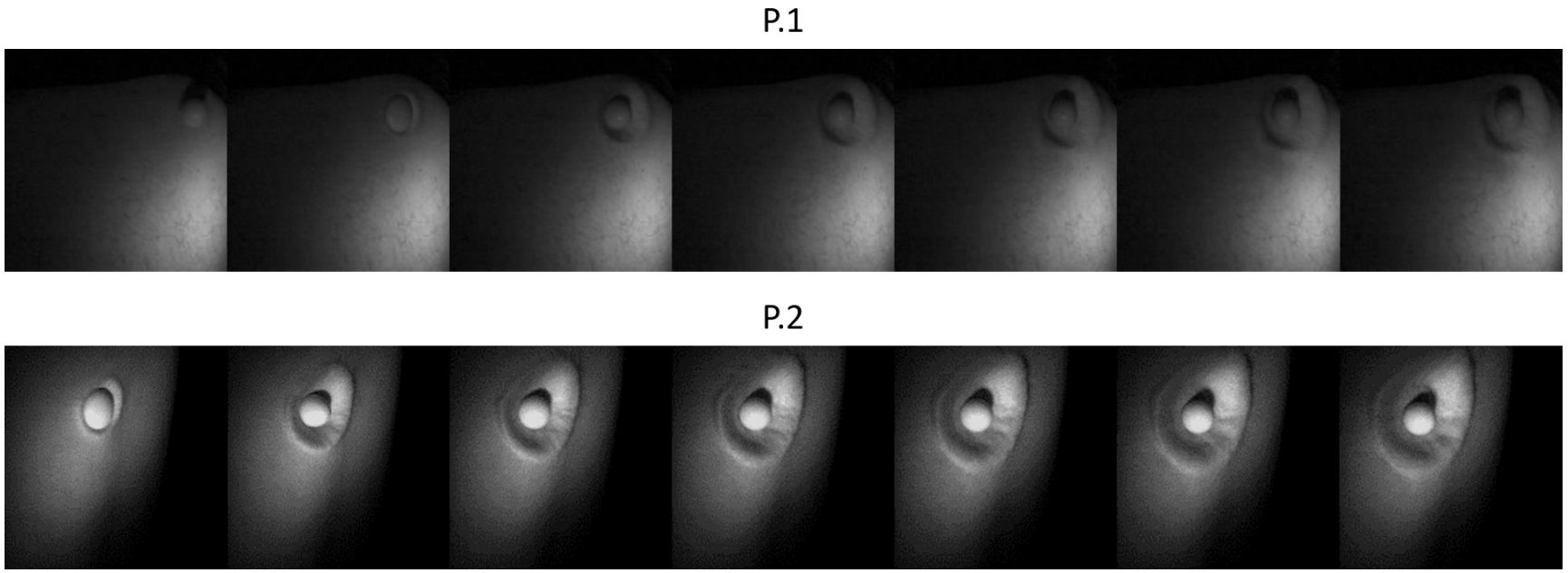

Figure 4-25 Tissue deformations observed for each thigh impact

4.9 Issues found

Through the course of the pilot study, several methodology issues were identified and needed to be addressed before a larger study could be initiated. There were two main issues identified:

1. Impact location
2. Lighting conditions

From these findings, it was clear that given the variations in arm size and back contours between individuals meant that a clear, direct impact could not consistently be obtained. This not only reduced the quantity of usable data which could be collected, it also increased the risk of participants being impacted in an unintended location, e.g. upper back or face. To eliminate the possibility of any significant injury, the thigh was chosen as the impact location for all future work.

Lighting conditions were also a problem and required altering during testing with the first participant. The LED light had to be repositioned to remove shadows and thus allow for clearer videos to be recorded. However, even with this change the initial stages of impact were not the clearest. This problem is linked with the recording frame rate. Currently, recording at 13,500 fps is not fast enough to clearly record the point of impact and the peaks plotted within the force profiles are based on 7 data points. Thus, frame rate needed to be increased and improved lighting would allow for this.

Given the lack of individual tissue composition characteristics, no specific conclusions could be made from the data. This was not considered a problem at this point as the pilot was to ensure safety of protocol, determine a specific impact location and gain an indication of the extent of bruising which could be perceived. However, given the impacts and injuries observed it was clear that a more detailed characterisation of individuals was required. Therefore, a short health questionnaire was created for use in the main study (see Chapter 5). Ideally a measurement of adiposity would also be carried out and prior to the pilot study, skin fold thickness

was planned to be measured as part of the larger study. However, on selecting the thigh as the impact location, skin fold thickness was excluded as it was impractical. Due to time constraints and alternatives (e.g. ultrasound), being unavailable, the decision was made to only use questionnaire answers in combination with BMI measurements of each participant.

4.10 Lighting and frame rate

4.10.1 New lighting

Following on from the problems highlighted within the pilot study, two 50W LED floodlights (daylight white) (lighting EVER LTD, UK), were purchased to provide greater illumination of the impact site. Unfortunately, although brighter than the single LED lamp, they did not provide constant illumination i.e. the light intensity fluctuated within the videos. Given this problem, new lighting had to once again be sourced. However, these lights could be used to evaluate higher frame rates. This was done using the same methods as done previously.

4.10.2 Frame rate findings

The change in light source allowed for recordings at frame rates of 20,000 up to 100,000 fps. These recording rates captured impacts over a greater number of frames, shown in Table 4-10. Therefore, there would be a greater number of data points which could be used to characterise the impacts.

Table 4-10 Approximate number of frames which categorise impacts for recording frame rates of 20000 - 100000 fps

Recording frame rate (fps)	Approximate number of frames	Number of frames capturing forward motion
20,000	9	4
30,000	14	7
40,000	21	9
50,000	19	7
60,000	24	8
75,000	31	9
100,000	52	14

A velocity profile was generated for each impact recorded at a different frame rate, to observe how clear a trace appeared (Figure 4-26). As frame rate was increased the number of data points available for each impact increased, creating a

more accurate profile of the impact. However, an increase in frame rate reduced the image resolution (quality). The camera software only allowed for distance measurements from pixel edge, thus although a more detailed impact was visually captured (as shown in Figure 4-27), the accuracy of distance measurements was reduced as the edge of the ball could not always be accurately selected. Combined with the error introduced by manual measurements, the clarity of each velocity profile began to reduce above 40,000 fps. Furthermore, the camera field of view was reduced with increasing frame rate (also shown in Figure 4-27). Thus, the higher frame rates carried the risk of missing the location of impact when testing was performed on individuals and not a wooden board.

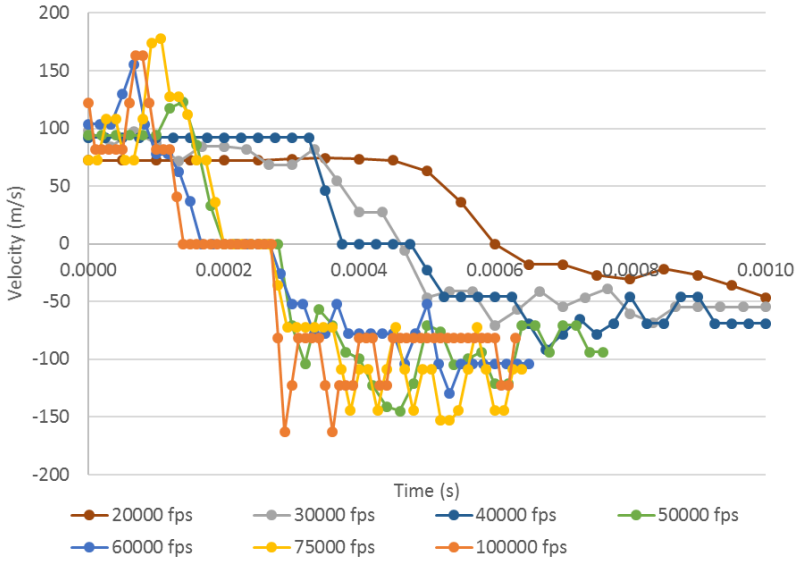

Figure 4-26 Velocity traces for impacts recorded at 20,000 to 100,000 fps

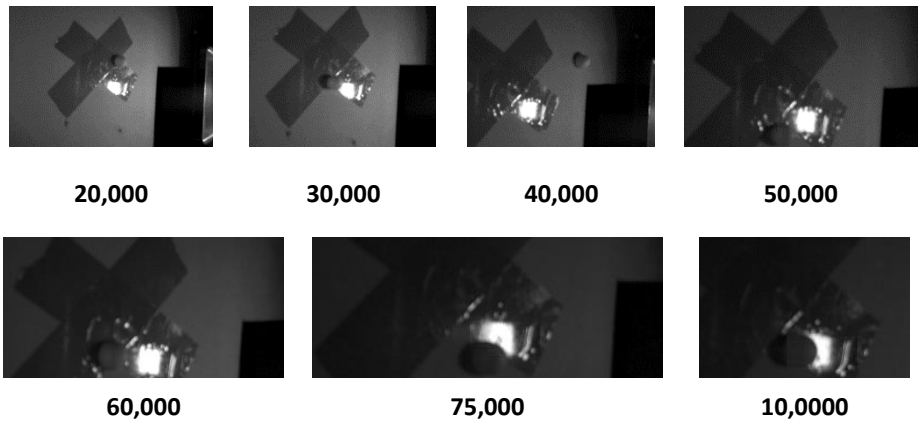

Figure 4-27 Point of impact image quality for 20,000 – 100,000 fps frame rates

4.10.3 Conclusions

From both the video recordings and the data which could be extracted, it was concluded that a frame rate of 40,000 fps was the optimum for recording impacts. After this preliminary testing was complete, LED lamps specifically for use for the high speed camera were obtained from Photron Ltd., and used throughout the rest of this research.

4.11 Data Collection

Given the error which was inevitably introduced from manually extracting data from the videos, it was decided to both automate the process and introduce a data filter – 4th order Butterworth low pass filter. The filter was applied with a sampling frequency of 40,000 Hz and a cut-off frequency of 3,500 Hz. This cut-off frequency was chosen as it visibly smoothed out the data with minimal loss of peak force.

4.11.1 Code development for video analysis

A function was developed in Matlab (Mathworks, 2016a) (University of Strathclyde, UK), which tracked the ball's centre of shape and movement frame by frame, measuring the movement of the ball's centre of mass, not only in the horizontal (x) direction but also the vertical direction (y). The process was not free of user input, with the outline of the ball being defined in the first frame to be used as a reference for all following frames.

For data processing, the filter was applied to the raw positional data. The processed data was used to calculate the total impacting velocity, acceleration and force of each impact. The equations used are listed below.

Velocity equations:

Eqn. 5

$$v_{x(i)} = \frac{d_{x(i+1)} - d_{x(i-1)}}{2\Delta t}$$

where $v_{x(i)}$ is the velocity in the x direction, d_x is the distance (filtered) travelled in the x direction and Δt, is the change in time.

Eqn. 6

$$v_{y(i)} = \frac{d_{y(i+1)} - d_{y(i-1)}}{2\Delta t}$$

where $v_{y(i)}$ is the velocity in the y direction, d_y is the distance (filtered) travelled in the y direction and Δt, is the change in time.

Eqn. 7

$$v = \sqrt{{v_x}^2 + {v_y}^2}$$

where v is the total velocity, v_x is the velocity in the x direction and v_y is the velocity in the y direction.

Acceleration equations:

Eqn. 8

$$a_{x(i)} = \frac{d_{x(i+1)} + d_{x(i-1)} - 2d_{x(i)}}{\Delta t^2}$$

where $a_{x(i)}$ is the acceleration in the x (horizontal) direction, d_x is the distance (filtered) travelled in the x direction and Δt, is the change in time.

Eqn. 9

$$a_{y(i)} = \frac{d_{y(i+1)} + d_{y(i-1)} - 2d_{y(i)}}{\Delta t^2}$$

where $a_{y(i)}$ is the acceleration in the y direction, d_y is the distance (filtered) travelled in the y direction and Δt, is the change in time.

Eqn. 10

$$a = \sqrt{{a_x}^2 + {a_y}^2}$$

where a is the total acceleration, a_x is the velocity in the x direction and a_y is the acceleration in the y direction.

Force equations:

Eqn. 11

$$f_x = ma_x$$

where f_x is the force in the x direction, m is the mass of the ball and a_x is the acceleration in the x direction.

Eqn. 12

$$f_y = ma_y$$

where f_y is the force in the y direction, m is the mass of the ball, a_y is the acceleration in the y direction. Gravity was ignored due to its negligible effect.

Eqn. 13

$$f = \sqrt{{f_x}^2 + {f_y}^2}$$

where f is the total force, f_x is the force in the x direction and f_y is the force in the y direction. Whilst the force applied to the ball is determined, Newton's 3rd law implies this is equal and opposite to the force of the ball on the tissue.

4.12 Comparison of data collection methods

With the introduction of the Matlab function, the data which it produced had to be compared to that from the chronograph and high speed camera recordings. This would both confirm its accuracy and whether automated data extraction was better than manually extracted data.

4.12.1 Methodology

A similar process to that described in Section 4.5.1 was used with some differences. As before, the camera was set up to record the ball as it travelled between the two IR sensors of the chronograph whilst the high speed camera was positioned perpendicular (at 90°), to the ball's path of travel.

In this case, the camera was set to record at 40,000 fps with a 1/frame second shutter speed. One of the LED lights sourced from Photron Ltd., was positioned in line with the camera, unlike before where it directed light towards the camera causing the ball's shadow to be recorded. A black backdrop was used to ensure high contrast between the ball and the background. This setup is shown in Figure 4-28. To improve

the reliability of the results, the number of tests performed was increased from 10 to 20.

Each video recording was analysed using the Matlab function and manual measurements were also taken. For the manual measurements, as before, the measurement scale within the function was calibrated based on the ball's vertical diameter. Again, the distance the ball travelled between frames was measured however, this time the centre of the ball was taken as a reference point, rather than the edge, due to the increased video clarity (Figure 4-29).

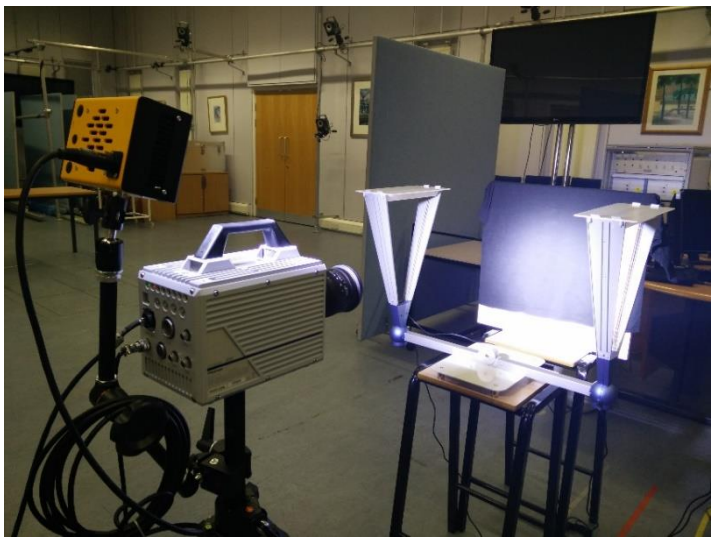

Figure 4-28 New setup for chronograph versus high speed camera testing

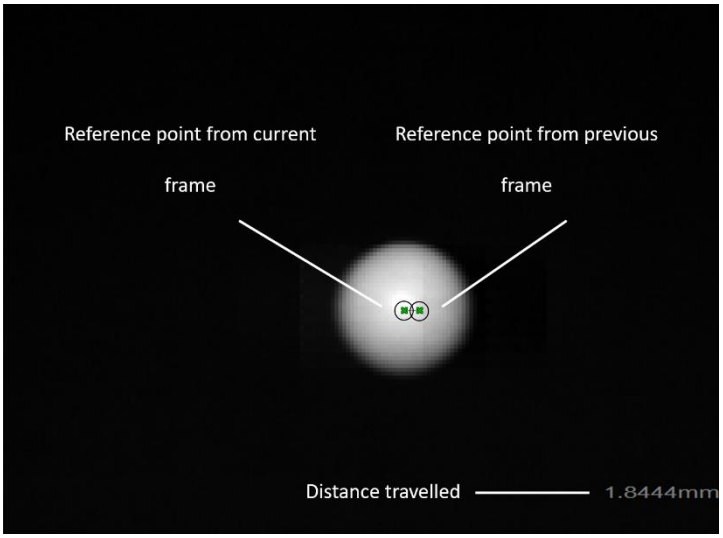

Figure 4-29 Measurement of distance ball travelled

For each video, approximately 74 manual distance measurements were made and combined so a plot of the ball's movement could be made. As with the 13,400 fps recordings there was an accuracy of ± half a pixel. For 40,000 fps, this equated to approximately ± 0.2326 mm but as stated earlier in Section 4.6.1, scale will change with each video given the location of the ball. Therefore, all velocity and force values will be reported to 3 significant figures.

Like before, velocity was calculated using Eqn. 1, with a change in time of 2.5×10^{-5} seconds. ANOVA (single factor), was used to determine statistical significance, at the 5% level.

4.12.2 Manual findings

Although the previous set up showed that manual measurements were significantly different to the chronograph readings, they were justified for use at that point in time. However, the improved equipment and data collection improved the accuracy of velocity calculations.

As before, manual measurements were not ideal and again found to be both visually (Figure 4-30), and statistically different ($p < 0.001$). The average difference was calculated to be 7.24 ± 1.60 ms^{-1}. Furthermore, working with the higher frame rate resulted in the distance travelled by the ball between frames being reduced. This caused a particular problem when locating the centre of the ball in each frame, as the measurement tool can only be placed at the edge of a pixel. As a result, where the ball's centre appeared to lie within a pixel, measurements were forced to either be over or under estimated.

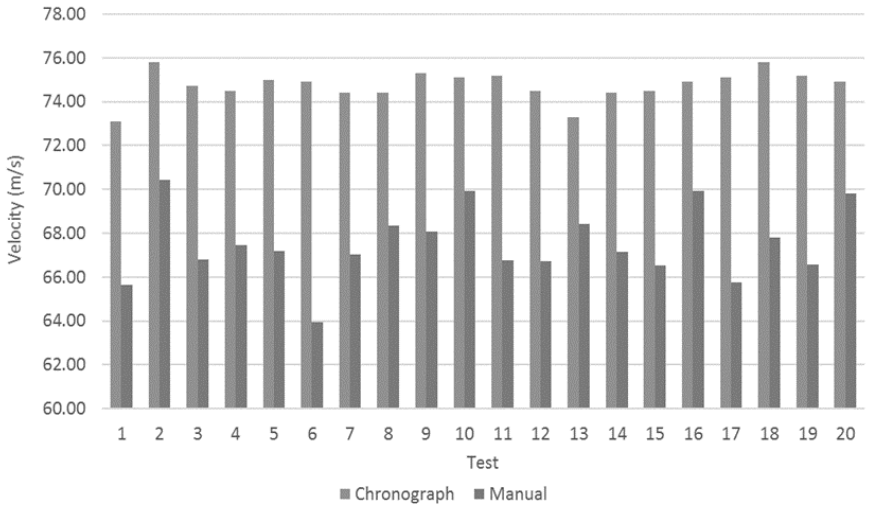

Figure 4-30 Plot of velocities recorded by the chronograph and by manual measurement over 20 tests

4.12.3 Findings of automated analysis

With the increased frame rate, a clearer representation of ball velocity was produced when each video was run through the Matlab function. However, it was clear that the use of the filter had an effect on data output. For this filter to work successfully, 15 data points at the beginning and approximately 15 data points at the end were required. Therefore, these 30 data points were excluded from all average velocity calculations (highlighted in Figure 4-31).

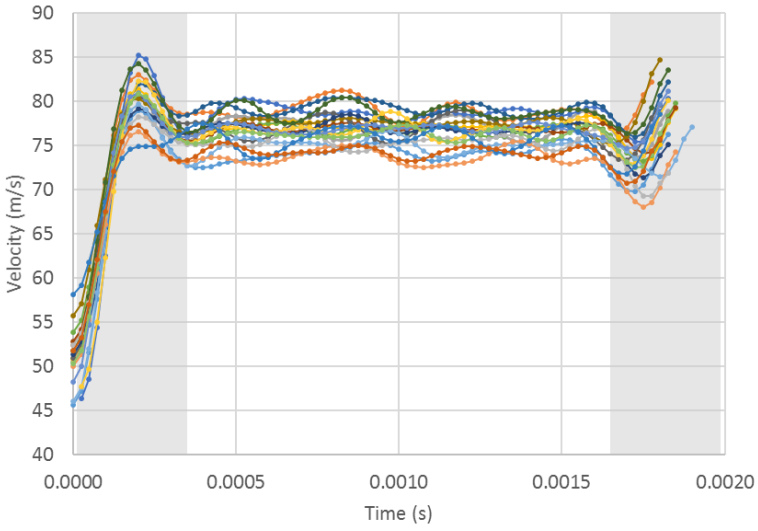

.

Figure 4-31 Plot of all 20 firing velocity traces with the excluded 30 data points highlighted

The Matlab function was found to calculate firing velocities much closer to those recorded by the chronograph (Figure 4-32), compared to those calculated

manually. However, statistically, there was still a significant difference ($p < 0.001$). With an average difference of 1.93 ± 1.41 ms^{-1} (Table 4-11), it was deemed that whilst there would always be an element of difference between the two measurement techniques, the use of the Matlab function resulted in a smaller difference from the chronograph readings compared to manually calculating velocity. Therefore, this automated method of data analysis would be implemented in future work.

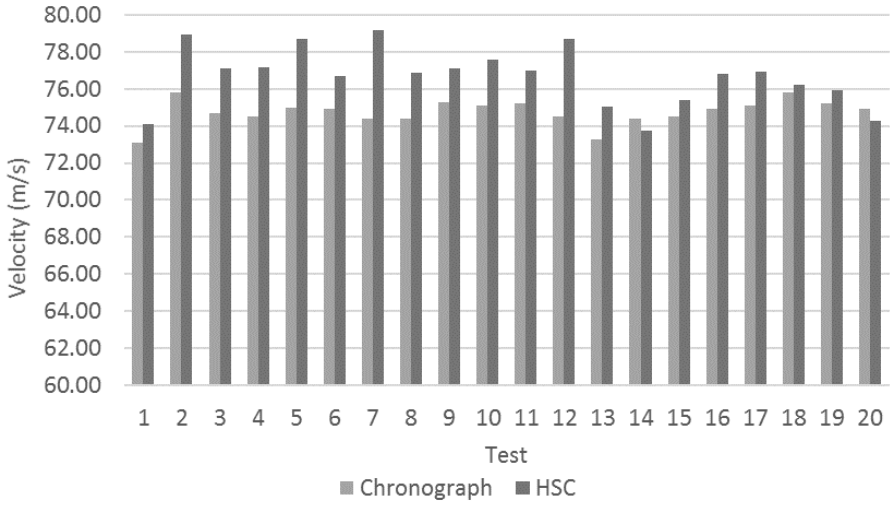

Figure 4-32 Plot of velocities recorded by the chronograph and high speed camera over 20 tests

Table 4-11 Velocities recorded by both the chronograph and the Matlab function

Test	Chronograph (m/s)	Average calculated (m/s)	Difference (m/s)
1	73.1	74.1	1.01
2	75.8	79.0	3.15
3	74.7	77.1	2.38
4	74.5	77.2	2.67
5	75.0	78.7	3.69
6	74.9	76.7	1.81
7	74.4	79.2	4.79
8	74.4	76.9	2.48
9	75.3	77.1	1.84
10	75.1	77.6	2.48
11	75.2	77.0	1.78
12	74.5	78.7	4.20
13	73.3	75.0	1.72
14	74.4	73.8	-0.65
15	74.5	75.4	0.92
16	74.9	76.8	1.92
17	75.1	76.9	1.83
18	75.8	76.2	0.41
19	75.2	76.0	0.75
20	74.9	74.3	-0.60
Average difference			1.93 ± 1.41

4.13 Repeated pilot experimentation

4.13.1 Ethical approval and volunteers

Given the change in equipment and data processing, pilot work had to be repeated before full ethical approval for a larger study could be sought. As in Section 4.7, this pilot work was approved by the University of Strathclyde's University Ethics Committee.

As before, the same two volunteers were recruited, one male and one female and no detailed personal characteristics were taken except for gender and age.

4.13.2 Pilot Methodology

Impact generation methods were the same as those used during the first pilot described in Section 4.7, with some minor changes.

Instead of single shots being directed to multiple anatomical locations, a single shot was directed onto the participant's thigh. The high speed camera was set up as before, with camera angle calculated to be approximately 50° for the first participant and approximately 52° for the second participant. The Photron LED light was used to illuminate the impact site for the video recordings. The camera was set to record at 40,000 fps and was manually focussed before use.

For the pilot work so far, impacts have been discussed in terms of their velocity and force, not the resultant severity of bruising (the bruises are shown in Section 4.17). It was found that the impact mark generated was too severe when impacts were directed to bare skin, causing damage which took longer than the expected 2 to 3 week period to heal (Figure 4-33). Furthermore, the contrast between the ball and skin during impact was not clear. Therefore, participants were asked to wear clothing over the impact site, such as black lycra cycle shorts, protecting the skin surface and improving video contrast.

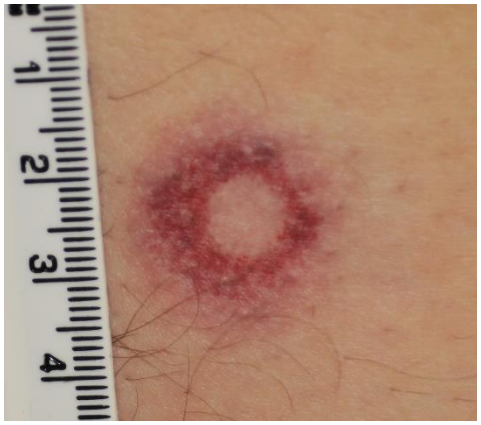

Figure 4-33 Severity of impact mark on the thigh, from impacts to bare skin

4.13.3 Pilot work findings

Although the use of black clothing improved the contrast of the ball within the video (Figure 4-34), the recorded videos were too dark and it was found that modifying brightness and contrast settings post-recording not only improved image clarity but allowed for some details to be observed, which were originally not visible. This is shown in Figure 4-35, where only part of the deformation is visible, but can be clearly seen after editing. The limitation of covering the skin is that it reduced the

detail associated with the tissue wave generated. As this wave could not be specifically quantified, the reduction of wave information could not be measured.

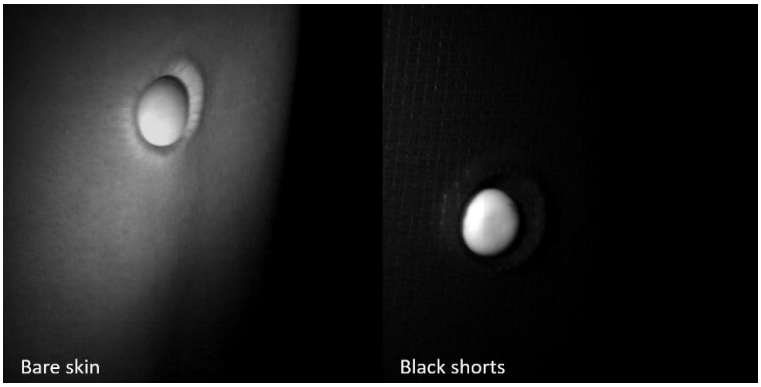

Figure 4-34 Improved video contrast of ball from thigh by introducing black shorts

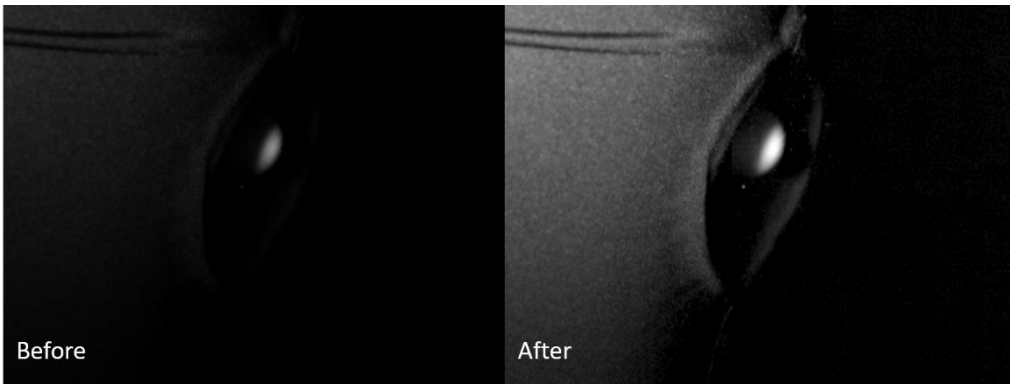

Figure 4-35 Video quality before and after contrast alterations

Like the previous pilot, the impacts could not be clearly recorded for both participants - the impact occurred just outside the camera's field of view, causing the tissue response to mask part of the impact (Figure 4-36). Even though measures which were put in place to improve repeatability of impacts, paintball markers do not fire consistently. This, combined with the variances in thigh shape between participants, means that there will always be a risk that some impacts may not be captured. Although this influenced what data could be extracted from the video, visual assessments could still be made.

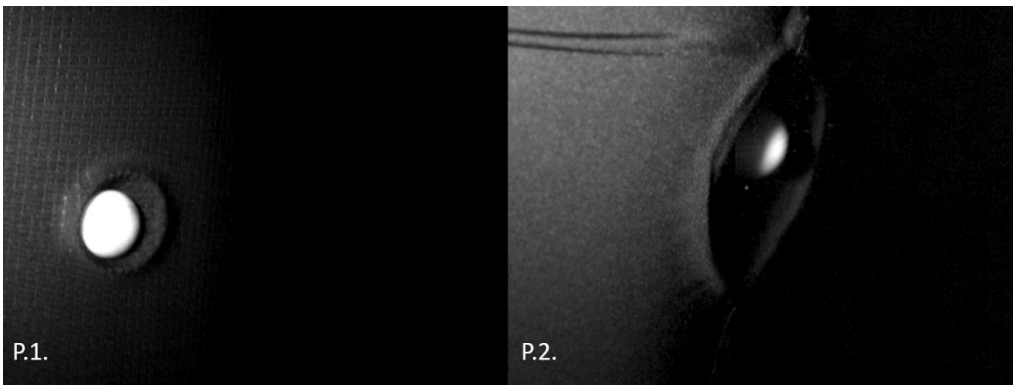

Figure 4-36 Clarity of both pilot impacts – P.1. impact in camera view, P.2. impact not completely in camera view

As seen previously with the introduction of improved lighting conditions and faster recording rate, the clarity of both ball and tissue deformations during impact was improved. The introduction of the black shorts improved the contrast of the ball from the skin, whilst the lighting ensured that the tissue deformations generated could still be observed. It was not possible to determine if the introduction of shorts reduced the level of deformation generated compared to bare skin – however it could be said to be minimal. It did have an effect on the appearance of the bruising generated (shown below in Figure 4-37).

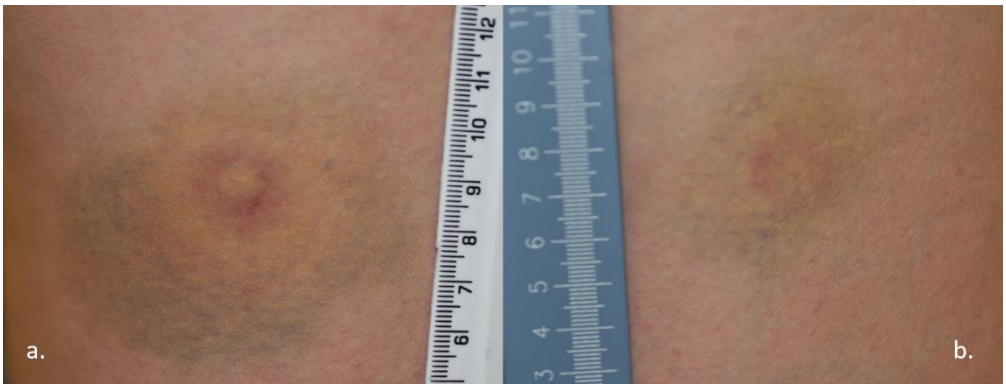

Figure 4-37 Effect of shorts on bruising a. bare skin impact b. shorts impact

As for data extraction, given the findings of Section 4.11, only the Matlab function was used to characterise impacts, with the first and last 15 data points being excluded. Compared to the previous pilot, the changes in methodology resulted in a clear pattern being identified, with peak force being characterised by a greater number of data points.

For the first participant, the results of both pilot tests can be compared (Table 4-12). Unlike the first pilot, the point of impact was able to be identified from the data, whereas before it was identified by watching the video recording.

Table 4-12 Impact characteristics from P.1 pilot tests to the thigh

Pilot Number	1	2
Impact velocity (m/s)	63.8	73.1
Impact time (ms)	0.444	0.444
Time to peak force (ms)	0.370	0.370
Peak impact force (N)	1,110	1,190

The same general force pattern was observed of two distinct peaks (Figure 4-38), however, the Matlab function gave a clearer trace whilst emphasising the inaccuracies found when manually extracting the data (i.e. less chance of over/underestimating values). A mechanical explanation of these peaks is presented in Chapter 7.

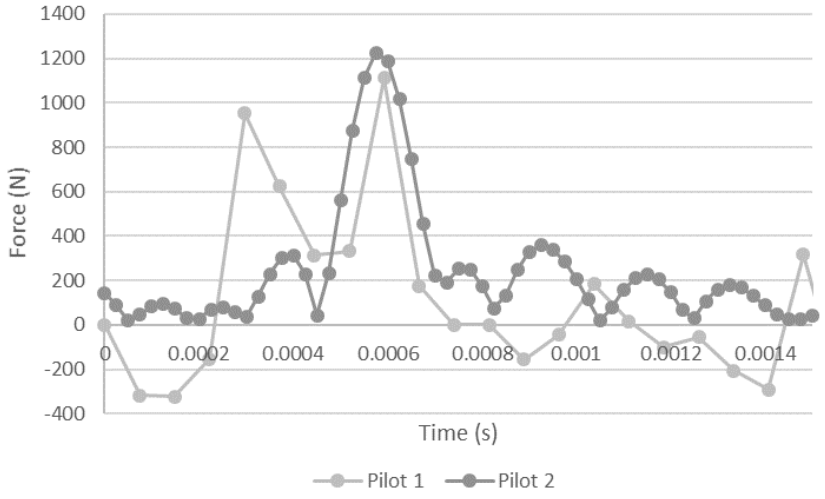

Figure 4-38 Force results for both pilot tests to the thigh for participant 1

With the 2nd pilot impact being characterised by a greater number of data points, the most prominent difference is at the first peak which represents the point of contact. There was a difference in impact velocity between the two tests (a

difference of + 9.25 ms^{-1}), which would have been expected to have resulted in a higher peak. The opposite was in fact observed (1st peak force decreased from pilot 1 to pilot 2). With the increase of data points and thus a more accurate impact characterisation, it is likely that the difference was due to manually extracting data from the videos, resulting in over estimations.

Another factor was the change in camera frame rate. With the second pilot containing a larger volume of data, the pattern is more representative of the impact compared to the first pilot. This combined with the move away from manual measurements explains the change in pattern.

The presence of the oscillations both before and after impact indicate that the Matlab function may not be tracking the centre of the ball's mass correctly, as a steady line would be expected to be seen. Instead, what is represented is the elastic oscillations of the ball shape as it travels through the air.

Comparison of the second participant's results was not possible and this is explained in the following section.

4.14 Pilot limitations

The main limitation for this pilot was that the impact data for P.2 could not be compared with P.1 or with the findings of the first pilot. This was a result of a combination of the extent of tissue deformation and camera angle, causing the impact to not be captured clearly.

A point of contact could be identified from the data. However, from the force trace produced (Figure 4-39), there were no two distinct peaks which followed the pattern previously observed.

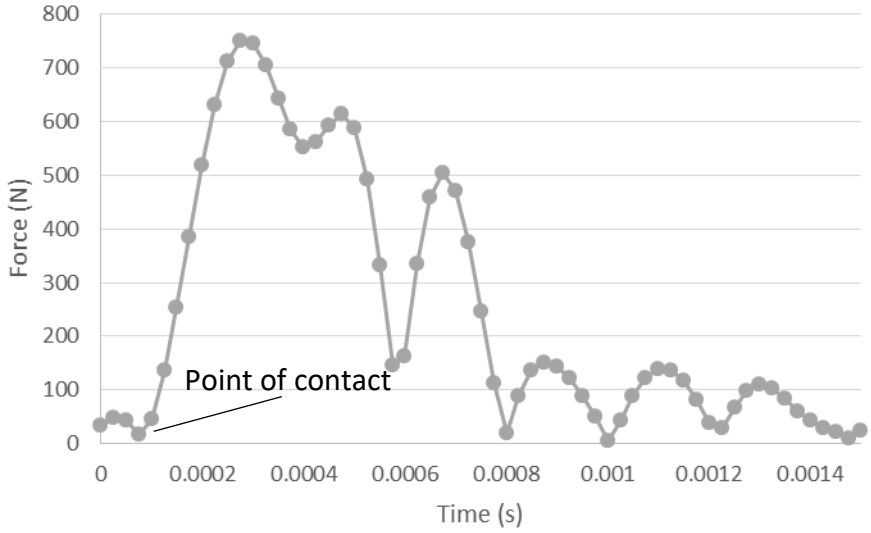

Figure 4-39 Force trace for P.2's second pilot thigh impact

Other issues encountered during this pilot included the equipment itself. During testing, the protective screen became problematic if the ball clipped the edge of the hole instead of passing straight through. This resulted in the impact location either being too high or low to be captured by the high speed camera. As this also increased the risk of unintended injury to participants, the decision was made to increase the diameter of the hole.

By looking at the accuracy results for a 6 m firing distance from Section 4.2.7, it would be expected that most shots would go through a hole of 8 cm (2SD). Precision measurements had been made using the centre of each impact but did not include the diameter of the ball itself (1.6 cm). To increase the hole diameter to 9.6 cm, given shots tended to clip the boards edge rather than fail to go through, was considered inappropriate. This was as if a ball was clip the edge later in the study there would be a greater risk of target impact location being missed or not caught by the high speed camera. Therefore, the diameter of the hole was increased by 1 cm (to 9 cm), in an attempt to both improve the success of direct impacts whilst ensuring the safety of participants.

4.15 Data analysis continued

4.15.1 Data from wooden board

As the Matlab function was shown to calculate marker velocity accurately, it was assumed that all following calculations were correct. However, when it came to accounting for camera angle, the methodology could be improved. Up until this point, the camera angle had been calculated based on positional and distance measurements made by the researcher. Even in marking out where the equipment should be placed for future tests, exact positioning could not be guaranteed. This therefore brought some variability into the results.

To determine the effect which this had, impacts were delivered to a wooden board and analysed.

4.15.2 Methodology

As performed in previous tests, the paintball marker was fired from a distance of 6 m onto a wooden board. The high speed camera was placed at an angle to the board (later calculated to be approximately 50°). The wooden surface was covered by black material to ensure a high contrast between the ball and background – thus replicating the experimental conditions which would go on to be implemented in the study. The chronograph was set up to ensure the paintball gun as firing at the previously stated safe limits.

As before, the camera was set to record at 40,000 fps, with the LED lighting being used to illuminate the target area. As in previous tests, the protective screen was positioned 50 cm in front of the wooden board, providing a predictable impact location which the camera could focus on. A total of 20 impacts were recorded. For data analysis, each video was run through the Matlab function, using the calculated camera angle. For each test, the first and last 15 data points were excluded and ANOVA (single factor), was used to determine statistical significance.

4.15.3 Findings

4.15.3.1 General findings

Overall, the use of the Matlab function give a clear, repeatable representation of each impact. For the velocity traces (Figure 4-40), the ball is not travelling at the same velocity for each impact; as expected given the variability of firing velocity (see Section 4.2.6). One test was excluded (test no. 9) as the material covering the board came loose, masking the ball during its impact with the board.

Like velocity, the force profiles generated followed the same pattern, as would be expected. The majority of peak forces ranged between 1,000 and 1,600 N (Figure 4-41). There are 2 distinct peaks after impact, which occur after the ball has left the skin. This is linked to the deformation of the ball as it returns to its original spherical shape.

ANOVA of all 19 impacts indicated that there was no significant difference between any of the velocity traces, or any force traces calculated (p = 0.258 and p = 0.378 respectively). This confirmed that the Matlab function is reproducible.

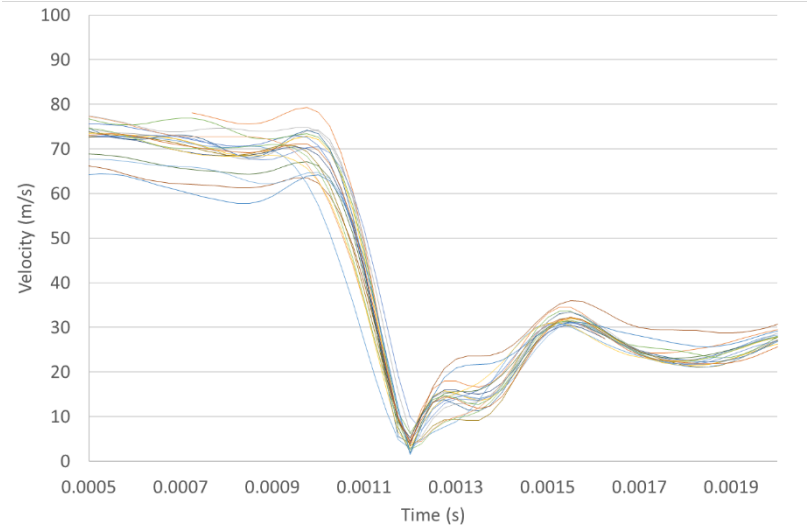

Figure 4-40 Velocity traces for each of the 19 wooden board impacts

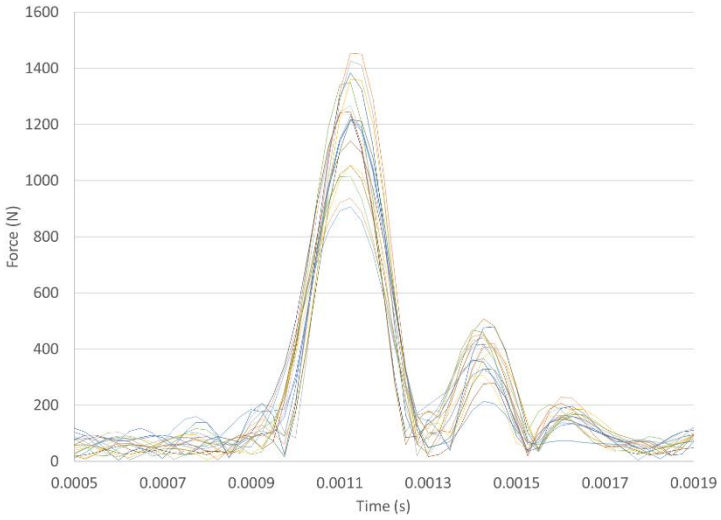

Figure 4-41 Force traces for each of the 19 wooden board impacts

4.15.4 Velocity calculation problems

Although the traces generated by the Matlab function were repeatable, there was a problem with the velocities calculated prior to impact. When compared to the recorded firing velocities, in some cases the impacting velocity was unexpectedly higher than the firing velocity (highlighted within Table 4-13). Impacting velocity was calculated by averaging approximately the first 34 data points before impact began. However, as not all recordings captured the ball pre-impact for the same length of time, there were not always 34 data points available.

Although the introduction of the Matlab function was found to improve velocity calculation accuracy, there was clearly a problem when the camera position changed from being perpendicular to the ball's path of travel. To eliminate this problem an alternative method of angle estimation had to be developed.

Table 4-13 Chronograph and Matlab calculated velocities compared

Test	Firing Velocity	Impacting Velocity
1	73.0	73.0
2	75.0	76.7
3	74.2	75.1
4	73.8	74.4
5	73.3	76.3
6	75.5	78.6
7	74.9	75.5
8	75.1	66.2
9	73.9	64.3
10	74.9	74.7
11	73.8	73.3
12	74.5	69.9
13	73.9	69.3
14	73.5	76.9
15	71.7	76.3
16	73.7	73.6
17	73.0	73.9
18	73.6	74.9
19	74.3	64.6
20	73.3	74.4

4.16 Scale setting

Up until this point, the measurement scale for each recording was based upon the diameter of the rubber ball and the camera angle which was calculated based on its position within the experimental setup.

As an alternative, the use of a grid scale was introduced (a 10 x 10 cm grid (Figure 4-42)). The intention was to record an image of this grid positioned on the ball's path of travel, then using this grid as the basis for setting the measurement scale. This would eliminate any inaccurate estimation of camera position and ultimately the need to know camera angle. In addition to this, the Matlab function itself was altered not only to accommodate the introduction of a scale, but to improve the ball tracking process.

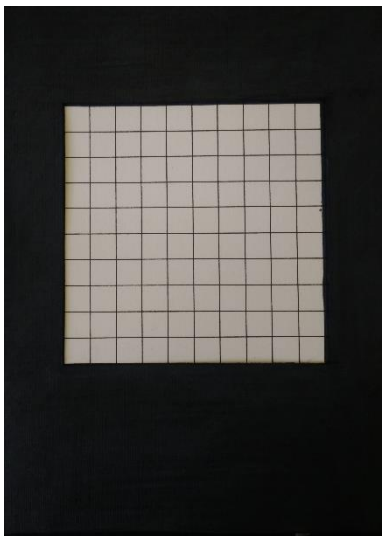

Figure 4-42 10 x 10 cm grid

4.16.1 Code alterations

For this to work, the function was set up to firstly import the image of the scale, then detect the 4 outermost corners (Figure 4-43). The two x and two y distances were then defined as 0.1 m in length, creating a pixel to meter ratio, which could then be applied as the scale for the recorded videos.

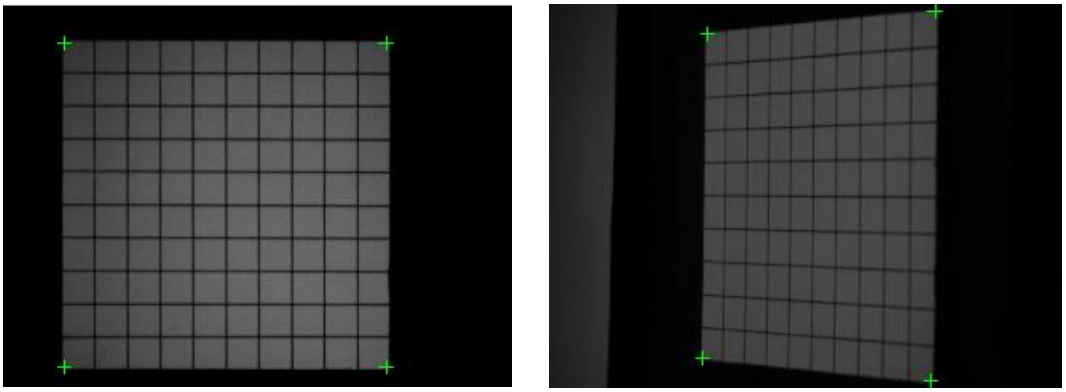

Figure 4-43 Corner detection of scale grid

Previously the ball tracking was based on the user outlining the shape of the ball in the first frame, then this information being used to locate the ball in each of the following frames. This made the process very time consuming and introduced some subjectivity when defining ball size/shape. As the videos contained a dark background, the function was changed to track the centre of any white object (in this case the ball). This removed the user subjectivity and substantially reduced the processing time required.

4.16.2 Scale setting accuracy

To assess the accuracy of the use of a grid scale, chronograph and high speed camera recordings were made of the paintball marker firing velocity and compared, using the high speed camera set up described in Section 4.11. A total of 40 recordings were made, 20 with the camera perpendicular to the ball's path of travel and 20 with the camera set at an unknown angle. As part of the code alterations, the 4^{th} order Butterworth filter which caused 30 data points to be excluded, was changed to a 7-point binomial filter to try reduce the amount of data being excluded.

4.16.3 Findings

Overall, the velocities calculated using the altered code appeared to be consistent. From the traces shown in Figure 4-44, it is clear that the again the filtering influences the data at the start and end of every recording. Therefore, before an average velocity for each test was calculated the first and last 4 data points were excluded from each test. These 8 points were also excluded from all future data.

Once the camera was moved to be at an angle to the ball's path, a similar trend was seen. However, unlike the perpendicular trials, each test showed decreasing velocity (Figure 4-45). This is likely to be due to the fact that for the scale image being at an angle, the dimensions are not perceived as equal. Therefore, at the start of the recording the ball appears larger moving further faster, while towards the end it appears smaller, moving slower.

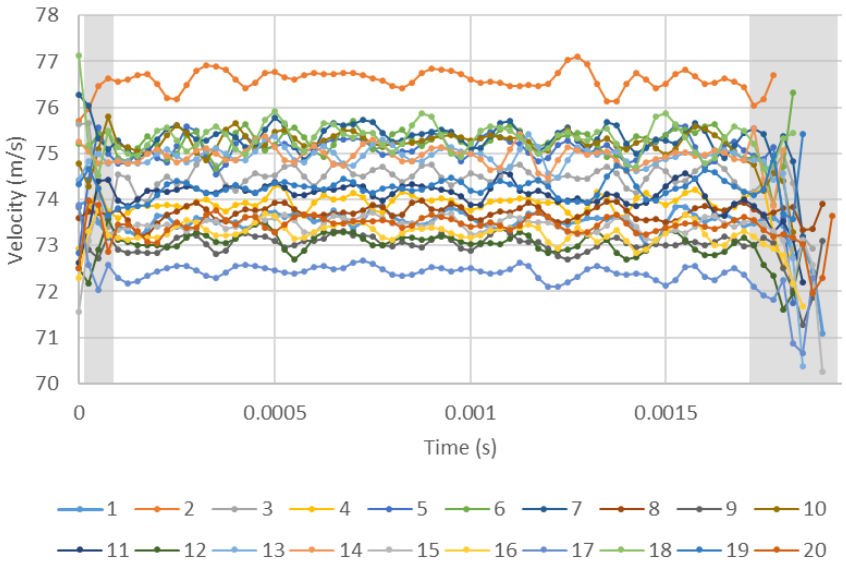

Figure 4-44 Perpendicular velocity traces for each test

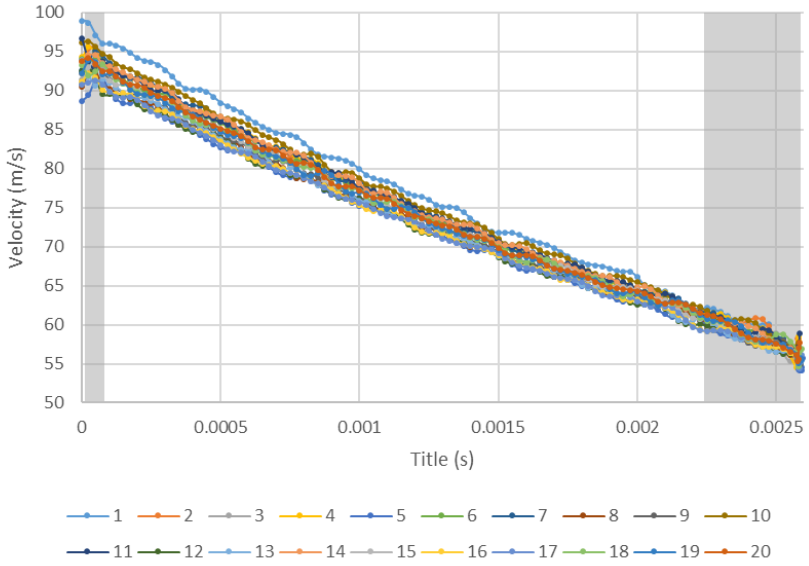

Figure 4-45 Angled velocity traces for each test

Although the change in camera angle appeared to produce different trends in velocity, when the average firing velocity was calculated for each test they appeared very similar to that recorded by the chronograph (Table 4-14). Although velocity estimations from the video recordings were higher than the chronograph, this occurred in all cases, bar one (highlighted within Table 4-14). However, in this case the difference can be considered negligible (0.02 ms^{-1}).

As previously mentioned, the chronograph was being taken as the 'gold standard' for recording firing velocity; as it is the standard method used. Although not perfect, the linearity observed is parallel and thus, similar to that of the chronograph in both perpendicular and angled cases (high r^2 values of 0.90 and 0.79 respectively) (Figure 4-46 and Figure 4-47).

Table 4-14 Comparison of firing velocities recorded by the chronograph and the high speed camera

Test	Perpendicular Camera		Angled Camera	
	Chronograph (m/s)	Camera (m/s)	Chronograph (m/s)	Camera (m/s)
1	71.3	73.5	75.1	76.9
2	74.4	76.6	73.4	73.9
3	72.3	74.5	71.7	74.0
4	71.9	73.9	72.7	74.1
5	73.2	75.1	70.3	71.0
6	72.9	75.3	71.9	73.8
7	73.5	75.4	72.8	74.1
8	71.9	73.7	70.5	72.0
9	71.3	73.1	71.3	72.3
10	73.5	75.3	73	74.7
11	72.7	74.1	71.3	73.9
12	71.5	73.1	70.9	71.6
13	73.4	75.0	72.3	72.3
14	73.2	75.0	73.2	74.4
15	72.2	73.5	72	72.9
16	72	73.3	70.8	71.8
17	71.1	72.4	70.7	71.4
18	73.2	75.3	71.7	72.6
19	72.1	74.3	71.9	72.6
20	71.6	73.5	72.5	73.2
Average Difference (m/s)	1.82±0.33		1.17±0.62	

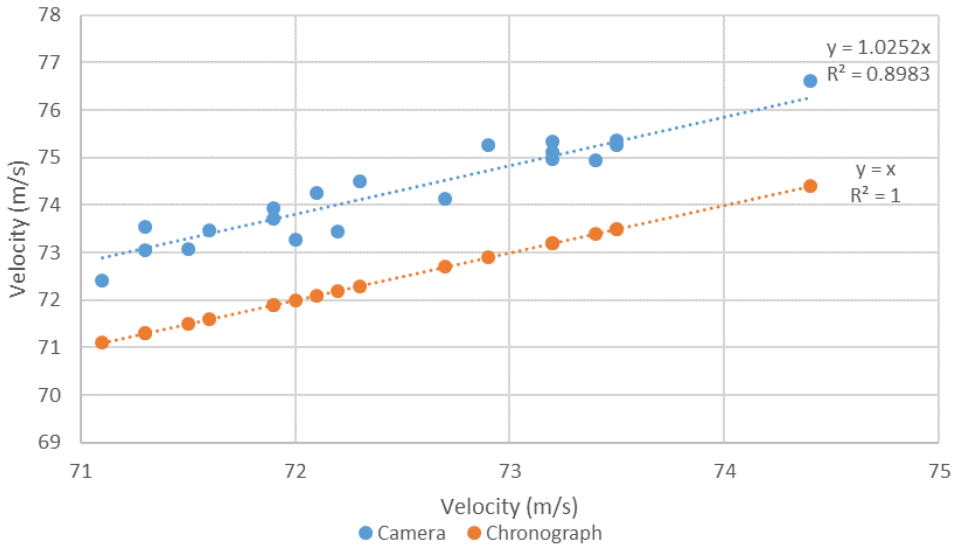

Figure 4-46 Correlation between chronograph and high speed camera perpendicular recordings

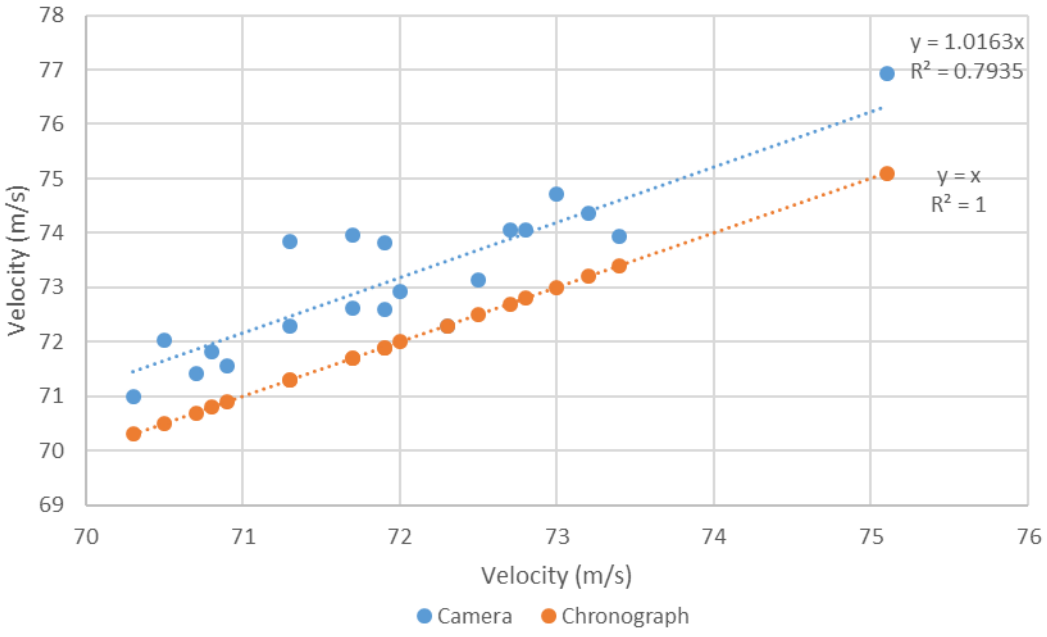

Figure 4-47 Correlation between chronograph and high speed camera angled recordings

Overall, it was found that the new code alterations caused the calculated velocities to have a higher difference when the camera was perpendicular to the ball's path of travel compared to the angled camera results. This was not considered to be a significant problem, particularly as any future work would involve the camera being set at an angle.

Furthermore, the differences between the camera recorded velocities and the chronograph velocities are minor (an average of 1.17 ms^{-1} for angled camera recordings). A correction factor was considered to apply to the velocity data to closer represent the chronograph readings. However, as previously stated within this chapter, although the chronograph is considered a gold standard no information on how chronograph accuracy was determined by the manufacturers could be found. Therefore, the differences observed between camera and chronograph were considered negligible and camera recordings considered accurate and thus applicable to all future work.

4.16.4 Impacts on board

With the changes made to the Matlab function, recordings of impacts onto a wooden board were repeated (as described in Section 4.14). These videos were then run through the new function to collect a reference impact force profile and see the if the changes altered the profile in any way. this would also confirm the complete reproducibility of the data collection method.

4.16.5 Findings

As seen with previous tests, the traces observed were similar for all tests. There was one exception to this (Test 3), where the impact occurred at a downwards angle at the bottom of the camera's field of view. This test was therefore excluded.

Unlike previous data, the forces (shown in Figure 4-48), did not show a singular clear peak. This is likely due to the ball tracking detecting the deformation of the ball in more detail than previously.

The first peak, reflected the point at which the ball has impacted with the board and began to slow in its forward motion whilst the second peak reflects the point at which the ball has fully deformed and ceased its forward motion. The third peak reflects the point at which the ball's directionality has changed and it has also elongated in shape prior to deflecting completely off the board (as shown in an example in Figure 4-49).

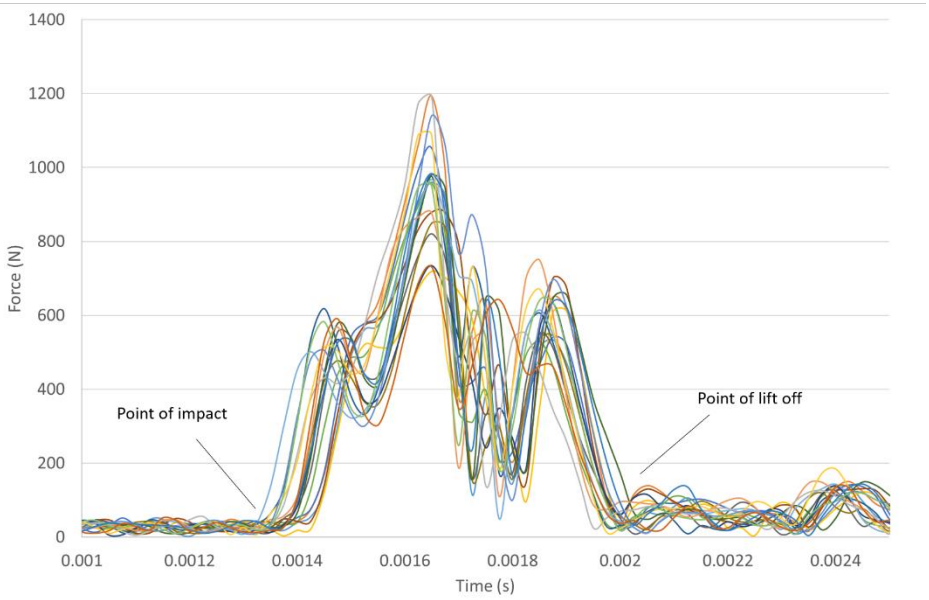

Figure 4-48 Force traces calculated using Matlab for blunt impacts delivered to a wooden board

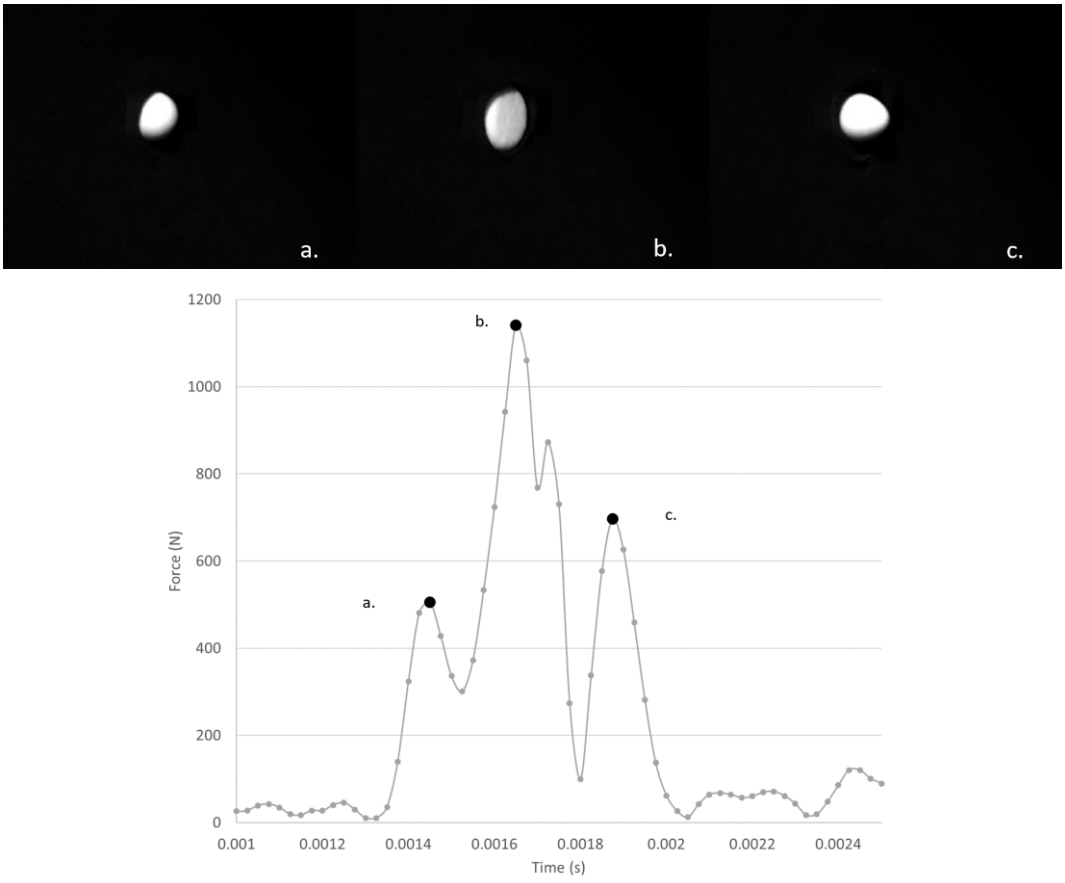

Figure 4-49 Example force profile with associated snapshots relative to its 3 distinct peaks a., b. and c.

This difference in pattern links closer to that observed for the pilot traces on human tissue. With impacts being delivered by the same object it would be expected that the pattern would be similar. However, it is anticipated that the levels of force and the timings for each peak will differ for human tissue, as the mechanics of each impact will be dependent on the stiffness of the impacted tissue.

It was therefore concluded that this final version of the Matlab function, making use of a 10 x 10 cm grid as a scale was repeatable, reliable and thus appropriate for use in determining the impact characteristics of a blunt impact by a reusable paintball.

4.17 Marker aim problem

4.17.1 The issue

Throughout all the pilot and methodology testing, it became apparent that the aim accuracy of the marker had reduced, with impacts becoming increasingly unpredictable and unable to go through the hole in the protective screen. It was considered that this may be due to either the equipment positioning (both marker and protective screen), changing slightly between use, the marker requiring to be re-oiled and cleaned or the effects of cylinder pressure decreasing during use. However, on accounting for all these parameters, the ability of the marker to consistently fire the reusable paintballs through the hole in the screen did not improve.

Another possibility considered was that the balls themselves became damaged throughout their use. This would therefore cause them the become either misshapen or less solid in structure and thus, would not fly through the air with the efficiency they had at the start of this study.

A new set of these reusable paintballs was purchased (Just Paintball, UK), and when used, the aim of the marker appeared to become more consistent. However, the number of shots to successfully go through the screen hole was limited. Therefore, reassessment of marker accuracy and precision was carried out.

4.17.2 Methodology

The marker was set up as in all previous testing, within a purpose built table mount positioned 6 m away from a target.

The target was again made by placing carbon paper between two sheets of A3 card, then securing it to a wooden board. Using a full cylinder or air, a total of 10 shots were fired at the target. A new target was then secured to the board and the process repeated a further 3 times. The aim of the marker, as indicated by the laser pointer guide, was also marked on each target to provide a point of reference when assessing the spread of impacts. All shots were fired at approximately 74 ms^{-1}.

4.17.3 Findings

Of the 40 shots gathered for this test, all were observed on the targets, with some observed to overlap with others (for target images, see Appendix E). As seen previously for the 6 m test, all impacts occurred within the same area. However, this impact area was in a different location to that seen in the initial accuracy and precision tests (Figure 4-50).

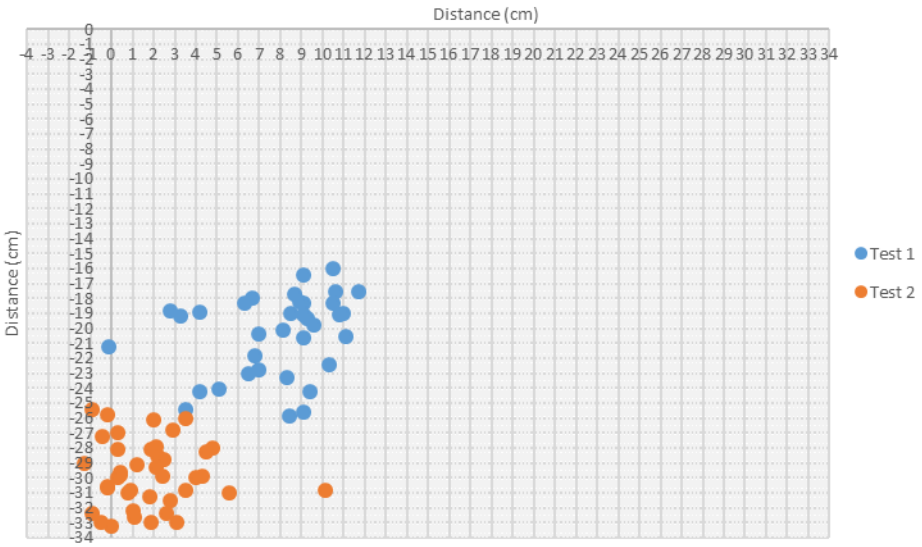

Figure 4-50 Plot of impact sites for all 6 m shots: Test 1 = impact location from original 6 m accuracy and precision test; Test 2 = impact location for reassessment of 6 m accuracy and precision test

Comparing the average impact locations, although in different areas, the spread of impacts was similar (Figure 4-51). Therefore, the mark on the screen to be used as

the laser guide reference point for shots delivered from 6 m was changed to reflect that of the new average impact location.

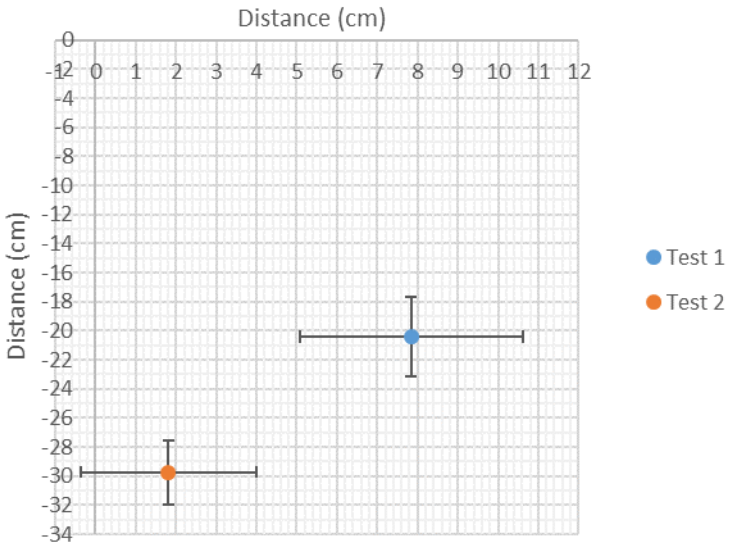

Figure 4-51 Plot of average impact locations for original and new 6 m accuracy and precision tests

4.18 Pilot imaging and analysis

Since purposeful injurious impacts were intending to be made on individuals, it was imperative that considerable pilot testing was undertaken to ensure that all data collected on volunteers would be useful and errors minimised wherever possible. So far, this chapter has detailed this pilot work for the mechanical characterisation of the impacts. The next section details pilot work regarding the development of chosen imaging methods for bruise characterisation.

To determine the suitability of colour, CP and IR photography, alongside L*a*b* colour measurements via computer software, a preliminary investigation was carried out. Images taken during the pilot work outlined earlier in this chapter were analysed. It should be noted that the primary aim of the pilot study was to determine safe and controlled bruise generation conditions, not to test photography techniques (hence not all imaging equipment being available during the full pilot testing period).

4.18.1 Colour photography

Bruising was photographed primarily using colour photography. Following impact, colour photographs were taken daily (excluding weekends), for 11 days, using

a Nikon D300 camera (Advanced Camera Services, England) with a micro Nikkor 60 mm lens (Advanced Camera Services, England). The camera was secured with a tripod, operated using the auto ISO and F-stop settings, manually focused and with the flash on. Images were taken under the same artificial lighting conditions each time. A ruler was used for scale in each image and no image standardisation was performed. Due to time constraints, sequential images could not be continued until the bruises had completely faded. Pilot work relates to the bruising generated on the thigh of each participant.

As previously stated, the main aim of the pilot was to establish a safe method of blunt impact generation; therefore, the photography which was carried out was simply to document the bruising and not an assessment of the imaging technique itself. However, at this point colour photography was noted as being capable of documenting bruising and the range of colours which may be presented (Figure 4-52).

4.18.2 CP photography

During the pilot work, CP imaging was able to be tested during the photography of P.2. by positioning polarising filters over the camera flash and lens at 90° to each other, no camera settings were changed. Although producing images which are darker and which contain less colour definition, the contrast between bruise and skin visibly appears improved Figure 4-53). As with the colour images, CP images were not standardised at this stage.

Figure 4-52 Timeline of pilot bruising for both participants. Photos taken immediately and 1 hour post impact, and days 3, 4, 6 and 7 post impact

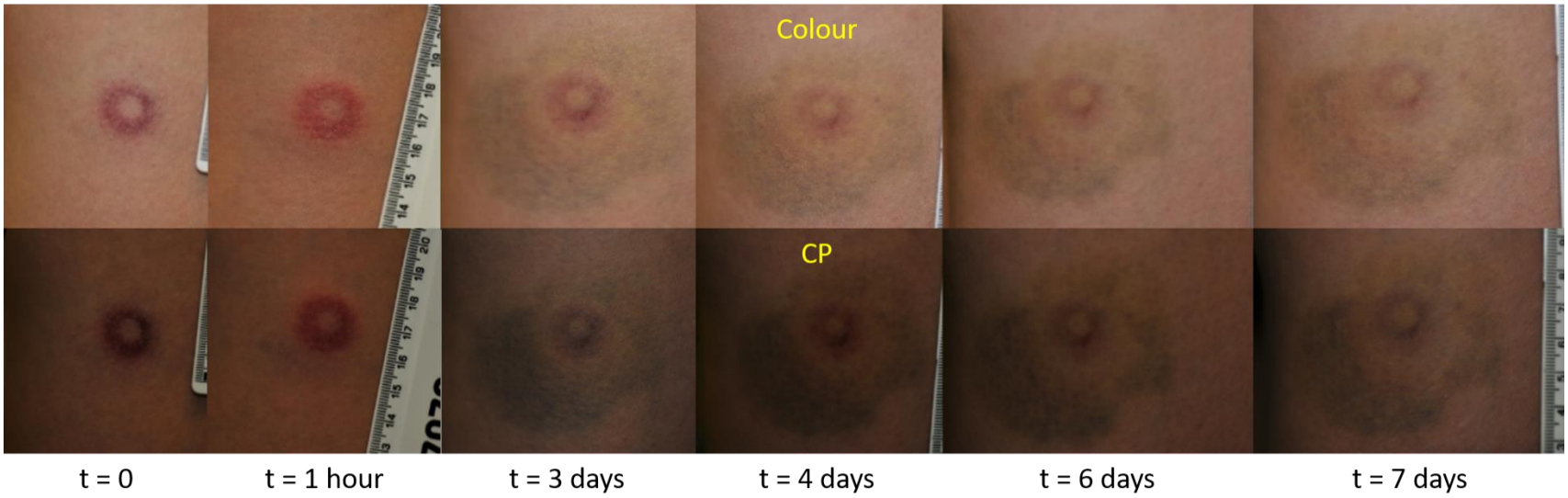

Figure 4-53 Colour and CP 1 week timeline for P.2. Photos taken immediately and 1 hour post impact, and days 3, 4, 6 and 7 post impact

4.18.3 IR photography

IR photography was not available as part of the pilot. Once an IR light source was purchased (Amazon, UK), practice images of accidental bruising were taken to determine appropriate camera settings and lighting conditions to be used in the main study. The light was positioned on the camera as this would allow the imaged object to be completely illuminated (no shadows). Images were not white balance corrected at this stage.

The IR light source was not purpose built for this type of photography and so its wavelength was measured to ensure it matched that which was advertised (850 nm), and thus within the detectable range of the camera (720 – 1100 nm). This was found to be true, with the light intensity being strongest at 850 nm (Figure 4-54).

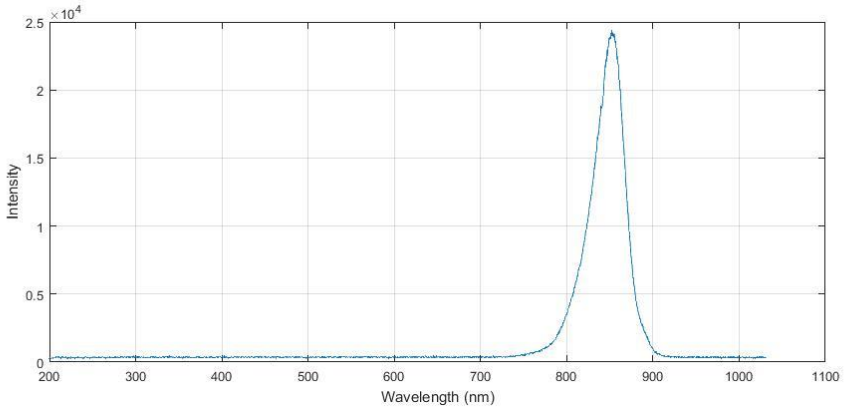

Figure 4-54 Measured wavelength of IR light source

Normally, IR photography using an artificial light source requires a dark environment, thus ensuring no influence or other sources such as sunlight. However, for this particular light source, a dark environment caused the image to be flooded with light. Adjusting the light position did allow for an image to be taken but was ruled out as it required to be close to a power source (making it an impractical setup) (Figure 4-55a). The addition of tracing paper over the LED lights to act as a diffuser did improve image clarity, though the images were still over exposed (Figure 4-55b).

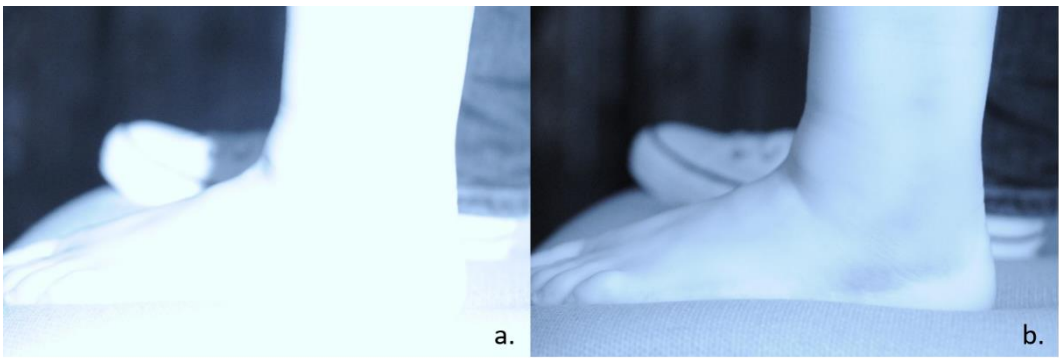

Figure 4-55 Examples of overexposed IR images a. uncovered light b. light covered with tissue paper

IR imaging was then attempted with artificial room lighting on. This successfully removed the problem of over exposure. Although, unconventional, images were taken of the room prior to the IR light source being used, showing the lighting did not influence the captured images.

The resultant images captured were able to detect bruising, and some examples of how this compared to the colour and CP images are shown in Figure 4-56 (note: these bruises were caused accidentally, are of an unknown age and presented with permission of the individuals).

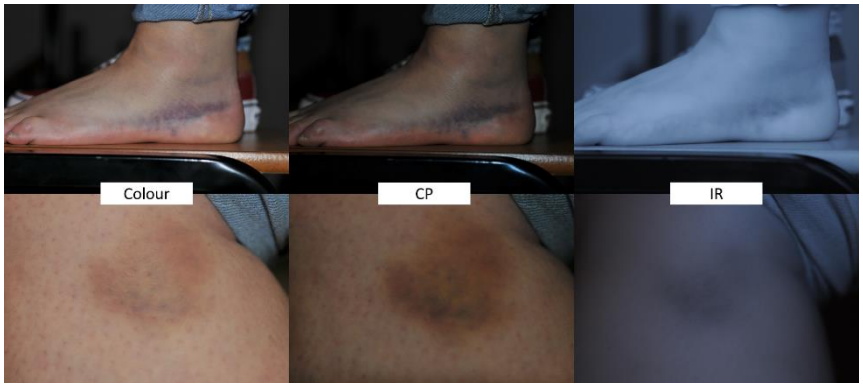

Figure 4-56 Examples of unstandardised colour, CP and IR of accidental bruising on the foot and leg

Early comparison of the three techniques indicated that CP improved image contrast compared to colour photography, while IR imaging looked to be best at capturing the darker areas of a bruise. However, without a complete timeline, an indication of the effectiveness of each technique for bruise documentation could not be determined.

4.18.4 Pilot L*a*b*

From the pilot participant's images, L*a*b* measurements were made using Photoshop to select bruise and non-bruise areas. This was based upon the method used by Baker et al., (2013), for contrast measurements and this then went on to be used in the main study (see methods Chapter 5 for full methodology).

Initial indications suggested that, given the bruising was of different sizes and colour intensity, a pattern did appear to be present. As shown in Figure 4-57, both bruises tended to lighten, go from red to green, and from blue to yellow. P.1 patterns appeared more variable in comparison to P.2 however, as previously indicated not all equipment was available at the time pilot imaging took place. Standardisation of the images was unable to be carried out and thus it was expected that the variability observed was due to this methodology limitation. Overall the results appeared promising for going onto a larger study with standardised images.

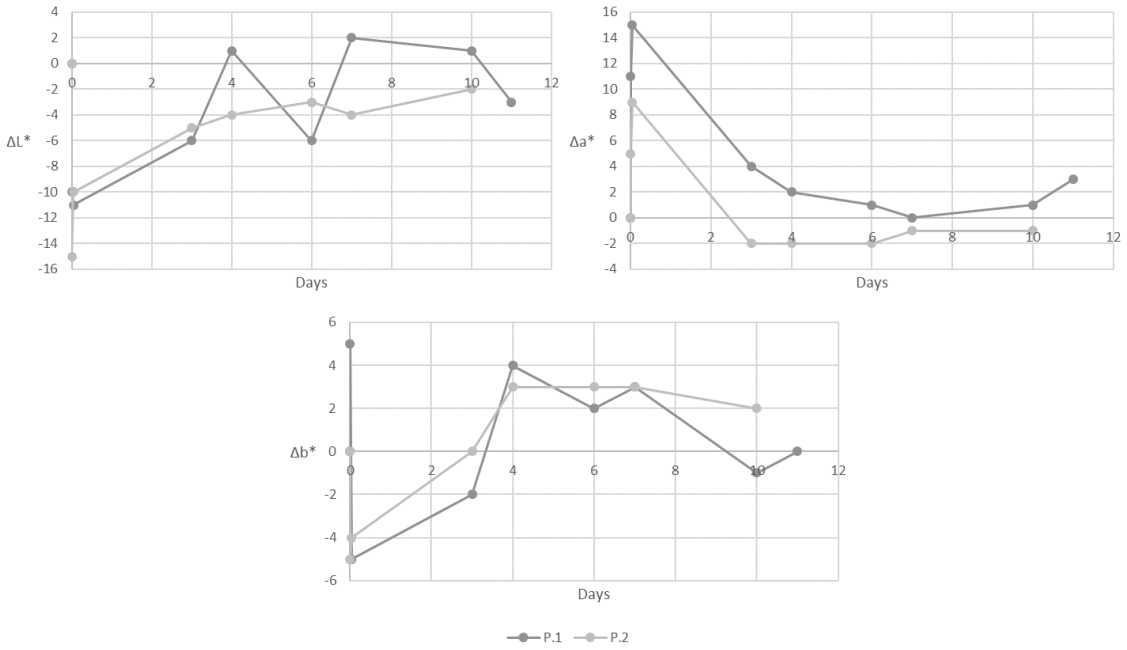

*Figure 4-57 Plots of L*a*b* values for both participants*

Chapter 5

Implemented Methodology

5.1 Ethical Approval

5.1.1 Ethical approval

Ethical approval for this study was obtained for the University of Strathclyde's University Ethics Committee. All recorded data was pseudo-anonymised for use in this study. For each participant, a unique 5-character code was generated using the last 2 letters of their postcode, the number of the month they were born and the first letter of their mother's maiden name. Personal details (name, email address and a contact number), were collected and only used to contact the participants directly to discuss arrangements for the study.

5.1.2 Exclusion criteria

Participants were to be aged between 16 and 60 years of age and to reduce the risk of any severe injury the following exclusion criteria were put in place:

- Anyone taking anti-coagulant or anti-platelet medications e.g. warfarin, dipyridamole, clopidogrel, ticlopidine, cilostazol and heparin
- Anyone who takes anti-inflammatory medication e.g. ibuprofen, diclofenac and aspirin on a regular basis
- Anyone taking oral or injectable steroids
- Anyone who had been diagnosed with any of the following medical conditions – coagulation deficiency, bleeding disorders, haemophilia, von Willebrand's disease, vitamin K deficiency, diabetes, sickle cell disease, anaemia, bone marrow disorders, any autoimmune disorder causing clotting problems, leukemia, thrombocytopenia, thrombocytosis, Bernard-Soulier syndrome, Wiskott-Aldrich syndrome, Glanzmann's thrombasthenia and polycythaemia rubra vera, heart disease, cancer stroke or transient ischaemic attack, nephritis, liver disease, Ehlers-danlos syndrome or other conditions causing problems with collagen formation and structure
- Anyone who has had an organ transplant
- Anyone who is pregnant
- Anyone who had donated blood or blood product in the past 60 days

- Anyone who had undergone major surgery or has significant scarring on the thigh which was to be tested

To keep data anonymous, anyone with any identifying marks, tattoos and/or piercings on the thigh which was to be tested, were also excluded.

5.1.3 Recruitment methods

Staff and students of the University of Strathclyde were invited to take part and if interested, provided with a participant information sheet detailing the purpose of the study, the level of commitment etc., expected from them as a participant, and the exclusion criteria. They were also provided with a consent form which was signed prior to participation in the study. The participant invitation letter, information sheet and consent form are shown in Appendix F.

5.1.4 General health questionnaire

Chapter 2 identified that there are many things which influence bruising, from diet to specific blood thinning medications. With the exclusion criteria preventing those at a greater risk of excessive bleeding from taking part, it was still necessary to take note of each individual's personal characteristics.

Each participant was asked to complete a general health questionnaire, providing information which would allow for participants to be categorised by age, gender, ethnicity, smoking habits, alcohol consumption, medication/food supplement intake and exercise habits. These characteristics would later go on to determine whether individual characteristics influenced blunt impact mechanics and/or bruise formation. The survey was adapted from one used by Scafide, (2012) and is shown in Appendix G.

5.2 Participant involvement

5.2.1 Part 1: Pre-impact

A total of 18 participants were recruited. They were instructed to wear tight fitting black shorts or similar, e.g. leggings, which would fully cover their thigh.

The height and weight of each participant was recorded and then three control images were taken of their right thigh – colour and CP using a Nikon D300 DSLR (Advanced Camera Services, UK), and IR using an IR converted Nikon D300 DSLR (Advanced Camera Services, UK). Both were fitted with a Nikkor 60 mm lens. For each person, both colour and CP images of an X-Rite ColourChecker (Amazon, UK) (Figure 5-1), were also taken to be used later for image standardisation. The same camera settings were used for each mode of photography for each participant (see Table 5-1). The room was fully lit with artificial neon tube lighting (i.e. no sunlight), to keep the lighting conditions as consistent as possible. The cameras were mounted to a height adjustable tripod to ensure images were always taken at 90° to the thigh (and later each area of bruising).

Figure 5-1 X-Rite ColourChecker

For CP images, polarising filters (Knight Optical, UK), were positioned at 90° to each other over the flash and lens. A separate IR light source (Amazon, UK), was used to illuminate the thigh during the IR photography (Note: room lighting was not switched off for IR photography). All images were saved as the raw file format which the camera produced (.NEF file).

Table 5-1 Camera settings used for each photography technique

Setting	Colour	CP	IR
Flash	On	On	Off
F-stop	4.5	4.5	4.5
ISO	Auto	Auto	Auto
Metering mode	Pattern	Spot	Pattern

5.2.2 Part 2: Impact generation

Participants were asked to stand behind the purpose built screen (University of Strathclyde, UK), with the lateral side of their right thigh positioned behind the gap in the screen. A marker was placed on the thigh in the area which was to be targeted and then lined up so that it could be seen through the screen hole (Figure 5-2). The approximate distance between board and thigh was 50 cm.

Figure 5-2 Example of how a participant's thigh was positioned behind the protective screen using the guidance marker

The Photron Fastcam SA4 high speed camera (Photron (Europe) Ltd., UK), with a single Photron High Power multi LED lamp (Photron (Europe) Ltd., UK), and fitted with a Sigma 24-70 mm lens (Photron (Europe) Ltd., UK), was positioned and manually focussed ready to capture the impact. The marker was then removed from the thigh and participants were provided with safety goggles to ensure, in the unlikely event that any stray shot was to bounce up towards their face.

A BT-4 Combat paintball marker (Just Paintball, UK), was secured within a purpose built table mount (University of Strathclyde, UK), at a distance of 6 m from the participant. Positioned in front of the marker was the CED M2 chronograph, fitted with IR screens (Competitive Edge Dynamics), to record the firing velocity for each participant, ensuring safe firing conditions.

The high speed camera was set to record and a single shot was fired at approximately 74 ms^{-1} and only repeated if the shot hit the screen rather than the participant. Reusable rubber paintballs (Just Paintball, UK) (2.6 g with 1.6 cm diameter), were used as the impacting object.

Immediately following impact, the impact site was photographed using the same colour, CP and IR imaging techniques used prior to impact generation. An ABFO NO.2 Bite Mark Reference Scale (Ebay, UK), was used in each photograph (Figure 5-3).

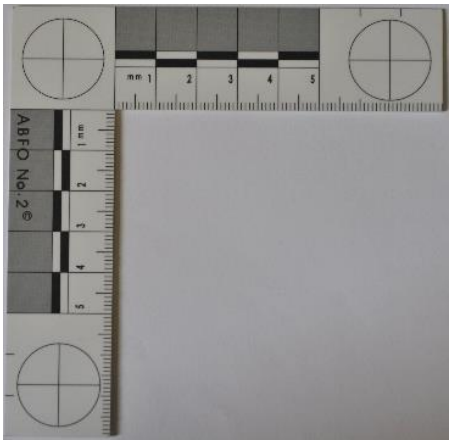

Figure 5-3 ABFO No. 2 bite mark scale

5.2.3 Part 3: Post-impact

Following each successful impact and without moving the position of the high speed camera, a 10 x 10 cm reference grid (University of Strathclyde, UK), was positioned in the ball's line of travel. This grid was then recorded using the high speed camera, to be used as a reference in each participant's data analysis.

For follow-up, participants were required to return to the Biomedical Engineering Department on a regular basis (either on days 1, 3, 5 etc. or 2, 4, 6 etc.), for the following 3 week period or until their bruise had fully healed (whichever was

shortest). In the case that bruising was still visible after the 3 weeks, participants were not required to return. The alternate day pattern was selected as it required the least time commitment from participants whilst still allowing for pattern identification.

For each of the follow-up visits colour, CP and IR images were taken of the impact site following the same methodology as mentioned previously, using the ABFO reference scale each time. Each day a colour and CP image was taken of the X-Rite ColourChecker, to be used for the standardisation of that day's images. All equipment is listed in Appendix H.

5.3 Data Extraction

5.3.1 Individual characteristics

In addition to the details collected within the health questionnaire, the body mass index (BMI), and body surface area (BSA), for each participant was calculated from their height and weight. Neither of these measurements were ideal as they did not provide information on the specific level of adiposity in the thigh, but were considered appropriate for grouping individuals together.

For BMI, it was calculated using Eqn. 14:

Eqn. 14

$$BMI = \frac{w}{h^2}$$

where, *w* is the individual's weight in kilograms and *h* is the individual's height in metres (Willacy, 2016). A list of the weight classifications relating to BMI are listed in Table 5-2.

Table 5-2 List of BMI classifications adapted from WHO, 2016

BMI (kg/m^2)	Classification
< 18.5	Underweight
18.5 – 24.99	Normal Range
25 – 29.99	Overweight
30 – 34.99	Obese Class I
35 – 39.99	Obese Class II
≥ 40	Obese Class III

Using the same height and weight data, BSA was calculated using Eqn. 15 (Willacy and Thomas, 2016):

Eqn. 15

$$BSA = \sqrt{h\left(\frac{w}{3600}\right)}$$

In addition to ethnicity, each participant's skin tone was recorded via calculation of their individual typology angle (ITA°) (Eqn. 16). This system has been utilised in several studies allowing for skin tones to be objectively listed from dark to very light, based on L* and b* values (Chardon et al., 1991; Del Bino et al., 2006; Scafide et al., 2016, 2013). These were taken from the standardised control images. For 3 participants an alternative standardised CP image was used, as metering mode had been set to pattern rather than spot. A full explanation of how images were standardised and measurements taken is listed in Section 5.3.3.

Eqn. 16

$$ITA° = \left[\tan^{-1}\left((L^* - 50)/b^*\right)\right]\left(\frac{180}{\pi}\right)$$

5.3.2 Mechanical parameters from high speed videos

For each participant's impact recording, a screenshot of the relevant grid scale was taken and saved. If necessary, the impact videos were altered to improve contrast and thus the visibility of deformation.

The scale and impact recording for each participant were then run through the Matlab function previously developed. From this, position, velocity, acceleration and force data of the ball were calculated and saved as an excel spreadsheet.

5.3.3 Image standardisation

5.3.3.1 Colour and CP standardisation

For each image a colour calibration was carried out, relating each image to the conditions of the day. Although attempts were made to keep lighting consistent, this calibration accounted for any unknown day-to-day changes.

This process involved creating a camera profile for each day, for each participant. Each colour chart image was opened within Adobe Photoshop Camera Raw and saved as a DNG file. Running this file through ColourChecker Passport Software (specifically for use with the ColourChecker chart), generated a camera profile which was then saved with a unique filename containing the participant reference code, whether it was a colour or CP image and the day on which the image was taken.

Opening the control, bruise and all relevant colour chart images within camera raw of Photoshop, the relevant camera profile can be applied to the control and bruise images (using the camera calibration tab). In addition to colour standardisation, the white balance was also adjusted. This was done by selecting both the participant image and the appropriate colour chart, using the white balance target tool to select the white square within the colour chart. Following this step, each participant image was opened within Photoshop.

At this point the standardisation process was complete and the control and bruise images were saved as TIFF files. This methodology was obtained from Breathing Color® and X-Rite (Color, 2016; X-Rite, 2016).

Bruise images were rotated so that the ABFO scale was aligned to the horizontal and vertical. Each image was then cropped to show only the scale and the

bruise, being saved as TIFF files. Figure 5-4 shows an example of an original then standardised image.

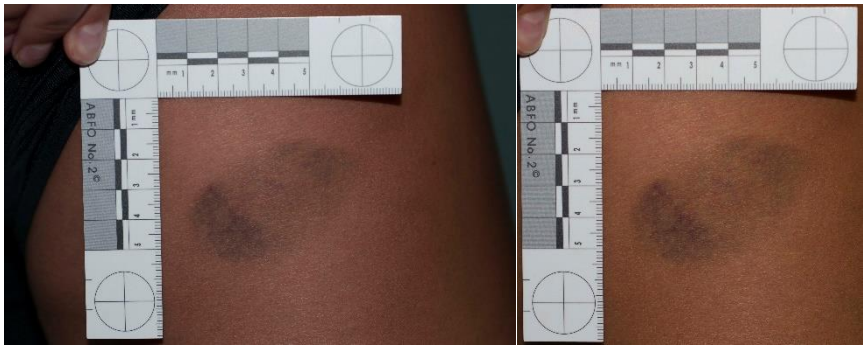

Figure 5-4 Effect of image standardisation A. pre-standardisation B. post-standardisation

5.3.3.2 IR standardisation and alteration

For these images there was no colour reference chart used and the white balance was set using the same method as used for the colour and CP images. A white part of the measurement scale was used as a reference for each day, with the scale in the day 0 image being used for each respective control image. Once standardised they were rotated and cropped as was done for the colour and CP images, then saved as TIFF files.

To improve the contrast of each bruise from the skin, each IR image was altered using the ''curves'' function of Photoshop. Once contrast appeared visibly improved, the image was also saved as a TIFF file. An example of each image pre- and post-standardisation alongside the altered, standardised image is shown in Figure 5-5.

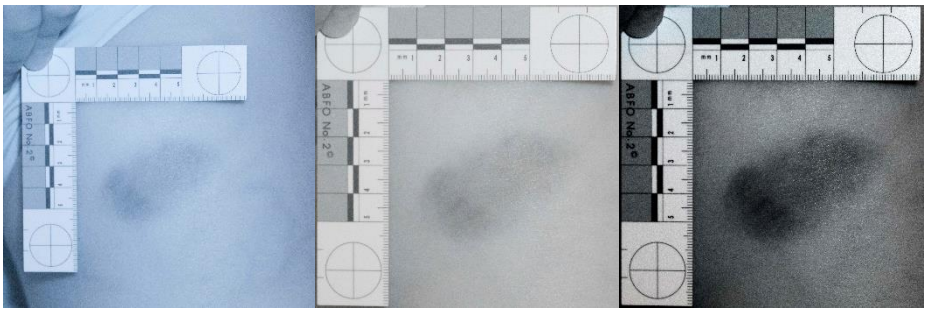

Figure 5-5 Effect of image standardisation A. pre-standardisation B. post-standardisation C. altered contrast Image data

5.3.4 Photoshop image analysis

5.3.4.1 Bruise size

For each standardised image (colour, CP, IR and altered IR), a custom measurement scale was set using the ABFO scale within the image. Image number 0 (immediately after impact), was excluded from all bruise measurements as the impact mark was much more prominent and it was not possible to clearly identify bruising.

Using the first follow up image (either day 1 or 2), the impact mark was selected and covered by a circular shape. The dimensions (height, width and area), of this shape were recorded and applied to all the images of that timeline.

Using the magnetic lasso tool, the outer edge of the bruise was selected and the dimensions recorded. Bruise area was calculated by subtracting the impact mark dimensions from the measured bruise area. However, as the bruising generally healed from impact location outwards, the expanding internal clear zone would be measured using the magnetic lasso tool and subtracted.

For the colour and CP day 0 images, the impact mark dimensions were measured. These dimensions were not chosen to be subtracted from the timeline images as described above, as they were smaller than those observed throughout the rest of the timeline. In addition, where a larger red area was observed around the impact mark, this was also recorded.

5.3.4.2 L*a*b* measurements

Conversion from RGB to L*a*b* colour mode was done for each of the colour and CP images.

Using the measurement scale within the image as a reference, a circular area with 1 cm diameter was used to select 2 areas within the bruise and 3 from the surrounding non-bruised skin.

From observation, it was clear that bruising had greater prominence towards the bottom of the bruise and lighter at the top, therefore the 2 chosen areas were selected to reflect this. Furthermore, these areas were outwith the impact mark area identified during bruise size measurements. The surrounding areas were, where possible, taken at the 12, 4 and 8 o'clock positions. The colours in each area were blurred using the average blur filter and then, using the colour sampler tool, the average L*, a* and b* values were recorded.

The averages of the bruised and non-bruised skin measurements were calculated and then the difference between the two taken as the L*a*b* profile for each bruise image.

5.3.4.3 Image contrast measurements

The contrast measurement of bruise from skin for each photography technique, was carried out using Photoshop following a method proposed by Baker et al., 2013.

All images were converted to greyscale, then three areas of non-bruised skin were selected at approximately 12, 4 and 8 o'clock positions relative to each bruise. Unlike the proposed method, 2 areas of each bruise rather than three were selected. This was due to the circular shape and varying bruise intensity for each image. The selected areas were approximately 1 cm in diameter, scaled using the measurement scale within each image. The selected areas for contrast measurement were the same areas as those chosen for the colour measurements in both colour and CP images.

The histogram tool within Photoshop provided the average luminosity for each area, a value ranging between 0 (black) and 255 (white). The average for both bruised and non-bruised areas were then calculated, with the difference between the two being recorded as the contrast value.

No contrast measurements were collected from images taken immediately after impact, as the impact mark and any immediate bruising were overlapping. The impact mark itself, was excluded from all measurements as it represented the tissue damage which occurred during the impact and not the bruising itself. Therefore, the

first image and last image, where bruising was no longer visible, were recorded as zero.

5.4 Statistical analysis

All statistics were performed using SPSS version 24. Pearson correlation coefficient test was performed on the data to determine the strength of any link between data sets. The Shapiro-Wilk test was conducted to confirm normal distribution of data, with the appropriate tests (t-tests (paired or independent), Wilcoxon-Signed Ranks test, Mann-Whitney or repeated measures ANOVA) being performed to test the effect of variables on bruise characteristics and photography technique. Test were conducted with a significance level of 5 %.

Chapter 6

Results

6.1 Participant characteristics

6.1.1 Characteristics

A total of 18 individuals volunteered for this study (8 males and 10 females), with an age range of 19 to 32 (average of 25.89 ± 3.66 years). BMI ranged from 19.46 (healthy), to 41.28 (obese class III), with an average class of overweight (26.19 ± 5.55). BSA ranged from 1.15 to 2.47 m^2 (average of 1.86 ± 0.27 m^2). The volunteer pool was predominantly White (15 of 18), with the other three being Arab, Asian or Black. This was broken down into specific ethnic categories, with 12 British, 2 Italian and the remaining 4 being African, Greek, Indian and Syrian. Only one participant was a current smoker and had been for 5 years, with a frequency of 1 to 10 cigarettes a day. One other participant stated they were a former smoker of 10 years, but were classified as non-smoker as this was the case at the time of the study. A total of 7 participants were taking either or both medications or supplements at the time of the study, whilst many participants stated they drank alcohol (16 of 18). Most (13) had a weekly intake of 1 to 10 units, 2 participants had 11 to 20 units a week while 1 participant had an intake of 21 to 30 units. All participants stated they took part in some form of weekly exercise, either cardio (6 of 18) or strength and cardio (12 of 18). The frequency of exercise ranged from once a week to 6 times a week.

Compared to similar studies, the number of parameters noted for each individual was extensive (excluding that used by Scafide et al., (2012), whose participant questionnaire was the basis for that used in this study). Furthermore, the number of volunteers was greater than in the majority of similar studies involving deliberately bruising individuals (Table 6-1). The objective of these studies included impact mechanics, muscle bruising, aging bruising and assessing observer subjectivity.

Where bruising was generated using a paintball marker, this study had a larger pool of volunteers than all listed studies excluding one (Scafide et al., 2013), where a significantly larger pool of people were recruited.

Table 6-1 List of known studies to deliberately bruise or deliver a blunt impact to study volunteers

Author	Method of impact/bruising	No. of participants
Black, 2013b	Drop mass system	5
Desmoulin and Anderson, 2011	Drop mass system	1
Grossman et al., 2011	Vacuum	9
Hawkins, 2014	Tennis ball machine	10
Lecomte et al., 2013	Drop mass system	12
Pilling et al., 2010	Vacuum	11
Randeberg et al., 2006	Paintball	1
Randeberg et al., 2010	Paintball	8
Randeberg and Hernandez-Palacios, 2012	Paintball	3
Scafide et al., 2013	Paintball	122
Thavarajah et al., 2012	Vacuum	20

6.1.2 Limitations

The health questionnaire completed by all participants provided an overview of the population tested. However, given the number of participants, the level of variation was ultimately limited. Given the recruitment age range of 16-60, the age range of those who took part (19-32), was relatively small. Although a range of ethnicities were represented, the majority were White and British, with most others being represented by only one individual. Therefore, they cannot be appropriately compared. This also applied to many of the other categories, for example the smoking and drinking habits of individuals. Although there could be an indication of a link between such characteristics and the resultant impacts and bruising, there was not enough to provide any conclusive results. However, within the categories of gender and BMI, there was a large enough variation to be included in the analysis.

6.1.3 Leg hair

During forensic investigations there is no requirement for hair removal before images of bruising are taken (Black, 2013b), therefore this was not a requirement of this study. Although not necessarily always the case, it was found in this particular study that males had a larger volume of hair on their thighs compared to females (Figure 6-1). This influenced the clarity of the outer boundary of bruises, particularly as they began to fade. Therefore, it is likely to have had an effect of area measurements (thought unlikely to be significant), along with the colour measurements as it cannot be excluded.

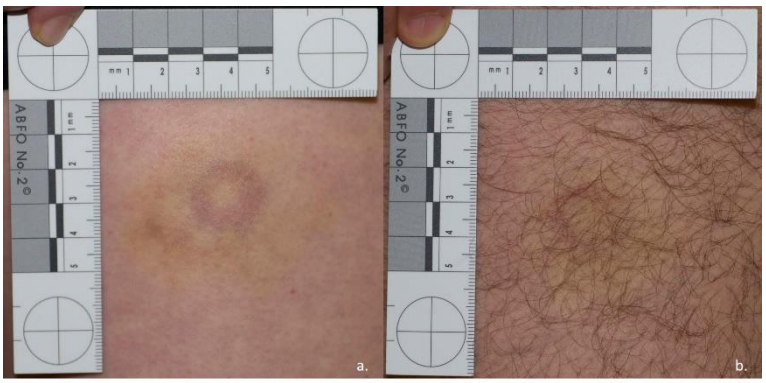

Figure 6-1 Influence of leg hair on outer boundary of yellowing bruise a. hairless b. dark hair present

6.2 Bruise results

6.2.1 Shape and colour

The majority of bruises presented as a doughnut shape – circular with a central clear zone. For some individuals, the bruise was more of an oblong shape indicating impact trajectory, or had a non-specific shape with no central clear zone. Each shape also gave an indication of the impact trajectory as would be expected (Georgieva et al., 2005b).

For direct blunt impacts delivered by a circular object, it is accepted that doughnut shaped bruising should be seen (at least for the first few days). This is as the impacting object forces blood to be directed away from the impact location, leaving a clear zone at the centre (Pounder, 2009; Randeberg et al., 2011; Scafide,

2012). For direct hits, the bruise generally had a circular shape (Figure 6-2a), while when the hit had a greater downward angle, or occurred towards the side of the thigh, the bruise had an oblong shape (Figure 6-2b). In one case the impact was at such an angle that the resultant bruise presented with no clear central zone (Figure 6-2c).

Figure 6-2 Examples of bruising shapes observed a. doughnut shaped b. oblong shaped c. non-specific shape

However it should be noted that in these cases, the impact direction was confirmed via the high speed camera videos. When the causation is unknown, the impact location and the effect of blood pooling and gravity should be taken into consideration before stating the impacting object's movement direction.

Subjectively, it appeared that bruise size relates to bruise severity – larger bruises presented with purple and blue tones, smaller bruises would only show yellow tones. Although this would be expected (larger bleed → larger bruise → increased colour intensity), the variance between individuals was significant given the consistent method of impact. Examples shown in Figure 6-3.

Figure 6-3 Comparison of two 3 day old bruises a. small bruise presenting mostly yellow tones b. large bruise presenting with blue, purple and yellow tones

6.2.2 Gravity influence

As extravasated blood will flow downwards due to gravity, this accounts for the intensity of bruising observed towards the bottom of the bruised area, compared to the top, for all participants.

For one participant, the bruise appeared in two parts (Figure 6-4). In addition to the doughnut bruising observed around the impact site, there was a smaller bruise located approximately 2 cm below. There was no evidence of the participant being struck a second time by a rebounding ball, the participant themselves did not sustain a second impact at a later time. Although not present 1 day post impact, the healing time and colour change suggested it was part of the same bruise (intra-person bruising appears to follow the same colour pattern when present on similar limbs i.e., 2 bruises on opposing forearms (Black, 2013b; Grossman et al., 2011)). This bruising could be due to some extravasated blood migrating downwards through channels within the subcutaneous tissues due to gravity, pooling externally to the impact site. The clear zone between the bruised areas could due to there not being a large volume of extravasated blood present in the area to be visible on the skin surface. There was no way to confirm or refute whether the smaller bruise being part of the original bruise and therefore, as it could not be excluded, both bruises were combined during analysis.

Figure 6-4 Bruise which presented as two separate bruises

6.2.3 Impact mark

Almost all bruises appeared with a red circular mark located within the central clear zone (examples seen in Figure 6-2). This could be considered either tissue damage or intradermal bruising. It was visible in some of the IR images, indicating that it is bruising. This could not be confirmed for all participants and the length of visibility ranged from the number of days the bruise itself was visible to over 30 days (Figure 6-5) (note the mark did fade with time and no permanent tissue damage occurred). It was also not possible find a link between the participants for which the mark lasted longer with the collected individual characteristics. Therefore, due to the uncertainty the mark was noted but excluded from the area measurements made.

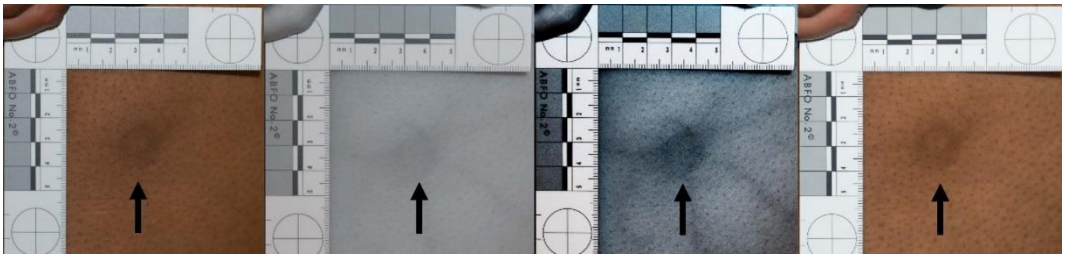

Figure 6-5 Example of the impact mark (indicated by the arrows), which was found to last much longer that the bruising which surrounded it. Each photo (colour, IR, altered IR and CP), taken 30 days post impact

A red area was also noted surrounding the impact site for most participants as skin tone influenced visibility. This was only visible immediately after impact occurred and varied in size between individuals (two examples are shown in Figure 6-6).

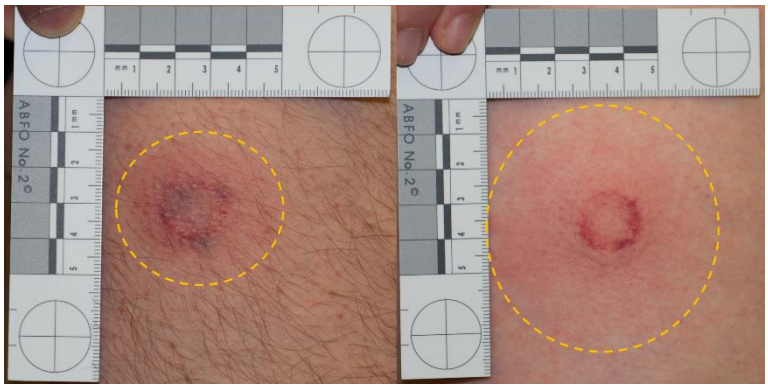

Figure 6-6 Examples of a visible red area surrounding the impact site immediately after impact

6.3 Videos

The high speed camera recordings specifically, they are visually very interesting. One notable factor was the visibility of immediate injury in the pilot work (Figure 6-7). This was only seen during these impacts due to their delivery to bare skin. It was concluded that the injury observed in the video was that of the impact mark/intradermal bruising seen immediately after impact. Given the frame rate (13,500 fps), it was evident that injury occurred within a fraction of a second. However, as it was generated at the point of impact, the ball itself masked this area of skin from the camera's field of view until it had been deflected clear. Thus, no exact time could be measured, but it would be less than the 0.002 s between the frame of ball impact and first frame which showed visible damage.

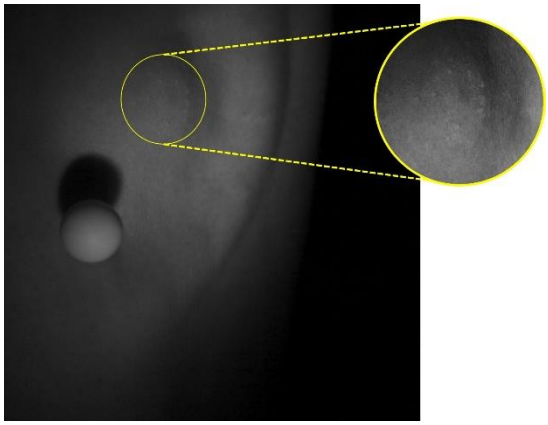

Figure 6-7 immediate identification of injury

For all main study impacts, each participant presented with varying levels of deformation. For comparison, a snapshot was taken from each video of the crest of each participant's deformation wave (Figure 6-8).

Although a subjective interpretation, some participants had a smaller deformation. With impacts being consistent for each participant, the smaller deformation indicated impacts to stiffer tissues. However, this could not be concluded purely on this visual analysis.

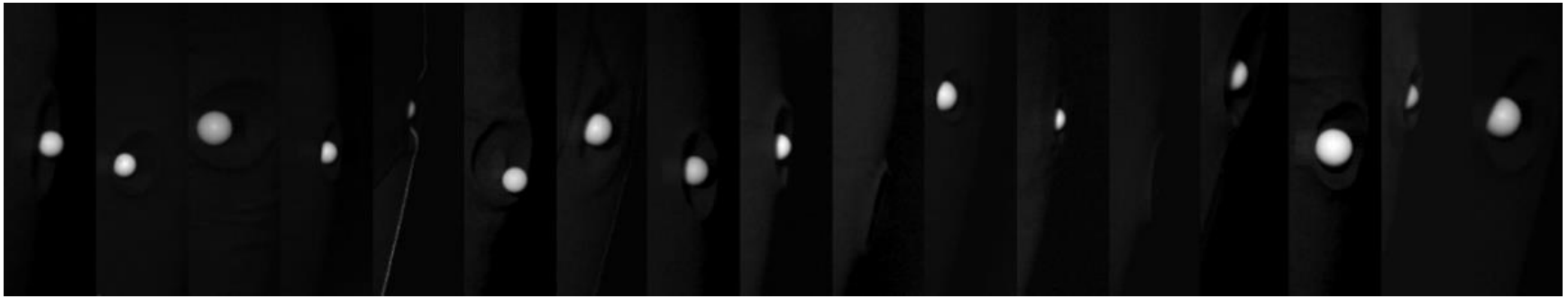

Figure 6-8 Snapshot of each participant's deformation (n =17)

6.4 Impact results

6.4.1 Firing and impact velocity

Firing velocity was expected to be approximately 74 ms^{-1} whilst always below 76 ms^{-1}. A full list of firing and impact velocities are shown in Table 6-2. As there was one unsuccessful video capture, only 17 of the 18 firing and impact velocities are listed. There was no correlation between firing and impacting velocity (r = 0.359, p = 0.157) due to the variable nature of the paintball marker and the use of a spherical projectile (Figure 6-9).

Table 6-2 List of firing velocities and their respective impact velocities

Firing velocity (ms^{-1})	**Resultant velocity on impact (ms^{-1})**
74.0	67.5
75.3	68.5
72.1	71.4
77.7	67.0
72.8	69.0
74.2	67.2
71.9	66.3
74.6	68.6
75.7	71.2
72.4	65.3
71.3	66.8
76.6	73.1
72.3	66.8
72.5	67.5
73.5	73.0
76.4	71.5
74.2	74.6
Average firing velocity (ms^{-1})	**Average impact velocity (ms^{-1})**
73.97 ± 1.87	69.15 ± 2.78

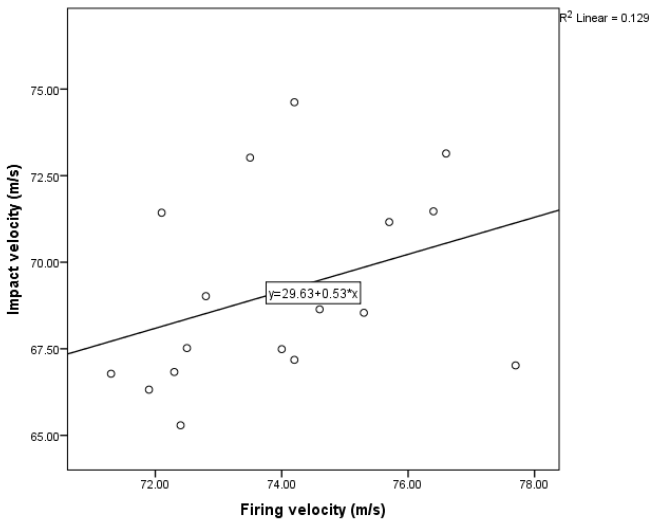

Figure 6-9 Correlation between firing velocity and the resulting impact velocity

6.4.2 Impact velocity and applied force

Some impacts were either not direct hits, or the ball was masked by tissue deformation. Therefore, a total of 5 participants were excluded (n = 13), as impact mechanics calculations would be inaccurate. For each impact, velocity and force both followed a general trend, thus showing that not only were impacts delivered with the same velocity, but the soft tissues of each participant responded in the same manner. A typical velocity and force profile is shown in Figure 6-10, all 12 others are shown in Appendix I.

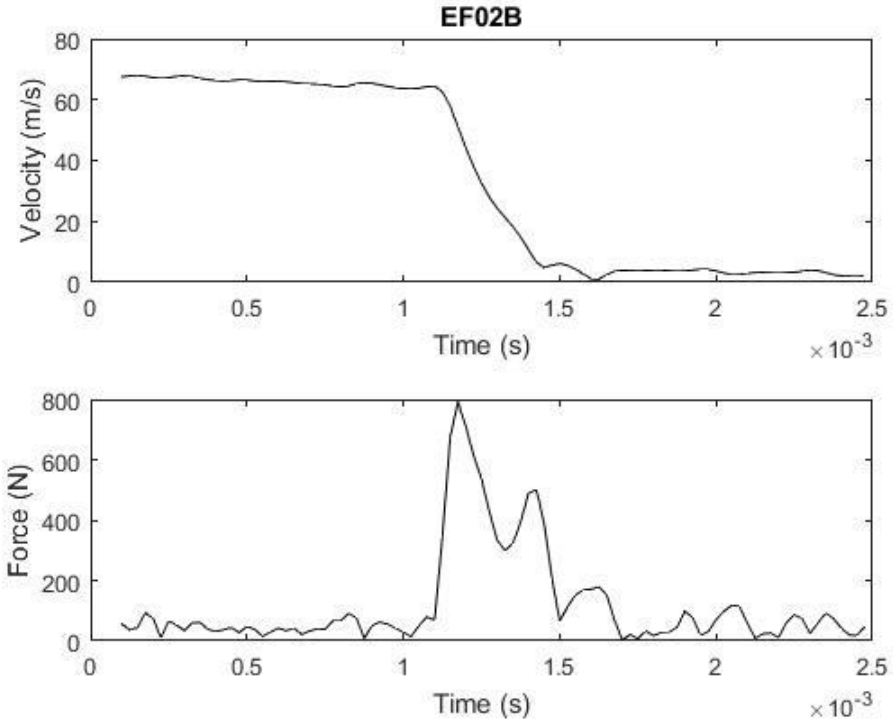

Figure 6-10 Typical velocity and force trace observed for the delivered blunt impact. Results shown are from participant EF02B

Although similar patterns were observed, there was variation between participants. Regarding velocity, the gradient relating to the impact varies in steepness between individuals, more so than when the ball is in flight, indicated by the greater SD shown in Figure 6-11 in the rapid deceleration phase. Therefore, it was concluded that the stiffness of the tissue was the factor responsible for this variance.

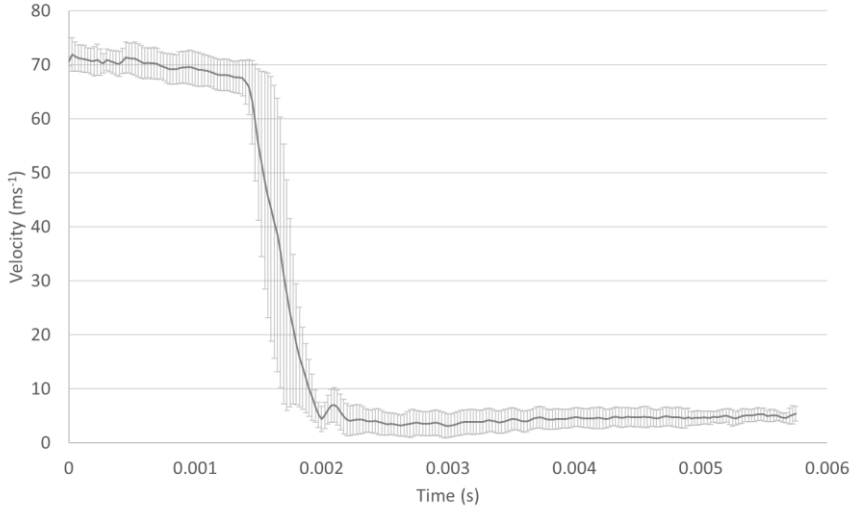

Figure 6-11 Average (±SD) velocity trace for all participant impacts

This was confirmed in the applied force profiles. For each individual impact there were 3 peaks observed. From the average force profile shown in Figure 6-12 (times aligned by the point of peak force), peaks 1 and 3 are well defined in comparison to the 2nd peak. The 3rd peak was excluded from the analysis, as explained in Section 7.2.

The applied force (1st peak), ranged from 749 N to 1,190 N, with an average of 917 ± 141 N. The 2nd peak ranged from 176 N to 730 N (average of 446 ± 178 N) for all participants. The time between both peaks ranged from 0.15 ms to 0.35 ms, with an average of 0.22 ± 0.06 ms.

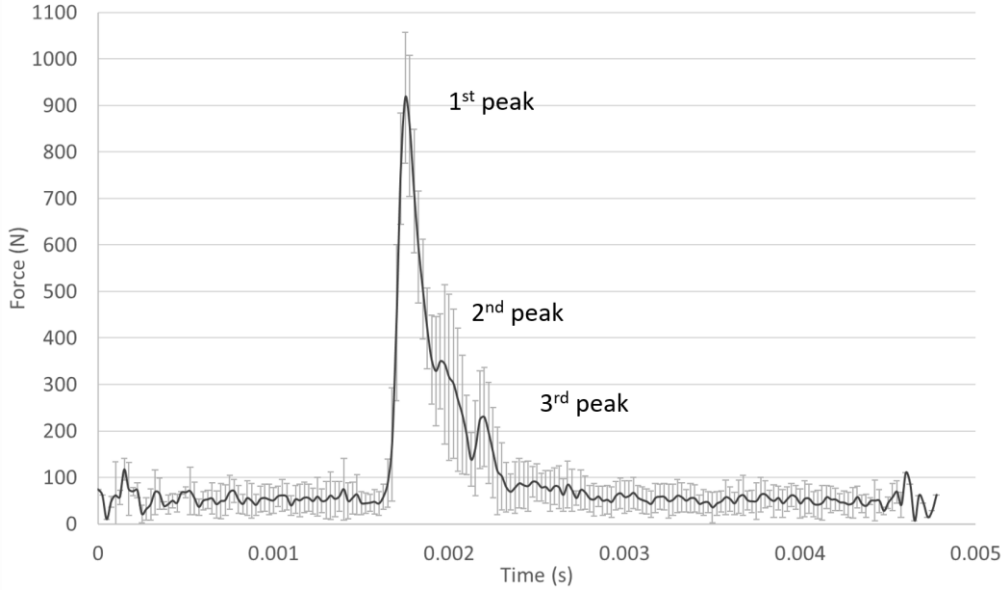

Figure 6-12 Average (±SD) force profile for all (13) participants

6.4.3 Force relative to tissue displacement

The first peak force appears at a displacement of approximately 5 mm (Figure 6-13). When viewed alongside the respective video frame, the applied force occurs at the point the ball is periodically embedded in the tissue whilst the surrounding tissue appears unresponsive (Figure 6-14).

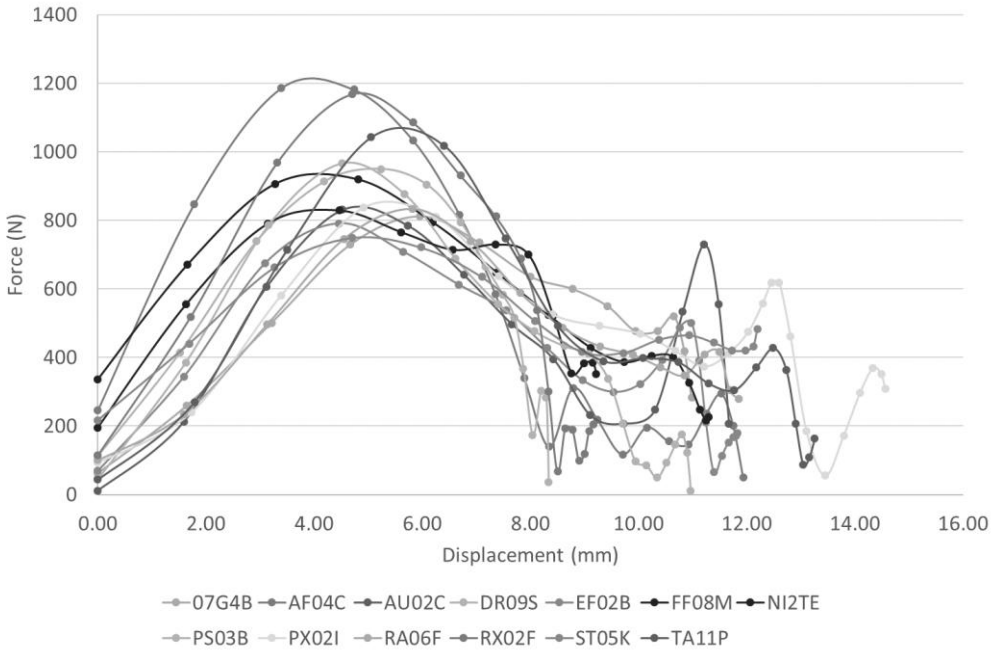

Figure 6-13 Plot of each participant's force and tissue displacement traces

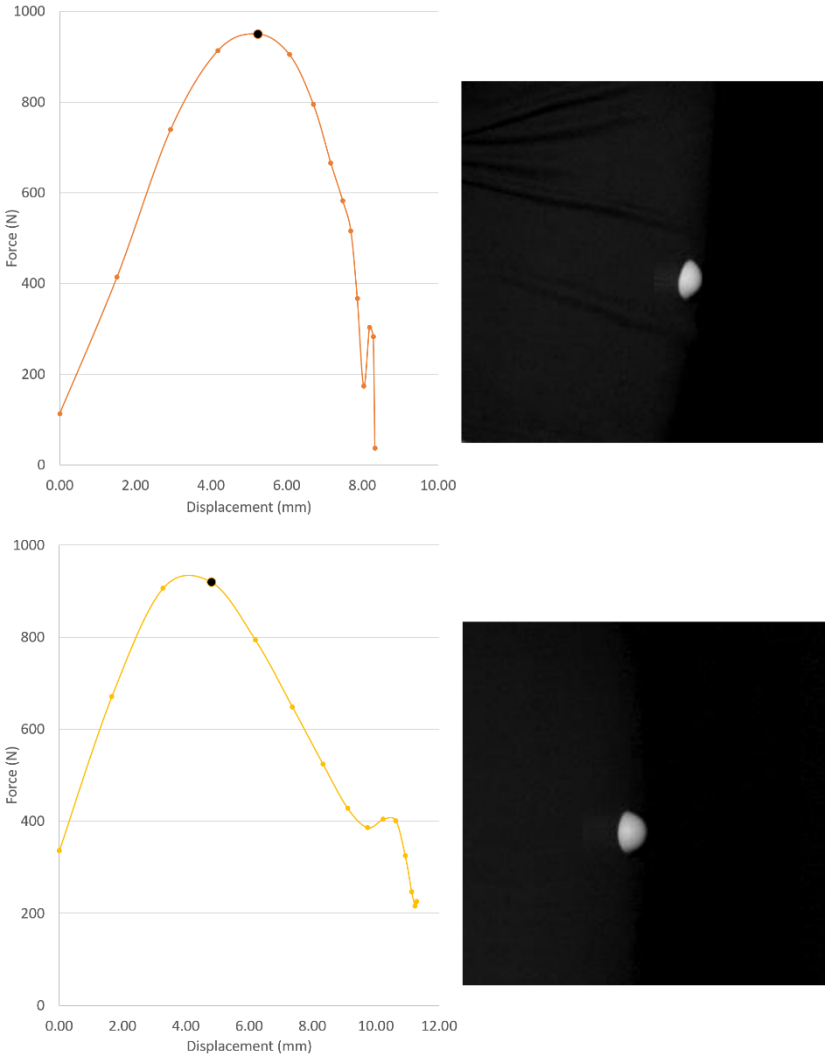

Figure 6-14 Two example force against displacement plots, with the respective ball and soft tissue deformation at peak force

The second peak force displacements ranged from 8.19 to 12.60 mm, with an average of 10.47 ± 1.41 mm. The time at which this displacement occurred also varied between participants. When viewed alongside the respective video frame (Figure 6-15), this peak force occurs at the point the ball has reached its maximum deformation and has ceased its forward motion into the thigh.

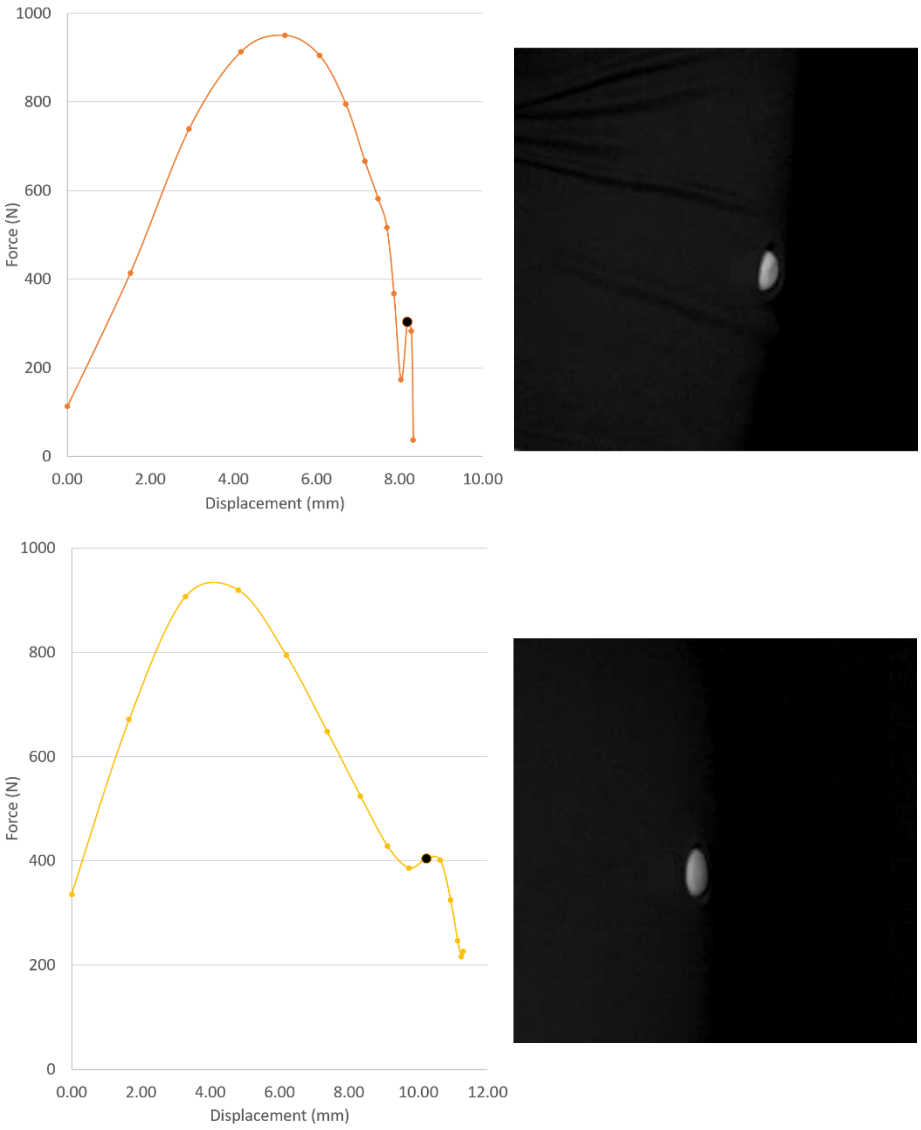

Figure 6-15 Two example force against displacement plots with respective ball and soft tissue deformation at the second peak force

A negative correlation between both first and second peak forces was identified (r = -0.639, p = 0.014) showing that the higher the initial peak, the lower the second peak observed (Figure 6-16).

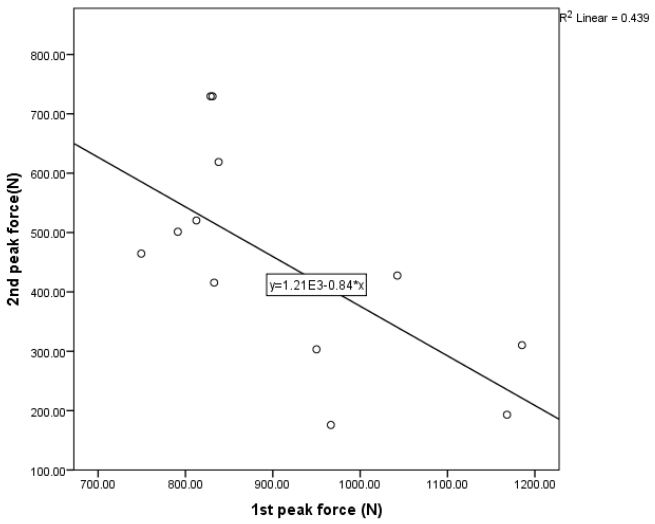

Figure 6-16 Correlation between the two peaks observed during each impact

6.4.4 Influence of the soft tissues

Combining both force and displacement results, it can be concluded that not only does the soft tissue influence the initial applied force, but also how the projectile's energy is transferred through the tissues.

6.4.4.1 Location

As previously stated, impacts were delivered to the lateral side of the right thigh of all participants. Although impact location may have varied slightly between individuals, the approximate impact location was the same for all participants (shown in Figure 6-17). It is assumed that skin, muscle and fat tissues were all affected when the blunt impact was delivered. Given the thigh is more muscular in nature compared to other anatomical locations and the adiposity of each individual was not quantified, whether the underlying muscle could have played a role in force dissipation and whether it became bruised itself is unknown. This could not be checked *in vivo* and so could not be completely ruled out as a possibility.

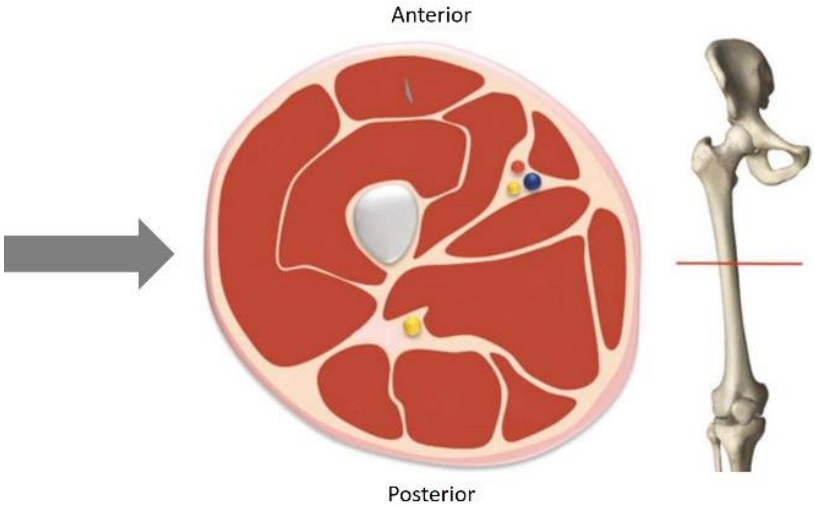

Figure 6-17 Sectional view of impacted thigh. Arrow indicated impact location. Skeletal image shows location of sectional image (Adapted from Silvestri et al. 2015)

6.4.4.2 Individual influence on impact

Of all the characteristics considered in the questionnaire, BMI was the only one found to have any significant correlation with the mechanics considered. The correlation between BMI and the first peak force (r = -0.567, p = 0.043), indicated that the lower the BMI the higher the peak force and thus suggesting a higher tissue stiffness of the thigh (Figure 6-18).

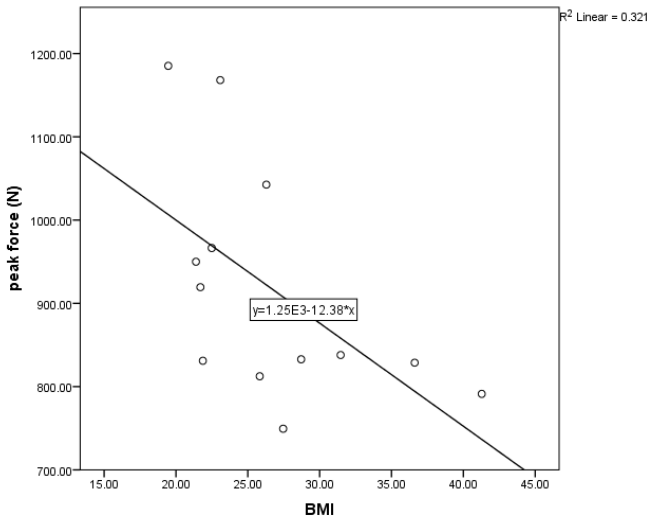

Figure 6-18 Correlation between BMI and peak force

BMI may increase the time period seen between both peak forces, however there was no significant correlation found (Figure 6-19) due to one outlier (r = 0.241, p = 0.427).

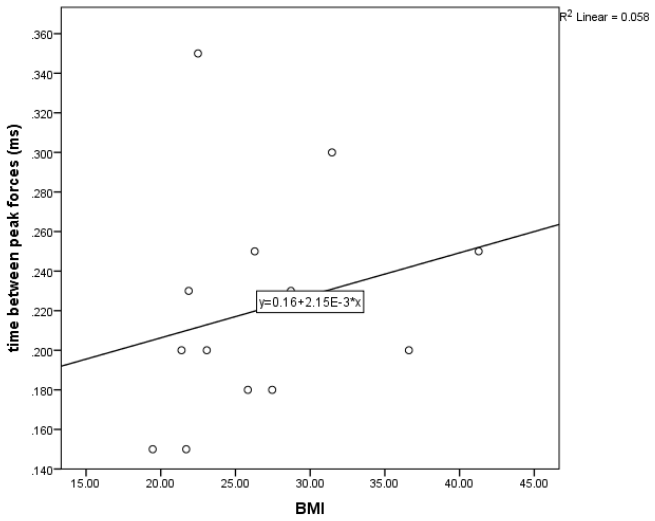

Figure 6-19 Time between 1st and 2nd peak forces relative to BMI

6.5 Impact on bruise extent

6.5.1 Area timelines

In general, bruising followed a pattern of increasing size over the first couple of days before reaching a maximum, then reducing as the healing process progressed. Each participant's timeline is shown in Figure 6-20 to Figure 6-23, relative to either colour, CP, IR or altered IR modality. For each image technique, the areas measured and the day of average peak bruise area (± SD), varied. For the IR measurements (Figure 6-22 and Figure 6-23), bruises were generally observed as being larger.

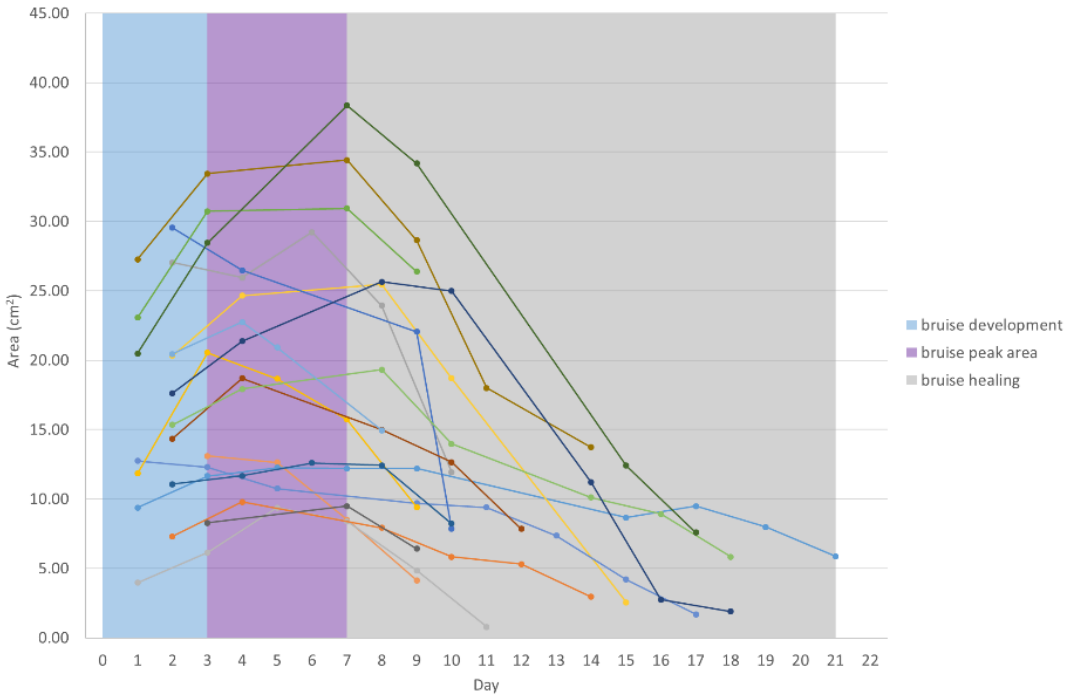

Figure 6-20 Bruise size timelines measured from colour images

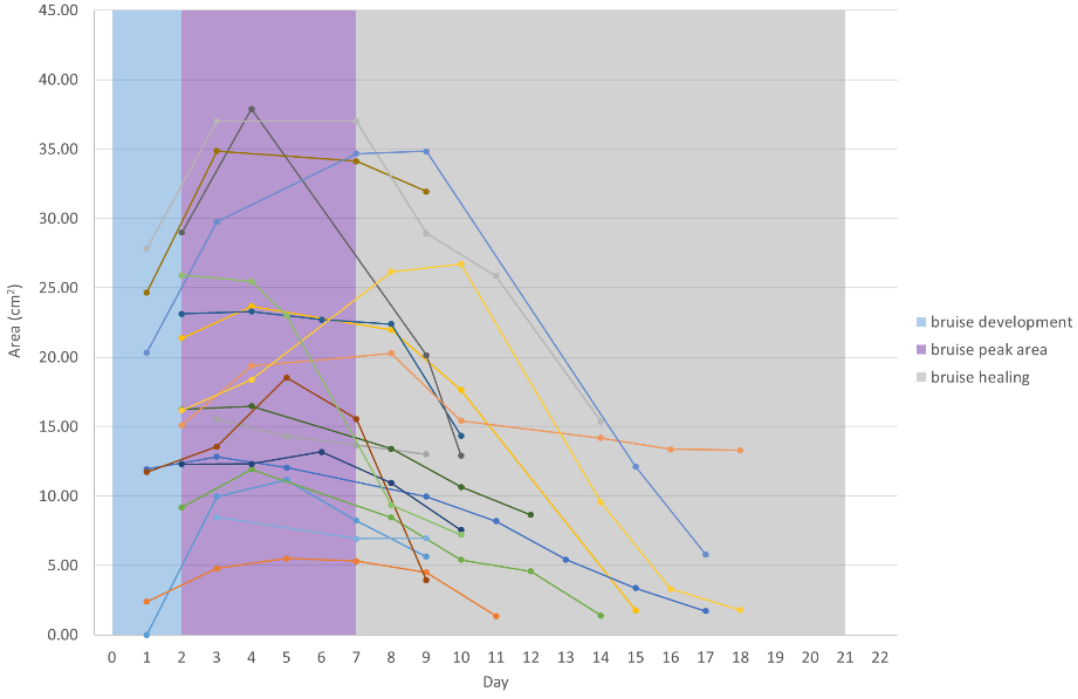

Figure 6-21 Bruise size timelines measured from CP images

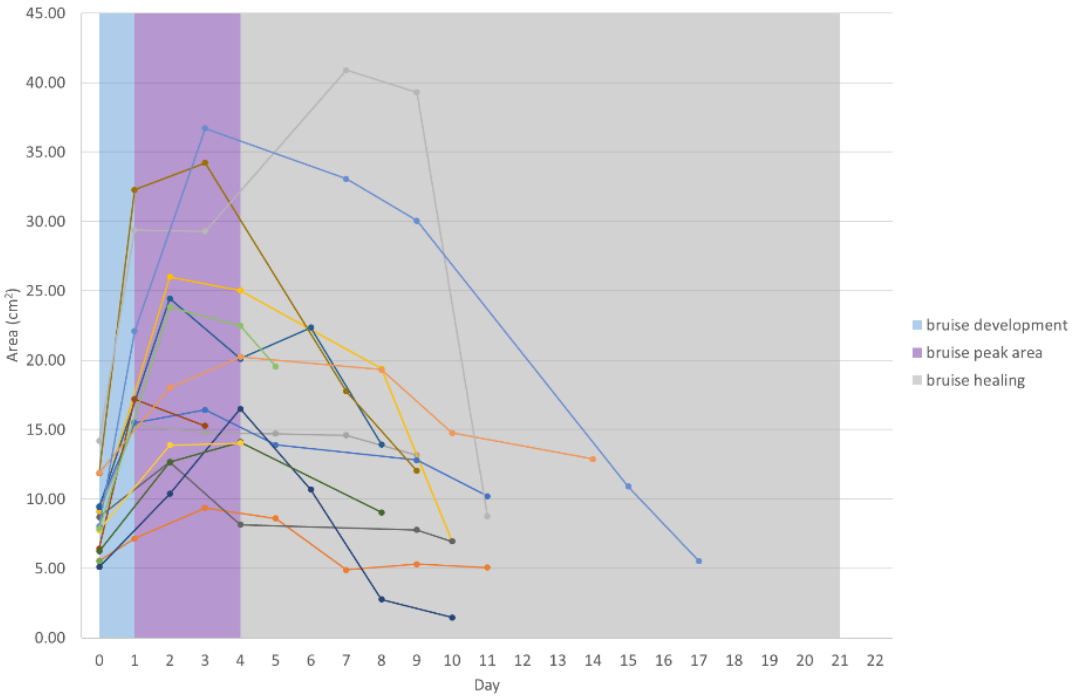

Figure 6-22 Bruise size timelines measured from IR images

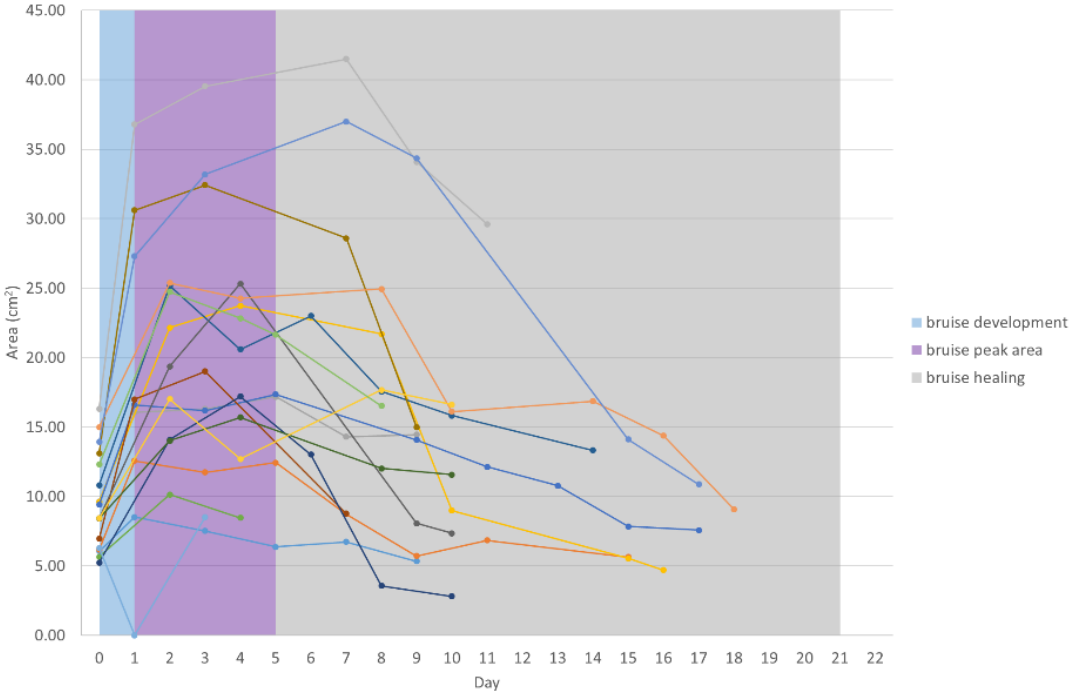

Figure 6-23 Bruise size timelines measured from altered IR images

6.5.2 Impact parameters and area

There was little correlation found between the impact parameters and the size of resultant injury. The only feature of impact which seemed to have any

influence was the maximum tissue displacement observed. Taken from the measurements of the colour images, a correlation between maximum tissue displacement and the impact mark area was observed (r = - 0.573, p = 0.041). Although not a completely linear relationship and only observed for one photography modality, it did indicate that the greater the deformation (i.e. deformation at the second peak force), the smaller impact mark area (i.e. less immediate, visible damage) (Figure 6-24).

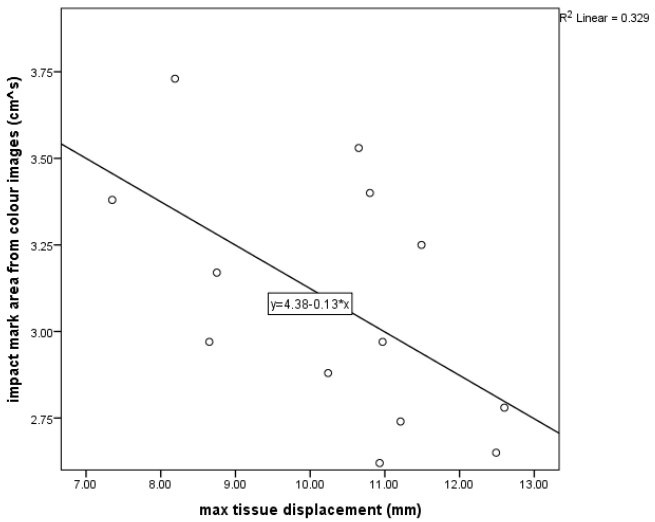

Figure 6-24 Correlation between maximum tissue displacement and the impact mark area taken from the colour images

It was also found that whilst a greater displacement produced a smaller impact mark, the mark itself also decreased in brightness (i.e. a lower L* value was recorded). This correlation (only seen for colour images Figure 6-25), indicated that the softer the tissues the more focused the damaged area would be (r = - 0.595, p = 0.032).

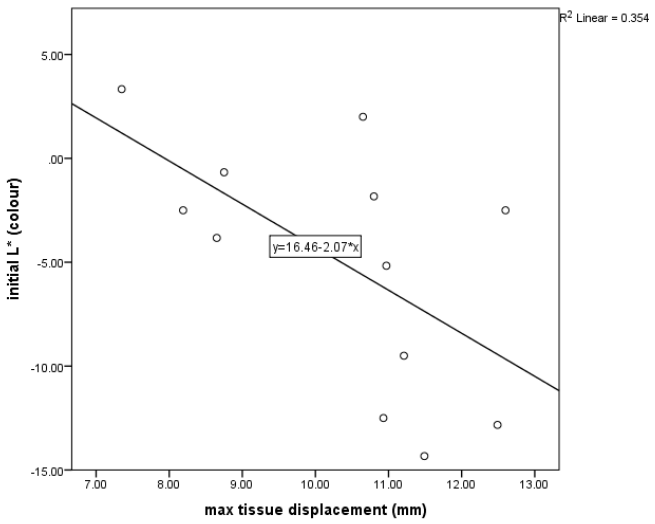

Figure 6-25 Correlation between maximum tissue displacement and the initial L value recorded*

6.5.3 Impact mark to maximum bruise area

The area measurements of the impact mark (in both colour and CP images), did not correspond with the extent of bruising eventually observed. However, the measurements of impact mark area from the IR images did have a correlation with the maximum areas measured from the colour (r = 0.556, p = 0.025), CP (r = 0.613, p = 0.012) and IR images (r = 0.703, p = 0.002) (Figure 6-26).

As this trend was seen only for the IR and subsequently the altered IR impact mark images, this would suggest that the immediate bleeding detected is a good indicator of the extent of bruising likely to be seen. Unsurprisingly, the greatest correlation was between impact mark area and the maximum area measured using IR photography.

The maximum areas from the colour and CP images were also found to correlate with the L* value of the initial impact mark (colour: r = - 0.566, p = 0.014 and CP: r = -0.603, p = 0.008) (Figure 6-27). This suggests that bruise size may be estimated by the initial 'darkness' of a bruise following impact, independent of the image being a colour or CP (i.e. the darker the initial bruise the larger the bruise will become). However, no specific calculation on bruise size could be achieved, particularly due to the variability which individuality brings to bruise formation.

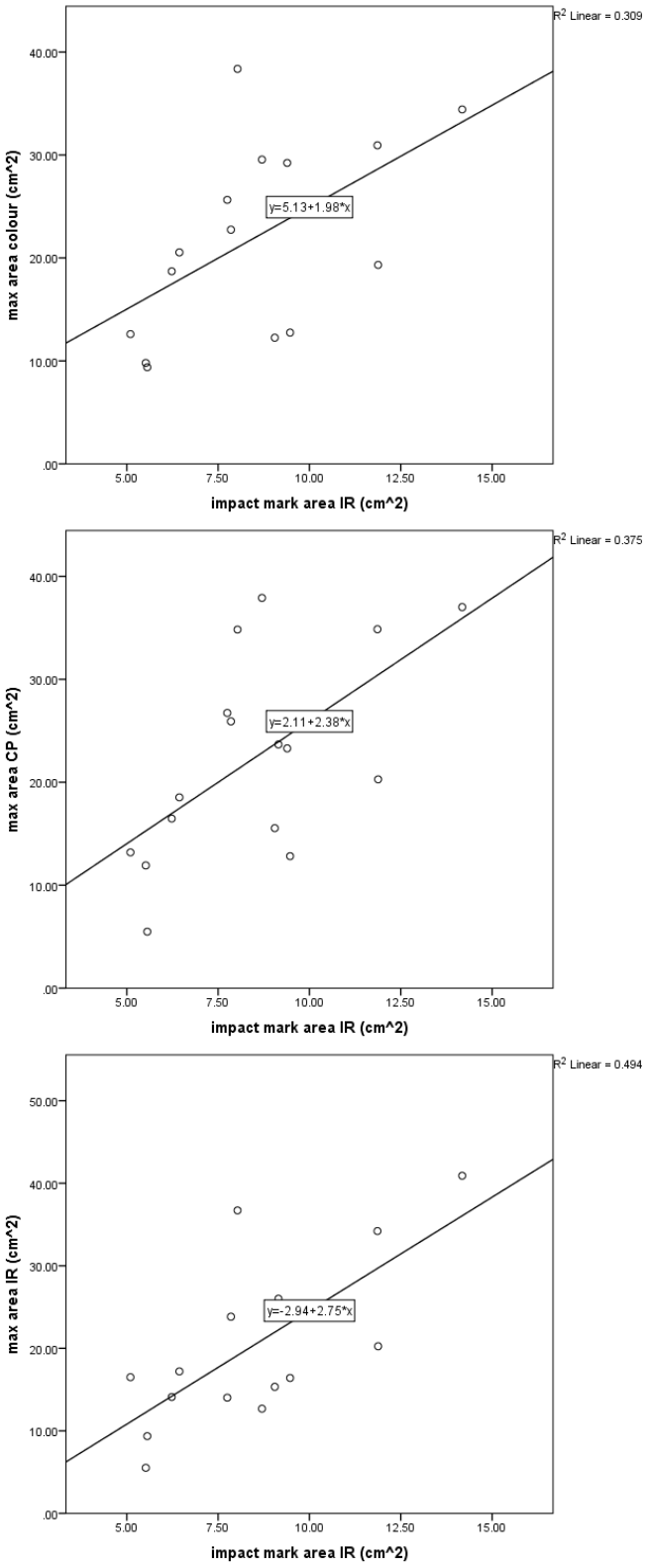

Figure 6-26 Correlations between IR measured impact mark area and the maximum bruised area measured from colour, CP and IR images

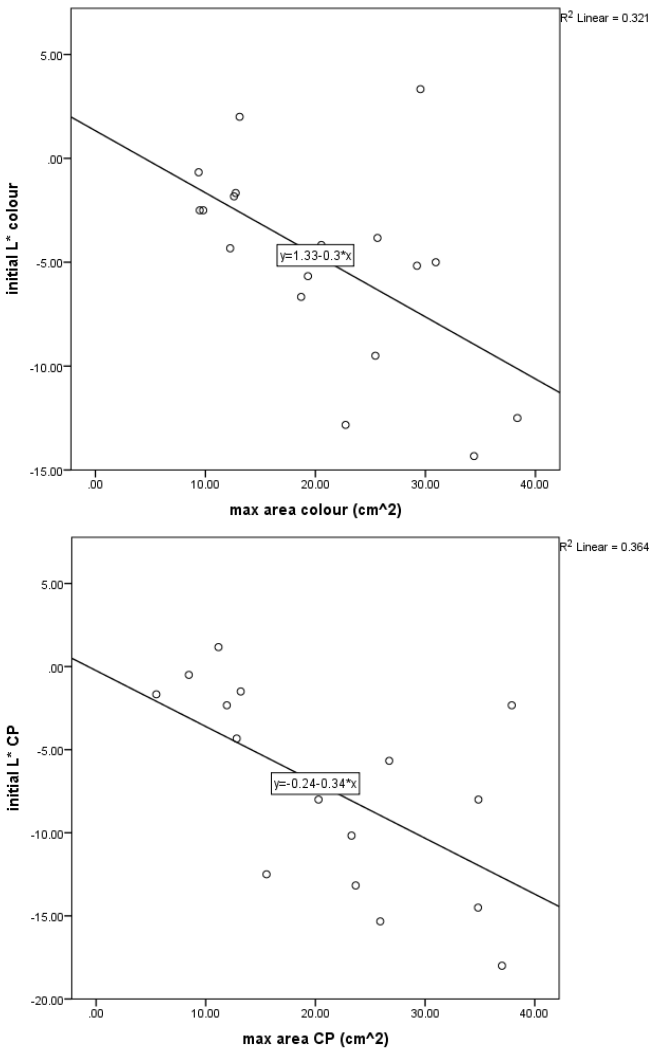

Figure 6-27 Correlation of max area measured in both colour and CP photography against their respective Initial L values*

6.5.4 Individual influence on bruising

Of all the individual characteristics which were noted for each participant, there was little evidence of a link between characteristics and impact mechanics and resultant injury. There was an indication that weekly alcohol intake may have influenced bruise size and days visible, however these results were excluded due to the small number in each group.

There was a link found between gender and the impact mark area observed from the IR images. As shown in Figure 6-28, the initial bleeding observed appeared larger for females and as for both genders the data had a normal distribution, an independent t-test, confirmed the difference between males and females to be

significantly different ($p < 0.05$). However, as gender was not found to have any correlation with bruise size (initial or peak), for any other imaging technique, it cannot be concluded with any certainty that gender influenced the bruising process overall.

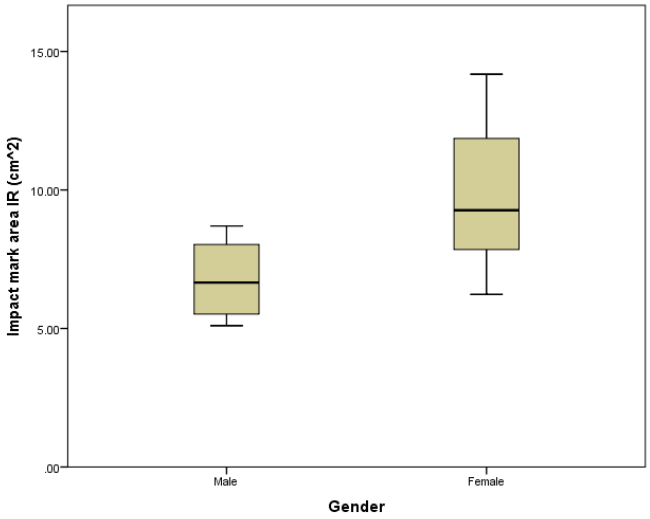

Figure 6-28 Box plot of impact mark area as measured from the IR images, against gender

With regards to bruise colour, the only individual characteristic to show any significant influence was gender on the lightness (L*) of the immediately visible impact mark, using both colour and CP techniques (Figure 6-29). This was proven by t-test for the colour technique and a Mann-Whitney Test for the CP technique (results for the male CP images were not normally distributed). Significance values were $p = 0.041$ and $p = 0.006$ for colour and CP techniques respectively.

This trend showed that initial injury was darker for females compared to males. However, there was an outlier within the male group, indicating that gender alone may not be appropriate in describing bruising in general.

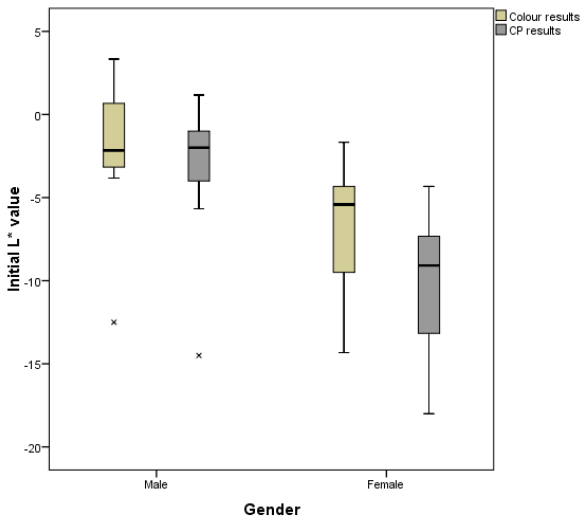

Figure 6-29 Box plot of the L values of the impact mark relative to gender*

6.6 Colour patterns for all participants

The L*a*b* colour system has produced similar patterns both in previous studies and the pilot work of this research, it was expected that the main study would produce similar results. However, that was not found to be the case. Furthermore, although some similarities could be seen, there was a wide range between the colour values measured (Figure 6-30).

In all cases, the patterns observed for each participant's colour image timeline matched the respective CP pattern, although at a different level. This would be expected, as CP photography enhances colours rather than changing them. This is seen when comparing the average of all colour measurements from each photography technique (Figure 6-31).

In both Figure 6-30 and Figure 6-31, there is a general trend over the lifetime of the bruises going from dark to light (ΔL*), green to red (Δa*) and blue to yellow (Δb*). The Δa* trend is less consistent of the three and does not match the pattern expected or noted in previous studies (Mimasaka et al., 2012; Scafide et al., 2013; Thavarajah et al., 2012). In each case the bruise must develop before a peak is seen, i.e. the bruise is not at it's darkest immediately after impact.

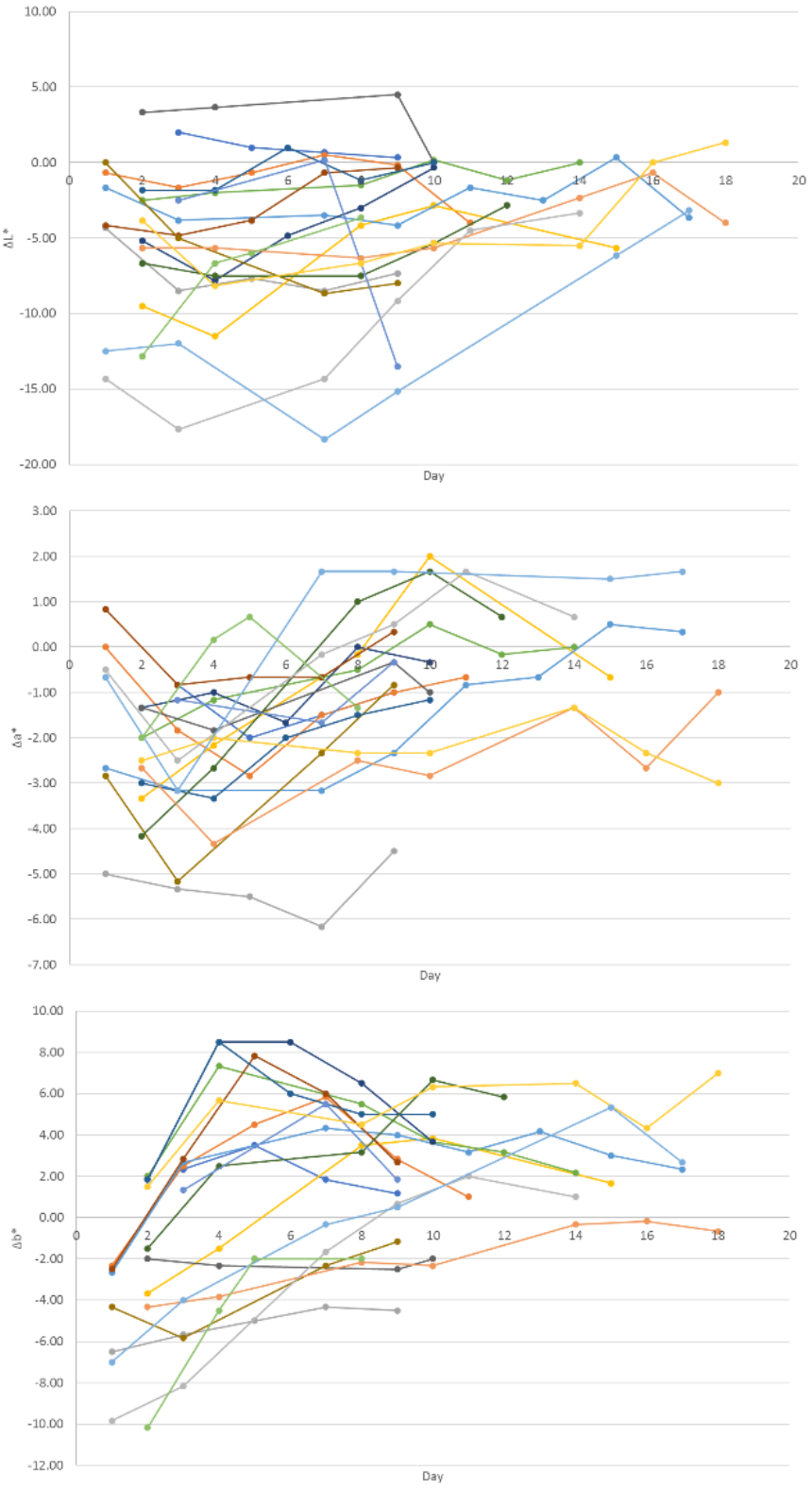

Figure 6-30 Each participant's ΔL, Δa* and Δb* traces from the colour images*

Given the healing process of bruising, it would be expected that the colours would go from red to green. The fact that this was not observed could be as a result

of the methodology itself (i.e. Photoshop cannot accurately measure colours as specific colour measurement tools can).

When averaging all participants, it was observed that in doing so the pattern definition was reduced. The approach of Scafide et al., 2013, was to separate individuals based on skin tone, whereas Thavarajah et al., 2012 specifically focused on dark skinned individuals. Therefore, as the colour patterns observed were not consistent for all participants, the results were categorised by skin tone.

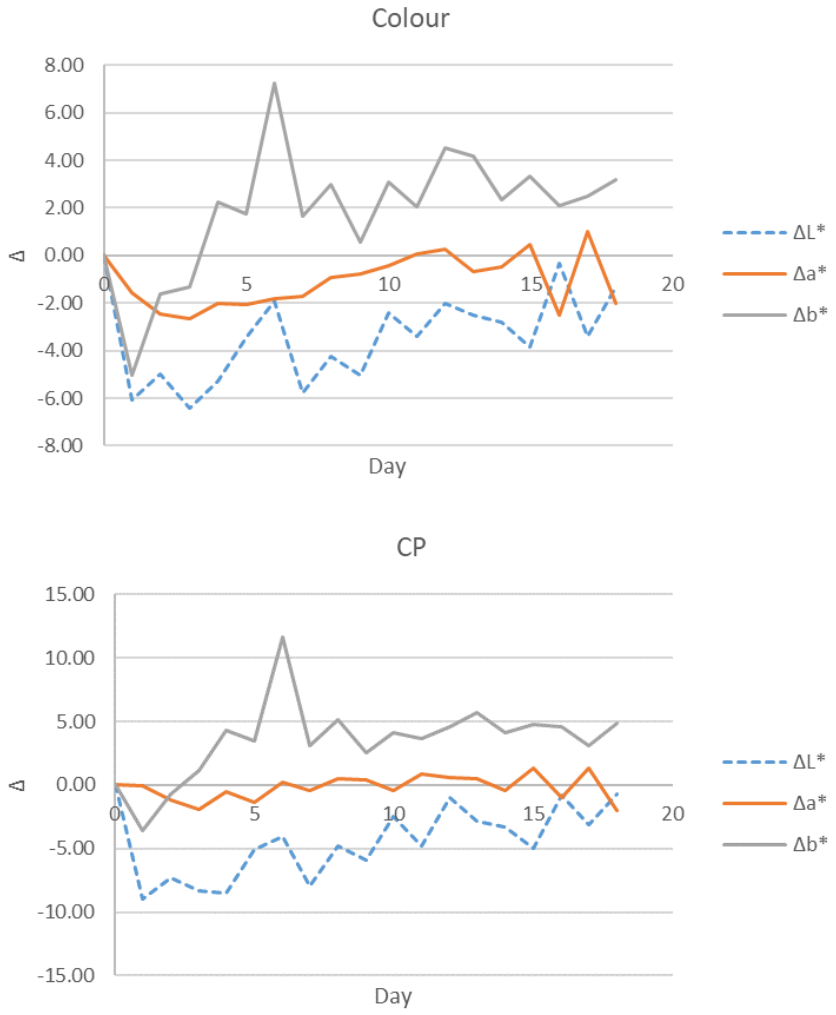

Figure 6-31 Average ΔL, Δa* and Δb* traces of both colour and CP photography techniques*

6.7 Categorisation by skin tone

A reported positive of L*a*b* measurements was in that it allowed for pattern identification regardless of skin tone. Therefore, the colour patterns collected in this study were then categorised based on the skin tone of each participant in two ways:

1. A simplified ITA° system categories (dark, medium and light).
2. All categories included in the ITA° system (dark, brown, tan, intermediate, light and very light)

Although the analysis (like the previous studies), did account for the skin tone by subtracting it from the bruise colours measured, skin tone would still have influenced the range of colours which were visible.

It would be expected that the level of each colour pattern (i.e. the intensity and range of colours), would vary between each skin tone category, with the pattern itself remaining the same (as seen in Scafide et al., 2013).

6.7.1 Simplified categories

6.7.1.1 Overall findings

Categorising individuals based on the simplified skin categories as done in a previous study (Scafide et al., 2013), was found to be unsuccessful. The range of values measured in each category overlapped with one another, visible in the plots of the average L*, a* and b* patterns for each skin tone (Figure 6-32). Although there were some distinct peaks observed, they were not considered significant as they were a likely result of the averaging process, which did not always include the same number of participants (bruising healed at different rates for different people).

For the CP images, the classification of individuals changed, with there being none defined as medium skin toned. Comparing the average results for light skin tones, the patterns observed between each photography technique was similar, with the most notable being a b* (yellow), peak on day 6 (Figure 6-33). For dark skin tones, as for the colour image findings, the patterns were also found to be similar (also shown in Figure 6-33).

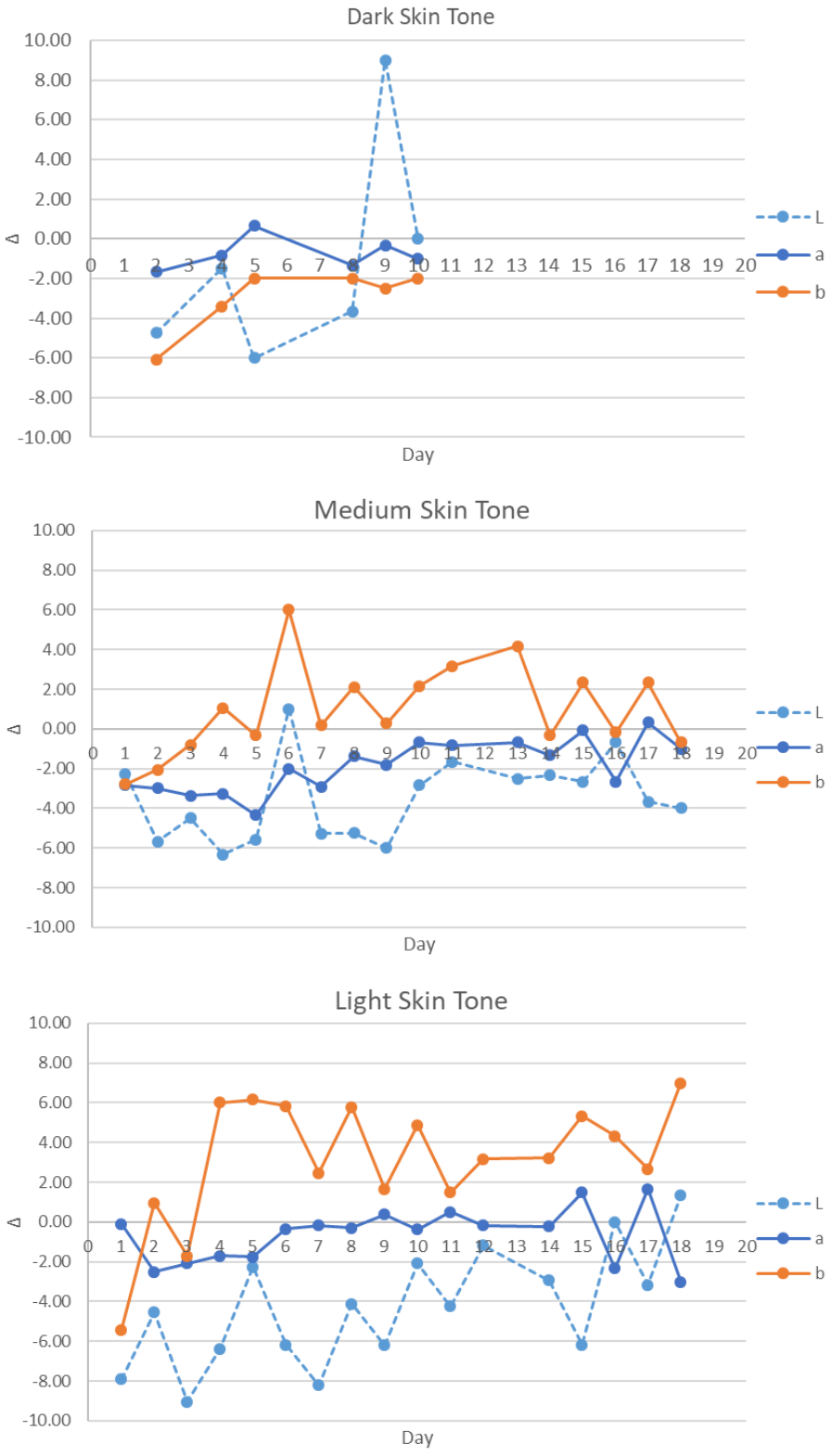

Figure 6-32 Average L, a* and b* patterns observed for dark, medium and light skin tones from the colour images*

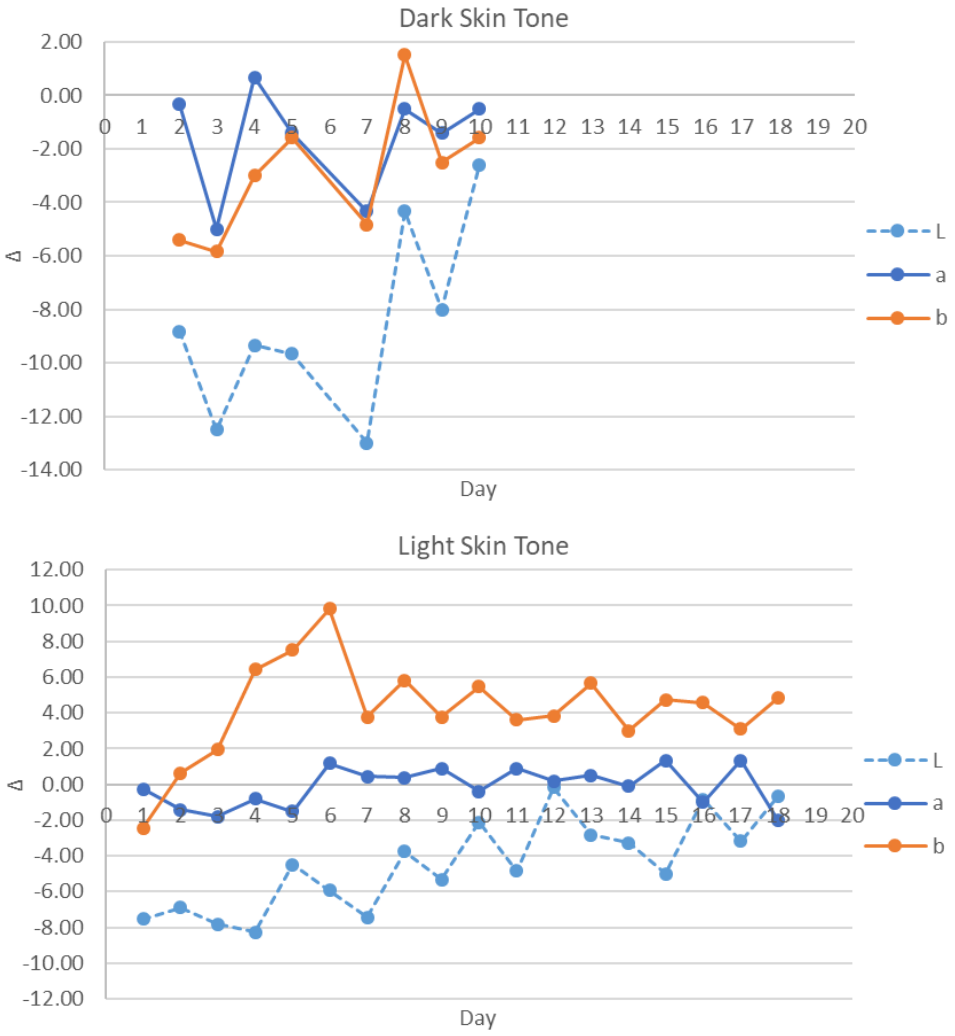

Figure 6-33 Average L, a* and b* patterns observed for dark and light skin tones from the CP images*

The patterns from CP images appeared characteristic to both light and dark skin tones, as the average L*, a* and b* patterns were lower for darker skin. However, when the patterns for each participant were plotted together, dark and light skin tones could not be differentiated from one another, thus could not be stated as characteristic of skin tone. The plots of all participants grouped by skin tone (both colour and CP results), are shown Appendix J.

6.7.1.2 Comparison

The interpretation of these results changed when presented in the same fashion as that seen in previously published work. To compare with Scafide et al. (2013), where this categorisation had shown success, the average patterns were

plotted from day 0 to day 4 (with day 0 being the origin), so the data was presented within the same range.

Once the results are presented in this manner, there did appear to be similarities between the findings. There was also a notable difference in measurement values between both studies (particularly when comparing L* and b* patterns).

For the L* measurements, although a difference was noted in the level of darkness measured for each skin tone, there was not a clear distinction between the each category (Figure 6-34). Even though the patterns did not exactly match those presented by Scafide et al., the general trends however, were present in the results – confirming that bruising will begin dark and become lighter with time.

There were no similarities found between the pattern observed for the change in a* values over the 4 day timeline, in fact the pattern observed was the opposite of that expected. Instead of going from red to green, the results indicated the bruising was green to begin with, becoming closer to a red tonality with time. Like the L* pattern, there was no clear distinction between the patterns observed for each skin tone (Figure 6-35).

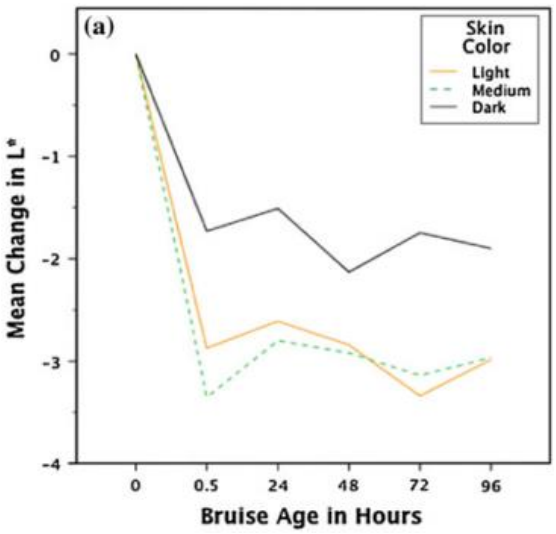

a. Results from Scafide et al., 2013 (adapted)
dark: n = 34, medium: n = 35, light: n = 34

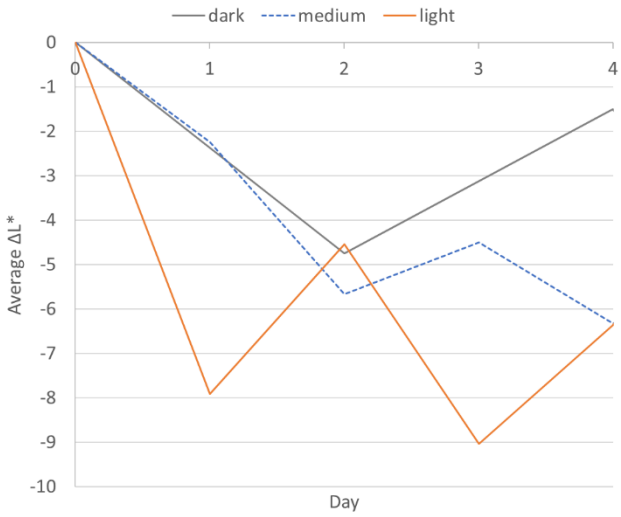

b. Colour study results
dark: n = 2, medium: n = 8, light: n = 8

Figure 6-34 Comparison of Scafide et al., 2013 change in L results and the results of this study's change in L* results*

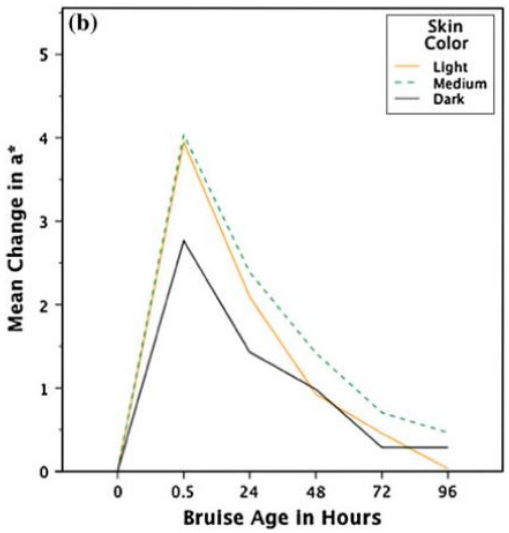

a. Results from Scafide et al., 2013 (adapted)
dark: n = 34, medium: n = 35, light: n = 34

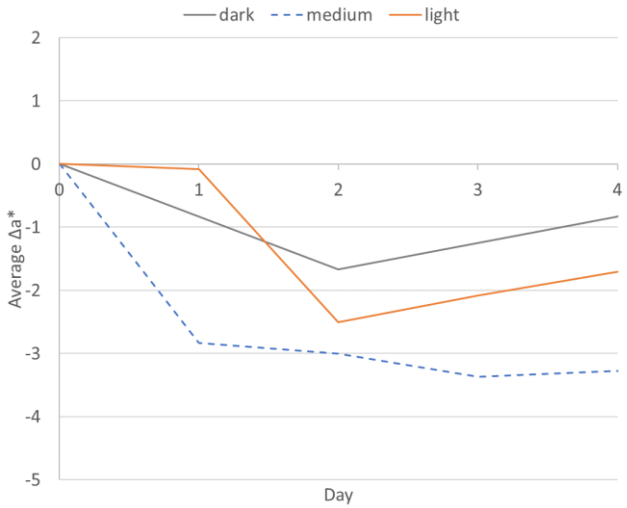

b. Colour study results
dark: n = 2, medium: n = 8, light: n = 8

Figure 6-35 Comparison of Scafide et al., 2013 change in a results and the results of this study's change in a* results*

For the b* patterns, there was a similarity between the patterns of this study and those which Scafide et al., presented (Figure 6-36). For both studies the patterns observed indicated a change in colour from blue to yellow. This was less clear in this study's results for medium skin tones and again, it could not be concluded that the patterns were characteristic of each skin tone.

Similar patterns were observed for the CP images, although as previously stated, this photography technique alters the level of values measured more than the patterns themselves.

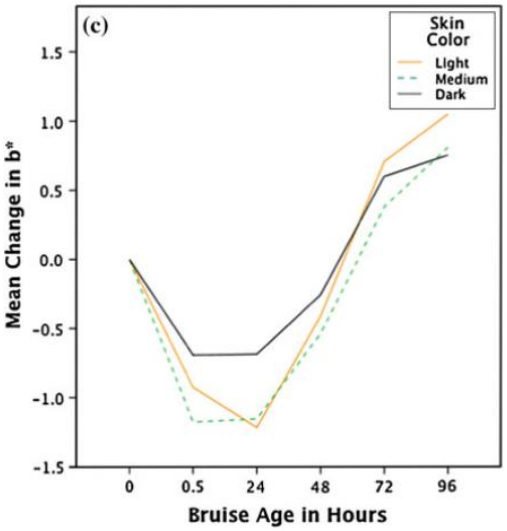

a. Results from Scafide et al., 2013 (adapted)
dark: n = 34, medium: n = 35, light: n = 34

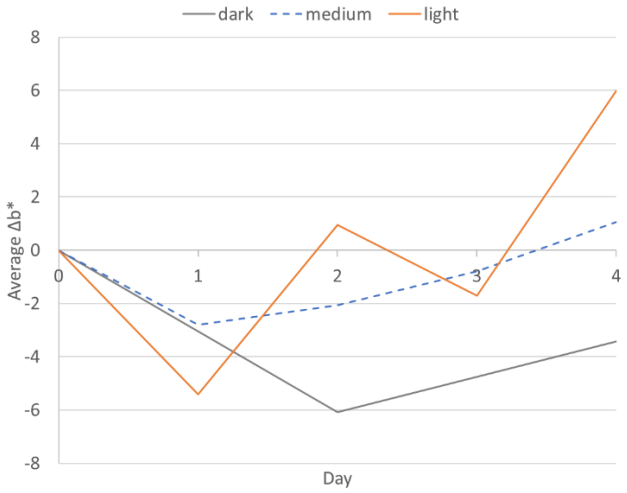

b. Colour study results
dark: n = 2, medium: n = 8, light: n = 8

Figure 6-36 Comparison of Scafide et al., 2013 change in b results and the results of this study's change in b* results*

6.7.2 All skin tone categories

Given the overlap in patterns observed when categorising skin tone as either dark, medium or light, expanding the categories to all those available using the ITA° system was investigated. Only plots of all patterns are considered, so any overlaps in patterns were visible and not lost by averaging.

As seen with the simple categories, the expanded list did not provide any clarity in showing whether skin tone influences the level of colour pattern observed.

This was concluded for measurements taken from both the colour and CP images. Given that more individuals became classified as having very light skin when CP photography was used, the ability to identify characteristic patterns was dramatically reduced. Comparison of the L* patterns from each imaging technique categorised by the expanded skin tones, is shown in Figure 6-37. The a* and b* pattern comparisons are shown in Appendix K.

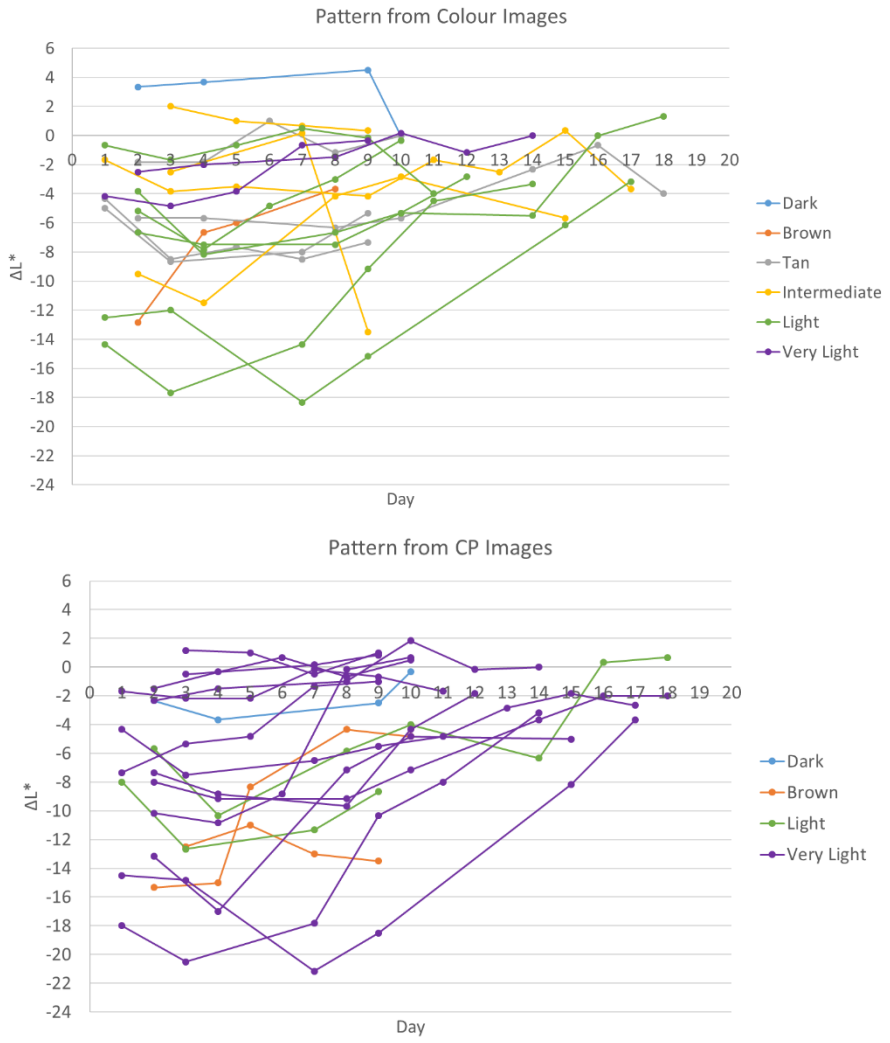

Figure 6-37 All L patterns taken from both colour and CP images, grouped by dark, brown, tan, intermediate, light and very light skin tones*

6.8 Categorisation by BMI

Individuals were grouped into three categories (healthy, overweight and obese), based on their calculated BMI. Subcategories of obese were excluded due to a lack of individuals for each section. The aim was to determine whether the pattern

of colours measured could be linked to an individual's build. All participant patterns were plotted together to avoid loss of definition generated by averaging those patterns within each category.

Like skin tone, it was not possible to attribute pattern range to category. For both the colour and CP photography techniques, the range of patterns observed would overlap with that seen for other categories. An example of the colour L* pattern is shown in Figure 6-38, indicating that the severity of bruise and the resulting colour change is not indicative of an individual's BMI. There were no clear associations for a* and b* patterns either. For the a* and b* colour patterns and L*, a* and b* CP patterns, see Appendix L.

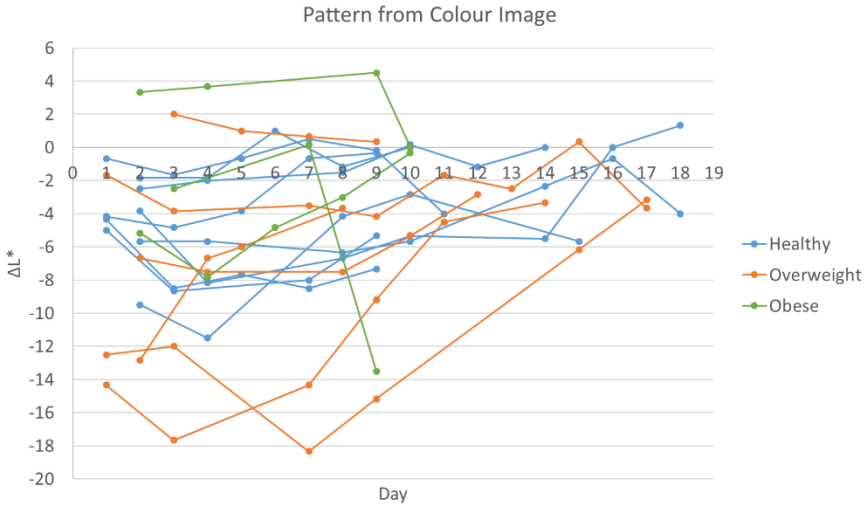

Figure 6-38 All L patterns taken from the colour images, categorised by BMI*

There was no known study to have used this approach in combination with this colour model to compare bruise colour patterns. Therefore, based on these findings, the use of the L*a*b* colour system to describe bruise colour progression for different BMI classifications, was concluded as unsuccessful.

6.9 Categorisation by gender

Individuals were grouped by their gender, 8 males and 10 females. Visually, it appeared that females presented with darker bruising than males, and this was reflected in the results (Figure 6-39). The perception of this result was more evident for the measurements taken from CP images (also shown in Figure 6-39). However,

there were exceptions and so it could not be conclusively stated that the L* patterns observed were characteristic of gender.

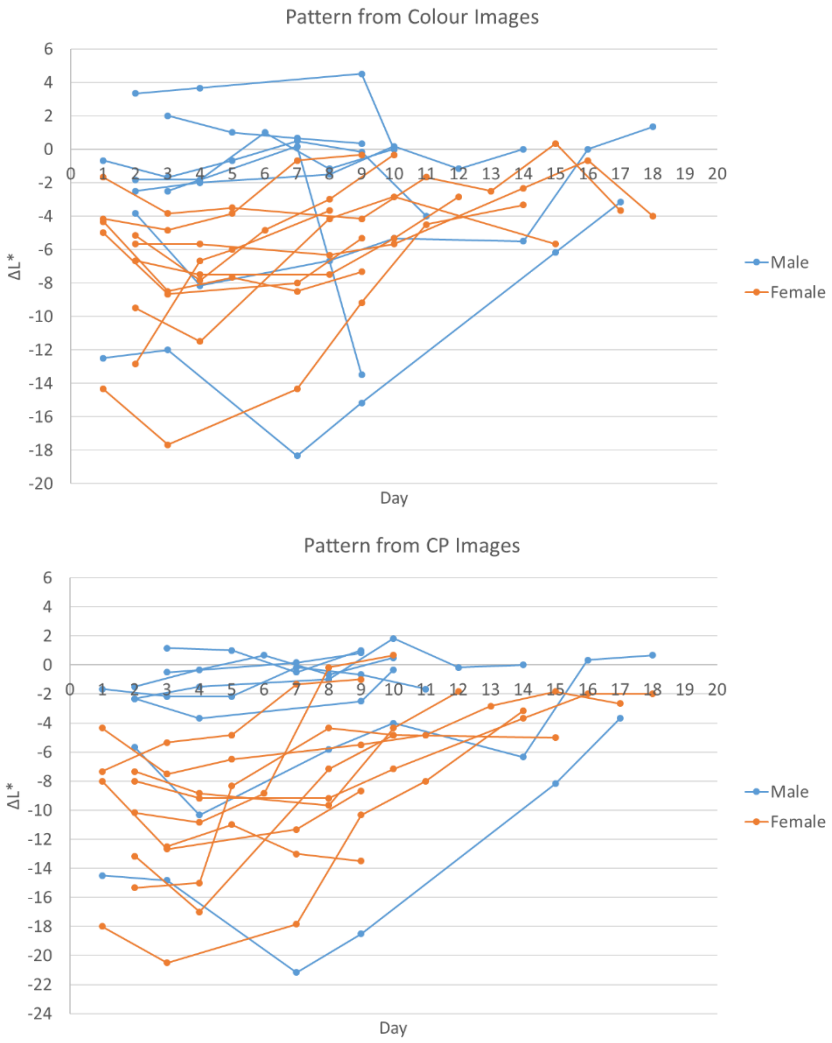

Figure 6-39 All L patterns taken from the colour and CP images, categorised by participant gender*

For the a* and b* patterns observed, there was a greater overlap in range therefore the patterns could not be stated as characteristic by gender. For all a* and b* patterns, see Appendix M.

Of the studies identified as having used this colour system in relation to bruising, Scafide et al. (2013), was the only one noted to consider and then comment on gender. Their findings suggested that gender had no significance in the prediction of bruise colour or how colour changed with time. That was found to be consistent with the range of a* and b* patterns between individuals of each gender observed in this study. However, the present findings surrounding the L* pattern did suggest that

gender somewhat plays a role in the severity (i.e. darkness) of bruising, particularly over the first half of a bruise timeline (approximately days 0 - 5). This could be of significance, yet as the range within each group varied and overlapped (one male participant presented with a bruise darkness similar to that shown by female participants), this could be an anomaly of the comparatively small sample size discussed earlier.

6.10 Effect of photography technique on bruise visibility

For colour and CP images, the first day on which bruising was recorded was the first day of return (either day 1 or day 2). Between both colour an CP images, only one case saw the day of initial visibility change from day 1 to day 3. IR imaging captured the immediate bruising present beneath the skin which had not become visible on the skin surface and to the naked eye. Therefore, IR imaging (and subsequently IR (altered) images) consistently allowed for early identification of bruising (Table 6-3).

Table 6-3 Average day bruise first visible for each photography technique

Photography technique	Average day bruise first visible
Colour	1.72 ± 0.67
CP	1.83 ± 0.71
IR	0 ± 0

For the number of days for which bruising was visible, the photography technique did not appear to have a significant impact. On average, bruising was visible a day less for IR imaging compared to colour or CP techniques (Table 7-4). Adjusting IR image contrast to determine if any unseen features could be detected, only increased the number of days of visibility to match that of the colour and CP images (Table 6-4). However, it did not reveal any bruising features which had not already been detected by the other techniques. CP photography improved visibility (though did not reveal any unseen features), by appearing to reduce the effect of leg hair masking the bruise whilst improving the contrast (Figure 6-40 shows an example of this effect).

A repeated measures ANOVA confirmed that there was no significant difference between techniques on the number of days a bruise was visible ($p = 0.157$). It was therefore concluded that no imaging technique had any significant advantage over any other in terms of identifying bruising which appears fully healed to the naked eye.

Table 6-4 Average number of days of bruise visibility for each photography technique

Photography technique	Average number of days visible
Colour	11.50 ± 3.57
CP	11.44 ± 3.71
IR	10.06 ± 4.31
IR (altered)	11.94 ± 4.37

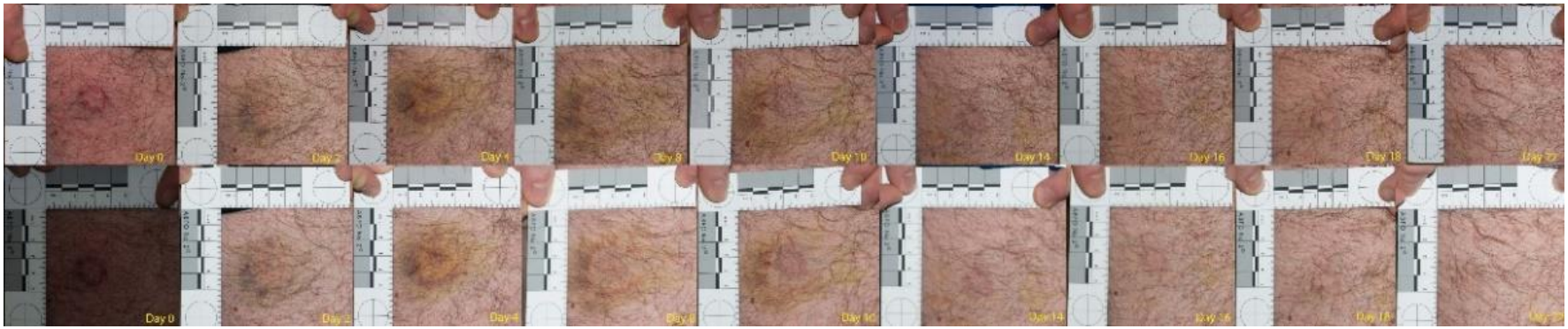

Figure 6-40 Timelines showing how CP photography lightens leg hair thus improving bruise clarity

6.11 Effect of photography technique on bruise contrast

6.11.1 Contrast at specific timepoints

Photography technique did appear to influence the contrast between bruised and non-bruised skin. For the average peak contrast of each technique, it was found that CP imaging provided the greatest contrast whilst IR the least. Unsurprisingly, by manually editing the IR images their contrast increased substantially (Table 6-5).

Table 6-5 Average peak contrast values for each photography technique

Photography technique	Average peak contrast
Colour	18.25 ± 10.79
CP	25.39 ± 17.89
IR	16.95 ± 5.70
IR (altered)	47.01 ± 17.22

A repeated measures ANOVA with the day of peak contrast and the value of peak contrast as within subject variables was performed. Results suggested that there was variation with day of contrast (results described later) and the peak value itself. Post-hoc analysis revealed that there was no difference in the level of peak contrast which colour and IR imaging could achieve (p = 0.375). Thus, once bruising was fully developed, IR photography (unaltered), provided no additional image clarity compared to standard colour photography.

There was a significant difference found between the peak contrast measurements for all other photography techniques (p < 0.001 in each case), with a correlation between one of the combinations – colour and CP (Figure 6-41). This showed that CP photography consistently provided greater contrast compared to colour photography, regardless of skin tone.

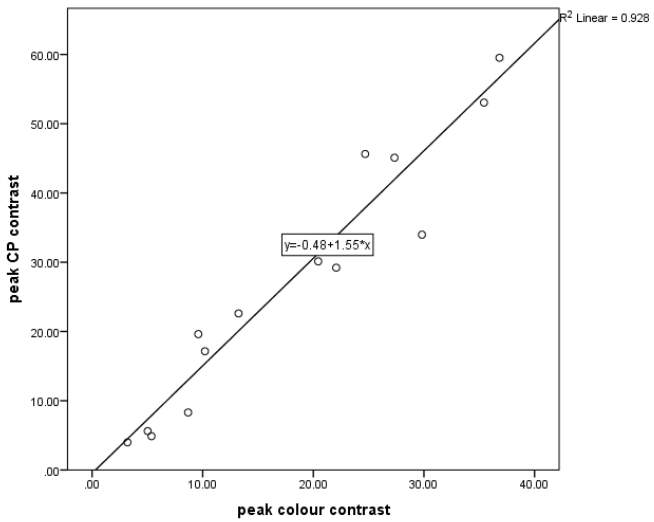

Figure 6-41 Positive correlation between colour and CP peak contrasts between bruised and non-bruised skin (r = 0.963, p < 0.001)

This improvement was generally seen over the full timeline, however as the bruise began to fade, the ability of either colour or CP photography to produce an image with clear contrast reduced. IR had the poorest contrast across the whole timeline, though was similar to the colour imaging results over the first 10 days. Although once altered the IR timeline had the greatest contrast, the trend was less defined and its effectiveness over the other methods dropped from day 12 onwards. The average contrast timelines for each photography technique is shown in Figure 6-42).

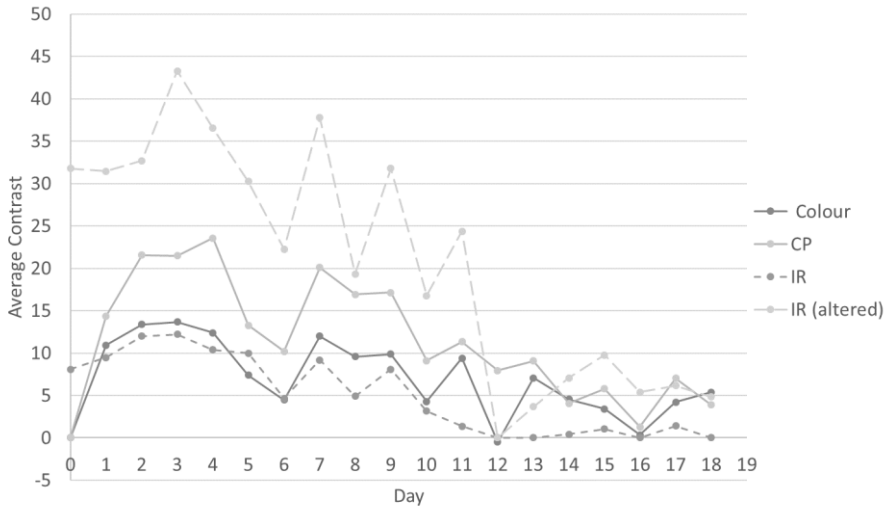

Figure 6-42 Average colour and CP contrast timelines for all participants

As previously stated, photography techniques were also found to influence the day at which peak contrast was observed. IR photography (both original images and altered), identified peak contrast approximately a day before the colour and CP images (Table 6-6).

Table 6-6 Average day peak contrast was observed for each photography technique

Photography technique	Average day of peak contrast
Colour	4.63 ± 2.71
CP	4.61 ± 2.20
IR	3.19 ± 2.59
IR (altered)	3.61 ± 2.77

From the post-hoc analysis of the repeated measures ANOVA, significant differences were found between the peak contrast days associated with the colour and IR images and the CP and IR images (see Table 6-7).

A possible explanation for this could be, that it takes time for bruising to initially become visible on the skin surface due to migration through the soft tissues. Therefore, as IR allows the visualisation of bruising beneath the skin surface, using this technique could be a more accurate way of documenting the healing time of a bruise.

Table 6-7 Calculated p-values for each photography technique comparison relating to the average day of peak contrast of bruise from non-bruise skin

Groups compared	*p* value
Colour and CP	0.806
Colour and IR	0.016
Colour and IR (altered)	0.199
CP and IR	0.004
CP and IR (altered)	0.104
IR and IR (altered)	0.085

6.11.2 Contrast by individual characteristics

As a characteristic average contrast timeline was identified in Figure 6-42, this data was assessed in more detail. Looking at all individuals together regardless of technique, the contrast patterns present with a wide variation of contrast, altering in intensity with technique. All contrast timelines are shown below in Figure 6-43 and Figure 6-44. Given the differences in contrast levels observed, this data was considered in the same manner as the colour pattern data, ungrouped and grouped by individual characteristics. As before skin tone, BMI and gender were considered.

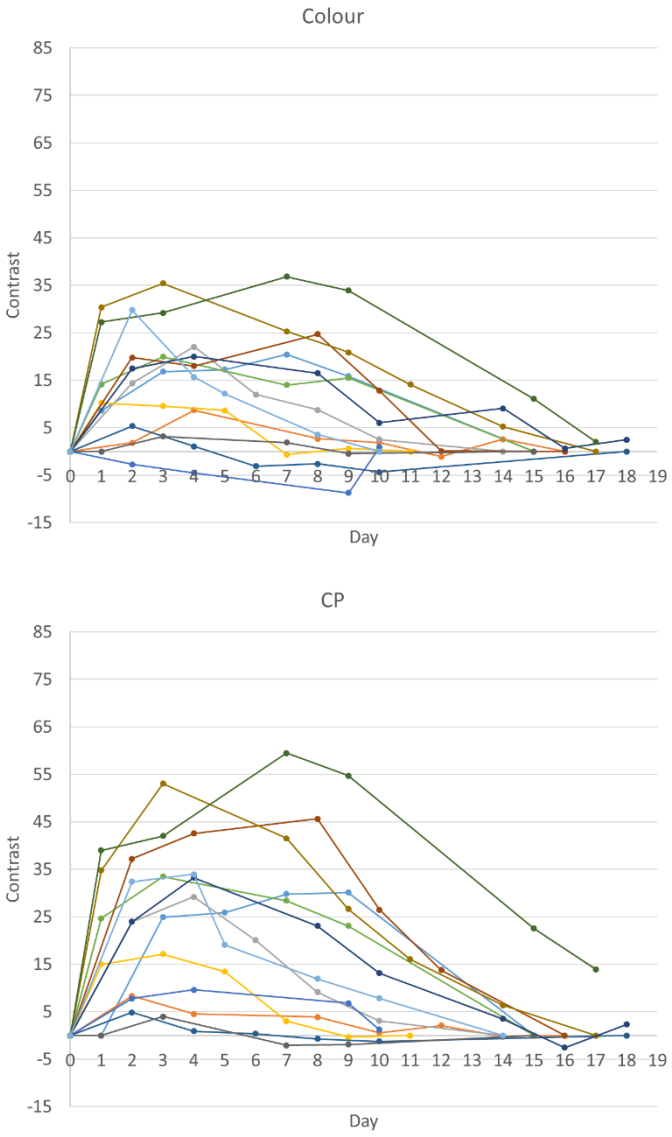

Figure 6-43 Each participant's contrast timeline taken from the colour and CP images

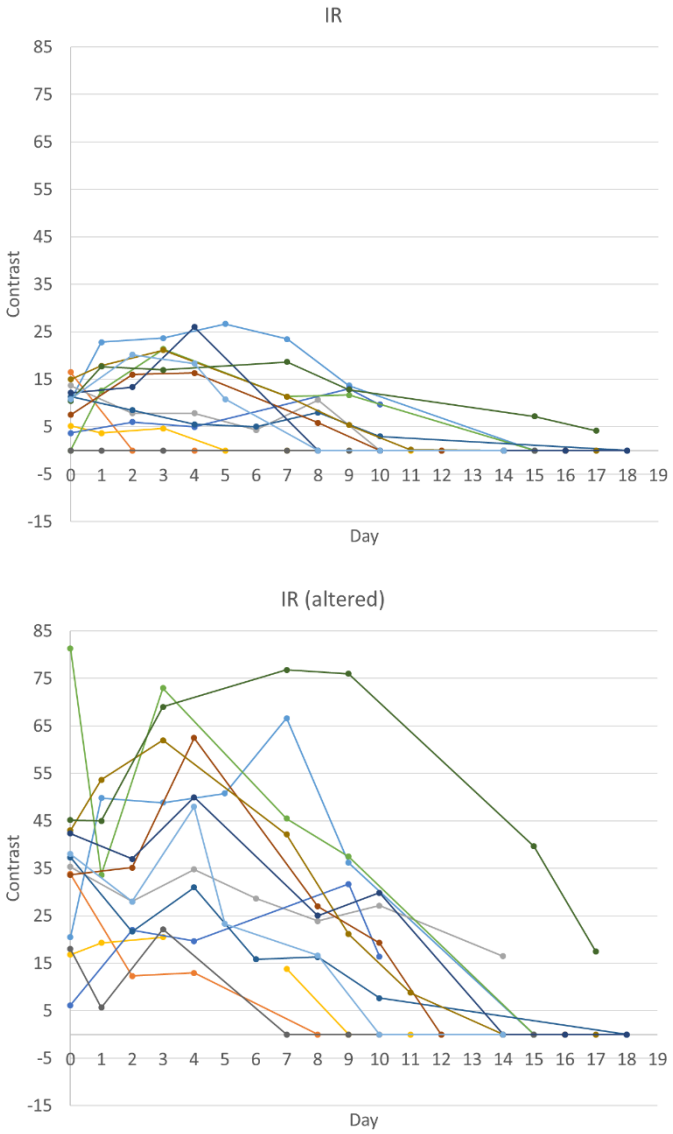

Figure 6-44 Each participant's contrast timeline taken from IR and IR (altered) images

6.11.2.1 Categorisation by simplified skin tone categories

For both simplified and all skin tone categories, the contrast timelines were only considered from the colour and CP images, as skin tone could not be determined from using IR.

For the simplified categories of dark, medium and light skin tones, the level of contrast observed could not be attributed to either group. For the colour images, each group presented with a wide variation and overlap with each group. Once considering the CP images which altered the skin tone classification to only dark and

light, again the contrast timelines overlapped. Therefore, contrast between bruise and non-bruise skin over the injury timeline was no influenced by the skin tone of the individual. Both colour and CP timelines are shown in Figure 6-45.

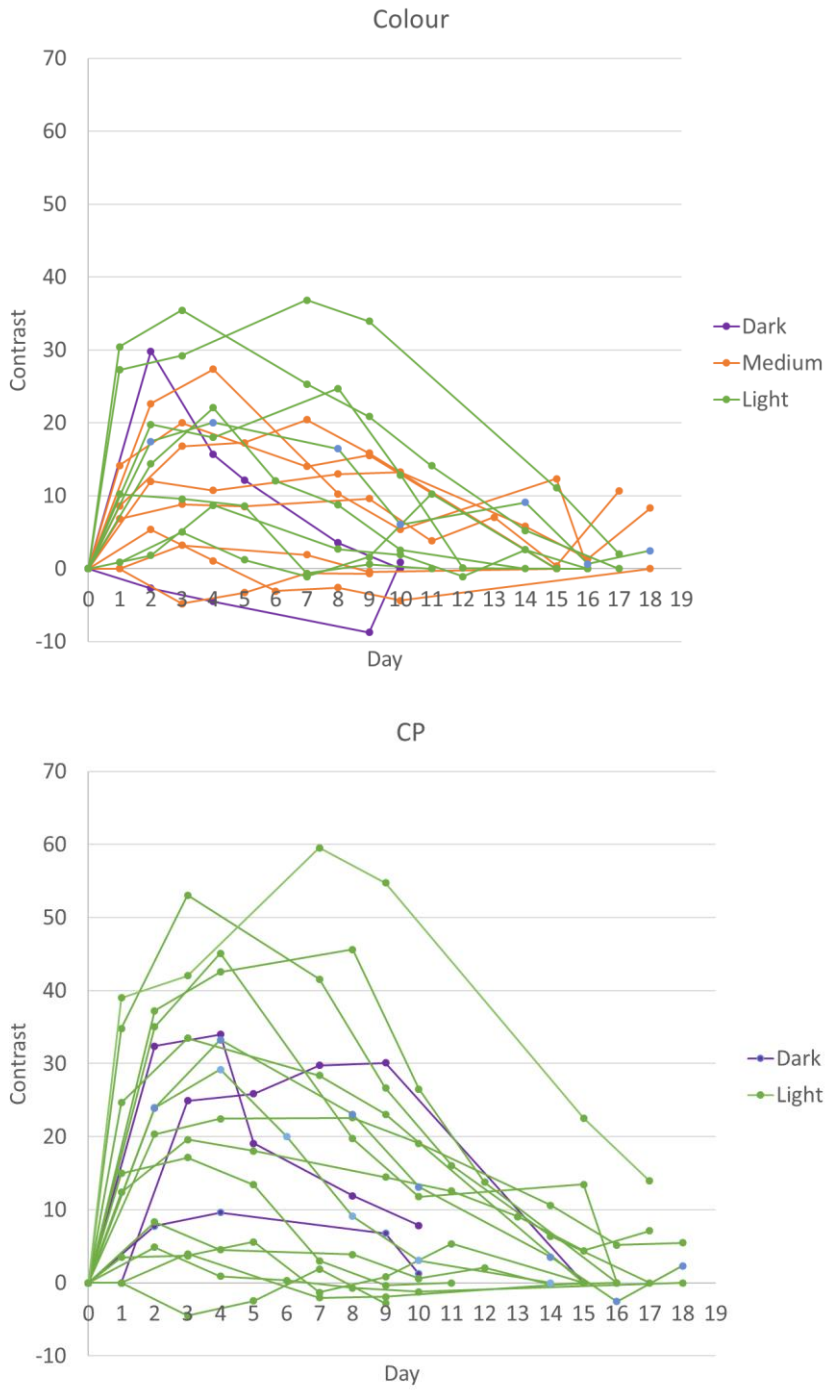

Figure 6-45 Each participant's contrast timeline, categorised by the simplified skin tone categories, for both colour and CP imaging techniques

6.11.2.2 Categorisation by all skin tone categories

As with the simplified skin tones, when expanded to include all skin tone groups, contrast levels could not be attributed to any group. Both colour and CP contrast timelines are shown below in Figure 6-46.

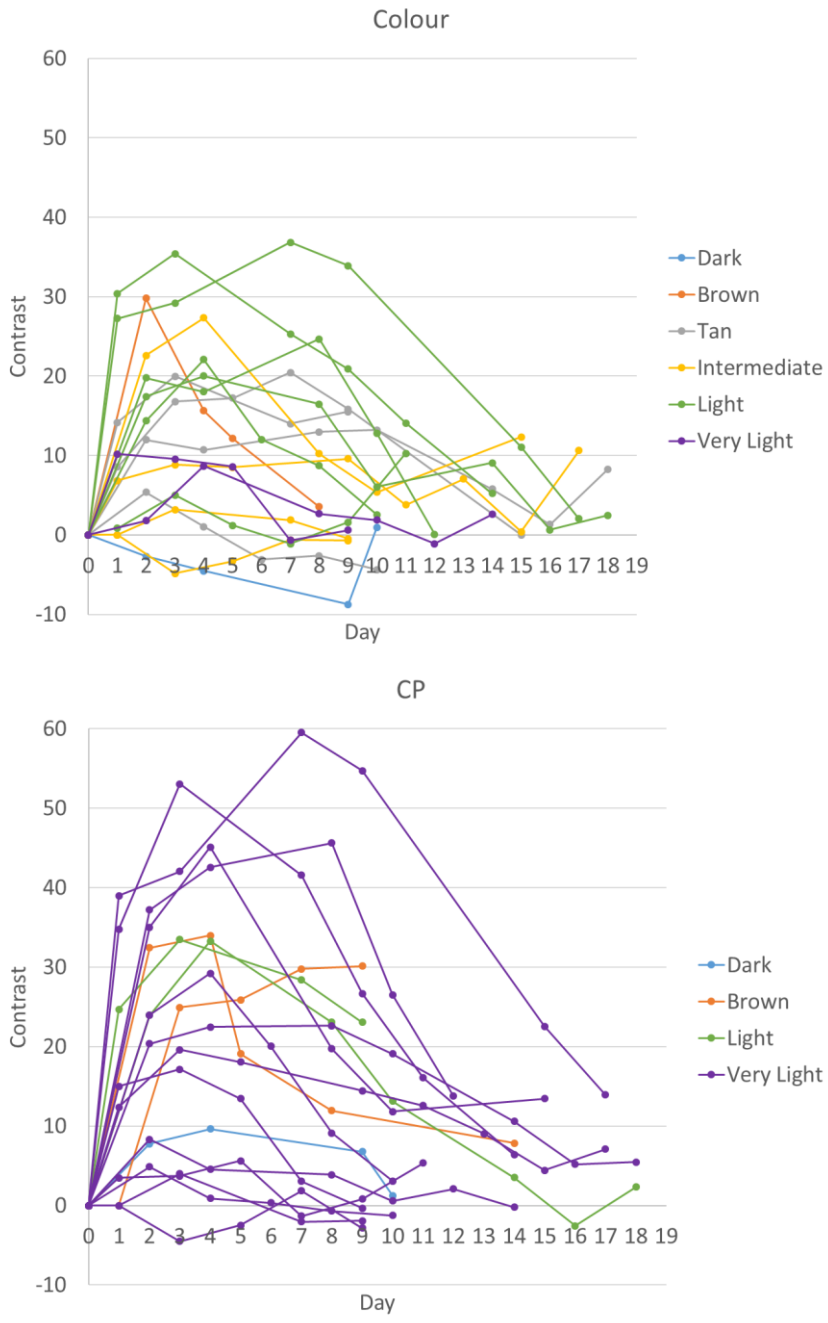

Figure 6-46 Each participant's contrast timeline, categorised by all skin tone categories, for both colour and CP imaging techniques

Looking at the colour image results, it could be argued that as skin tone goes from dark to light, the level of contrast increases, with the exception of very light skin tones. However, as seen before the patterns for each group overlap with those from other groups so this observation cannot be considered conclusive.

For the CP results, the ability to see any category is reduced as the majority become classed as having very light skin tone, thus making it impossible to attribute contrast level with skin tone category.

6.11.2.3 Categorisation by BMI

Individuals were again grouped into three categories of healthy, overweight and obese based on their calculated BMI. This was to determine whether contrast levels could be attributed to an individual's build.

For the colour and CP (as shown in Figure 6-47), it generally appears that contrast increases for those with a higher BMI, however this did not apply to those classed as obese whilst again, there was overlap between each category.

For the IR and subsequently IR (altered) images, the contrast timelines observed again could not be attributed to BMI categories (Figure 6-48). The use of IR appeared to give a more variable range of patterns, i.e. the overlap between groups was more significant than with the colour and CP techniques. Furthermore, the levels varied even more once contrast levels had been altered, making group categorisation impossible.

Therefore, as found for skin tone, it was not possible to link contrast range with BMI category, regardless of imaging technique.

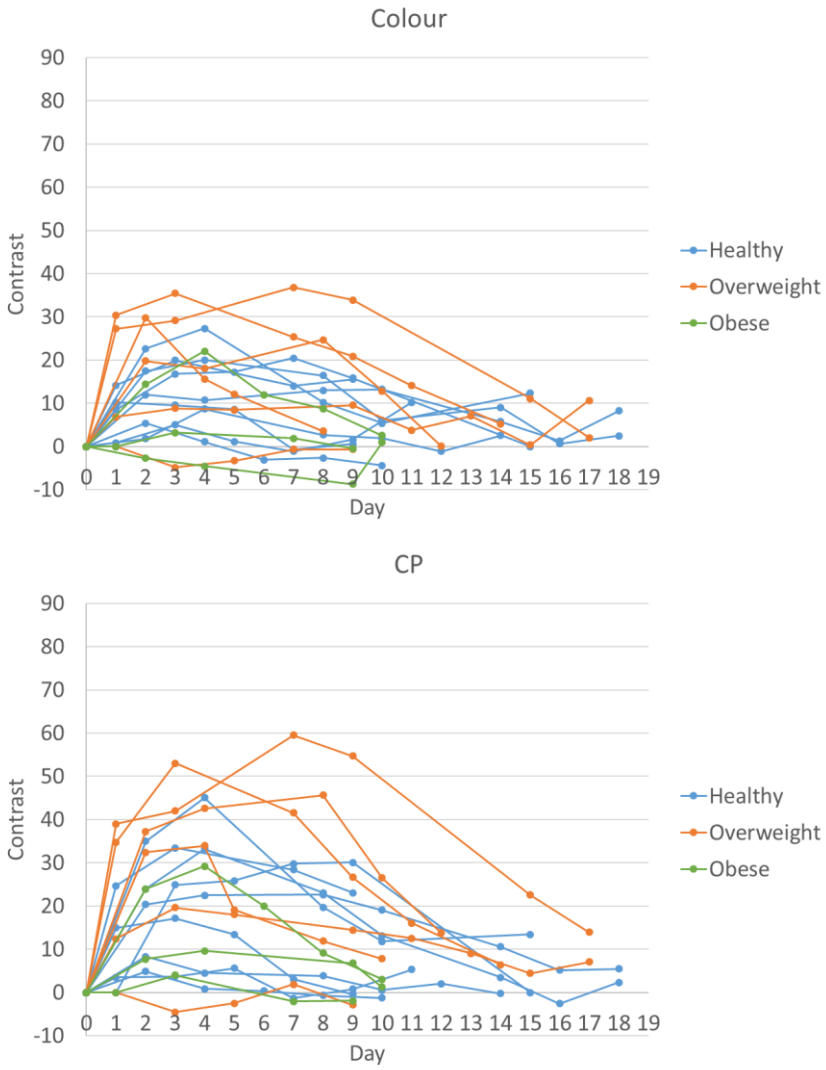

Figure 6-47 Each participant's contrast timeline, categorised by BMI, for both colour and CP imaging techniques

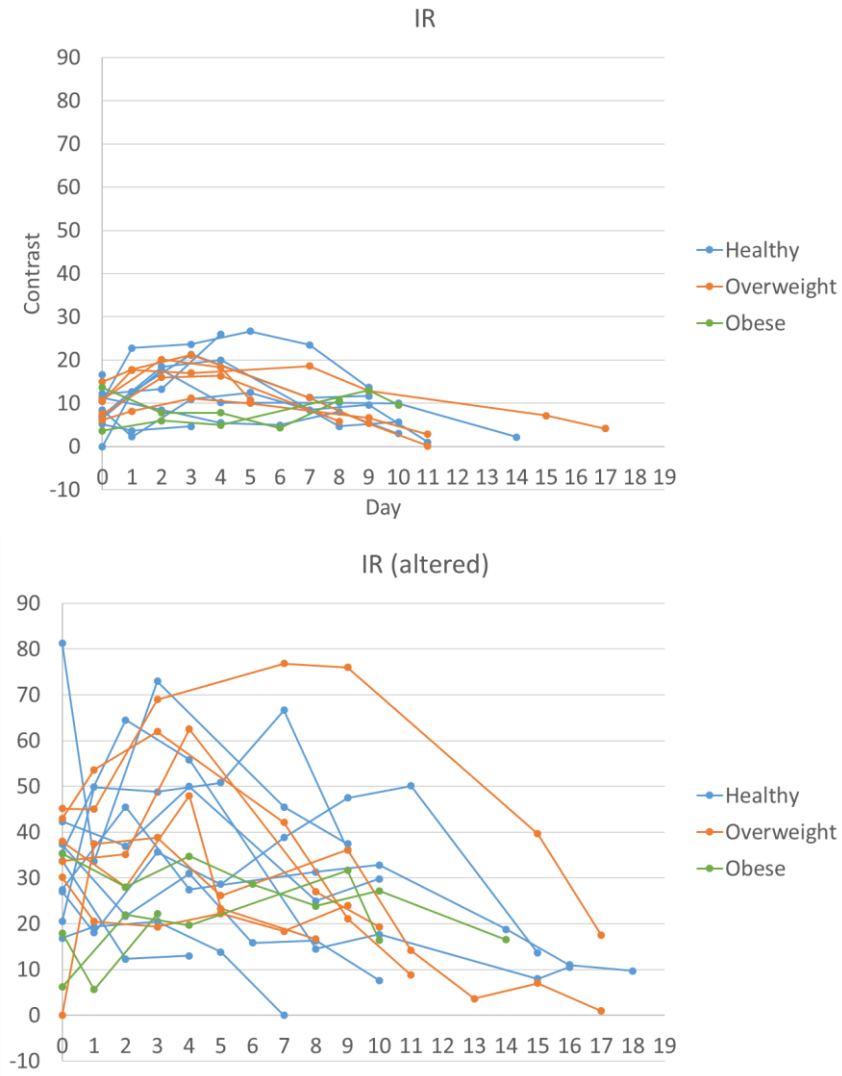

Figure 6-48 Each participant's contrast timeline, categorised by BMI, for both IR and IR (altered) imaging techniques

6.11.2.4 Categorisation by gender

Individuals were grouped by their gender (8 males and 10 females), to determine whether contrast could be attributed to either group.

For the colour and CP techniques (Figure 6-49), the contrast timelines showed that in general, female's had greater contrast between bruised and non-bruised skin across their respective timelines. However, this could not be conclusively stated as there were exceptions to this in each case.

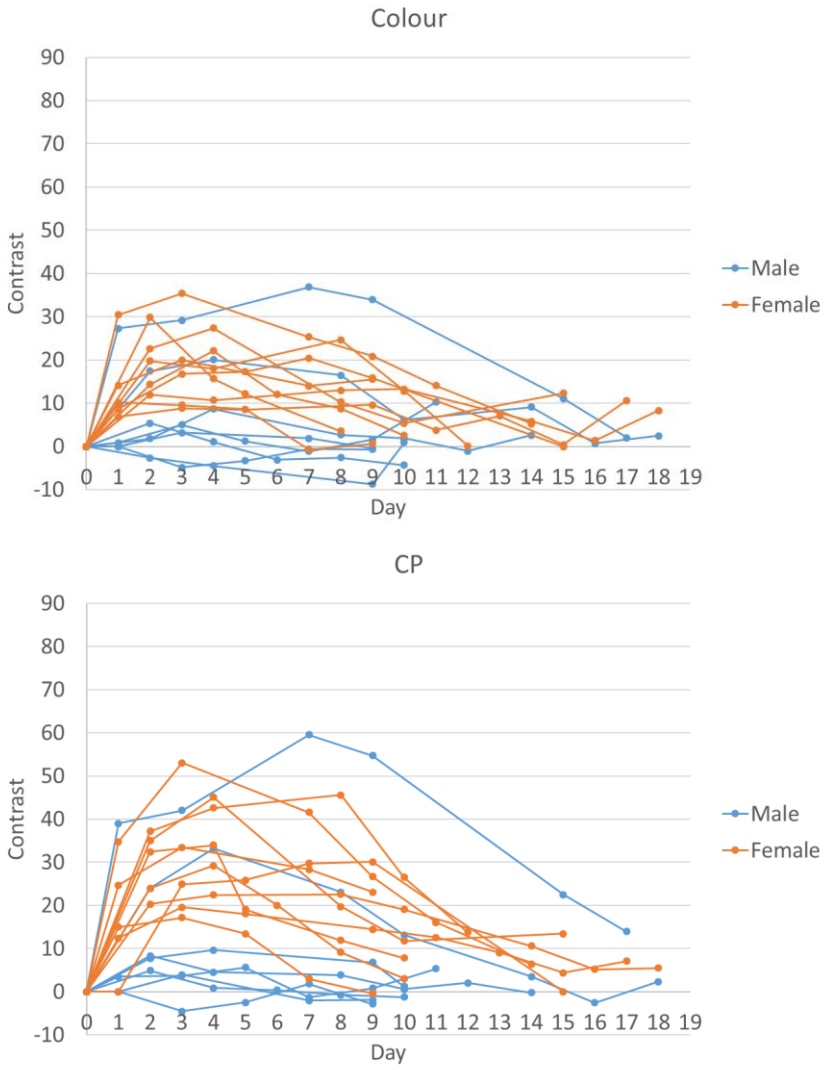

Figure 6-49 Each participant's contrast timeline, categorised by gender, for both colour and CP imaging techniques

Any indication that contrast results could be categorised by gender was lost when considering the IR photography techniques (shown in Figure 6-50). The overlap in range of contrast levels was increased, particularly once the contrast levels were manually altered, thus this was unsuccessful.

For all characteristics considered (skin tone, BMI and gender), the general pattern of an increasing contrast was observed for approximately the first 5 days, before dropping as the bruise fades. There was no known study to have considered this approach to contrast measurement whilst comparing individual results in this

manner. Therefore, it was concluded that contrast could not be describe bruise contrast progression for any of the considered categorisation groups.

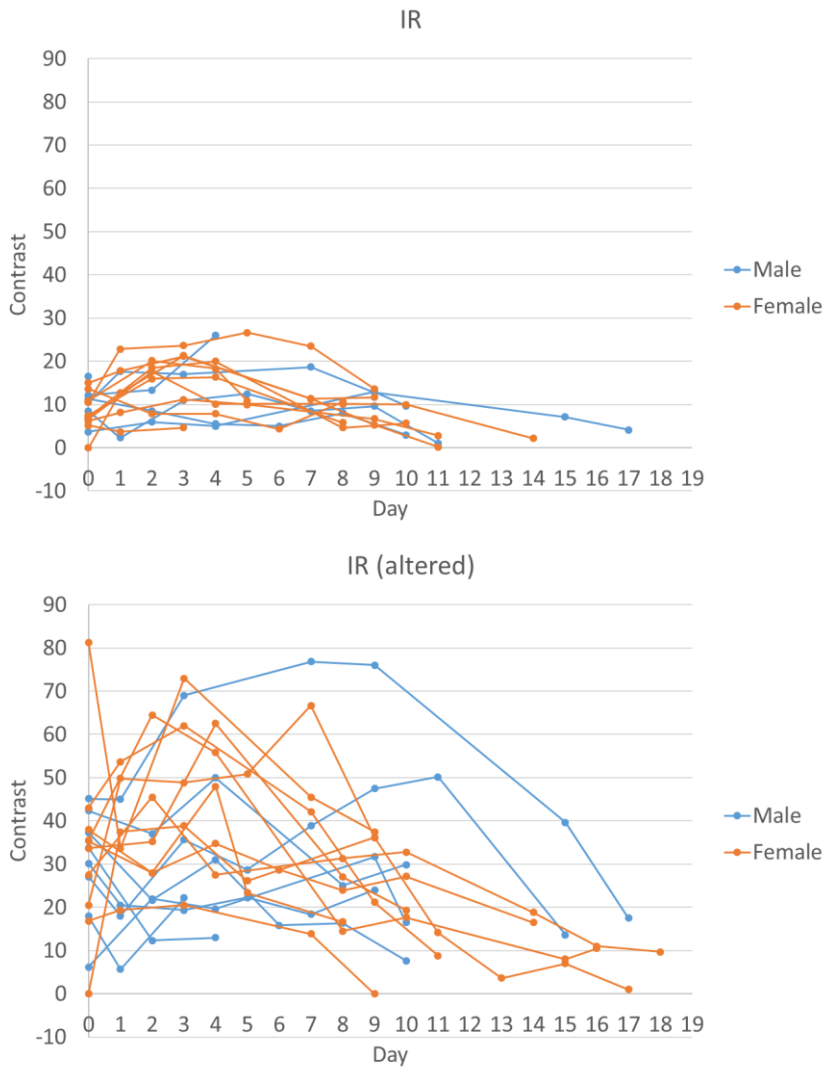

Figure 6-50 Each participant's contrast timeline, categorised by gender, for both IR and IR (altered) imaging techniques

6.11.3 Contrast over whole timeline

Baker et al., (2013), used a grouping system of days 1 to 3, 4 to 6 and 8 to 10 when assessing timeline contrast. This was also used in this research, however the last group was changed to days 7-10, as there was no reason to exclude day 7 data.

Overall contrast was greatest for the first 3 days, decreasing from day 4 onwards (Figure 6-51). The photography technique found to have the greatest contrast was CP photography, however this changed once the IR images were altered

(i.e. contrast was manually increased). The variation in contrast varied not only between techniques but also between participants. These contrast trends were also visible to the naked eye, as shown in Figure 6-52, which is an example of a full bruise timeline documented by all imaging methods and the IR (altered) images. All timelines not shown in this chapter can be found in Appendix N.

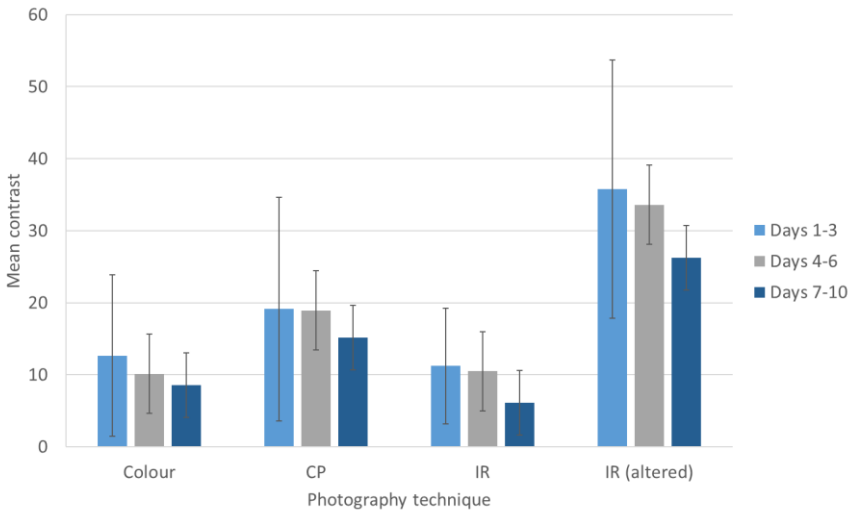

Figure 6-51 Bar chart of the average contrast measured for different time periods for each photography technique

CP photography increased the definition of the outer bruise boundary compared to colour photography, for all skin tones. However, with only one dark skinned participant (see Figure 6-53), this finding requires additional confirmation.

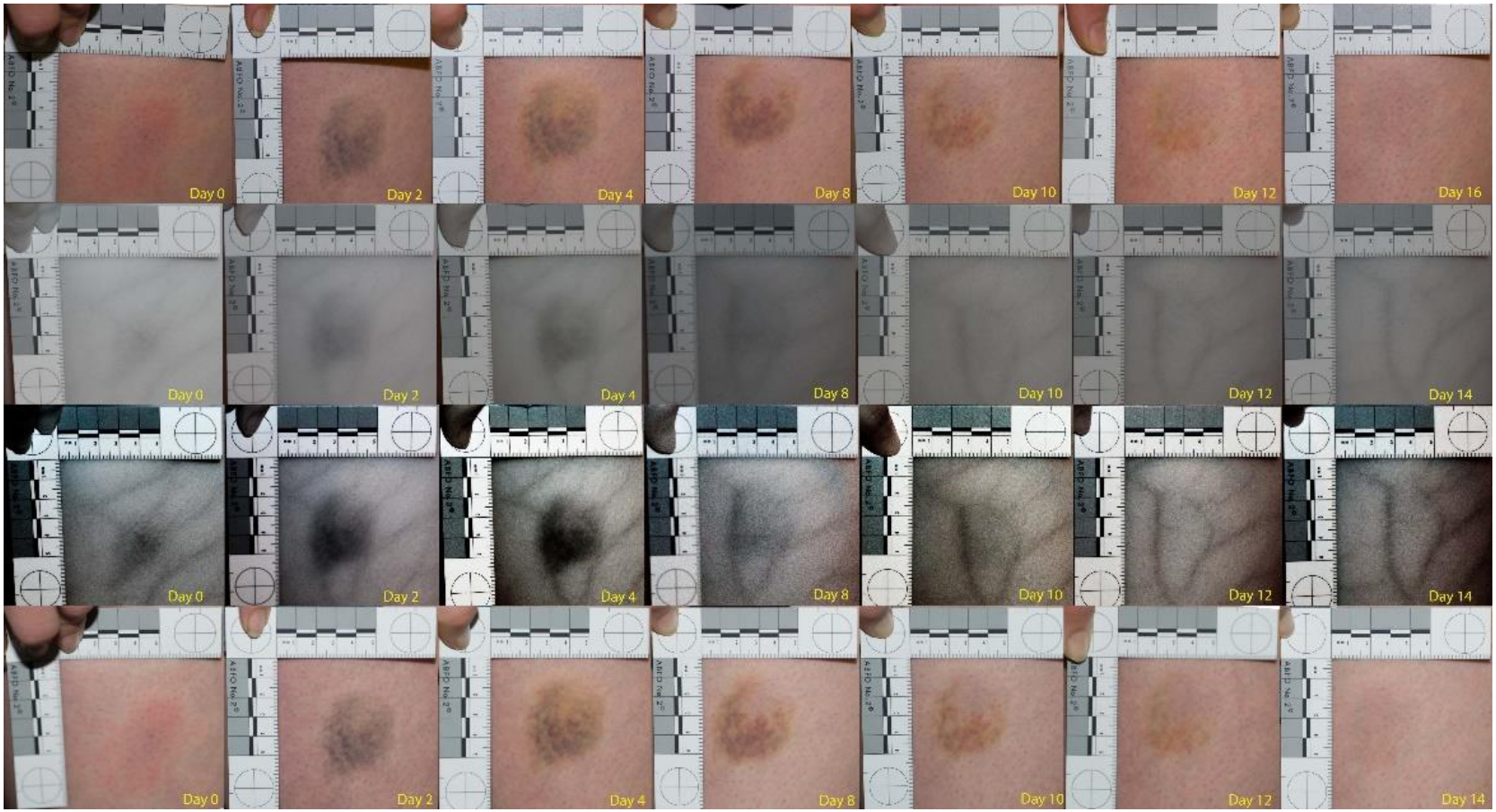

Figure 6-52 Example of bruise timeline captured by all photography techniques. From top to bottom: colour, IR, IR (altered) and CP images (Participant PS08M

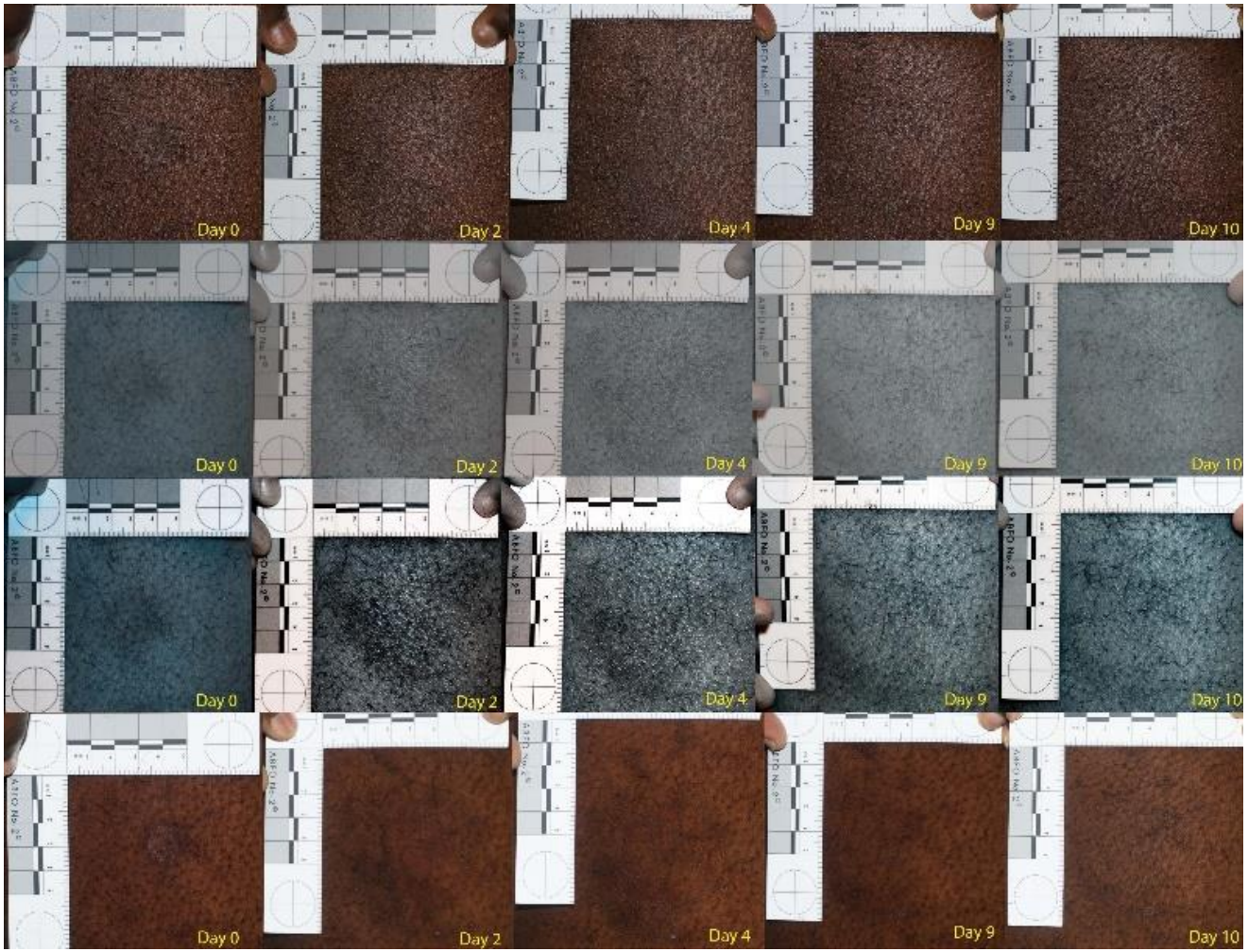

Figure 6-53 Clarity of bruise on dark skin, for each photography technique. From top to bottom: colour, IR, IR(altered) and CP images (Participant NI2TE)

IR imaging provided contrast between bruised and non-bruised areas on dark skin where visible identification was unclear (Figure 6-53). Although information on bruise shape could be inferred from all image types, IR (and subsequently the altered IR images), provided the clearest profile. It was noted that definition was less than that which was seen on the lighter skin tones.

It should be noted that with IR's ability to capture the skin's underlying vasculature, this could reduce the clarity of the outer bruise boundary if there was any overlap, particularly in the later stages of bruise healing (see Figure 6-52). Furthermore, vasculature could not be removed from the image before analysis, although it should be noted that vasculature was not observed in all cases, even after image alteration (see Figure 6-54).

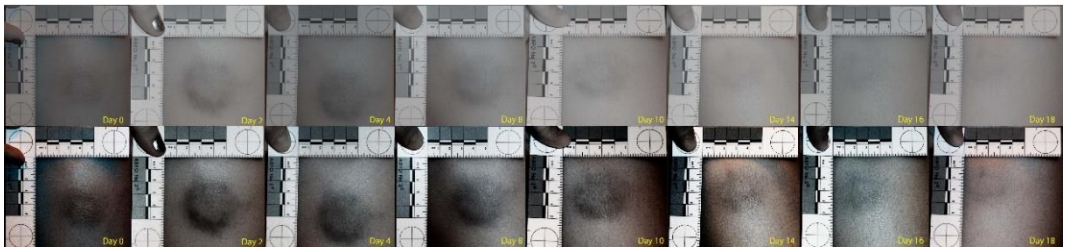

Figure 6-54 IR and IR (altered), image timelines for a bruise where no underlying vasculature was captured

6.12 Effect of photography technique on bruise colour

CP photography was found to influence the bruise colour levels measured. For the first day on which the bruise was visible, the L* (lightness) values were on average lower for CP when compared to the colour images. For the average a* (red to green) values, CP images are more positive which was also seen for the average b* (blue to yellow) values (Table 6-8). Statistically (paired t-test), for each colour model parameter the differences resulting from photography technique were found to be significantly different for only the L* values ($p < 0.001$). This can be explained by the impact mark appearing as a red mark on all individuals (i.e. there was little to no difference in the mark appearance).

*Table 6-8 Average L*a*b* values for the initial bruise (i.e. the day which it was first visible), for colour and CP images*

Photography technique	Mean initial bruise colour values		
	L*	a*	b*
Colour	-4.88 ± 4.86	-1.64 ± 1.84	-2.08 ± 4.27
CP	-7.31 ± 5.67	-0.96 ± 1.81	-1.49 ± 3.99

CP photography also significantly (paired t-test) increased the average peak b* value observed (Table 7-9, $p < 0.001$), which is noteworthy as yellow is the colour considered most valuable when analysing bruising. Furthermore, the average day on which the peak b* values (also shown in Table 6-9) was found to be the same for each technique ($p = 0.886$).

Table 6-9 Average peak b value and day of peak b* for colour and CP images*

Photography technique	Mean peak b* colour value	Day
Colour	3.66 ± 4.04	7.89 ± 4.13
CP	5.48 ± 4.41	7.78 ± 3.44

6.13 Effect of photography technique on bruise area measurements

The maximum area of bruising generated varied significantly between individuals, ranging from 5.49 cm^2 to 41.5 cm^2 (across all photography techniques). By splitting the range of maximum areas into thirds, bruising could be categorised as small, medium or large. The categories are shown in Table 6-10.

Table 6-10 Overall bruise area range and the resultant ranges for classification of bruising as small, medium and large

Minimum Area	Maximum area	Range	Third of range
5.49 cm^2	41.5 cm^2	36.01 cm^2	12.00 cm^2
Size Categories			
Small < 17.49 cm^2	17.49 cm^2 < Medium < 29.5 cm^2		Large > 29.5 cm^2

Photography technique was found to influence the area measurements of the impact mark, initial surrounding red area and the maximum bruise area. The average area of each feature (Table 6-11), colour and CP were closest overall. However, with the IR images detecting immediate bruising not visible to the eye, the impact mark appeared larger. In addition, by altering IR image contrast to enhance the bruise visibility, area measurements were larger still. All techniques have a similar average when the bruise appears at its largest.

Table 6-11 Average area of the impact mark, surrounding red mark and max bruise (cm^2), for each imaging technique. Impact mark and surrounding red mark measured at Day 0, with max area being the largest area measured for each bruise, irrespective of day.

Photography technique	Average area (cm^2)		
	Impact mark	Surrounding red mark	Max bruise
Colour	3.31 ± 0.76	24.79 ± 9.75	20.79 ± 9.22
CP	3.05 ± 0.55	22.87 ± 10.00	21.00 ± 10.16
IR	8.51 ± 2.55	-	20.47 ± 9.96
IR (altered)	9.54 ± 3.39	-	21.06 ± 9.30

The standard deviations are all relatively small for the impact mark where the measured shape had a clear edge regardless of technique. This increases for the IR and IR (altered) images, as a greater area of blood pooling is detected and the boundary has less definition to that seen in the colour and CP images. The increase in value of the measurements from IR to IR (altered) images, resulted in them being similar to the averages calculated for colour and CP. For the surrounding red mark (only visible in the colour and CP images), skin tone influenced its definition,

therefore area varied between individuals and a larger standard deviation was observed. This also applied to the maximum bruise area for all imaging techniques.

Statistically, the differences between colour and CP impact mark areas were found to be significant (Wilcoxon Signed Ranks Test: p = 0.001) and the IR and IR (altered) impact mark areas were also found to be significantly different (paired t-test: p = 0.004). The measurements of the surrounding red mark and maximum bruise sizes were all found to be similar. The only significant difference observed was between the maximum areas measured in the IR and IR (altered) showing that IR was the least consistent of all techniques. Therefore, photography technique had a significant influence in the documentation of immediate bruising, which may or may not have been distinguishable from a surface impact mark. For older bruising these differences are no longer present, thus the techniques were all as a good as each other when capturing bruise size.

Using different image techniques resulted in a change in the number of participants per size category (small medium and large). The majority appeared to be either small or medium regardless of imaging technique (Table 6-12).

Table 6-12 Number of participants with small, medium and large bruising, observed in each of the 3 photography techniques and the IR (altered) images

		Photography technique			
		Colour	**CP**	**IR**	**IR (altered)**
Bruise size	**Small**	7	8	9	8
	Medium	7	6	4	7
	Large	4	4	3	3
	Total	18	18	16	18

Chapter 7

Discussion

7.1 Visual analysis

This visual analysis is the main limitation of this video analysis. As the camera was manually positioned in each test, the camera's field and angle of view varied between individuals and, combined with the unpredictability of impact location, the extent of tissue wave perceived could have been effected. Camera angle also influenced identification of wave peak, as a completely side on view hid the internal part of the deformation along with the impacting ball. Although the camera distance influenced the scale of each video, it does not hide the fact that the extent of deformation varied. Future work could utilise this method in such a way that the wave could be tracked, rather than the ball. For example, by applying reflective material to the shorts (or bare skin), in a similar way to that used gait analysis. In doing so a greater understanding of energy dissipation by soft tissues could be investigated between different individuals.

A notable problem, not only in consistency of camera angle, was the resolution of the images. With the setup as it was, although the lighting allowed for recording at a greater frame rate, this did reduce the quality of recording. Although not necessarily a problem as the ball was clearly identifiable (important for the analysis), if any future study was to focus on the tissue deformation then it should be taken into consideration.

Another problem which can be seen in the videos is the shorts, although tight fitting shorts were requested and in some cases supplied, the different materials which were ultimately used, did fit differently on different people. Clearly the more lycra based shorts fitted smoothly over the thigh (which was the ideal scenario), but where the material was more cloth based, it was not as flush against the skin. It is not expected that this significantly influenced any of the results. If this study was to be repeated, ensuring all participants have the exact same clothing would reduce and variation of skin surface damage and the possibility of material masking part of the impacting object.

7.2 Impact mechanics

The methodology used allowed for clear characterisation of each impact, impact velocity and applied force being clearly identifiable.

How the force is transferred to the thigh can be described through the 3 peaks observed. Although the 3rd peak was excluded from analysis, when viewed alongside the respective video frame, it occurred at the point at which the ball had undergone an elongation deformation (as also seen during method development). Furthermore, it could not be determined whether the ball was free from contact with the soft tissue at this point, due to both the soft tissue deformations masking the base of the ball and the opaque nature of the ball itself (shown in Figure 7-1).

In all videos, the ball was seen to undergo such deformations as its shape oscillated around the spherical. This was reflected in all the results as oscillations were seen after this 3rd peak. However, given the known state and directionality of the ball at this point, it was concluded that this peak was likely the first of the ball deformation oscillations.

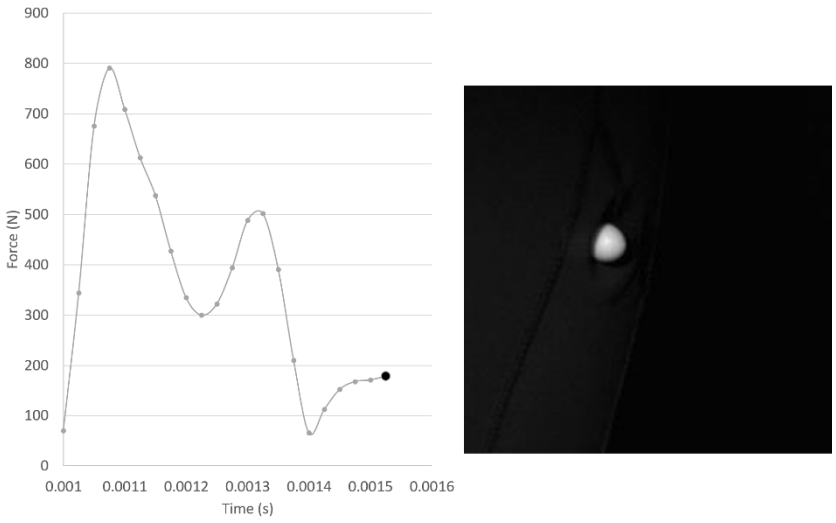

Figure 7-1 Example of force trace alongside the respective video frame, showing elongation of the ball shape as it begins its rebound off the impacted thigh

The impact of a hyperelastic sphere on a compliant, viscoelastic medium is a very complex mechanical interaction. This problem deserves significant analysis and modelling, out with the scope of this thesis. The causes of the repeatable impact characteristics can only be hypothesised.

The 1st peak force has already been defined as the applied force at the point at which the ball initially comes into contact with the soft tissue, and significant deformation has yet to occur – i.e. rapid deceleration of the ball at the point of contact.

Considering the viscoelastic properties of the tissues, by definition they are not fully solid. As the deformation during impact increases, the tissue beneath the impact is compressed. Given a non-linear stress-strain relationship, tissue stiffness may rapidly increase resulting in a 2nd peak force.

Another possibility is that the impact induced pressure wave is reflected back and the resultant interaction between this wave and ball is what gives the 2nd peak. It cannot be concluded whether reflection occurs from the muscle or bone with the variability between individuals being due to their own body composition.

With the specific adiposity of each individual's thigh being unknown, it was difficult to come to any conclusion as to the extent to which tissue composition influenced the applied force and its dispersion during these impacts. For the first 2nd peak hypothesis a greater adiposity would result in a greater deformation before the 2nd peak was observed.

Referring to the method development for this study, impacts to the wooden board also presented with the same 3 peak pattern. This suggests that the second hypothesis of a reflected pressure wave likely as the stiffness of the board did not change. Assuming an equivalent change in momentum between participants, the impulse of a force is also constant. A high 1st peak would imply a lower 2nd peak and vice versa. This is what is shown in Figure 7-2, where BMI increases the 1st and 2nd peak forces decrease and increase respectively. However, although a correlation between BMI and the 1st peak force has already been identified, there was not one

for BMI and the 2nd peak force (r = 0.507 and p = 0.077). This was likely a reflection of the volunteer pool, where higher BMI's could have been attributed to individuals who had a more muscular build than in having a higher adiposity. Therefore, adiposity likely influenced the level of force transmitted through and reflected back to the skin surface and would be a more appropriate measure (compared to BMI) in this case.

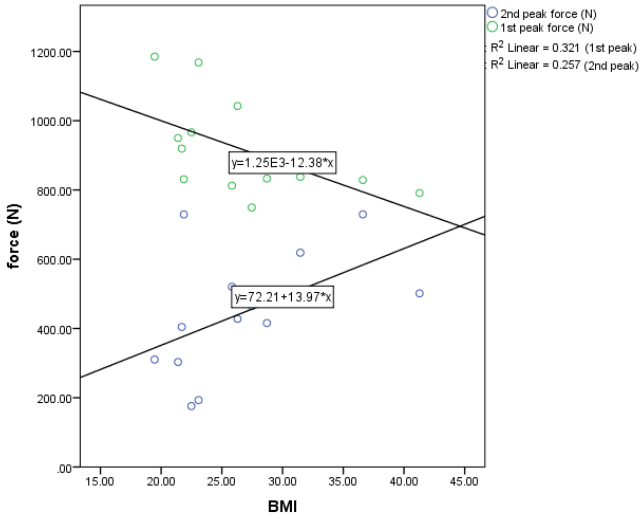

Figure 7-2 Plot of both 1st and 2nd peak forces against the BMI of each participant

An alternative explanation for both 2nd and 3rd peaks is that both reflect oscillations in ball shape. This would be based on the premise that the wave produced both once fired and during impact within the ball caused the deformations. It was not possible to measure the oscillations pre-impact however as the 2nd peak occurs at a measured timepoint and its material is known, this could be tested for both human tissue and wooden board impact (from the methodology development Figure 4-48 (page 130) was chosen as the methods used for data analysis matched that of the main study). Using the speed of sound through rubber (approximately 54 m/s^{-1} (Plack, 2014)) and the average time between 1st and 2nd force peaks, the distance at which a wave would travel through the ball could be estimated (shown in Table 7-1).

Given that the ball is seen to have a large deformation at this point during impact and each distance calculated is shorter than the diameter of the ball (1.6 cm), the idea that both 2nd represents a ball oscillation is also a likely hypothesis. Therefore, future work would be required to prove this hypothesis as the

measurements are only estimations given the previously acknowledged errors in data accuracy and the effect of tissue composition during the impacts to the thigh.

Table 7-1 Average distance calculated for a shockwave to travel through the rubber ball during impacts to a wooden board and to the thigh

	Average time between 1st and 2nd peak force (ms)	**Average distance travelled by wave (cm)**
Wooden Board Impact	0.168	0.907
Human Tissue Impact	0.219	1.18

Tissue composition not only appeared to influence the force applied to the tissue, but also the time this takes to happen. The results also indicated that in general, an increased BMI increased peak-to-peak time.

Maximum tissue displacement was taken at the point of the 2nd peak force, as after this point the ball appeared to begin to change direction, thus bounce off the skin. The problem with this system as a whole was that it could not be stated conclusively that this was the exact point of directional change, as both the ball and tissue deformations overlap.

However, the tissue deformations did visibly differ between individuals. As in the pilot work of this research, for some individuals a shallow wave was seen to propagate across the thigh, while for others a wave with a much more defined edge was seen. Unfortunately, it was not possible to clearly identify wave size as the shorts worn by participants reduced the definition (unavoidable consequence of the experimental setup). Therefore, no link could be made between wave size, propagation distance and resultant bruising. It is hypothesised that a crested wave would result in greater shear forces and in turn greater tissue damage and bruising. All impact videos are shown in the electronic Appendix O.

7.3 Linking impact to bruise

Although the specifics of individual variance could not be quantified, a theory on how impacts result in bruising can be made. The process seen during this study was a complex system of not only a deformable impact surface, but also the

impacting object. This increased the complexity of the interaction between the two, which could not be captured through a visual assessment due to the high speed camera setup.

Given the impact interaction, it is clear that the tissue at the point of contact was compressed and that this resulted in a deformation wave propagating outwards away from this site. As previously discussed in this thesis, the focus of the majority of blunt impact research is on the mechanics of traumatic and/or fatal injuries rather than comparatively minor bruising. However, on reassessment, one article did provide such an explanation and though the context is again traumatic injury, the theory still applies.

Cooper and Taylor, (1989), described both compression and shear waves in terms of blunt impact, starting with compression. These waves tend not to generate significant damage (e.g. lacerations) to tissues, but can cause vessel rupture. They also stated that such waves will also reflect off structures within the tissue and this in turn both increases the localised pressure on the impact site and within the tissues. For shear waves, they related this to deformation of internal organs adjacent to specific impact sites.

Although their focus was on large impacts to the chest, their descriptions apply to this research. The hypothesis of the 2nd peak force observed being a reflected pressure wave, could in turn explain the impact mark formation with the two opposing forces compressing the intradermal blood vessels. This then would cause a build up of pressure and subsequent vessel rupture.

However, as the bruising generally presented with a central clear zone (doughnut shape), it can be assumed that the compressive pressures generated within the tissue were not high enough to result in direct subcutaneous vessel rupture. Therefore, it is likely that the shear waves which were produced were responsible for the surrounding bruising observed.

These shear forces originate from where the tissue is stretched around the impacting object rather than directly beneath it, which after impact springs back to

its original state, causing a wave which propagates through the tissue, as was seen in each of the video recordings. Both sites of compressive and shear forces are shown in Figure 7-3.

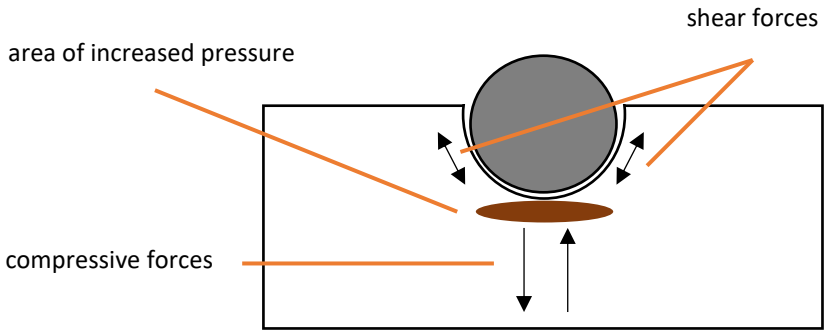

Figure 7-3 Schematic showing sites where compressive and shear forces are found during blunt impact

As the generated wave travels outwards, away from the impact site, the shear forces within the tissues would rupture the underlying vasculature, resulting in the characteristic doughnut shaped bruising. The variances in bruise severity could therefore be linked to the magnitude of the wave generated, which in turn is linked to the tissue properties which are characteristic of the individual. Referring to this study's pilot work, the individual with the larger wave and more defined edge experienced more extensive bruising. Therefore, it is likely that this property could explain the variation of bruising observed within the main study, however as the black shorts worn by participants reduced the visibility of the shear waves in the videos, this could not be confirmed.

In addition, these findings also provide explanation for why individuals can present with no visible external bruising yet have fatal internal injuries (as described by Byard in 2012). Given that generally speaking, a blood flow is required for a bruise to form, where an impact has resulted in immediate death, no bruising would form. Yet, given the proposed theory from this study's results, it would be expected to find some intradermal bruising at the point of impact.

It could therefore be concluded that where a blunt impact is lower than that which can be reflected back to the skin surface the pressure at the contact point is not high enough for intradermal bruising to occur. Therefore, the damage resulting

from the movement of internal structures during impact are what result in fatal injury, while the skin surface appears undamaged.

7.4 L*a*b* colour model

7.4.1 Overview

One of the proposed advantages of the L*a*b* colour system over others such as the RGB system, is that not only does it allow for a characteristic bruise colour pattern to be identified, but it can also associate pattern with skin tone. In this case, it was concluded that the measured L*, a* and b* patterns were not characteristic of dark, medium or light skin tones over the full bruise timeline. This was as a result of patterns for each individual in each category overlapping with that of the other categories (i.e. no definitive boundaries for each skin tone were identified).

Over the initial 4 day period there was a similarity in trend noted, but it did not clearly match with previous research using this specific classification system. There are a number of explanations which could explain why the patterns were not closer to those presented by Scafide et al., 2013. The difference in the values measured were expected to differ as the methodology of measurement differed (Scafide et al., used a colourimeter in their study, a digital camera and Photoshop used in this study). However, the timing of data collection could have altered the pattern. With the data collection being on alternate days the averaging of data was not of all individuals in that category, only of those present on those days.

Furthermore, the number of participants in this study being much lower than that of Scafide et al., which could have influenced the clarity of the trend. The spread of participants between each group was not as even as that in Scafide et al., while imaging technique altered the spread of individuals in each group (shown in Table 7-2).

Table 7-2 Comparison of subject numbers per skin tone category for both this study and Scafide et al., 2013

Skin tone	This study (Colour images)	This study (CP images)	Scafide et al., (2013)
Dark	2	3	34
Medium	8	0	35
Light	8	15	34
Total	18	18	103

This trend had been reported by other studies (Mimasaka et al., 2010; Thavarajah et al., 2012; Yajima et al., 2003), and so it would be presumed that even with lower participant numbers, the pattern would still be observed in these results.

The difficulty in comparing the results with Scafide et al., was that they focused on an early time period of a bruise life span where there was a definitive pattern present. However, this study showed that when pattern analysis was extended to the full healing period the variability in bruise colour and how this changed with time increased. This therefore lead to an inability in finding a trend which could be associated with either dark, medium or light skin tones, regardless of photography technique.

Another problem in comparing to the results presented by Scafide et al., is that there were no error bars to show whether the groups are as distinct as they appear. This is problematic as if all the individuals tested do not conform to L*, a* and b* trends, then they cannot be considered as characteristic rendering them inappropriate for use in a forensic context.

The similar results presented by the other studies (Mimasaka et al., 2010; Thavarajah et al., 2012; Yajima et al., 2003), analysed bruising over a 10 day period. Between days 4 and 10 their patterns become less defined and this was also reflected in the present study.

As previously shown, imaging technique altered the spread of individuals per group. When the skin tone categories were expanded and thus more specific, the spread of individuals per category changed with photography method. For the colour images, there was at least one participant for each category when calculated from a colour image. However CP photography had a lightening effect, resulting in tan, intermediate and the majority of light skin tones to be reclassified. Hence a majority

then being classed as having a very light skin tone. The number of participants per skin tone category is shown in Table 7-3.

Table 7-3 Number of individuals in each of the 6 skin tone categories for each photography method

Skin tone	Colour Images	CP images
Dark	1	1
Brown	1	2
Tan	4	0
Intermediate	4	0
Light	6	2
Very Light	2	13

Using this expanded skin tone list, the L*a*b* colour system was not characteristic of the new categories. This was found for both colour and CP images. No similar previous work is known to have employed the full ITA° categorisation system when assessing bruising on different skin tones and for Scafide et al., categories were simplified for ease of use.

Therefore, as the L*a*b* system had not produced characteristic patterns based on skin tone, alternative individual characteristics were considered. Based on available participant characteristics and those commonly associated with bruising tendency, BMI and gender were considered.

7.4.2 Discussion

Overall, the use of the L*a*b* colour system for identifying a characteristic colour pattern, which could be used to indicate bruise age, was inconclusive.

Both versions of skin tone categorisation methods were inconsistent, indicating that either the system itself or the measurement technique was inappropriate. Given that this study (and other published work), has identified average patterns based on skin tone over approximately the first week of a bruise timeline, does suggest that this approach has potential.

The patterns from each participant did show similarities to the general pattern which would be expected. For example, the average L* patterns compared with the results which Scafide et al. presented showed bruising generally appeared darker on light and medium skin tones when compared to dark skin tones. This was expected, as lighter skin tones provide a greater contrast between bruised and non-

bruised skin. The similar average patterns seen for medium and light skin tones both here and by Scafide et al., could not be said to be characteristic due to their overlapping. Similar conclusions were made for the a* and b* patterns due to the overlap seen between skin tone categories, suggesting that the colours perceived within a bruise are influenced by more than just the tone of the surrounding skin.

Characterisation by skin tone was limited, whilst the lack of individuals per group in this study made it difficult to conclude this system could be used to indicate the age of a bruise. The previous use of average patterns could be hiding individual variation, as seen in this study. This in turn could undermine the ultimate aim of ageing such injuries and potentially lead to inappropriate evidence in court. When investigating the expanded skin tone list, gender and BMI as alternative categorisation methods, the clarity of a characteristic pattern with limited overlap with others, was unable to be identified.

There may have been an interaction effect of BMI and gender on the patterns observed, but given the limited variation within the volunteer pool it was not appropriate to analyse these subgroups.

However, the lack of success here could be more indicative of having used digital photography and Photoshop over a more robust system which measures directly from the skin. This could in turn explain why the a* trend of green to red was observed and not one of red to green as previously found, based the accepted colour progression of a bruise.

7.4.3 Possible alternatives to colour models

As a definitive colour pattern was not found as part of this study, it can be concluded that this approach was not appropriate for aging bruising and/or removing subjectivity of interpretation. As previously mentioned, the use of this colour model has shown positive results. However, the three main studies to do so, did not discuss how the level of bruising influenced results. This is of concern, as our results indicate that for consistent impacts, range of colours produced vary significantly. Therefore,

the probability of seeing such a pattern for all bruises, and being able to infer age without knowing specific bruise causation, is currently not possible.

While the aim of using a colour pattern system is to provide a method of aging bruises, a possible alternative lies away from assessing colour. One such study focused on histology as a method of assessing and ageing bruising, combining histology with photography and spectrophotometry for colour measurement (Hughes and Langlois, 2011). They used 15 bruises from 10 subjects during post mortem and noted a link between the level of yellow within a bruise (based on the L*a*b* colour system) and FD490 (a value representing the level of haemoglobin degradation products as detected by a spectrophotometer). Although admittedly weak, this would be expected as yellow tones indicate blood breakdown. There was also some success in linking spectrophotometry with histology, as where the FD490 value indicated a greater volume of degradation products, histological testing indicated little to no iron present within the sample. This would be expected, as when broken down the iron within the blood is removed by the body. Therefore this, combined with Fronczek et al., 2015, (see below) does indicate that by taking and analysing a biopsy of a bruise, an indicator of age could be determined. Furthermore, this would completely remove the influence of skin tone, however being an invasive technique, this is not ideal. The research within this area is limited as it is more commonly applied to the identification of internal organ damage, analysis of tumours or other abnormalities. Therefore, further investigation into the practicalities surrounding application of such a method is required.

A similar approach has used an immunohistochemical technique, where biopsies were taken from the outer boundary of 101 skin wounds (of known age), on living participants (Fronczek et al., 2015). The wounds assessed included bruises, abrasions, bites, stabbings, scratches, those caused by fireworks and those of unknown causation (bruises being the majority (69%)). They were specifically assessing at the number of various inflammatory markers with the aim to create a scoring system and therefore age wounds. Unfortunately, this study did not distinguish the results associated with each type of wound and they acknowledge this

as a limitation. However, they were able to associate the number of inflammatory cells observed with specific timeframes after bruising, e.g. CD68 (found on white blood cells) at 4 days). Although exact days/times cannot be associated to inflammatory markers at this time, this is a promising approach. By sampling at the outer boundary of the wound, the variation between size of wound is excluded. However, by not differentiating between wound types, the specific markers could vary. Furthermore, if wound age is unknown, this could cause doubt as maximum marker volume could vary between participants, dependent on wound type.

Compared to measuring colour patterns, histological approaches have the advantage of being completely independent of subjectivity and false representation of bruising via imaging. As bruise appearance can vary significantly between individuals but be of the same age, this could also offer an alternative to measuring colour directly from the skin *in vivo*. Again, the influence of bruise severity is unknown. As it would be preferable to age bruising via a non-invasive method, taking biopsies would be unfavourable due to the discomfort experienced by an individual.

Another possible alternative is hyperspectral imaging (HSI). Unlike conventional photography HSI is based on the use of the RGB colour system, HSI allows for images to be taken using a larger range of wavelengths, from IR to UV (Lu and Fei, 2014; Payne et al., 2007). Where colour models produce a value for each channel, HSI produces a spectral signature, which can be associated with specific locations (or pixels) within the image (Lu and Fei, 2014). When used to image bruising, the theory is that the spectra relative to bruised tissue will change over time as the injury heals, thus generating a characteristic pattern, which could then be used to age the injury. This approach has been investigated for use in the food industry (Baranowski et al., 2012; Garrido-Novell et al., 2012; Jiang et al., 2016) and less so within a medical/forensic context where it has shown success. A study by Stam et al., (2011), showed for 3 bruises, they could be aged relatively accurately (Table 7-4) when recorded and assessed using a computer model which they had previously developed (Stam et al., 2010). Although data was limited and the bruises were not aged exactly, this process provided a more quantitative analysis than that which

visual and colour pattern analysis can currently provide. Other studies have attempted to utilise HSI in this manner (Randeberg et al., 2006; Randeberg and Hernandez-Palacios, 2012a, 2012b), with success, however a fully developed HSI methodology and data analysis protocol is not yet available.

Table 7-4 Results of Stam et al., (2011), showing a relatively low time difference in bruise age estimation when using HSI results in combination with a pre-developed computer model

Bruise 1		Bruise 2		Bruise 3	
Age	**Error**	**Age**	**Error**	**Age**	**Error**
0.9 day	0.5 h	3.1 day	2.3 h	2.1 day	12 h
2.2 day	6 h				
5 day	9 h				

7.4.4 Conclusion

Although a general trend for each component of the L*a*b* colour model was observed, there were no trends which could be conclusively linked to individuals based on their skin tone, BMI or gender. With the Photoshop analysis being relatively primitive compared to the colourimetry measurements made by other studies, it is likely that Photoshop analysis is too simple and subjective in comparison (e.g. by manually selecting sampling locations). Therefore, a standard colour pattern could not be identified and the use of computer software was not suitable for colour pattern analysis. Success in identifying a bruise healing pattern could be more likely found within any, or a combination of suggested alternative methods. Although this could lead to the use of more complex imaging equipment, it could provide more accurate results and possibly a means of aging bruising, whist remaining a non-invasive technique.

7.5 Photography techniques

Regarding how bruise visibility is affected by photography technique, the findings of this study match that which was seen within other research. For the photography types assessed in this study it would be expected that CP would be better than colour photography overall with some advantage over IR photography.

CP photography did not capture bruising earlier than any other the other techniques, but did provide a greater contrast between bruised and non-bruised skin than either colour or IR photography. This was due to the reduced glare caused by the reflection of light from the skin surface, an advantage noted in other studies (Baker et al., 2013; Benson et al., 2008; Lawson et al., 2015, 2011). When considering the contrast of bruise from non-bruised skin,

For the IR findings, these were to be expected in theory (i.e. clearer for younger bruising). IR photography is commonly used to detect vasculature, whether it be for vein pattern analysis or mapping veins as part of a medical procedure (Gupta et al., 2016; Hsia et al., 2017; Lingyu and Leedham, 2006; Shrotri et al., 2010; Zharov et al., 2004). Its use is based on the ability of haemoglobin to absorb IR light and so creating images where the vasculature appears as dark areas. As the blood which has formed a bruise is broken down with time, the IR absorbance of the blood is reduced, thus resulting in the effectiveness of IR imaging of bruises to be reduced. However, the results were contradictory to the findings of the study by Rowan et al., (2010), which is commonly reported as having success, although it has not been successfully reproduced. A possible reason for their success could be that the bruising was deeper within the tissue and IR detected it whilst it did not appear visible on the skin surface. Alternatively, it could also be possible that they made a mistake in their results (shown in Figure 7-4).

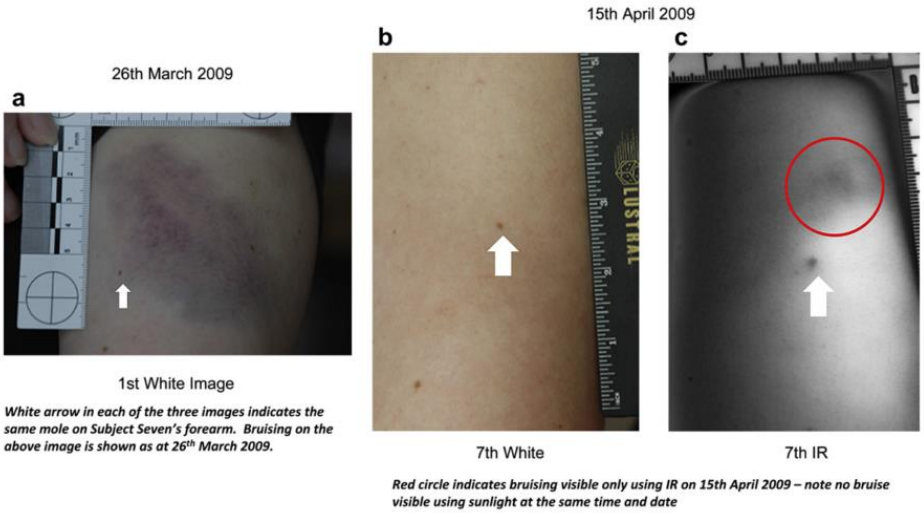

Figure 7-4 Result of Rowan et al., (2010), showing successful identification of bruising no longer visible to the naked eye a.image taken 1 day after bruise was sustained, b. bruise appears to have faded to the naked eye and c. IR detection of bruising on same day the bruise appears healed.

At first inspection, there does not appear to be anything wrong, hence why many studies have reported their success and have continued to pursue this method as a possible alternative to standard photography (including this one). However, when taking a closer look at the images demonstrating bruise detection, it could be possible that the image was taken of an alternative location on the upper arm of the subject.

On the subject's skin, there are several predominant freckles which could be mistaken for the one specifically highlighted in Figure 7-4a visible on either side of the original bruise. It could be possible that the chosen landmark is a freckle from the opposite (top) side of the where the bruise was. Given how the follow up images Figure 7-4b and Figure 7-4c have been cropped, there is no way of being sure that they have used the same landmark freckle or not. Furthermore, for the two follow up images having been taken on the same day, the use of a different scale (both in brand and units) casts doubt on their findings. Although it is possible different scales could have been used by accident, this was not stated.

With regards to their positive result, the authors did suggest that the variability of sunlight which they used for illumination could have been a factor in successful (and unsuccessful) bruise detection.

It should be noted that the author did conclude that overall, their IR imaging setup did not identify any significant bruising once it was no longer visible. Subsequent studies have failed to produce positive results when using more consistent lighting (i.e. artificial lighting). Furthermore, the findings of this study suggest that IR cannot detect bruising which is not visible to the naked eye, but may be more beneficial in imaging bruising at the earlier stages of its timeline.

By manipulating the IR images, contrast was increased, however this provided no improvement to bruise visibility at the point at which the bruise appears fully healed to the naked eye.

Photography technique did effect the day at which peak contrast was observed. IR photography (both original and altered images), identified peak contrast as being a day before that seen in the colour and CP images. A possible explanation could be that as it can take time for bruising to become visible on the skin surface (migration through the soft tissues), this delay is visibility applies to the full timeline. As IR allows visualisation of beneath the skin surface, this could be a more accurate way of not only identifying but describing the timeline of a bruise.

As previously mentioned, photography technique did effect the day at which peak contrast was observed. For contrast over all bruising timelines, IR (altered) images provided the greatest contrast. However, considering the three techniques, IR performed the worst overall. Although IR imaging has the advantage of improving bruise contrast on darker skin tones, CP photography provided the greatest contrast overall. These findings matched those of Baker et al., (2013), thus confirming that CP photography was a better method of documenting bruising. The differing levels of image clarity provided by each technique resulted in a significant difference in the immediate impact area measurements made. This difference was only observed between visible and non-visible light imaging techniques. Furthermore, for maximum bruise area, the only variance worth noting was between IR and IR (altered) techniques. No imaging technique allowed for any additional information to be extracted from images, therefore the improved image clarity benefited

documentation but not dimensional analysis of bruising. This is not something known to the author to have been addressed within other studies.

When considering the contrast progression over a bruise timeline, although imaging technique did alter the level of contrast observed, the specific levels captured could not be conclusively attributed to either the skin tone, BMI or gender of the participants. This indicated that although bruising appears with a predictable change in contrast, contrast level itself is not predictable enough to allow for accurate injury age estimation based on the characteristics considered in this case.

A limitation of the IR and IR (altered) images was in that, not only did they capture bruising but also the underlying vasculature. This may have influenced the accuracy of bruise boundary identification where injury and vasculature overlapped, though could not be avoided during analysis. IR does however provide an opportunity to map the vasculature of an area and investigate whether that influences the resulting bruise. The ability to investigate this was not possible due to the lack of vasculature identified across all participants.

IR photography removes the influence of skin surface markings/anomalies on bruise observation, for example abrasions and freckles (Bernstein et al., 2013). From the results, it is not clear if this was successfully done as such skin markings were not visible on many participants. There were some instances where the impact mark was clearly identifiable in the colour and CP images and not within the IR images. However, with the mark likely to be surface bruising rather than skin damage, this would explain why for some participants, the mark was identifiable across all photography types.

The improved contrast provided by CP photography did alter the colouring of the images and thus the L*a*b* colour measurements made, particularly when considering the levels of yellow measured. Although the day at which peak yellow was measured was not altered between colour and CP, the intensity change was significant. This was influential as it is the main colour to be considered when determining bruise age. Therefore, if CP photography became standard for bruise

documentation whilst visual analysis was still the norm, caution would have to be taken when providing an opinion on bruise age. At this point it is unknown if the change in colour measurements were a true or false representation of the injury itself, thus further research in this area would be recommended.

Although concluding that CP photography would be beneficial in bruise documentation, there may however be an alternative imaging technique which could provide a clearer image of bruising, even when not visible to the naked eye. This could be an ALS system or ultrasound imaging, as discussed in Chapter 3.

7.5.1 Conclusion

It can be concluded that between colour, CP and IR photography, CP was best at documenting bruising, providing the greatest contrast between bruised and non-bruised skin. No technique captured detail not visible to the naked eye with the exception of IR imaging, which itself allowed for visualisation of immediate injury not yet visible on the skin surface. With the research by Baker et al., (2013) being the only directly comparative study, these findings matched those as published by them. By enhancing contrast of the IR images, contrast was improved beyond that seen in the CP images. However, no additional information could be extracted from the IR (altered) image. Given these findings, a combination of alternative methods could be a more beneficial approach for future research in this area.

Chapter 8

Final Discussions

8.1 Review of aims and objectives

At the start of this research, the overall aim was to improve the viability of bruising as a piece of evidence to a court. Although a very common injury (both within and out with a forensic context), an understanding of the fundamentals of their formation was lacking. This problem relates to the specific response of tissue to an impact and how different tissue compositions behave, not only between individuals but also with anatomical location. Furthermore, an accurate method for documentation and analysis of bruising, where size colour and causation information could be inferred, does not exist. Colour photography is currently the accepted method, though widely acknowledged as being inaccurate. Whilst assessment of severity of the force which generated a bruise is based on a subjective, visual interpretation.

Therefore, this research aimed to improve the understanding and interpretation of bruising through:

1. Characterisation of bruising mechanics using a controlled method of blunt impact generation.
2. Assessment the suitability of colour, cross polarised and infrared photography techniques for imaging bruising, in terms of the extent of information which can be extracted (e.g. bruise size and colour range).
3. Investigation into the use of a colour model for pattern identification within a healing bruise, which could allow for a more accurate age estimation for bruising.
4. Determination as to whether the information extracted from each image type (bruise characteristics and colour model values), can be linked back to the bruising mechanics which caused their formation.

These aims were tackled whilst taking into consideration the individuals themselves, i.e. their anthropometric characteristics. The hypothesis was that this information would provide a greater understanding of how the body itself influences injury potential.

Each of these aims were successfully met with the hypothesis being correct. However, where it would have been presumed that a greater understanding would be achieved in terms of how much influence anthropometric characteristics had over injury potential, it was in fact the opposite. The fact that this influence could not be quantified (given a controlled blunt impact), emphasised the current uncertainties surrounding bruise formation and the need for more extensive work in this field. Colour patterns and photography techniques were successfully investigated although results were not as conclusive as expected. This was due to the chosen methodology, evaluated in the following section.

8.2 Methodology evaluation

The methodology developed and used within this research aimed to provide a simple and repeatable way to determine whether the mechanics of an impact influenced the resultant bruising and how individual characteristics affected the extent of bruising seen. Although there were some limitations, the methodology did successfully meet this aim.

8.2.1 Characterisation of bruise mechanics

As discussed within Chapter 4 the velocities derived from the high speed camera could not be confirmed as truly correct. Although high speed camera values correlated with those measured by the chronograph, the lack of published chronograph accuracy means that the variance between chronograph and 'true' velocity was unquantifiable. However, given the 'gold standard' status of a chronograph as velocity recording equipment, this limitation did not affect this study's results.

All experimental equipment was simple to use, however given the chosen method of bruise formation, there was always a chance that impacts may not be recorded by the high speed camera. Of the 18 impacts delivered, only one was missed by the camera. This was caused by the projectile clipping the edge of the hole in the protective screen, deflecting it downwards, causing the impact to occur out with the camera's field of view. The camera was moved further away from the participant in

later experiments, thus increasing the camera's field of view. As it was impossible to predict if another shot would clip the board this was the only way to ensure that if it happened again, the impact would still be captured.

There was an issue with the tissue response masking the ball from the high speed camera's field of view during impact. This limited the quantity of usable data from the video recordings. This could not be prevented with the current setup, as the extent of tissue wobble was unpredictable. If this experiment was to be repeated, further consideration should be given to the position of the camera. Siting it in a more parallel position to the projectile's trajectory, at a safe distance for it to not be damaged nor to restrict the positioning of the protective screen could be more appropriate. An alternative method of impact generation could be beneficial in terms of ease of recording, however that would compromise the simplicity and repeatability of the chosen impact generation method.

The only other factor to influence video data collection was the clothing of one participant. Black, tight fitting shorts or leggings were specified and worn by all. However, in one case the clothing had a prominent seam at the impact site, causing interference with the Matlab analysis. Clothing with such a prominent seam should be avoided in future. Furthermore, as clothing did appear to have an effect on tissue wave propagation, alternative clothing types should be considered (either a thinner material or if more appropriate, test bare skin). Future work should consider supplying clothing to keep material type and thickness consistent for all participants.

It could not be guaranteed that each participant would be shot first time, with the protective screen deflecting the off-target projectiles away from the participant. This ensured that participants did not have to spend too long anticipating the impact (either one or two shots was the norm). However, for one or two participants it took approximately five shots before impact. This was likely due to the pressure within the gas cylinder beginning to drop, therefore affecting firing consistency. This was an inconvenience for participants which could not have been predicted as cylinder pressure was still above the 1,500 psi in each case.

General setup time of the experimental equipment was not ideal (approx. 1 hour). This affected the recruitment process as laboratory availability became limited. This in turn made recruitment of participants difficult. There was a keen interest by many to take part and although the time each participant would be expected to give was fairly short, the three week timespan and available start dates resulted in people unable to take part. Furthermore, those who did take part could not always return on all required dates.

Further studies would benefit from a greater number of participants. Eighteen were recruited in this study and compared to the majority of similar studies, this was a larger pool of people than had previously been achieved. There are cases where over 100 people have been recruited (Scafide et al. 2013), but participants were offered a financial incentive to take part, something which was deemed inappropriate for this study.

The individual characteristics that were collected, although giving a profile of each participant, were basic in nature. Ideally, specific characterisation of the impacted thigh would have been carried out i.e. a measure of adiposity. During method development, skinfold thickness measurements were proposed as a measure of body fat. Although not without limitations (whole body measure and not limb specific), body fat would have been a useful characteristic. This was abandoned once the thigh was chosen over other locations such as the upper arm, as skin fold measurements are impractical and furthermore, body fat is calculated from measurements taken from the upper body only. Specific measure of both muscle and fat composition should be performed in any future study to give a greater understanding of which soft tissues are, if at all, influential in impact dissipation and bruise formation.

8.2.2 Suitability of colour, CP and IR photography

The overall methods used did satisfy the aim of assessing both the positives and negative of each photography technique. However, this did also have some limitations.

The photography process used was straightforward, with participants spending no more than 10 minutes having their photographs taken on each follow-up day. Although participants may not have been able to return at their previously agreed time, the fact that the process took such a short time made rearrangement of follow-up relatively easy, therefore maximising the volume of data available to collect.

The IR imaging was difficult to keep consistent due to the brightness of the chosen light source. Steps were taken to reduce this by diffusing the light with tracing paper and having the room artificially lit with no natural light. This is different to normal protocol, where a dark room would be used to ensure no interference from external light sources. To show that the IR images were not influenced by the room lighting, images were taken prior to the study commencing, which showed the camera was only sensitive to the chosen IR light source (i.e. the captured image was black). As described in Section 4.17 the IR light wavelength was confirmed to be 850 nm as claimed by the supplier and therefore within the camera's detectable range. Nonetheless, the risk of overexposure was difficult to control. By adjusting camera distance however, this effect was then found to be minimised. Despite this making the method unconventional, it was proven appropriate for use. However, future work should consider a purpose built IR illuminator or flash to ensure optimal illumination.

8.2.3 Investigation of the L*a*b* colour model for pattern identification

The use of Photoshop for photo analysis (bruise dimensions, colour profiles and contrast), was easy and simple. Therefore, the aim of assessing the suitability of the L*a*b* colour model was successfully carried out.

As Photoshop is a readily available piece of software, this makes its use preferable over that of more expensive equipment and allows for data collection with minimal user subjectivity during size measurements and defining bruise outline.

8.2.4 Bruise analysis

In addition to the specific details of each aim, bruise characteristics themselves (such as area measurement), were carried out to be used in assessment of how the generated blunt impact related to the size of injury observed.

It was found that analysis of the photographs was simple, although very time consuming. Furthermore, it involved visually and manually deciding on where bruise boundaries were. Part of the problem with current bruise analysis is that it is subjective and this could not be completely removed from this study when defining where bruise boundaries were. This in turn reduced the repeatability of this method as user input was required. Although all analysis was carried out by one assessor thus reducing the variability between measurements, automation of photo analysis would completely remove this subjectivity. Unfortunately, generation of such software was not possible in this case. This problem has been previously examined most recently, and somewhat successfully, by Johnson et al., 2016. Their approach was to develop a Matlab algorithm which could identify a bruised area within an image. For a prominent red/purple bruise, they were able to do this; however, it was not able to include the faded outer edge. Furthermore, the authors themselves admit it would not be appropriate for identifying more faded or bruising that is yellow in colour (as show in Figure 8-1). Therefore, defining outer boundaries visually was more accurate than currently available automated methods, particularly as bruising becomes more faded over time.

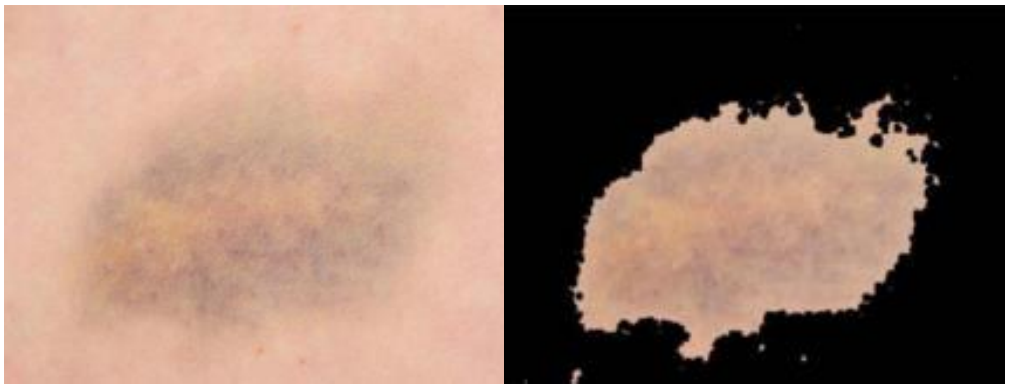

Figure 8-1 Example of the accuracy of current bruise boundary detection methods (Adapted from Johnson et al. 2016)

8.3 Experimental considerations

8.3.1 The bruises

The bruising produced was surprisingly different for all participants. For the rubber ball impacts, a characteristic doughnut shaped bruise was observed and where this shape varied, the angle of impact had varied.

There are a wide variety of terms which can be used to describe bruising (for example contusion or haematoma), however from the start the word 'bruise' has been the chosen terminology. The bruising generated was mostly subcutaneous, while the tissue response during impact suggested that the impact mark was intradermal which resulted from the increased pressure at the impact site.

8.3.2 Relations between experimental parameters

The assessment of photography technique was fairly inconclusive in that there was no overall best technique, each had their strengths and limitations. However, for documenting bruising, CP imaging was found to give the clearest representation of bruising whilst minimising the effect of light reflection from the skin. IR photography did show strengths in the early stages of bruising as it could enhance the visibility of subcutaneous bleeding. Furthermore, measurements of bruise area for IR taken immediately after impact did provide an indication to the extent of bruising which would then be seen, yet the correlation is not strong enough to be used as a reliable predictor. As individual variability strongly influenced the results, there may be better alternatives to standard photography for identifying, documenting and interpreting bruising.

Bruising presented a wide range of colours and sizes, with no immediately obvious link to the cause of variation. The colour model indicated that over the course of bruise formation and healing that colours develop and fade to a similar timeframe. Though the intensity and range of colour tones varied between individuals and could not be described as characteristic to different groups of individuals. The results of the main study did contradict those seen within the pilot study, specifically for the a*

pattern. The pilot trend matched that seen within previous studies and indicated that computer analysis of bruise colour could be a viable alternative to more expensive techniques. However, between the pilot and main study, not only did the number of participants increase, but the methodology was standardised to remove variability. In turn, this seems to have altered the expected pattern substantially. It could be that the limited number of pilot participants, and fewer imaging days, created a false representation of the expected pattern. Regardless, the main study findings although unsuccessful, did add to the knowledge that visual interpretation of colour is inaccurate, showing the extent of colour variability which could be seen.

This variability not only raised the inaccuracies in visually ageing bruising but also in describing the level of force which caused the injury. In this study force was quantifiable and the tissue response found to be predictable in each case. The only exceptions were when the impact was a glancing blow rather than a direct hit and when tissue response masked the ball from the camera's field of view.

The result of these impacts show that anthropometric characteristics have as important role in bruise potential as the level of force of an impact. There was a distinct lack of correlations able to be made from the information collected, with BMI and gender being the only ones to show a correlation.

The correlations identified between BMI and peak force demonstrate how tissue stiffness influenced generated force. BMI was not influenced by gender and did not appear to have any effect on the resulting bruise area. This emphasised how force cannot be considered a conclusive link to bruise appearance. Tissue displacement did appear to influence the resulting bruise area and the intensity of the impact mark however the correlation was not strong enough to use it as a predictor of bruise size. Combined it is clear tissue stiffness is an important factor in bruise development; however further, more detailed research into this topic is required.

Gender appeared to have an influence over the impact mark both in size and intensity however, could not be linked to the resultant bruising seen. Therefore,

gender alone cannot define bruising potential, and with the lack of other viable characteristics, the specific reasons for why gender had an influence over the immediate bruise appearance could not be explained.

8.4 Bruising as evidence

Given that this study kept impact velocity as a constant variable and force could be quantified, the conclusion of either a 'mild, moderate or severe' impact being responsible for a bruise (as is done within a forensic context), could not be made based on bruise appearance. The variability of injury susceptibility between individuals is widely acknowledged and noted during bruise assessments. However, it was not found to have ever been investigated in any depth. Many of the anthropometric variables taken into consideration were found to provide little or no explanation as to why one person bruises differently to another. This may have been due to the low range within the volunteer pool (e.g. majority were caucasian and regularly took part in sporting activities), or that other variables which could not be considered may have a larger influence over bruising (e.g. adiposity). This raises serious questions over whether visually assessing bruising should ever be used within a medico-legal context.

There is also an argument to be had against discussing impacts simply by force. During method development, it was found that the impact forces produced by a paintball marker were approximately 1,850 N when delivered to a solid surface, whilst approximately 917 N when impacting soft tissues. The current terminology within the forensic context, does not take into account that force is not a universal value for one impacting object when striking different tissues (under constant conditions).

This is evident when going back and comparing impacting conditions for various studies. Although published work focuses on force as the important parameter, for those studies which generated blunt impacts within a similar context to that used within this study energy could be inferred. As shown in Table 8-1, the varied impact forces reflect less varied applied energy values. Looking at Scafide's

reported impact force of 210 N compared to the 917 average of this research (ignoring the previously discussed error with their value calculation), it would be assumed that Scafide's delivered impact was much less severe than that in this study, however, the reported energy value is similar as would be expected, given the same methodological approach. Even when considering both examples listed for this research, where methodology was the same, force approximately doubled with changing surface, yet energy remained around 6 J in each case (difference of ± 0.23 J). Another advantage in using energy over force, is that it allows for an easier comparison of different methodologies, as other mechanical parameters can be inferred much easier than when force is reported.

Therefore, a false impression of the severity of a bruise causing impact may be given when force is the sole parameter considered.

Table 8-1 Published examples of forces generated as part of a controlled blunt impact with their associated applied energy

Author	Impact force (N)	Energy (J)
This research (wooden board)	1,850	5.99
This research (thigh impacts)	917 (average)	6.22
(Desmoulin and Anderson, 2011)	342 to 874	3 to 10.8
(Scafide, 2012)	210	7.18
(McBrier et al., 2009)	718.9 to 1032.7 181.9 to 244.5	1.05 to 1.83
(Black, 2013b)	181.46 to 213.39	0.79 to 1.32
(Farrugia et al., 2012)	2,996 (average) 2,592.5 (average)	66.84
(Sharkey et al., 2012)	3,200	96

Bruising generally indicates that some form of impact has occurred, or that an individual may be susceptible to bruising due to medication or an underlying medical condition. Bruising alone is not necessarily given the same weight of importance as

other evidence types (e.g. DNA or fingerprints), which can be used to show with little doubt that a specific individual was responsible for a specific event. However, bruises are commonly considered the first indicator of assault or abuse, particularly when dealing with children. This research has shown that the use of bruising for defining the severity of an impact (particularly where there is no evidence to suggest a specific causation), alongside defining a timeframe for when bruising occurred, is completely unsuitable given the current visual assessment methodology and the lack of a fully developed alternative.

However, where an individual presents with unexplained injuries, bruising should still be considered as an indicator that a possible impact has occurred, until such time it can be excluded as being accidental or symptomatic, rather than malicious.

The use of CP photography should be considered for the documentation of bruising for forensic and/or medical purposes. It has shown advantages over the standard colour photography technique and may be more appropriate for recording bruising as they appear on an individual. However, to go on and use CP images to discuss bruise colour and prominence does not remove the problem of subjective bruise interpretation. Furthermore, as CP imaging emphasised bruise appearance by removing reflected light, this would likely influence how an expert would interpret bruise age, severity and the level of force which generated the injury. This was demonstrated in the area measurements of bruises, where the recorded values differed for each photography technique.

Although the IR imaging did not provide any significant advantage in capturing bruising, where an alleged assault has been reported at the time of the offense occurring, IR imaging could be used as supplementary to either colour or CP imaging. This would provide an indication of the level of immediate injury and that expected to appear which, although would not remove subjective interpretation, would provide an additional resource for an expert to use in forming an opinion. The use of IR imaging for older bruising (i.e. 7 days or older), would in contrast be unlikely to aid bruise interpretation.

8.5 Conclusions and future work

The approach of this research, although built from experimental procedures already used in other published studies, shows originality in that it combines all aspects of bruise analysis. Impact force, documentation technique and visible bruise colour are all important to bruise analysis, though never studied in combination. Yet this is exactly what is expected of those required to describe such injuries in court.

By looking at each aspect individually and also in combination, this study has shown the need for greater knowledge surrounding bruise formation and healing timelines. The photography methods selected presented with some advantages over the standard colour photography method and so where appropriate, should be considered for use in the documenting of bruising. However, for a more accurate documentation and ultimately interpretation of bruising, alternative methods may be better suited in improving bruise documentation overall.

Although colour patterns were observed, they would not be suitable for use within a forensic context. There was no pattern which could be attributed to the range and intensity of colours seen, and there was an extensive variation between all participants. This may have been due to using computer analysis as the measurement tool, rather than measuring colours directly from the skin (e.g. with a colourimeter). Therefore, an improved documentation and analysis system is still required to replace subjective visual assessments.

When characterising force profiles from a standard impact, the system was strongly influenced by the soft tissues themselves rather than the force. The link between individuality and bruise severity was highlighted, showing that anthropometric characteristics may be more important to describing bruising than the level of force which may have caused their formation.

The novelty of this study and its findings show that it should be used as a precursor to future work, where bruising should always be considered within the context of the individual and the impacting conditions, particularly as individuality

was concluded to be significantly influential on results. To continue to investigate bruising solely on appearance would be fundamentally wrong.

Although experimental work has the advantage of accurately demonstrating how this type of injury varies for individuals, if it were supplemented with computer modelling a detailed understanding of the localised effect to all soft tissues could be achieved. When assessing individuality, future work should consider a more detailed approach to characterising individuals (e.g. measure adiposity rather than BMI) with a larger pool of volunteers. Combined with alternative documentation and interpretation methodology (e.g. ALS photography and automated bruise area measurements), a clearer and more accurate understanding of bruise injuries could be achieved.

Different anatomical locations should also be considered to not only continue to assess person-to-person variability, but also how bruising differs across the body. This approach should not only test different locations, but also measure skin tension for these locations.

Anatomical variance, like anthropometric characteristics, is commonly discussed in published work but never quantified for a standardised impact. Only once a complete understanding of how all aspects of bruising link together would bruise injuries become a reliable form of evidence within a forensic context.

Chapter 9

References and Appendices

9.1 References

Aboutalebi, S., Stetson, C.L., 2005. Paintball purpura. J. Am. Acad. Dermatol. 53, 901–902. doi:10.1016/j.jaad.2005.05.019

Adamec, J., Jelen, K., Kubovy, P., Lopot, F., Schuller, E., 2010. Forensic biomechanical analysis of falls from height using numerical human body models. J. Forensic Sci. 55, 1615–1623. doi:10.1111/j.1556-4029.2010.01445.x

Affagard, J.-S., Bensamoun, S.F., Feissel, P., 2014. Development of an inverse approach for the characterization of in vivo mechanical properties of the lower limb muscles. J. Biomech. Eng. 136, 111012-1-111012–8. doi:10.1115/1.4028490

Aggrawal, A., 2016. Forensic medicine and toxicology for MBBS, 1st ed. Avichal Publishing Company, New Delhi.

Ambay, A.R., Stratman, E.J., 2007. Paintball: dermatologic injuries. Cutis 80, 49–50.

Angelopoulou, E., 1999. The reflectance spectrum of human skin. Tech. Reports 1–14.

Ashrafi, M.R., Shabanian, R., Mohammadi, M., Kavusi, S., 2006. Extensive mongolian spots: a clinical sign merits special attention. Pediatr. Neurol. 34, 143–145. doi:10.1016/j.pediatrneurol.2005.07.010

Bahr, R., Krosshaug, T., 2005. Understanding injury mechanisms: a key component of preventing injuries in sport. Br. J. Sports Med. 39, 324–329. doi:10.1136/bjsm.2005.018341

Baker, H.C., Marsh, N., Quinones, I., 2013. Photography of faded or concealed bruises on human skin. J. Forensic Identif. 63, 103–125.

Baranowski, P., Mazurek, W., Wozniak, J., Majewska, U., 2012. Detection of early bruises in apples using hyperspectral data and thermal imaging. J. Food Eng. 110, 345–355. doi:10.1016/j.jfoodeng.2011.12.038

Bariciak, E.D., Plint, A.C., Gaboury, I., Bennett, S., 2003. Dating of bruises in children: an assessment of physician accuracy. Pediatrics 112, 804–807. doi:10.1542/peds.112.4.804

Beeson, S., Mayer, J.W., 2008. Sources of Light and Color, in: Patterns of Light: Chasing the Spectrum from Aristotle to LEDs. Springer Science and Business Media, New York, NY, pp. 75–90.

Benson, P.E., Shah, A.A., Willmot, D.R., 2008. Polarized versus nonpolarized digital images for the measurement of demineralization surrounding orthodontic brackets. Angle Orthod. 78, 288–293. doi:10.2319/121306-511.1

Bernstein, M., Nichols, G., Blair, J., 2013. The use of black and white infrared photography for recording blunt force injury. Clin. Anat. 26, 339–346. doi:10.1002/ca.22078

Bilo, R.A.C., Oranje, A.P., Shwayder, T., Hobbs, C.J., 2013a. Blunt-force trauma: bruises, in: Cutaneous Manifestations of Child Abuse and Their Differential Diagnosis. Springer Berlin Heidelberg, Berlin, Heidelberg, pp. 63–103. doi:10.1007/978-3-642-29287-3

Bilo, R.A.C., Oranje, A.P., Shwayder, T., Hobbs, C.J., 2013b. Evaluating suspicious skin findings in children, in: Cutaneous Manifestations of Child Abuse and Their Differential Diagnosis. pp. 25–61. doi:10.1007/978-3-642-29287-3

Black, G.A., 2013a. Protocol for the documentation of physical injuries.(Personal Coommunication)

Black, H.I., 2013b. The biomechanics of bruising. MSc Thesis, University of Strathclyde.

Blankenbaker, D.G., De Smet, A.A., Vanderby, R., McCabe, R.P., Koplin, S.A., 2008. MRI of acute bone bruises: timing of the appearance of findings in a swine model. Am. J. Roentgenol. 190, 1–7. doi:10.2214/AJR.07.2693

Bohnert, M., Baumgartner, R., Pollak, S., 2000. Spectrophotometric evaluation of the colour of intra-

and subcutaneous bruises. Int. J. Legal Med. 113, 343–348.

Boks, S.S., Vroegindeweij, D., Koes, B.W., Bernsen, R.M.D., Hunink, M.G.M., Bierma-Zeinstra, S.M.A., 2007. MRI follow-up of posttraumatic bone bruises of the knee in general practice. Am. J. Roentgenol. 189, 556–562. doi:10.2214/AJR.07.2276

Bolliger, S.A., Ross, S., Oesterhelweg, L., Thali, M.J., Kneubuehl, B.P., 2009. Are full or empty beer bottles sturdier and does their fracture-threshold suffice to break the human skull? J. Forensic Leg. Med. 16, 138–142. doi:10.1016/j.jflm.2008.07.013

Burgin, L. V, Aspden, R.M., 2007. A drop tower for controlled impact testing of biological tissues. Med. Eng. Phys. 29, 525–530. doi:10.1016/j.medengphy.2006.06.002

Burgmüller, M., Pemp, B., Dunavölgyi, R., Sacu, S., Buehl, W., 2014. Reproducibility of a new colour test. Ophthalmol. Int. J. Ophthalmol. 231, 177–179. doi:10.1159/000356722

Buttaravoli, P., Leffler, S.M., 2012. Contusion (bruise), in: Minor Emergencies. Elsevier, Philadelphia, pp. 530–534. doi:10.1016/B978-0-323-07909-9.00137-9

Byard, R.W., 2012. How reliable is external examination in identifying internal injuries - casper's sign revisited. J. Forensic Leg. Med. 19, 419–421. doi:10.1016/j.jflm.2012.02.002

Byard, R.W., Langlois, N.E.I., 2015. Bruises: Is it a case of the more we know, the less we understand?''. Forensic Sci. Med. Pathol. 11, 479–481. doi:10.1007/s12024-015-9661-0

Carloway, Lord, Brodie, Lord, Drummond Young, Lord, 2015. Appeal against conviction by Ian Geddes against Her Majesty's Advocate.

Carloway, Lord, Paton, Lady, Malcom, Lord, 2016. Note of appeal against conviction by George Donald Smith against Her Majesty's Advocate.

Carmichael, S.W., 2014. The tangled web of Langer's lines. Clin. Anat. 27, 162–168. doi:10.1002/ca.22278

Carson, H.J., 2010. Patterns of ecchymoses caused by manner of death and collateral injuries sustained in bruising incidents: Decedent injuries, profiles, comparisons, and clinicopathologic significance. J. Forensic Sci. 55, 1534–1542. doi:10.1111/j.1556-4029.2010.01490.x

Ceylan, H., McGowan, A., Stringer, M.D., 2002. Air weapon injuries: a serious and persistent problem. Arch. Dis. Child. 86, 234–235.

Challis, J.H., Pain, M.T.G., 2008. Soft tissue motion influences skeletal loads during impacts. Exerc. Sport Sci. Rev. 36, 71–75. doi:10.1097/JES.0b013e318168ead3

Chardon, A., Cretois, I., Hourseau, C., 1991. Skin colour typology and suntanning pathways. Int. J. Cosmet. Sci. 13, 191–208.

Chirali, I.Z., 2014. Traditional chinese medicine cupping therapy, 3rd ed. Elsevier Ltd, London.

Choudhury, A.K.R., 2014a. Characteristics of light sources, in: Principles of Colour Appearance and Measurement. Volume 1: Object Appearance, Colour Perception and Instrumental Measurement. Woodhead Publishing, pp. 1–52. doi:10.1533/9780857099242.1

Choudhury, A.K.R., 2014b. Colour and appearance attributes, in: Principles of Colour Appearance and Measurement. Volume 1: Object Appearance, Colour Perception and Instrumental Measurement. Woodhead Publishing, pp. 103–143. doi:10.1533/9780857099242.103

Choudhury, A.K.R., 2014c. Object appearance and colour, in: Principles of Colour Appearance and Measurement. Volume 1: Object Appearance, Colour Perception and Instrumental Measurement. Woodhead Publishing, pp. 53–102. doi:10.1533/9780857099242.53

Choudhury, A.K.R., 2014d. Principles of colour perception, in: Principles of Colour Appearance and Measurement. Volume 1: Object Appearance, Colour Perception and Instrumental Measurement. Woodhead Publishing, pp. 144–184. doi:10.1533/9780857099242.144

Číhalová, L., Hynčík, L., 2008. Impact injury prediction by FE human body model. Appl. Comput. Mech. 2, 243–254.

Color, B., 2016. How to create camera profiles using the ColourChecker Passport with Adobe CS5 [WWW Document]. Breath. Color Adv. Print Media Blog. URL http://www.breathingcolor.com/blog/how-to-create-camera-profiles-using-the-colorchecker-passport-with-adobe-cs5/ (accessed 10.13.16).

Cooper, G.J., Taylor, D.E., 1989. Biophysics of impact injury to the chest and abdomen. J. R. Army Med. Corps 135, 58–67. doi:10.1136/jramc-135-02-04

Cormier, J., Manoogian, S., Bisplinghoff, J., Rowson, S., Santago, A., McNally, C., Duma, S., Bolte Iv, J., 2010. The tolerance of the nasal bone to blunt impact. Ann. Adv. Automot. Med. 54, 3–14.

Cowan, S., Hunt, A.C., 2008. Wounding, in: Mason's Forensic Medicine for Lawyers. Tottel Publishing Limited, West Sussex, England, pp. 112–127.

Cox, W.A., 2011. Pathology of blunt force traumatic injury.

Crandall, J.R., Bose, D., Forman, J., Untaroiu, C.D., Arregui-Dalmases, C., Shaw, C.G., Kerrigan, J.R., 2011. Human surrogates for injury biomechanics research. Clin. Anat. 24, 362–371. doi:10.1002/ca.21152

Crawford, H., 2003. Survivable impact forces on human body constrained by full body harness.

Crawford, M., 2010. Physical abuse: pitfalls and challenges. Paediatr. Child Health (Oxford). 20, 566–570. doi:10.1016/j.paed.2010.08.004

Cromwell, T.A., 2011. The challenges of scientific evidence [WWW Document]. Scottish Counc. Law Report. Macfadyen Lect. URL http://www.scottishlawreports.org.uk/publications/macfadyen-2011.html (accessed 9.1.14).

Cuper, N.J., Klaessens, J.H.G., Jaspers, J.E.N., de Roode, R., Noordmans, H.J., de Graaff, J.C., Verdaasdonk, R.M., 2013. The use of near-infrared light for safe and effective visualization of subsurface blood vessels to facilitate blood withdrawal in children. Med. Eng. Phys. 35, 433–440. doi:10.1016/j.medengphy.2012.06.007

de Mayo, B., 2015. The everyday physics of hearing and vision. Morgan & Claypool Publishers, San Rafael, CA. doi:10.1088/978-1-6270-5675-5

Del Bino, S., Sok, J., Bessac, E., Bernerd, F., 2006. Relationship between skin response to ultraviolet exposure and skin color type. Pigment Cell Res. 19, 606–614. doi:10.1111/j.1600-0749.2006.00338.x

Desmoulin, G.T., Anderson, G.S., 2011. Method to investigate contusion mechanics in living humans. J. Forensic Biomech. 2, 1–10. doi:10.4303/jfb/F100402

Dimitrova, T., Georgieva, L., Pattichis, C., Neofytou, M., 2006. Qualitative visual image analysis of bruise age determination: a survey. Conf. Proc. Annu. Int. Conf. IEEE Eng. Med. Biol. Soc. 1, 4840–4843. doi:10.1109/IEMBS.2006.259596

Diridollou, S., Vabre, V., Berson, M., Vaillant, L., Black, D., Lagarde, J.M., Grégoire, J.M., Gall, Y., Patat, F., 2001. Skin ageing: changes of physical properties of human skin in vivo. Int. J. Cosmet. Sci. 23, 353–362. doi:10.1046/j.0412-5463.2001.00105.x

Doughty, S., 2011. Family torn apart in 15-minute court case by Judge James Orrell [WWW Document]. Dly. Mail. URL http://www.dailymail.co.uk/news/article-1359252/Family-torn-apart-15-minute-court-case-Judge-James-Orrell.html (accessed 9.1.14).

Dynamics, C.E., 2014. The CED M2 chronograph.

Elshimy, N., Gandhi, A., 2013. A teenager with lumbar striae distensae (when a bruise is not a bruise). Br. Med. J. Case Reports bcr2013201962-bcr2013201962. doi:10.1136/bcr-2013-201962

Engin, A.E., 2014. Forensic biomechanics. J. Forensic Biomech. 5, 102.

Engineering360, I., 2015. High speed cameras information [WWW Document]. URL http://www.globalspec.com/learnmore/video_imaging_equipment/video_cameras_accessories/high_speed_cameras (accessed 3.23.15).

Escoffier, C., de Rigal, J., Rochefort, A., Vasselet, R., Lévêque, J.-L., Agache, P., 1989. Age-related mechanical properties of human skin: an in vivo study. J. Invest. Dermatol. 93, 353–357.

Farrugia, K.J., Riches, P., Bandey, H., Savage, K., NicDaéid, N., 2012. Controlling the variable of pressure in the production of test footwear impressions. Sci. Justice 52, 168–176. doi:10.1016/j.scijus.2011.11.002

Force, T., 2014. History of paintball [WWW Document]. URL http://www.teamforceuk.com/history-of-paintball.php (accessed 6.23.14).

Fronczek, J., Lulf, R., Korkmaz, H.I., Witte, B.I., van de Goot, F.R.W., Begieneman, M.P. V, Schalkwijk, C.G., Krijnen, P.A.J., Rozendaal, L., Niessen, H.W.M., Reijnders, U.J.L., 2015. Analysis of inflammatory cells and mediators in skin wound biopsies to determine wound age in living subjects in forensic medicine. Forensic Sci. Int. 247, 7–13. doi:10.1016/j.forsciint.2014.11.014

Fuller, J., 2015. How high-speed photography works [WWW Document]. How St. Work. URL http://electronics.howstuffworks.com/high-speed-photography3.htm (accessed 6.5.15).

Gade, R., Moeslund, T.B., 2014. Thermal cameras and applications: A survey. Mach. Vis. Appl. 25, 245–262. doi:10.1007/s00138-013-0570-5

Garrido-Novell, C., Pérez-Marin, D., Amigo, J.M., Fernández-Novales, J., Guerrero, J.E., Garrido-Varo, A., 2012. Grading and color evolution of apples using RGB and hyperspectral imaging vision cameras. J. Food Eng. 113, 281–288. doi:10.1016/j.jfoodeng.2012.05.038

Gaudart, J., Pétrakian, J.-P., 2005. Evaluation of a chromatometer: a new method for blue-yellow or green-red visual comparisons, and anomaly screening techniques. Med. Sci. Monit. 11, MT39-MT52.

Geerligs, M., 2010. Skin layer mechanics. Eindhoven University of Technology. doi:978-90-74445-92-4

Georgieva, L., Dimitrova, T., Angelov, N., 2005a. RGB and HSV colour models in colour identification of digital traumas images, in: International Conference on Computer Systems and Technologies. pp. 1–6.

Georgieva, L., Dimitrova, T., Stoyanov, I., 2005b. Computer-aided system for the bruise color's recognition, in: International Conference on Computer Systems and Technologies. pp. 1–6.

Gibson, M., 1934. The electromagnetic spectrum. Students Q. J. 4, 140–145. doi:10.1049/sqj.1934.0010

Gooch, G., Williams, M., 2007. A dictionary of law enforcement. Oxford University Press Inc., Oxford.

Greenwald, R.M., Janes, P.C., Swanson, S.C., McDonald, T.R., 1998. Dynamic impact response of human cadaveric forearms using a wrist brace. Am. J. Sports Med. 26, 825–830.

Grossman, S.E., Johnston, A., Vanezis, P., Perrett, D., 2011. Can we assess the age of bruises? An attempt to develop an objective technique. Med. Sci. Law 51, 170–176.

Gundersen, H.M., 2007. An application of image processing techniques for enhancement and segmentation of bruises in hyperspectral images. Norwegian University of Science and Technology.

Gupta, P., Srivastava, S., Gupta, P., 2016. An accurate infrared hand geometry and vein pattern based authentication system. Knowledge-Based Syst. 103, 143–155. doi:10.1016/j.knosys.2016.04.008

Hainsworth, S. V, 2013. How much force?, in: Rutty, G.N. (Ed.), Essentials of Autopsy Practice. Springer London, London, pp. 151–170. doi:10.1007/978-0-85729-519-4

Hannon, P., Knapp, K., 2008. Forensic biomechanics. Lawyers & Judges Publishing Company Inc., Tucson.

Hardy, C., 2017. Enquiry from Competitive Edge Dynamics: Technical enquiry.

Harris, T.L., Flaherty, E.G., 2011. Bruises and skin lesions, in: Jenny, C., Lowen, D.E., Pierce, M.C., Kellogg, N.D., Frasier, L.D., Amaya-Jackson, L., Cohen, J.A., Laskey, A.L., Barron, C.E. (Eds.), Child Abuse and Neglect: Diagnosis, Treatment and Evidence. Elsevier Inc., Missouri, pp. 239–251. doi:10.1016/B978-1-4160-6393-3.00029-4

Hawkins, J., 2014. Athletic injury management models in humans. J. Athl. Enhanc. 3, 1–5.

Hayes, W.C., Erickson, M.S., Power, E.D., 2007. Forensic injury biomechanics. Annu. Rev. Biomed. Eng. 9, 55–86. doi:10.1146/annurev.bioeng.9.060906.151946

Heath, K.J., Byard, R.W., 2015. Suction pump injuries mimicking child abuse. Forensic Sci. Med. Pathol. 11, 626–628. doi:10.1007/s12024-015-9684-6

Helm, T., Bir, C., Chilstrom, M., Claudius, I., 2016. Ultrasound characteristics of bruises and their correlation to cutaneous appearance. Forensic Sci. Int. 266, 160–163. doi:10.1016/j.forsciint.2016.05.022

Hershberger, W., 2004. Taming those annoying highlights: cross-polarization flash macro photography [WWW Document]. URL http://www.naturescapes.net/articles/techniques/taming-those-annoying-highlights-cross-polarization-flash-macro-photography/ (accessed 5.6.15).

Hildebrandt, C., Raschner, C., Ammer, K., 2010. An overview of recent application of medical infrared thermography in sports medicine in Austria. Sensors 10, 4700–4715. doi:10.3390/s100504700

Holzapfel, G.A., 2000. Biomechanics of soft tissue, in: Lemaitre, J. (Ed.), Handbook of Material Bahaviour: Nonlinear Models and Properties. Academic Press, Graz, Austria, pp. 1–15.

Hospital, G.O.S., 2013. Mongolian blue spots [WWW Document]. URL http://www.gosh.nhs.uk/medical-information/search-for-medical-conditions/mongolian-blue-spots/mongolian-blue-spots-information/ (accessed 7.2.14).

Hsia, C.-H., Guo, J.-M., Wu, C.-S., 2017. Finger-vein recognition based on parametric-oriented corrections. Multimed. Tools Appl. 1–18. doi:10.1007/s11042-016-4296-z

Huang, L., Bakker, N., Kim, J., Marston, J., Grosse, I., Tis, J., Cullinane, D., 2012. A multi-scale finite element model of bruising in soft connective tissues. J. Forensic Biomech. 3, 1–5. doi:10.4303/jfb/235579

Hughes, V.K., Ellis, P.S., Langlois, N.E.I., 2004. The perception of yellow in bruises. J. Clin. Forensic Med. 11, 257–259. doi:10.1016/j.jcfm.2004.01.007

Hughes, V.K., Ellis, P.S., Langlois, N.E.I., 2006. Alternative light source (polilight) illumination with digital image analysis does not assist in determining the age of bruises. Forensic Sci. Int. 158, 104–107. doi:10.1016/j.forsciint.2005.04.042

Hughes, V.K., Langlois, N.E.I., 2011. Visual and spectrophotometric observations related to histology in a small sample of bruises from cadavers. Forensic Sci. Med. Pathol. 7, 253–256. doi:10.1007/s12024-010-9221-6

Iivarinen, J.T., Korhonen, R.K., Julkunen, P., Jurvelin, J.S., 2011. Experimental and computational analysis of soft tissue stiffness in forearm using a manual indentation device. Med. Eng. Phys. 33, 1245–1253. doi:10.1016/j.medengphy.2011.05.015

Imaging, F., 2015. About high-speed digital video cameras [WWW Document]. URL http://www.fastecimaging.com/support/resources/about-hsv (accessed 7.1.15).

Innocence, W.T., 2014. Exonerees: Sabrina Butler [WWW Document]. Witn. to Innocence. URL http://www.witnesstoinnocence.org/exonerees/sabrina-butler.html (accessed 9.1.14).

Ionescu, I., Guilkey, J.E., Berzins, M., Kirby, R.M., Weiss, J.A., 2006. Simulation of soft tissue failure using the material point method. J. Biomech. Eng. 128, 917–924. doi:10.1115/1.2372490

Jackson, J., Carpenter, S., Anderst, J., 2012. Challenges in the evaluation for possible abuse: presentations of congenital bleeding disorders in childhood. Child Abuse Negl. 36, 127–134. doi:10.1016/j.chiabu.2011.09.009

Jiang, Y., Li, C., Takeda, F., 2016. Nondestructive detection and quantification of blueberry bruising using near-infrared (NIR) hyperspectral reflectance imaging. Nat. Publ. Gr. 1–14. doi:10.1038/srep35679

Johnson, B., Member, S., Fazel-rezai, R., Member, S., 2016. Contusion (bruise) segmentation and diagnosis: A graphical user interphase approach, in: IEEE International Conference on Electro Information Technology (EIT). pp. 744–749.

Kaczor, K., Clyde Pierce, M., Makoroff, K., Corey, T.S., 2006. Bruising and physical child abuse. Clin. Pediatr. Emerg. Med. 7, 153–160. doi:10.1016/j.cpem.2006.06.007

Kassab, G.S., Sacks, M.S., 2016. Structure-based mechanics of tissues and organs, Structure-Based Mechanics of Tissues and Organs. Springer, New York, NY. doi:10.1007/978-1-4899-7630-7

Kenny, T., 2012. Aspirin and other antiplatelet medicines [WWW Document]. URL www.patient.co.uk/health/aspirin-and-other-antiplatelet-medicines (accessed 8.26.14).

Kent, R.W., Forman, J.L., Bostrom, O., 2010. Is there really a “cushion effect?”: a biomechanical investigation of crash injury mechanisms in the obese. Obesity 18, 749–753. doi:10.1038/oby.2009.315

Kieser, J., Whittle, K., Wong, B., Waddell, J.N., Ichim, I., Swain, M., Taylor, M., Nicholson, H., 2008. Understanding craniofacial blunt force injury: a biomechanical perspective, in: Tsokos, M. (Ed.), Forensic Pathology Reviews, Forensic Pathology Reviews. Humana Press, Totowa, NJ, pp. 39–51. doi:10.1007/978-1-59745-110-9

Kim, G., Kim, G.-H., Park, J., Kim, D.-Y., Cho, B.-K., 2014. Application of infrared lock-in thermography for the quantitative evaluation of bruises on pears. Infrared Phys. Technol. 63, 133–139. doi:10.1016/j.infrared.2013.12.015

Kim, O., Lines, C., Duffy, S., Alber, M., Crawford, G., 2013. Modeling and measuring extravascular hemoglobin: aging contusions, in: Schlesinger, M. (Ed.), Applications of Electrochemistry in Medicine. Springer Science and Business Media, pp. 381–402.

Kim, O., McMurdy, J., Lines, C., Duffy, S., Crawford, G., Alber, M., 2012. Reflectance spectrometry of normal and bruised human skins: experiments and modeling. Physiol. Meas. 33, 159–175. doi:10.1088/0967-3334/33/2/159

King, A.I., 2004. Impact biomechanics. Bridg. Natl. Acad. Eng. 34, 11–16.

Knott, L., 2014a. Haemophilia A (factor VIII deficiency) [WWW Document]. URL http://www.patient.co.uk/doctor/haemophilia-a-factor-viii-deficiency (accessed 10.6.14).

Knott, L., 2014b. Haemophilia B (factor IX deficiency) [WWW Document]. URL www.patient.co.uk/doctor/haemophilia-b-factor-ix-deficiency (accessed 10.6.14).

Kong, L., Caspall, J., Duckworth, M., Sprigle, S., 2008. Assessment of an ultrasonic dermal scanner for skin thickness measurements. Med. Eng. Phys. 30, 804–807. doi:10.1016/j.medengphy.2007.10.002

Konkle, B.A., 2011. Acquired disorders of platelet function. Am. Soc. Hematol. 2011, 391–396.

Kruger, G., Kerins, B., Kirby, J., Raol, D., Valvano, M., 2010. Skin hardness and elasticity measurement device. University of Michigan.

Langlois, N.E.I., 2007. The science behind the quest to determine the age of bruises: a review of the english language literature. Forensic Sci. Med. Pathol. 3, 241–251. doi:10.1007/s

Langlois, N.E.I., Gresham, G.A., 1991. The ageing of bruises: a review and study of the colour changes with time. Forensic Sci. Int. 50, 227–238.

Langlois, N.E.I., Ross, C.G., Byard, R.W., 2013. Magnetic resonance imaging (MRI) of bruises: a pilot study. Forensic Sci. Med. Pathol. 9, 363–366. doi:10.1007/s12024-013-9456-0

Lawson, Z., Dunstan, F., Nuttall, D., Maguire, S., Kemp, A., Young, S., Barker, M., David, L., 2015. How consistently do we measure bruises? A comparison of manual and electronic methods. Child Abus. Rev. 24, 28–36. doi:10.1002/car

Lawson, Z., Nuttall, D., Young, S., Evans, S., Maguire, S., Dunstan, F., Kemp, A.M., 2011. Which is the preferred image modality for paediatricians when assessing photographs of bruises in children? Int. J. Legal Med. 125, 825–830. doi:10.1007/s00414-010-0532-7

Lecomte, M.M.J., Holmes, T., Kay, D.P., Simons, J.L., Vintiner, S.K., 2013. The use of photographs to record variation in bruising response in humans. Forensic Sci. Int. 231, 213–218. doi:10.1016/j.forsciint.2013.04.036

Lee, W., Khoo, B., 2010. Forensic light sources for detection of biological evidenced in crime scene investigation: a review. Malaysian J. Forensic Sci. 1, 17–27.

Lewis, J.B., 1984. Medico-legal studies: contusions, ecchymoses, cutaneous hypostases and their relation to legal medicine. Med. Leg. J. 1, 553–566.

Li, Z., Huan, Z., Byard, R.W., 2015. Bruising caused by traditional Chinese massage therapy (ba sha) complicating the assessment of a case of fatal child abuse. J. Forensic Leg. Med. 36, 49–51. doi:10.1016/j.jflm.2015.08.012

Limmen, R.M., Ceelen, M., Reijnders, U.J.L., Joris Stomp, S., de Keijzer, K.C., Das, K., 2013. Enhancing the visibility of injuries with narrow-banded beams of light within the visible light spectrum. J. Forensic Sci. 58, 518–522. doi:10.1111/1556-4029.12042

Lingyu, W., Leedham, G., 2006. Near-and far-infrared imaging for vein pattern biometrics, in: Proceedings of the IEEE International Conference on Video and Signal Based Surveillance. pp. 1–6.

Lombardi, M., Canter, J., Patrick, P.A., Altman, R., 2015. Is fluorescence under an alternate light source sufficient to accurately diagnose subclinical bruising? J. Forensic Sci. 60, 444–449. doi:10.1111/1556-4029.12698

Lu, G., Fei, B., 2014. Medical hyperspectral imaging: a review. J. Biomed. Opt. 19, 1–23. doi:10.1117/1.JBO.19.1.010901

Mackay, M., 2007. The increasing importance of the biomechanics of impact trauma. Sadhana 32, 397–408.

Maguire, S., Mann, M.K., Sibert, J., Kemp, A., 2005. Can you age bruises accurately in children? A systematic review. Arch. Dis. Child. 90, 187–189. doi:10.1136/adc.2003.044073

Mangold, K., Shaw, J.A., Vollmer, M., 2013. The physics of near-infrared photography. Eur. J. Phys. 34, S51–S71. doi:10.1088/0143-0807/34/6/S51

Martini, F.H., 2004. Fundementals of anatomy and physiology, 6th ed. Pearson Education Inc., San Francisco.

Martini, F.H., Nath, J.L., 2009. Fundementals of anatomy and physiology, 8th ed. Pearson Education Inc., San Francisco.

McBrier, N.M., Neuberger, T., Okita, N., Webb, A., Sharkey, N., 2009. Reliability and validity of a novel muscle contusion device. J. Athl. Train. 44, 275–278. doi:10.4085/1062-6050-44.3.275

McKinley, M., O'Loughlin, V.D., 2006. Animation: hemoglobin breakdown [WWW Document]. Hum. Anat. URL http://highered.mheducation.com/sites/0072495855/student_view0/chapter21/animation__

hemoglobin_breakdown.html (accessed 1.29.15).

Meredith, M., 2012. Mom cleared in child abuse investigation; “bruises” are birth marks [WWW Document]. KDVR Fox 31 Denver News. URL http://kdvr.com/2012/04/05/mom-suspected-of-child-abuse-cleared-after-spots-found-to-be-birth-mark/ (accessed 8.22.14).

Mimasaka, S., Ohtani, M., Kuroda, N., Tsunenari, S., 2010. Spectrophotometric evaluation of the age of bruises in children: measuring changes in bruise color as an indicator of child physical abuse. Tohoku J. Exp. Med. 220, 171–175. doi:10.1620/tjem.220.171

Mimasaka, S., Oshima, T., Ohtani, M., 2012. Characterization of bruises using ultrasonography for potential application in diagnosis of child abuse. Leg. Med. 14, 6–10. doi:10.1016/j.legalmed.2011.09.007

Miodownik, M., 2013. How to: make a liquid that’s also a solid [WWW Document]. BBC Sci. URL http://www.bbc.co.uk/science/0/22880407 (accessed 2.17.17).

Mueller, W.H., 1982. The changes with age of the anatomical distribution of fat. Soc. Sci. Med. 16, 191–196.

Muhlestein, D., 2014. Difference between a mechanical and an electropneumatic paintball gun [WWW Document]. URL http://paintball.about.com/od/markersguns/tp/Differences-Between-A-Mechanical-And-An-Electropneumatic-Paintball-Gun.htm (accessed 12.11.14).

Mukamal, K.J., Massaro, J.M., Ault, K.A., Mittleman, M. a, Sutherland, P.A., Lipinska, I., Levy, D., D’Agostino, R.B., Tofler, G.H., 2005. Alcohol consumption and platelet activation and aggregation among women and men: the Framingham Offspring Study. Alcohol. Clin. Exp. Res. 29, 1906–1912. doi:10.1097/01.alc.0000183011.86768.61

Munang, L.A., Leonard, P.A., Mok, J.Y.Q., 2002. Lack of Agreement on Colour Description Between Clinicians Examining Childhood Bruising. J. Clin. Forensic Med. 9, 171–174. doi:10.1016/S1353-1131(02)00097-4

Nash, K.R., Sheridan, D.J., 2009. Can one accurately date a bruise? state of the science. J. Forensic Nurs. 5, 31–37. doi:10.1111/j.1939-3938.2009.01028.x

Nuzzolese, E., Di Vella, G. Di, 2012. The development of a colorimetric scale as a visual aid for the bruise age determination of bite marks and blunt trauma. J. Forensic Ondontostomatology 30, 1–6.

Odin, L., 2010. How a Tippmann A5 Works [WWW Document]. URL https://www.youtube.com/watch?v=hyUZrnvt2Zw (accessed 12.11.14).

Ogedegbe, H.O., 2002. An overview of hemostasis. Lab. Med. 33, 948–953.

Olds, K., Byard, R.W., Winskog, C., Langlois, N.E.I., 2016a. Validation of ultraviolet, infrared, and narrow band light alternate light sources for detection of bruises in a pigskin model. Forensic Sci. Med. Pathol. 12, 435–443. doi:10.1007/s12024-016-9756-2

Olds, K., Byard, R.W., Winskog, C., Langlois, N.E.I., 2016b. How useful are ultraviolet, infrared, and narrow band light sources for enhancing occult bruises in cases of assault? Forensic Sci. Med. Pathol. 12, 209–210. doi:10.1007/s12024-016-9756-2

Olds, K., Byard, R.W., Winskog, C., Langlois, N.E.I., 2017. Validation of alternate light sources for detection of bruises in non-embalmed and embalmed cadavers. Forensic Sci. Med. Pathol. 13, 28–33. doi:10.1007/s12024-016-9822-9

Ono, I., 2011. A study on the alterations in skin viscoelasticity before and after an intradermal administration of growth factor. J. Cutan. Aesthet. Surg. 4, 98–104.

Özkalipci, Ö., Volpellier, M., 2010. Photographic documentation, a practical guide for non professional forensic photography. Torture 20, 45–52.

Özkaya, N., Nordin, M., Goldsheyder, D., Leger, D., 2012. Fundementals of biomechanics, 3rd ed.

Springer, New York, NY.

Pain, M.T.G., Challis, J.H., 2002. Soft tissue motion during impacts: their potential contributions to energy dissipation. J. Appl. Biomech. 18, 231–242.

Paintball, E., 2014. The history of paintball [WWW Document]. URL http://empirepaintball.com/the-history-of-paintball (accessed 6.23.14).

Palmer, M., Brodell, R.T., Mostow, E.N., 2013. Elder abuse: dermatologic clues and critical solutions. J. Am. Acad. Dermatol. 68, 37–42. doi:10.1016/j.jaad.2011.03.016

Pasi, K.J., Collins, P.W., Keeling, D.M., Brown, S.A., Cumming, A.M., Dolan, G.C., Hay, C.R.M., Hill, F.G.H., Laffan, M., Peake, I.R., 2004. Management of von Willebrand disease: a guideline from the UK Haemophilia Centre Doctors' Organization. Haemophilia 10, 218–231. doi:10.1111/j.1365-2516.2004.00886.x

Paul, S.P., Matulich, J., Charlton, N., 2016. A new skin tensiometer device: computational analyses to understand biodynamic excisional skin tension lines. Sci. Rep. 6, 30117. doi:10.1038/srep30117

Payne-James, J., Crane, J., Hinchliffe, J.A., 2005. Injury Assessment, Documentation, and Interpretation, in: Stark, M.M. (Ed.), Clinical Forensic Medicine: A Physician's Guide. Totowa, NJ, pp. 127–158.

Payne, G., Langlois, N., Lennard, C., Roux, C., 2007. Applying visible hyperspectral (chemical) imaging to estimate the age of bruises. Med. Sci. Law 47, 225–232. doi:10.1258/rsmmsl.47.3.225

Pilling, M.L., Vanezis, P., Perrett, D., Johnston, A., 2010. Visual assessment of the timing of bruising by forensic experts. J. Forensic Leg. Med. 17, 143–149. doi:10.1016/j.jflm.2009.10.002

Piva, A., 2013. An overview on image forensics. ISRN Signal Process. 1–22. doi:10.1016/j.steroids.2009.10.005

Plack, C.J., 2014. The Sense of Hearing, Second. ed. Psychology Press. Taylor & Francis Group, New York, NY.

Possley, M., 2012. Sabrina Butler [WWW Document]. Natl. Regist. Exonerations. URL http://www.law.umich.edu/special/exoneration/Pages/casedetail.aspx?caseid=3078 (accessed 9.1.14).

Pounder, D., 2009. Blunt force injuries.

Purslow, P.P., Wess, T.J., Hukins, D.W., 1998. Collagen orientation and molecular spacing during creep and stress-relaxation in soft connective tissues. J. Exp. Biol. 201, 135–142.

Quan, M.B., Edwards, C., Marks, R., 1997. Non-invasive in vivo techniques to differentiate photodamage and ageing in human skin. Acta Derm. Venereol. 77, 416–419.

R. Vadivambal, D.S.J., 2014. Applications of thermal imaging in agriculture and food industry: a review. Adv. Remote Sens. 3, 128–140.

Rai, B., Kaur, J., 2013. Different types of light in forensic photography, in: Evidence-Based Forensic Dentistry. Springer Berlin Heidelberg, Berlin, Heidelberg, pp. 131–139. doi:10.1007/978-3-642-28994-1

Randeberg, L.L., Baarstad, I., Løke, T., Kaspersen, P., Svaasand, L.O., 2006. Hyperspectral imaging of bruised skin. Proc. SPIE 6078, 1–11.

Randeberg, L.L., Hernandez-Palacios, J., 2012a. Hyperspectral imaging of bruises in the SWIR spectral region. Proc. SPIE Photonic Ther. Diagnostics VIII 8207, 1–10.

Randeberg, L.L., Hernandez-Palacios, J., 2012b. Hyperspectral imaging as a tool for fluorescence imaging and characterization of skin bruises. Imaging Appl. Opt. Tech. Dig. 1–3.

Randeberg, L.L., Larsen, E.L.P., Svaasand, L.O., 2010. Characterization of vascular structures and skin bruises using hyperspectral imaging, image analysis and diffusion theory. J. Biophotonics 3, 53–

65.

Randeberg, L.L., Skallerud, B., Langlois, N.E.I., Haugen, O.A., Svaasand, L.O., 2011. The optics of bruising, in: Welch, A.J., Gemert, M.J.C. (Eds.), Optical-Thermal Response of Laser-Irradiated Tissue. Springer Netherlands, Dordrecht, pp. 825–858. doi:10.1007/978-90-481-8831-4

Randeberg, L.L., Winnem, A.M., Langlois, N.E.I., Larsen, E.L.P., Haaverstad, R., Skallerud, B., Haugen, O.A., Svaasand, L.O., 2007. Skin changes following minor trauma. Lasers Surg. Med. 39, 403–413. doi:10.1002/lsm.20494

Rangger, C., Kathrein, A., Freund, M.C., Klestil, T., Kreczy, A., 1998. Bone bruise of the knee: histology and cryosections in 5 cases. Acta Orthop. Scand. 69, 291–294.

Rawlings, A. V, 2006. Ethnic skin types: are there differences in skin structure and function? Int. J. Cosmet. Sci. 28, 79–93. doi:10.1111/j.1467-2494.2006.00302.x

Rodriguez, G., 2014. How does a paintball gun work [WWW Document]. URL http://www.life123.com/sports/extreme-sports/paintball/how-does-paintball-gun-work.shtml (accessed 12.9.14).

Rowan, P., Hill, M., Gresham, G.A., Goodall, E., Moore, T., 2010. The use of infrared aided photography in identification of sites of bruises after evidence of the bruise is absent to the naked eye. J. Forensic Leg. Med. 17, 293–297. doi:10.1016/j.jflm.2010.04.007

Sanders, J.E., Goldstein, B.S., Leotta, D.F., 1995. Skin response to mechanical stress: adaptation rather than breakdown - a review of the literature. J. Rehabil. Res. Dev. 32, 214–226.

Saukko, P., Knight, B., 2004. The pathology of wounds, in: Knight's Forensic Pathology. Oxford University Pres Inc., New York, NY, pp. 136–173.

Sbicca, J.A., Hatch, R.L., 2012. Target lesions and other paintball injuries. J. Am. Board Fam. Med. 25, 124–127. doi:10.3122/jabfm.2012.01.110120

Scafide, K.N., Sheridan, D.J., Taylor, L.A., Hayat, M.J., 2016. Reliability of tristimulus colourimetry in the assessment of cutaneous bruise colour. Injury 1–6. doi:10.1016/j.injury.2016.01.032

Scafide, K.R.N., 2012. Determining the relationship between skin colour, sex, and subcutaneous fat and the change in bruise colour over time. Johns Hopkins University.

Scafide, K.R.N., Sheridan, D.J., Campbell, J., Deleon, V.B., Hayat, M.J., 2013. Evaluating change in bruise colorimetry and the effect of subject characteristics over time. Forensic Sci. Med. Pathol. 9, 367–376. doi:10.1007/s12024-013-9452-4

Sharkey, E.J., Cassidy, M., Brady, J., Gilchrist, M.D., NicDaeid, N., 2012. Investigation of the force associated with the formation of lacerations and skull fractures. Int. J. Legal Med. 126, 835–844. doi:10.1007/s00414-011-0608-z

Shen, W., Niu, Y., Mattrey, R.F., Fournier, A., Corbeil, J., Kono, Y., Stuhmiller, J.H., 2008. Development and validation of subject-specific finite element models for blunt trauma study. J. Biomech. Eng. 130, 1–13. doi:10.1115/1.2898723

Sherman, D., Bir, C., Viano, D., Haacke, E.M., 2003. Evaluation and quantification of bruising, in: The American Society of Biomechanics 29th Annual Meeting. Cleveland, p. 1.

Shkrum, M.J., Ramsay, D.A., 2007. Forensic pathology of trauma: common problems for the pathologist. Humana Press, Totowa, NJ.

Shrotri, A., Rethrekar, S.C., Patil, M.H., Kore, S.N., 2010. IR-webcam imaging and vascular pattern analysis towards hand vein authentication 5, 876–880.

Silver, F.H., Freeman, J.W., DeVore, D., 2001. Viscoelastic properties of human skin and processed dermis. Ski. Res. Technol. 7, 18–23.

Silvestri, E., Muda, A., Orlandi, D., 2015. Ultrasound anatomy of lower limb muscles. A practical guide.

Springer.

Sosta, J., 2014. Marker internal operation.

Spilsbury, B., 1939. The medico-legal significance of bruises. Medico-Legal Rev. 7, 215–227.

Spinks, J., 2007. Easy bruising. Found. Years 3, 219–221. doi:10.1016/j.mpfou.2007.08.001

Stam, B., Gemert, M.J.C. Van, Leeuwen, T.G. Van, Aalders, M.C.G., 2012. How the blood pool properties at onset affect the temporal behavior of simulated bruises. Med. Biol. Eng. Comput. 50, 165–171. doi:10.1007/s11517-012-0860-5

Stam, B., van Gemert, M.J.C., van Leeuwen, T.G., Aalders, M.C.G., 2010. 3D finite compartment modeling of formation and healing of bruises may identify methods for age determination of bruises. Med. Biol. Eng. Comput. 48, 911–921. doi:10.1007/s11517-010-0647-5

Stam, B., van Gemert, M.J.C., van Leeuwen, T.G., Teeuw, A.H., van der Wal, A.C., Aalders, M.C.G., 2011. Can color inhomogeneity of bruises be used to established their age? J. Biophotonics 4, 759–767.

Stephenson, T., 1995. Bruising in children. Curr. Paediatr. 5, 225–229. doi:10.1016/S0957-5839(05)80034-X

Strangman, G., Boas, D.A., Sutton, J.P., 2002. Non-invasive neuroimaging using near-infrared light. Biol. Psychiatry 52, 679–693. doi:10.1016/S0006-3223(02)01550-0

Tanaka, N., Kaneko, M., 2006. Skin surface shock wave. Conf. Proc. Annu. Int. Conf. IEEE Eng. Med. Biol. Soc. 1, 4123–4126. doi:10.1109/IEMBS.2006.259937

Tetley, C., 2005. The photography of bruises. J. Vis. Commun. Med. 28, 72–77. doi:10.1080/01405110500104043

Tham, L.M., Lee, H.P., Lu, C., 2006. Cupping: From a biomechanical perspective. J. Biomech. 39, 2183–2193. doi:10.1016/j.jbiomech.2005.06.027

Thavarajah, D., Vanezis, P., Perrett, D., 2012. Assessment of bruise age on dark-skinned individuals using tristimulus colorimetry. Med. Sci. Law 52, 6–11. doi:10.1258/msl.2011.011038

Tidy, C., 2012. Platelet function disorders (thrombocytopathy) [WWW Document]. URL www.patient.co.uk/doctor/platelet-function-disorders-thrombocytopathy (accessed 10.13.14).

Tidy, C., 2014a. Vitamin K deficiency [WWW Document]. doi:10.3945/an.111.001800.1.

Tidy, C., 2014b. Vitamin K deficiency bleeding [WWW Document]. URL www.patient.co.uk/doctor/vitamin-k-deficiency-bleeding (accessed 8.26.14).

Turnbull, Lord, Bracadale, Lord, Dorrian, Lady, 2017. Appeal against conviction by Rachel Trelfa or Fee against Her Majesty's Advocate.

Turner, M., 2016. Interview with Dr. Marjorie Turner. 12th April.

UPT, 2014. Buying your first gun [WWW Document]. URL http://www.upt.pitt.edu/jcramer/webclass/krupa/guides/firstgun.htm (accessed 12.10.14).

Vanezis, P., 2001. Interpreting bruises at necropsy. J. Clin. Pathol. 54, 348–355.

Varith, J., Hyde, G.M., Baritelle, A.L., Fellman, J.K., Sattabongkot, T., 2003. Non-contact bruise detection in apples by thermal imaging. Innov. Food Sci. Emerg. Technol. 4, 211–218. doi:10.1016/S1466-8564(03)00021-3

Venus, M., Waterman, J., McNab, I., 2011. Basic physiology of the skin. Surgery 29, 471–474. doi:10.1016/j.mpsur.2011.06.010

Viano, D.C., King, A.I., 2000. Biomechanics of chest and abdomen impact, in: The Biomedical Engineering Handbook. Volume 1. CRC Press, pp. 369–380.

Viano, D.C., King, A.I., Melvin, J.W., Weber, K., 1989. Injury biomechanics research: an essential element in the prevention of trauma. J. Biomech. 22, 403–417.

Vij, K., 2011. Textbook of forensic medicine and toxicology: principles and practice, 5th ed. Elsevier India.

Walilko, T.J., Viano, D.C., Bir, C.A., 2005. Biomechanics of the head for Olympic boxer punches to the face. Br. J. Sports Med. 39, 710–719. doi:10.1136/bjsm.2004.014126

Ward, M.G.K., Ornstein, A., Niec, A., Murray, C.L., 2013. The medical assessment of bruising in suspected child maltreatment cases: a clinical perspective. Paediatr. Child Health 18, 433–442.

Watson, A.A., 1989. Forensic medicine - a handbook for professionals. Gower Publishing Company Limited, Aldershot, England.

Whitehall, J., Kenny, T., 2012. Topical Steroids [WWW Document]. doi:10.1016/B978-1-4377-0847-9.00013-1

Whitehall, J., Kenny, T., 2013. Anticoagulants [WWW Document]. URL www.patient.co.uk/health/anticoagulants (accessed 8.26.14).

WHO, 2016. BMI classification [WWW Document]. URL http://www.who.int/mediacentre/factsheets/fs311/en/ (accessed 10.12.16).

Willacy, H., 2016. BMI calculator [WWW Document]. URL http://patient.info/health/bmi-calculator-leaflet (accessed 10.12.16).

Willacy, H., Thomas, H., 2016. Body surface area calculator (Mosteller) [WWW Document]. URL http://patient.info/doctor/body-surface-area-calculator-mosteller (accessed 10.12.16).

Wilson, E.F., 1977. Estimation of the age of cutaneous contusions in child abuse. Pediatrics 60, 750–752.

Winnem, A.M., Randeberg, L.L., Larsen, E.L.P., Lilledahl, M.B., Haugen, O.A., Skallerud, B., Svaasand, L.O., 2007. Biomechanical characterization of soft tissue injuries. Proc. SPIE Photonic Ther. Diagnostics III 6424, 1–10.

Witmer, W.K., Lebovitz, P.J., 2012. Clinical photography in the dermatology practice. Semin. Cutan. Med. Surg. 31, 191–199. doi:10.1016/j.sder.2012.06.004

Wright, F.D., Golden, G.S., 2010. The use of full spectrum digital photography for evidence collection and preservation in cases involving forensic odontology. Forensic Sci. Int. 201, 59–67. doi:10.1016/j.forsciint.2010.03.013

X-Rite, 2016. ColourChecker Passport user manual. X-Rite Photo, Michigan, USA.

Xu, F., Lu, T.J., Seffen, K.A., 2008. Biothermomechanical behavior of skin tissue. Acta Mech. Sin. 24, 1–23. doi:10.1007/s10409-007-0128-8

Yajima, Y., Funayama, M., 2006. Spectrophotometric and tristimulus analysis of the colors of subcutaneous bleeding in living persons. Forensic Sci. Int. 156, 131–137. doi:10.1016/j.forsciint.2003.09.022

Yajima, Y., Nata, M., Funayama, M., 2003. Spectrophotometric and tristimulus analysis of the colors of subcutaneous bleeding in living persons. Leg. Med. (Tokyo). 5, S342–S343.

Zhao, J.Z., Narwani, G., 2007. Biomechanical analysis of hard tissue responses and injuries with finite element full human body model.

Zharov, V.P., Ferguson, S., Eidt, J.F., Howard, P.C., Fink, L.M., Waner, M., 2004. Infrared imaging of subcutaneous veins. Lasers Surg. Med. 34, 56–61. doi:10.1002/lsm.10248

Zioupos, P., 2014. Forensic biomechanics. J. Mech. Behav. Biomed. Mater. 33, 789–801. doi:10.1016/j.jmbbm.2013.11.005

9.2 Appendices

Appendix A

Empire BT-4 Combat Marker SOP

SOP Adapted from Empire BT-4 Series Markers Owner's Manual

Getting Started

Do not install an air cylinder or load paintballs into your marker until you feel completely confident with your ability to handle your marker safely.

Keep your finger out of the trigger guard and away from the trigger; point the muzzle of the marker in a safe direction at all times. Keep the marker in safely until ready to operate.

Always keep your marker pointed in a safe direction. Always use a barrel plug or barrel blocking device. Always use paintball specific eye protection which meets or exceeds EN 166:2001 specifications in any areas where paintball markers may be discharged.

Safe Mode

The safety should be set to ''SAFE'' (red marking on safety will not be visible).

Barrel Installation

Marker must be degassed, hopper removed, contain no paintballs and the marker must be in ''SAFE'' mode.

1. Place the threaded end of the barrel into the front opening of the marker body.
2. Turn the barrel clockwise until it stops (do not over tighten).
3. Install a barrel blocking device to prevent the accidental discharge of a paintball.

Air Cylinder Installation

Before pressurising the marker:

1. Ensure you and anyone within range are wearing suitable eye protection.
2. Double check that all screws are tightened and no parts are loose before installing the tank.
3. Ensure a barrel plug is in place.
4. Make sure there are no paintballs in the marker.
5. Set marker to ''SAFE'' mode.

Pressurising the marker:

1. While pointing the marker in a safe direction, cock the marker by pulling the cocking knob located on the left side of the marker until it clicks and stops.
2. Release the cocking knob, the marker is now cocked.
3. Locate the air cylinder adapter at the base of the pistol grip.
4. Position the marker so that the air cylinder is pointed upwards while keeping the muzzle of the marker pointed in a safe direction.
5. Insert the threaded cylinder valve end into the adapter.
6. Without pushing the cylinder, twist the cylinder clockwise and allow the threads to draw the cylinder into the marker until it stops. Your marker is now charged.

Loading Reusable Paintballs

1. Make sure the marker is set to ''SAFE'' mode.
2. Ensure you and anyone within range are wearing suitable eye protection.
3. Load the .68 calibre reusable paintballs, leaving room for them to move about inside the loader.

Firing the Marker

1. Place the empty loader onto the marker and secure into place.
2. Ensure you and anyone within range are wearing suitable eye protection.
3. Cock the marker and apply the air cylinder to pressurise the marker.
4. Put the paintballs in the loader.
5. Remove the barrel plug.
6. Aim the marker in a safe direction and set the safety to the ''FIRE'' position.
7. Aim the marker at the target.
8. Place your finger on the trigger and pull with a smooth squeezing motion.

Velocity Adjustment

Always check the velocity of the marker before use. At no time should the velocity exceed 300 feet per second (approx. 91.44 meter per second).

1. Ensure you and anyone within range are wearing suitable eye protection.
2. While pointing the marker in a safe direction, remove the barrel blocking device.
3. Point the marker over a chronograph that will measure the velocity of the paintballs discharged by the marker.
4. Set the marker to ''FIRE'' mode.
5. Pull the trigger and check the reading on the chronograph.
6. Locate the velocity adjuster screw on the left side of the marker.

7. Using a 5/32'' hex key, turn the screw inward or clockwise to reduce the velocity and outward or counter clockwise to increase the velocity of the paintballs discharged from the marker.

Unloading your Marker

1. Ensure you and anyone within range are wearing suitable eye protection.
2. Make sure the barrel plug is properly installed and the marker is set to ''SAFE'' mode.
3. Loosen the loader clamping screw. While holding the paintball hopper in place, invert the marker so that the hopper is below the marker.
4. Remove the loader and all paintballs.
5. While pointing the marker in a safe direction, remove the barrel plug.
6. Keep the marker pointed in a safe direction and pull the trigger several times to ensure there are no balls remaining in the chamber barrel.
7. Properly re-install the barrel blocking device and set the marker to ''SAFE'' mode.

Removing Air Cylinder

1. Ensure you and anyone within range are wearing suitable eye protection.
2. Make sure the barrel plug is properly installed and the marker is set to ''SAFE'' mode.
3. Point the marker in a safe direction and turn the cylinder counter clockwise about ¾ of a turn. This allows the cylinder valve to close without damaging the cylinder o-ring.
4. While pointing the marker in a safe direction, disengage the safety.
5. Keeping the marker pointed in a safe direction, pull the trigger until the remaining air is expelled and it fails to re-cock.
6. Unscrew the cylinder from the marker.

CED M2 Chronograph SOP – Indoor Use Only

SOP Adapted from CED M2 Chronograph Manual

Chronograph Construction

Mount the foldable mounting bracket to the table mount and attach both sensors to the each end of the bracket. Ensure they are pushed on as far as they will go until the end of the bracket is firmly against the back wall of the sensor. Adjust the pressure plate screws located on the bottom of each sensor, to tighten them in place, keeping it from moving during use. Ensure that the fixed end of the mounting bracket is facing forward.

Install the IR screen set. The grey arms slide into each side of the sensor and the white top screens fit onto each sidearm. The charged NiMH rechargeable battery pack or an AC power supply must be connected for use. Green lights on both screens indicate power. If red or no lights are lit, check the power supply.

Attach the cables from the sensors to the CED M2 Chronograph unit. Remember the front sensor must be plugged into the ''START'' jack and the rear sensor into the ''STOP'' jack. Open the CED M2 Chronograph unit and press the ''ON/OFF'' button to activate the chronograph.

Chronograph Use

Fire each projectile through the IR screen windows. For each shot, the current velocity will appear on the LCD display, along with the cumulative amount of shots received. When you wish to store a ''string'' of velocities or store all the data received, simply press the ''STO'' button and the data will be stored into memory. When the unit is turned off, the current string of velocities recorded will automatically be stored into memory.

Appendix B

Images of impact locations

Firing distance of 4 m

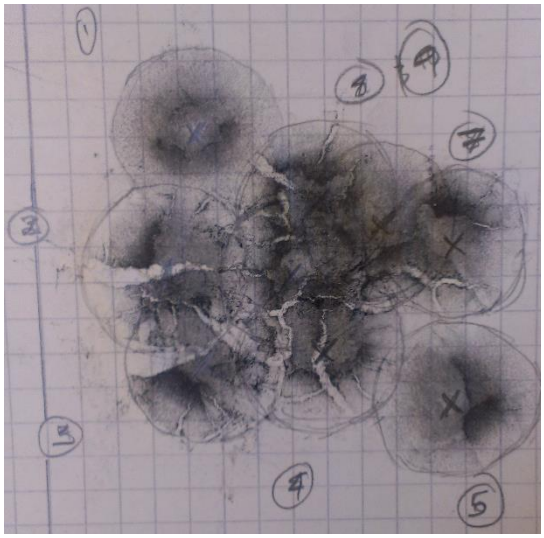

Test 1 – 9 impacts identified

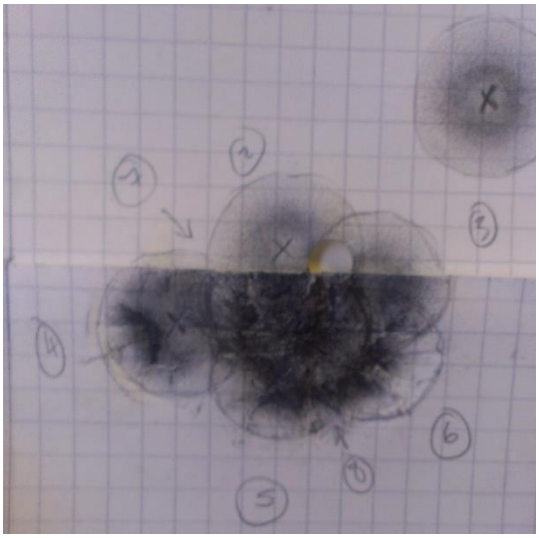

Test 2 – 8 impacts identified

Test 3 – 10 impacts identified

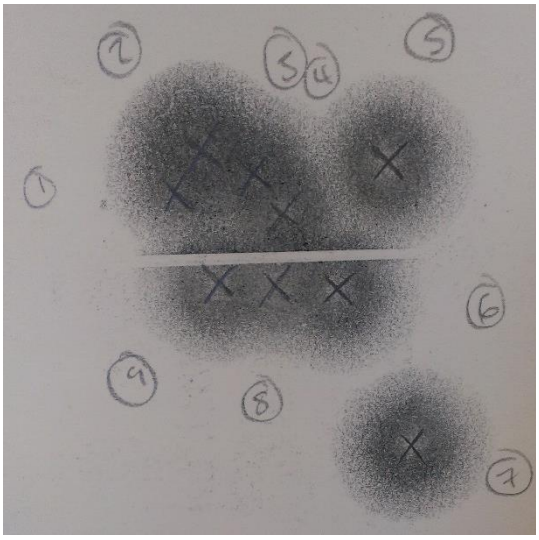

Test 4 – 9 impacts identified

Firing distance of 5 m

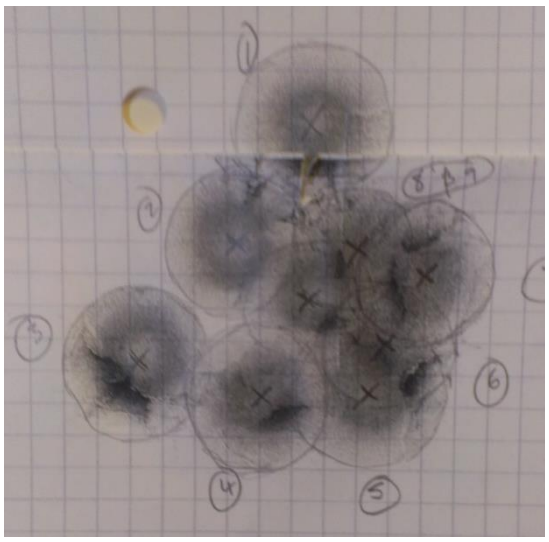

Test 1 – 9 impacts identified

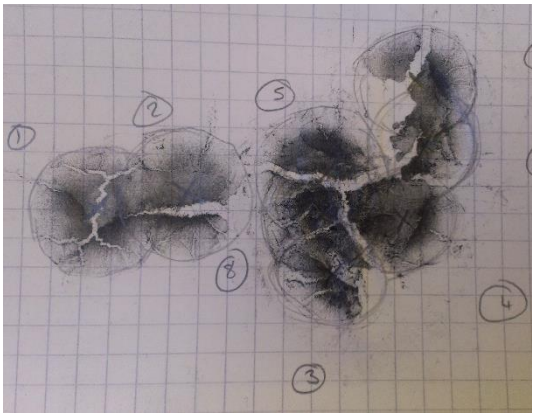

Test 2 – 8 impacts identified

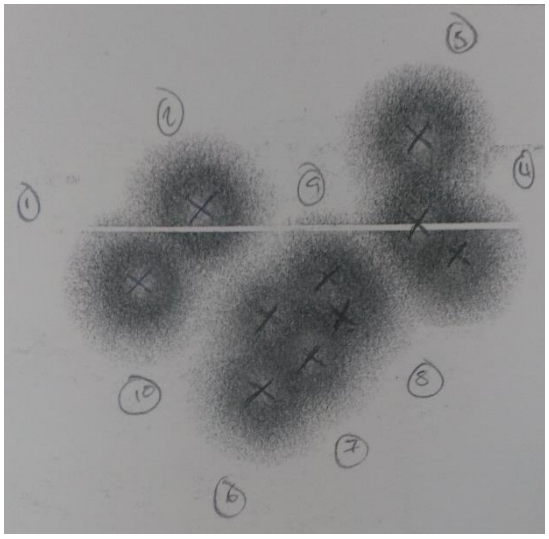

Test 3 – 10 impacts identified

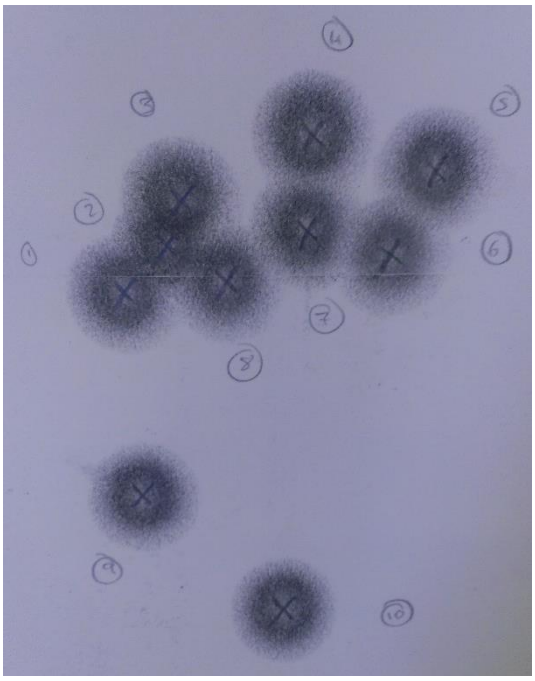

Test 4 – 10 impacts identified

Firing distance of 6 m

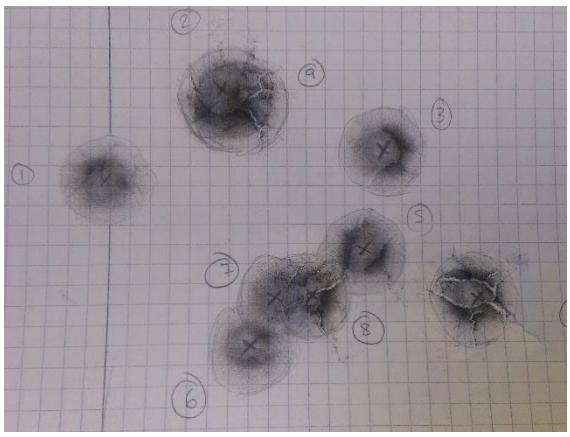

Test 1 – 9 impacts identified

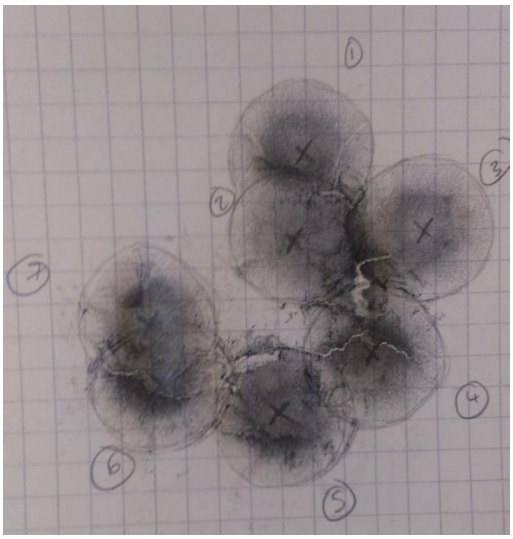

Test 2 – 7 impacts identified

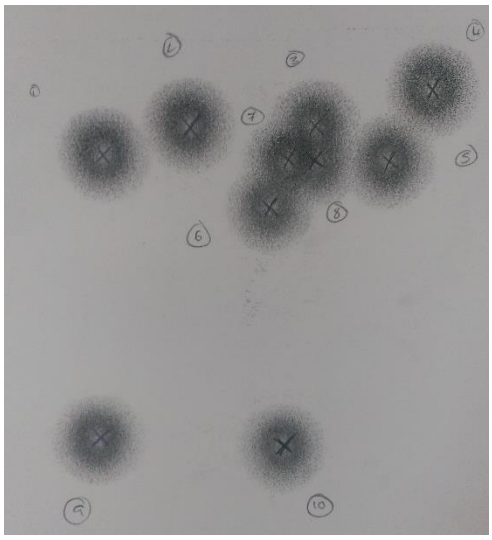

Test 3 – 10 impacts identified

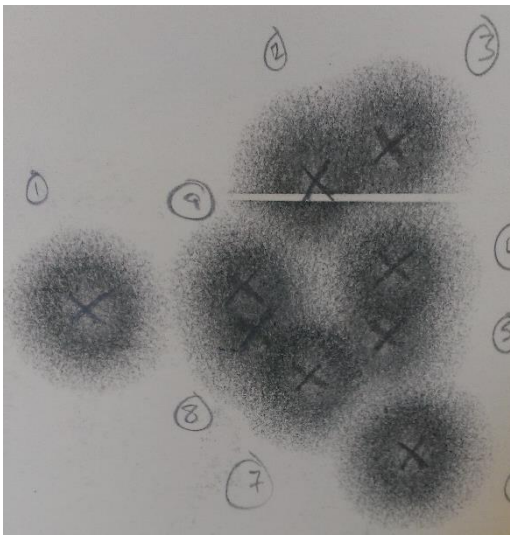

Test 4 – 9 impacts identified

Firing distance of 7 m

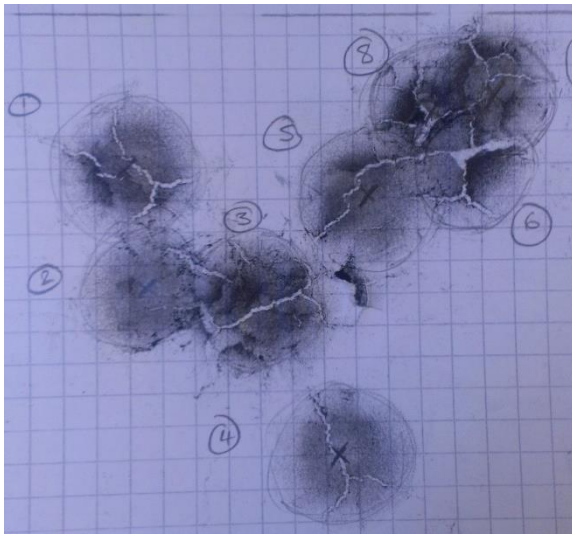

Test 1 – 8 impacts identified

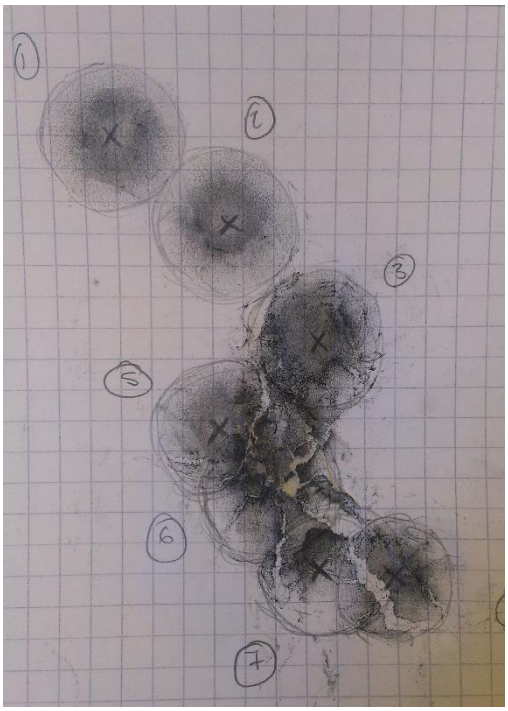

Test 2 – 7 impacts identified

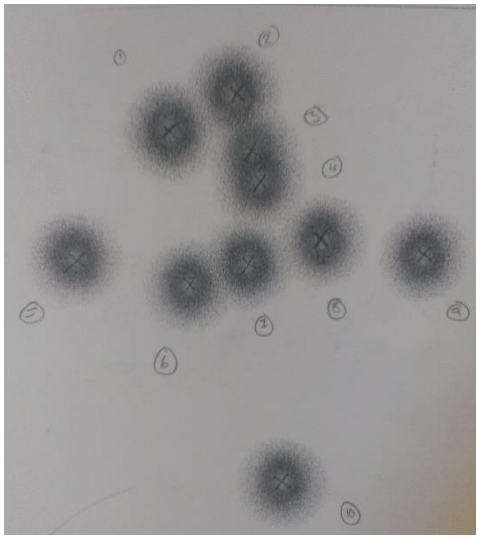

Test 3 – 10 impacts identified

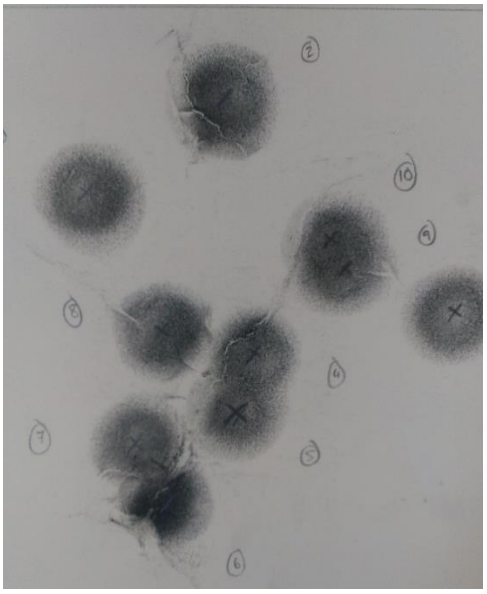

Test 4 – 10 impacts identified

Firing distance 8 m

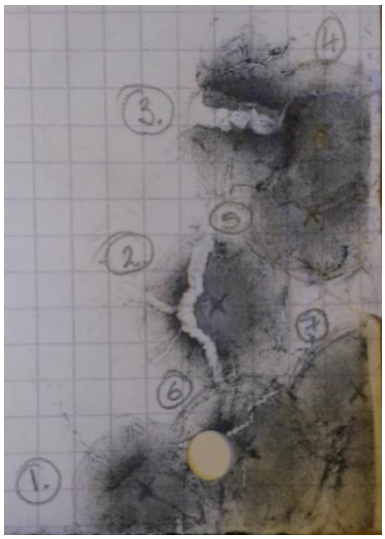

Test 1 – 7 impacts identified

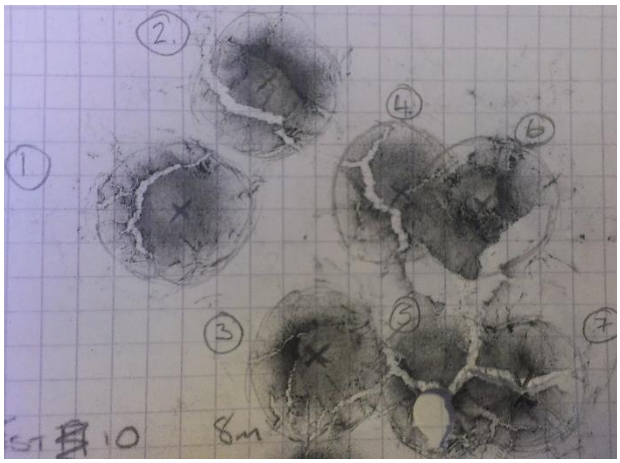

Test 2 – 7 impacts identified

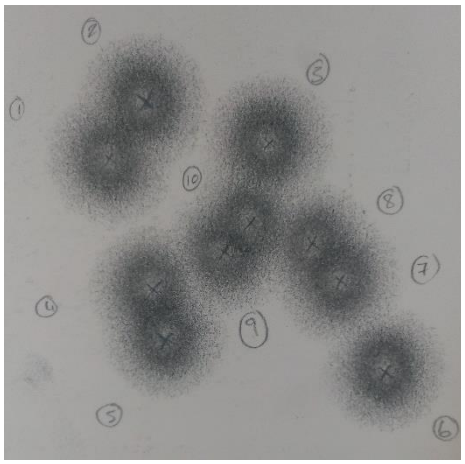

Test 3 – 10 impacts identified

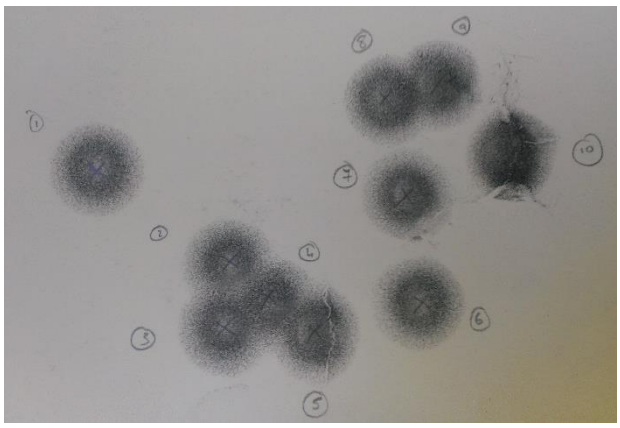

Test 4 – 10 impacts identified

Appendix C

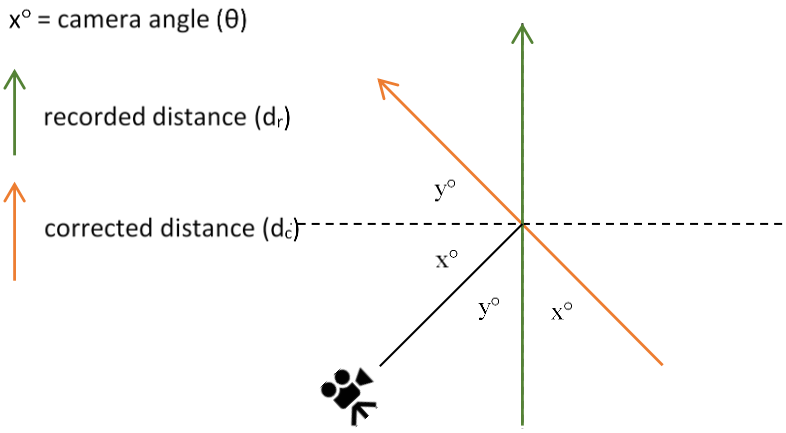

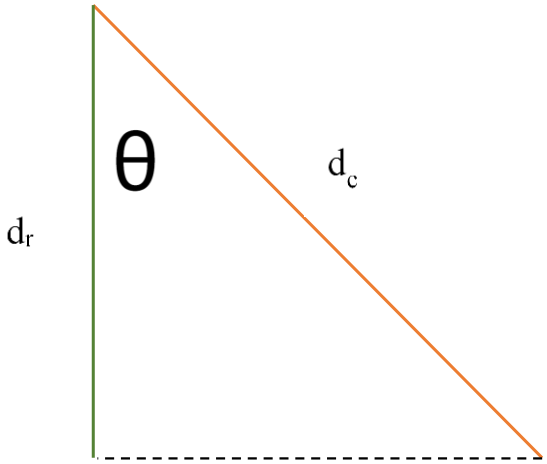

$$\cos\theta = \frac{d_r}{d_c}$$

$$d_c \cos\theta = d_r$$

$$\boldsymbol{d_c = \frac{d_r}{\cos\theta}}$$

Appendix D

From:	Ethics
Sent:	20 August 2015 15:32
To:	Heather Black
Cc:	Ethics
Subject:	FW: Approval: UEC15/47 Riches/Coupaud: The Biomechanics of Bruising

From: Ethics

Sent: 20 August 2015 15:20

To: Philip Riches; Sylvie Coupaud

Cc: Ethics

Subject: Approval: UEC15/47 Riches/Coupaud: The Biomechanics of Bruising

ETHICAL AND SPONSORSHIP APPROVAL

Dear Phil & Sylvie

I can confirm that the University Ethics Committee (UEC) has approved this protocol and appropriate insurance cover and sponsorship have now also been confirmed.

I would remind you that the UEC must be informed of any changes you plan to make to the research project, so that it has the opportunity to consider them. Any change of staffing within the research team should be reported to UEC.

The UEC would also expect you to report back on the progress and outcome of your project, with an account of anything which may prompt ethical questions for any similar future project and with anything else that you feel the Committee should know.

Any adverse event that occurs during an investigation must be reported as quickly as possible to UEC and, within the required time frame, to any appropriate external agency.

The University agrees to act as sponsor of the above mentioned project subject to the following conditions:

1. That the project obtains/has and continues to have University/Departmental Ethics Committee approval.
2. That the project is carried out according to the project protocol.
3. That the project continues to be covered by the University's insurance cover.
4. That the Director of Research and Knowledge Exchange Services is immediately notified of any change to the project protocol or circumstances which may affect the University's risk assessment of the project.
5. That the project starts within 12 months of the date of this letter.

As sponsor of the project the University has responsibilities under the Scottish Executive's Research Governance Framework for Health and Community Care. You should ensure you are aware of those responsibilities and that the project is carried out according to the Research Governance Framework.

On behalf of the Committee, I wish you success with this project.

Kind regards

Helen

Helen Baigrie

Contracts Manager

Research & Knowledge Exchange Services

University of Strathclyde

Graham Hills Building

50 George Street

Glasgow

G1 1QE

Direct Line +44 (0) 141 548 4539

Fax +44 (0) 141 552 4409

http://www.strath.ac.uk/ri/

Information for university staff can be found on the R & KE Portal: www.strath.ac.uk/rkeportal

The Internationalisation Information Portal for staff is available at https://moss.strath.ac.uk/internationalisation

Appendix E

Images of impact locations from second test from 6 m

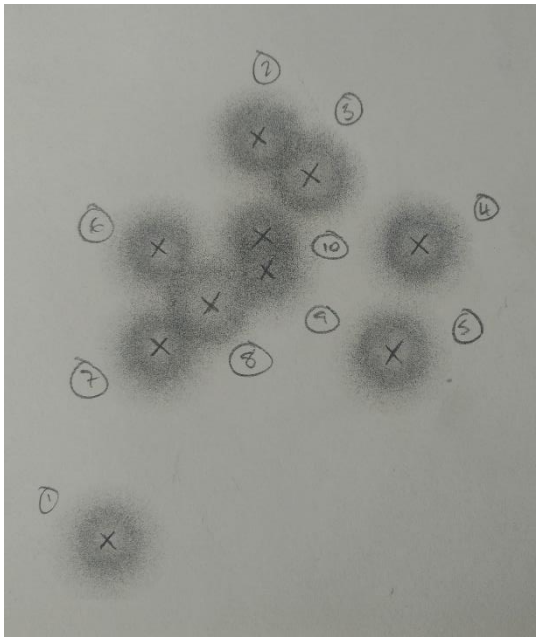

Test 1 – 10 impacts identified

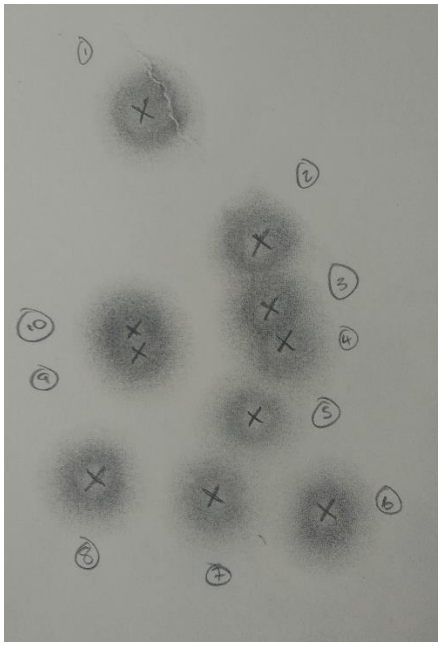

Test 2 – 10 impacts identified

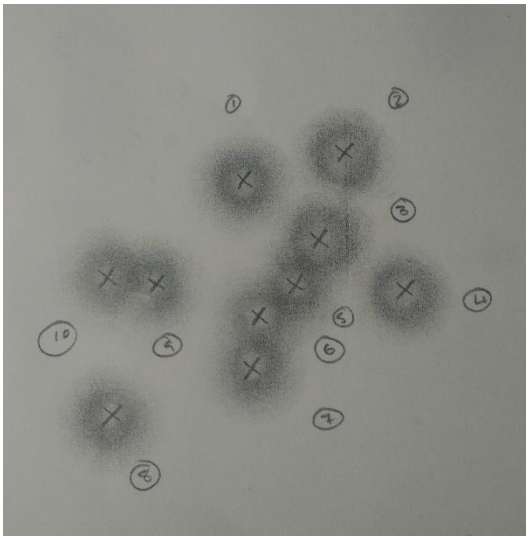

Test 3 – 10 impacts identified

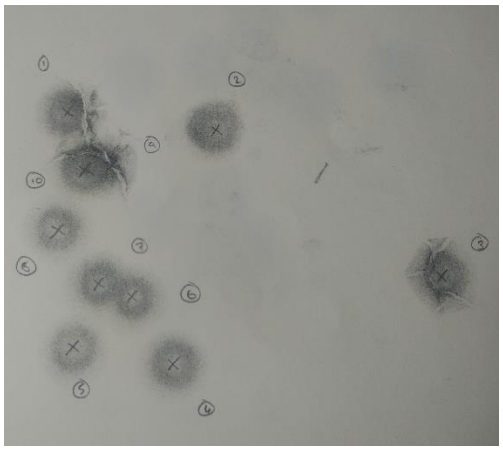

Test 4 – 10 impacts identified

Appendix F

Participant Invitation Letter

Name of department: Biomedical Engineering

Title of the study: The biomechanics of bruising

You are being asked to participate in a study that is being conducted by myself and my supervisors at the University of Strathclyde and has been approved by the University Ethics Committee.

The objective of this study is to understand the mechanical conditions surrounding the formation of a bruise. The study also aims to assess if there is any relationship between the colour changes of a bruise and the passage of time after the impact which caused the bruise. To do this we will use a paintball marker and reusable paintball to create a bruise, which we will then photograph using a variety of different (non-harmful), imaging techniques over a number of days (up to 3 weeks).

Little is known about the mechanical conditions of bruise formation and this research could develop a link between the physical appearance of a bruise with an estimated force and time of creation. If successful, this research would be very useful in forensic science investigations into the validation of assault timelines.

The impact of creating a bruise will generally hurt and we fully understand any reticence in volunteering. However, we are fully committed to answering these important research concerns and if there is a way to do this without causing pain we would obviously follow that route. We believe that the provided information sheet describes an important experiment and we hope that you understand our belief that the potential long term benefits of this work outweigh the short-term pain. The experiment has been piloted on the researchers themselves and we would not put you in any position that we are not willing to be in ourselves. If you have previously played paintball, you will be familiar with the level of pain and type of bruising that we are talking about. If you don't have any paintballing experience it should feel similar to a hard hit, like that experienced when you stub your toe, and may sting for a short time afterwards.

The information sheet hopefully provides a clear explanation of the study including the research aims, benefits, risks and also what participation would mean for yourself and any implications concerning your involvement. If there is any aspect of the study which is unclear that you would like further information on, please contact myself, or either of my supervisors, and we will be happy to answer your questions. Our contact details can be found at the end of the information sheet.

Thank you for your time.

Heather Black

PhD Biomedical Engineering Student

Participant Information Sheet for Volunteers

What is the purpose of this investigation?

The objective of this study is to understand the mechanical conditions surrounding the formation of a bruise including the force of impact and energy of impact required. The study also aims to objectively assess the colour changes of the bruise, visible and non-visible, over an approximate 3 week time period.

Do you have to take part?

No. Participation is entirely voluntary and it will require a significant commitment on your behalf if you agree to take part. If you decide to participate you will be asked to sign a form to confirm that the study was clearly explained to your and that you agree to take part. You will be free to withdraw at any time without giving a reason. For Strathclyde students and staff, the relationship you have with the University will not be affected in any way should you choose not to take part, or to withdraw yourself or your data, from the study.

What will you do in the project?

You will be required to attend the Department of Biomedical Engineering in the Wolfson Building on a regular basis at the same time of day over an approximate 3 week period. On the initial day of study, you will be asked to complete a short health questionnaire and measurements of your height and weight will be taken. You will be subject to a single impact from a reusable, non-paint filled paintball from a distance of 6 m, hitting the thigh. Photographs of the thigh will be taken before and after impact. Although we will give you a warning, you will not be aware of when the exact moment of impact will occur and the impact will be recorded via a high speed camera. You are required to wear tight fitting black lycra/cycle shorts if you do not have your own they can be provided for you and the whole process should take no longer than 1 hour.

We will ask you to attend the department every other day so that we can take photographs of the bruise up to a 3 week period or until the bruise is no longer visible using any of the imaging techniques employed in this study.

You may be asked to return at a weekend however, it is acknowledged that this may not always be possible and we will accommodate requests to avoid weekend return visits.

All photographic sessions should not take longer than 15 minutes.

It is requested that you do not:

- Apply self-tanning cream or spray tan within 2 or 3 weeks of taking part respectively, and to refrain from their use over the impacted area for the duration of the study
- Deliberately sun-tan the bruised area during your participation in this study
- Take any illegal drugs or drink alcohol 24 hours prior to taking part in the study
- Take any anti-inflammatory medication 24 hours prior to study

You will not receive any payment or reimbursement for your participation.

Why have you been invited to take part?

You have been invited to take part because you are a healthy person between 16 and 60 years. The investigators of this study aim to link the mechanics of bruise formation with their appearance over time, in an attempt to aid forensic investigations which may involve victims of alleged assault. Therefore, to perform such a study on anything other than human volunteers would not be appropriate.

Below is a list of exclusion criteria, if you are aware of these applying to yourself, unfortunately we will not be able to accept you as a volunteer but we appreciate your time in reading this information sheet.

Exclusion criteria:

- Anyone taking any anti-coagulants or anti-platelet medications – warfarin, dipyridamole, clopidogrel, ticlopidine, cilostazol and heparin.

  This type of medication prevents blood clot formation. If you were to take part there is a chance that you could bleed excessively, sustaining a more severe injury than intended for this study.

- Anyone who takes any anti-inflammatory medication e.g. ibuprofen, diclofenac and aspirin on a regular basis

  These medications can alter platelet function in the blood, reducing the body's ability to form a blood clot. Therefore, as with taking anti-coagulants, there is a chance that you could have an increased level of bleeding, sustaining a more severe injury than intended for this study.

- Anyone taking any oral or injectable steroids

  Steroids are a form of anti-inflammatory medication and can have side effects including thinning of the skin. This makes you more susceptible to bruising and could lead to greater injury than intended for this study.

- Anyone who has been diagnosed with any of the following medical conditions – coagulation deficiency, bleeding disorders, haemophilia, von Willebrand's

disease, vitamin K deficiency, diabetes, sickle cell disease, anaemia, bone marrow disorders, any autoimmune disorder causing clotting problems, leukemia, thrombocytopenia, thrombocytosis, Bernard-Soulier syndrome, Wiskott-Aldrich syndrome, Glanzmann's thrombasthenia and polycythaemia rubra vera, heart disease, cancer stroke or transient ischaemic attack, nephritis, liver disease, Ehlers-danlos syndrome or other condition causing problems with collagen formation and structure

- Anyone who has had an organ transplant
- Anyone who is pregnant
- Anyone who has donated blood or blood product in the past 60 days
- Anyone who has undergone major surgery or has significant scarring on the thigh which is to be tested
- Anyone with identifying marks, tattoos and/or piercings on thigh which is to be tested

What are the potential risks to you in taking part?

During the study you are likely to experience immediate and/or short term pain at (and around), the impact site. The pain experienced will depend on how you personally experience pain, but it is expected the pain will cause tolerable discomfort or at worst, distressing pain which dulls down over time (similar to stubbing your toe).

It is the intention to create bruises that last a number of days which causes short term damage to be made to the muscles. There is a minor possibility that a haematoma (blood clot), could be formed as a result of the impact, causing pain lasting much longer than expected (2-3 weeks or more), but will heal with time.

If you decide that afterwards you have experienced more pain that expected and feel it is necessary to take a painkiller (e.g. paracetamol), it is asked that you make the research team aware. Please do not take any anti-inflammatory medication (e.g. ibuprofen), as it may have effect on bruise development.

Providing that you've had no unusual bruising in the past, it is expected that there would be no long term effect of you taking part.

What happens to the information in the project?

All personal details will remain confidential and all results will be anonymous, identifiable only through a coded system. This will only be available to the research team. All information will be stored on password protected computers and all personal details will be deleted/destroyed once the study is complete. Anonymised electronic data, including photographs, will be kept indefinitely by the University by

both my supervisors for potential further use. I will not keep any photographs once the thesis is submitted.

You will be able to remove your data from the project at any time. Just let us know. However, we cannot retract published data or photographs.

The University of Strathclyde is registered with the Information Commissioner's Office who implements the Data Protection Act 1998. All personal data on participants will be processed in accordance with the provisions of the Data Protection Act 1998.

Thank you for reading this information – please ask any questions if you are unsure about what is written here.

What happens next?

If you would like to take part in the study you will be asked to sign a consent form to confirm you are happy to proceed. You will also be asked to complete a short general health survey prior to testing, which can be done either online or on paper. You will be asked for some personal details (name, age etc.), but they will only be used to link your survey answers with images taken during the study. At this point all details will be made anonymous and the other answers given (e.g. smoking habits and skin type), will remain confidential, only being used during results analysis.

If you do not wish to be involved in this study, we thank you for your time and consideration.

Researcher contact details:	**Chief Investigator details:**
Heather Black	Dr. Philip Riches
Biomedical Engineering Unit	Biomedical Engineering Unit
University of Strathclyde	University of Strathclyde
106 Rottenrow East	106 Rottenrow East
Wolfson Centre Glasgow	Wolfson Centre Glasgow
G1 0NW	G1 0NW
07889297750	0141 548 5703
heather.black@strath.ac.uk	philip.riches@strath.ac.uk

This investigation was granted ethical approval by the University of Strathclyde Ethics Committee.

If you have any questions/concerns, during or after the investigation, or wish to contact an independent person to whom any questions may be directed or further information may be sought from, please contact:

Secretary to the University Ethics Committee

Research & Knowledge Exchange Services

University of Strathclyde

Graham Hills Building

50 George Street

Glasgow

G1 1QE

Telephone: 0141 548 3707

Email: ethics@strath.ac.uk

Consent Form for Participants

Name of department: Biomedical Engineering

Title of the study: The biomechanics of bruising

- I confirm that I have read and understood the information sheet for the above project and the researcher has answered any queries to my satisfaction.
- I understand that my participation is voluntary and that I am free to withdraw from the project at any time, up to the point of completion, without having to give a reason and without any consequences. If I exercise my right to withdraw and I don't want my data to be used, any data which have been collected from me will be destroyed.
- If applicable, I understand that as a student/staff member of the University of Strathclyde, the relationship I have with the University will not be affected in any way if I choose to withdraw from the project at any time.
- I understand that I can withdraw from the study any personal data and unpublished data and photographs at any time.
- I understand that any information recorded in the investigation will remain confidential and no information that identifies me will be made publicly available.
- I confirm that no exclusion criteria apply to myself.
- I consent to have high speed video of the impact on my thigh taken

Optional:

- I consent to photographs/videos of my thigh being used in publications and talks

Yes No

Please circle

(PRINT NAME) Hereby agree to take part in the above project

Signature of Participant: Date:

Appendix G

Health Questionnaire

As mentioned on the information sheet, you are asked to complete this survey.

It is divided into 4 sections:

1 - Personal Details

2 - Identifying Code

3 - General Health Survey

Answers given in Section 1 will only be used to contact you during the study. The unique code which you create for yourself in Section 2 will be used to create a labelling system for each individual, whilst ensuring that data collected remains anonymous.

Answers given in Sections 3 will be used in analysis of results and all personal details will remain private and confidential.

Your details will not be distributed and any which are published within completed work will be made anonymous, thus will not be traceable back to yourself.

If you have any questions, please contact myself at heather.black@strath.ac.uk or at 07889297750.

Heather Black

PhD Biomedical Engineering Student

Section 1

Personal details.

Name:

Email Address:

Contact Telephone Number:

Section 2

Unique identifying code.

Please create your own unique code using the last 2 letters of your postcode, the number of the month you were born (01 = Jan, 02 = Feb etc.) and the first letter of your mother's maiden name.

Section 3

The following questions refer to you and your general health.

Age:

Gender:

Male/Female

How would you describe your ethnic origin? Please tick.

- Arab (please specify) _____
- Asian (please specify) _____
- Black (please specify) _____
- Mixed or multiple ethnic groups (please specify) _____
- White (please specify) _____
- Other _____

Have you regularly smoked cigarettes or cigars at any time in the last 10 years?

Yes / No

If you currently or previously have smoked cigarettes or cigars regularly, how long have you been smoking cigarettes for? If you wish not to answer, please enter N/A below

If you do smoke cigarettes, how many cigarettes do you have per day? Please tick.

- 1-10
- 11-20
- 21-30
- Other _____
- Rather not say

If you drink alcohol, how many units do you drink per week on average? Please tick.

Note*:

1 unit = half a pint of ordinary strength beer, lager or cider (3-4 % strength), small measure/25 ml of spirits (40 % strength), or standard measure/50 ml fortified wine, e.g. port or sherry (20 % strength).

1.5 units = a small glass/125 ml of ordinary strength wine (12 % strength) or a standard pub measure/ 35 ml of spirits (40 % strength)

*Source - www.patient.co.uk

- 1-10 units
- 11-20 units
- 21-30 units
- Other _____
- Rather not say

Please list all medications (prescription or over the counter), including contraceptives, vitamins, herbal remedies and food supplements (e.g. fish oil, ginkgo biloba) which you currently take and the frequency at which you take them. If you take no medications etc., or would rather not fill in any details, please state this below.

In a typical week, how often do you exercise?

What type of exercise do you do?

- Strength training (e.g. weight lifting)
- Cardio training (e.g. cycling)
- Both strength and cardio
- None
- Other _____

<u>For investigator use only</u>

Participant Height: _____ Weight: _____

Appendix H

Equipment	Source
CED M2 Chronograph	Centre for Anatomy and Human Identification, University of Dundee, UK
Compressed Air Cylinder	Just Paintball, UK
Compressed Air Supply	Aquatron Dive Store, UK
Custom Built Paintball Marker Table Mount	Department of Biomedical Engineering, University of Strathclyde, UK
Empire BT-4 Combat Paintball Marker	Just Paintball, UK
HAMA Red Laser Pointer 2518 (Class 2 Laser)	RS Components, UK
IR Converted Nikon D300 Camera	Advanced Camera Services, UK
IR Light Source – 48 LED Illuminator	Amazon, UK
Laser Pointer Purpose Built Clamp	Department of Biomedical Engineering, University of Strathclyde, UK
Nikkor 60 mm Lens	Advanced Camera Services, UK
Nikon D300 DSLR Camera	Advanced Camera Services, UK
Photron Fastcam SA4 High Speed Camera	Photron (Europe) Ltd., UK
Photron High Power LED Kit (2x Multi LED lamps)	Photron (Europe) Ltd., UK
Purpose Built Screen	University of Strathclyde, UK
Reusable Paintballs	Just Paintball, UK
Sheet Polariser	Knight Optical, UK
Sigma 24-70 mm f/2.8 Lens	Photron (Europe) Ltd., UK
X-Rite ColourChecker	Amazon, UK

Appendix I

Participant velocity and force profiles

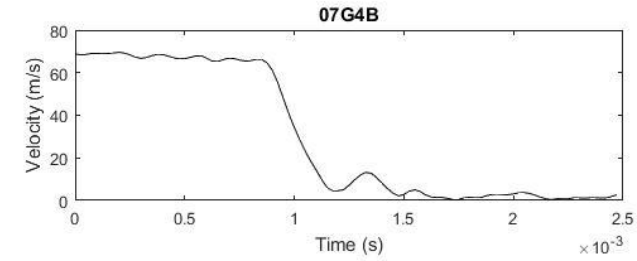

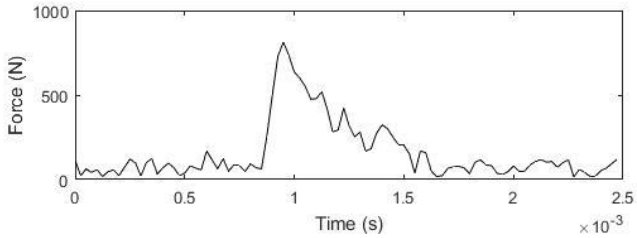

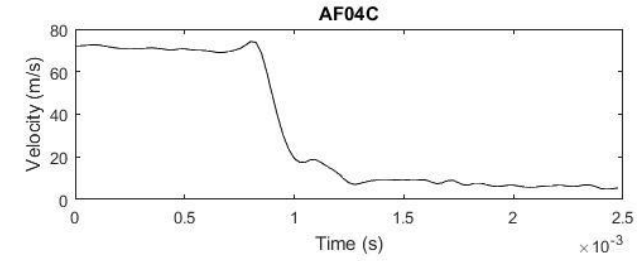

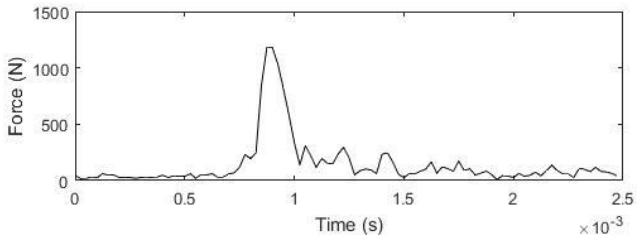

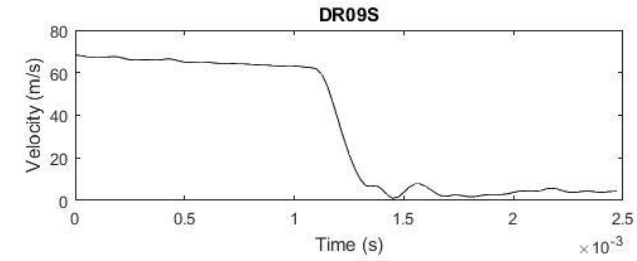

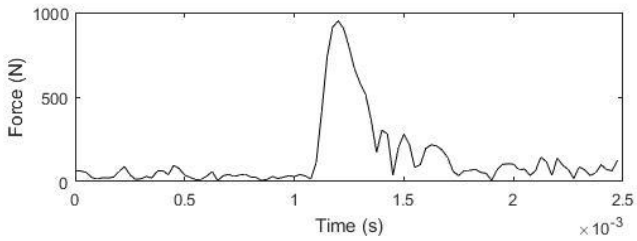

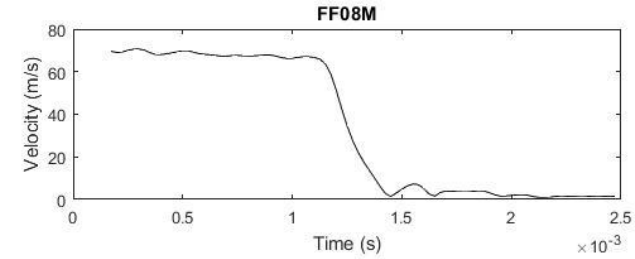
FF08M
Velocity (m/s)
Time (s)
×10^-3

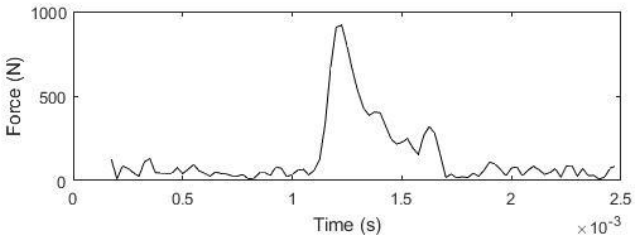
Force (N)
Time (s)
×10^-3

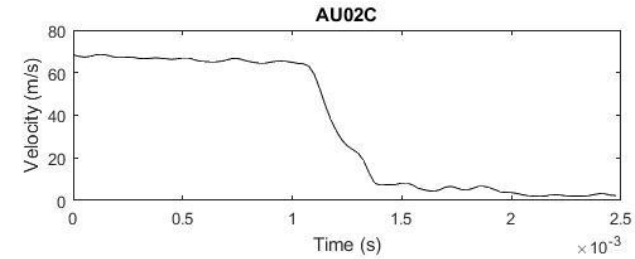
AU02C
Velocity (m/s)
Time (s)
×10^-3

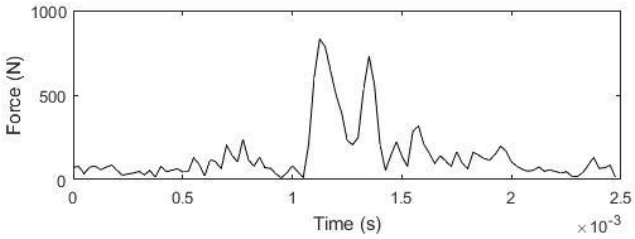
Force (N)
Time (s)
×10^-3

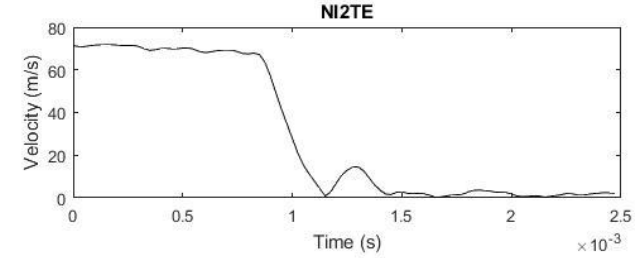
NI2TE
Velocity (m/s)
Time (s)
×10^-3

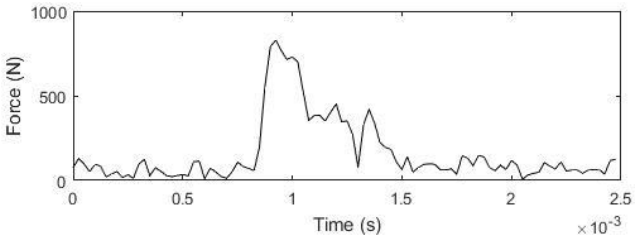
Force (N)
Time (s)
×10^-3

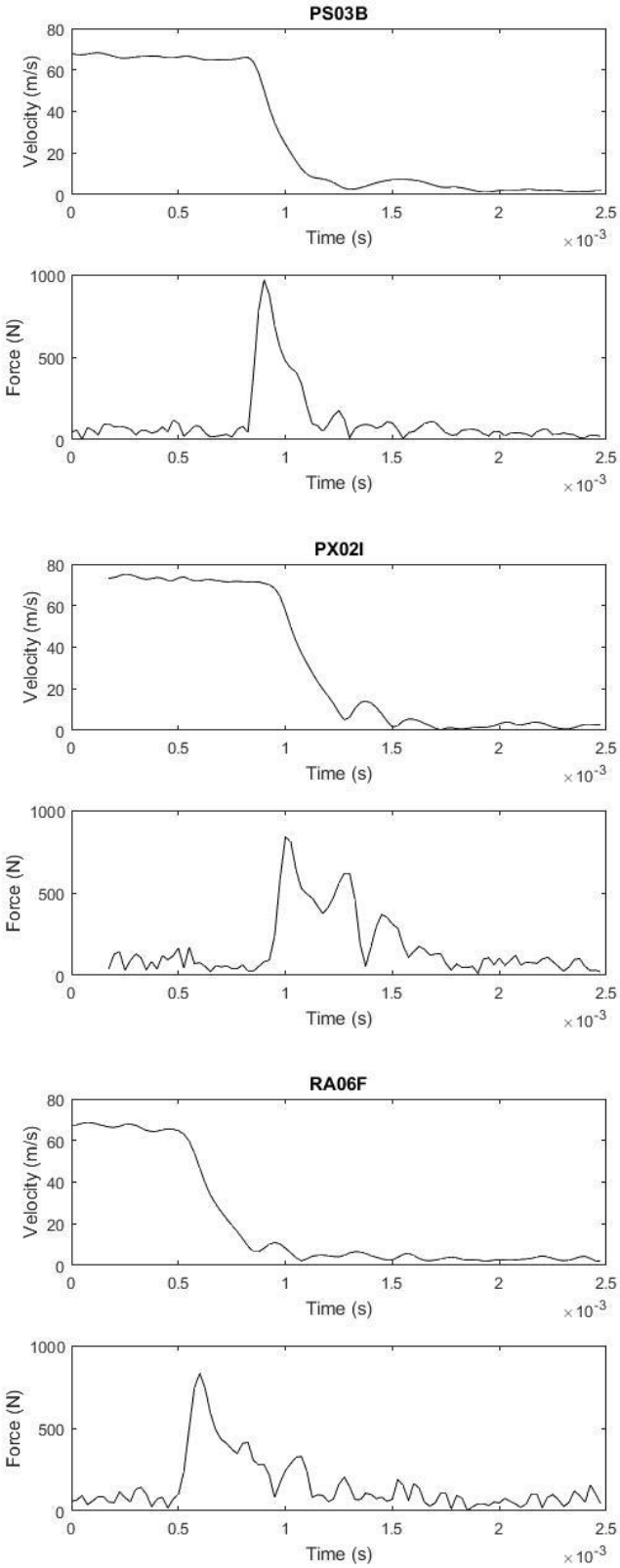
PS03B
Velocity (m/s)
Time (s)
×10^-3
Force (N)
Time (s)
×10^-3
PX02I
Velocity (m/s)
Time (s)
×10^-3
Force (N)
Time (s)
×10^-3
RA06F
Velocity (m/s)
Time (s)
×10^-3
Force (N)
Time (s)
×10^-3

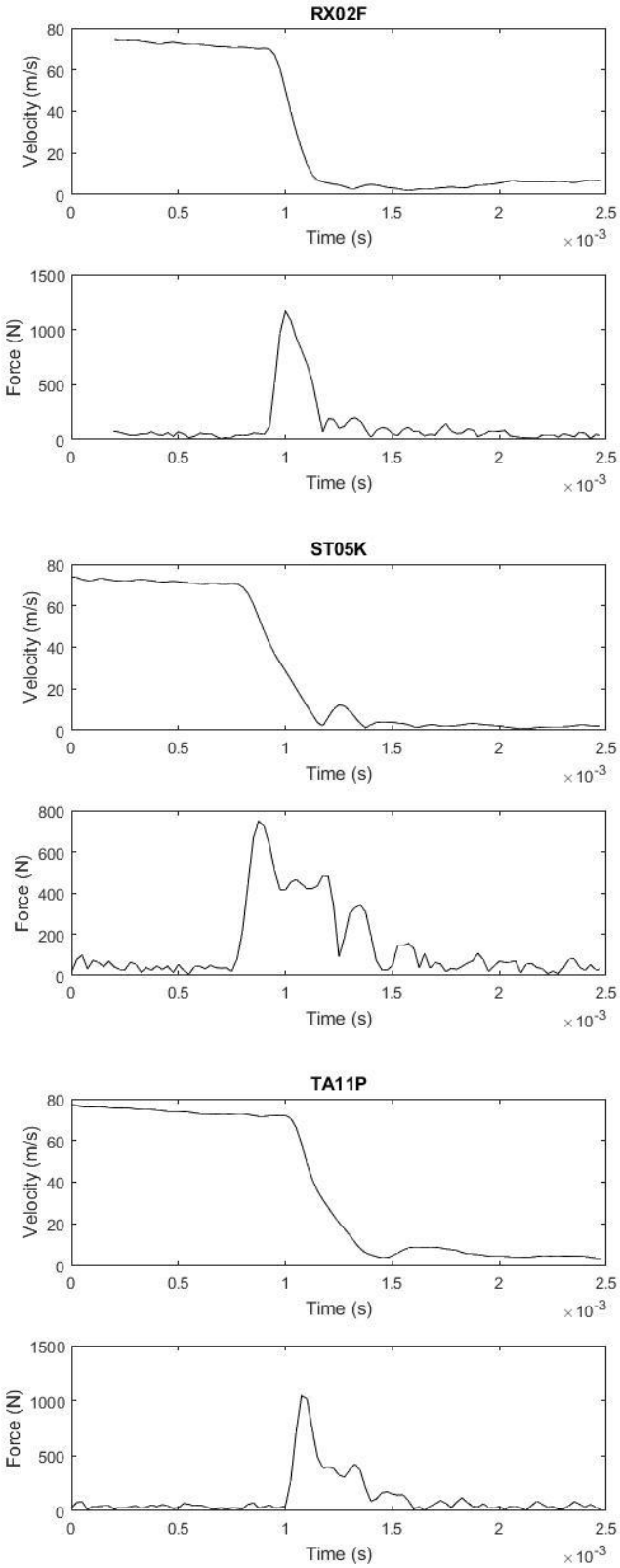
RX02F
Velocity (m/s)
Time (s)
×10^-3
Force (N)
Time (s)
×10^-3
ST05K
Velocity (m/s)
Time (s)
×10^-3
Force (N)
Time (s)
×10^-3
TA11P
Velocity (m/s)
Time (s)
×10^-3
Force (N)
Time (s)
×10^-3

Appendix J

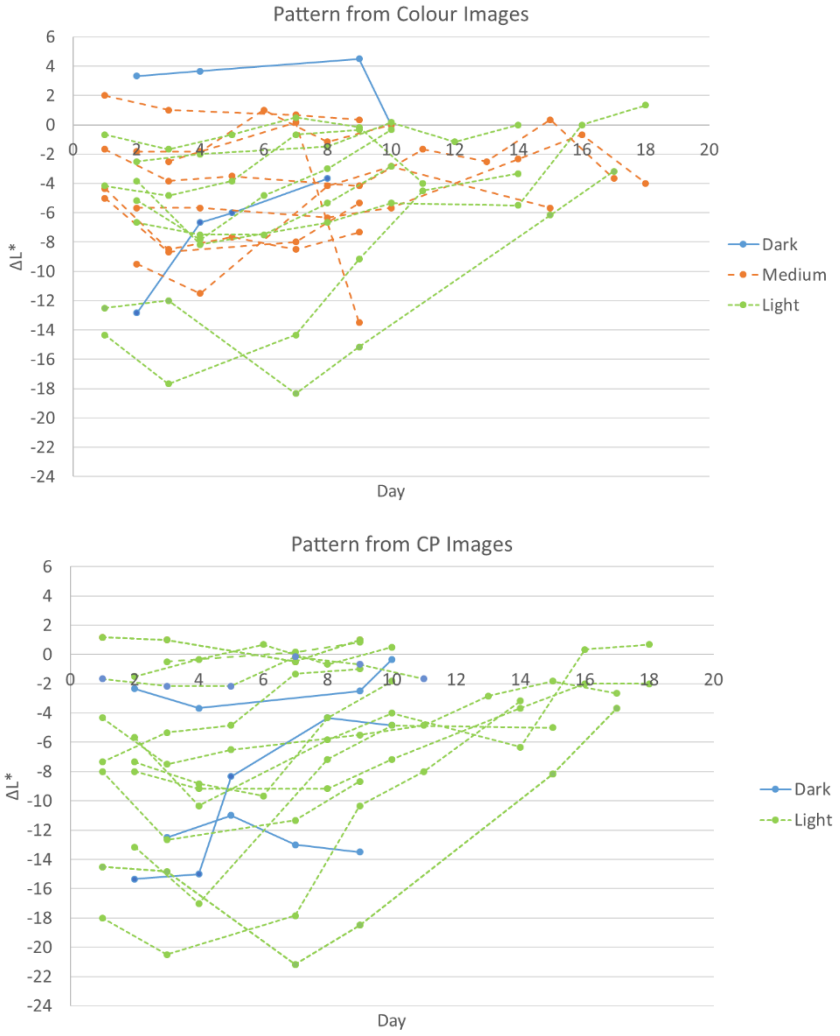

All L* patterns taken from both colour and CP images, grouped by dark, medium and light skin tones

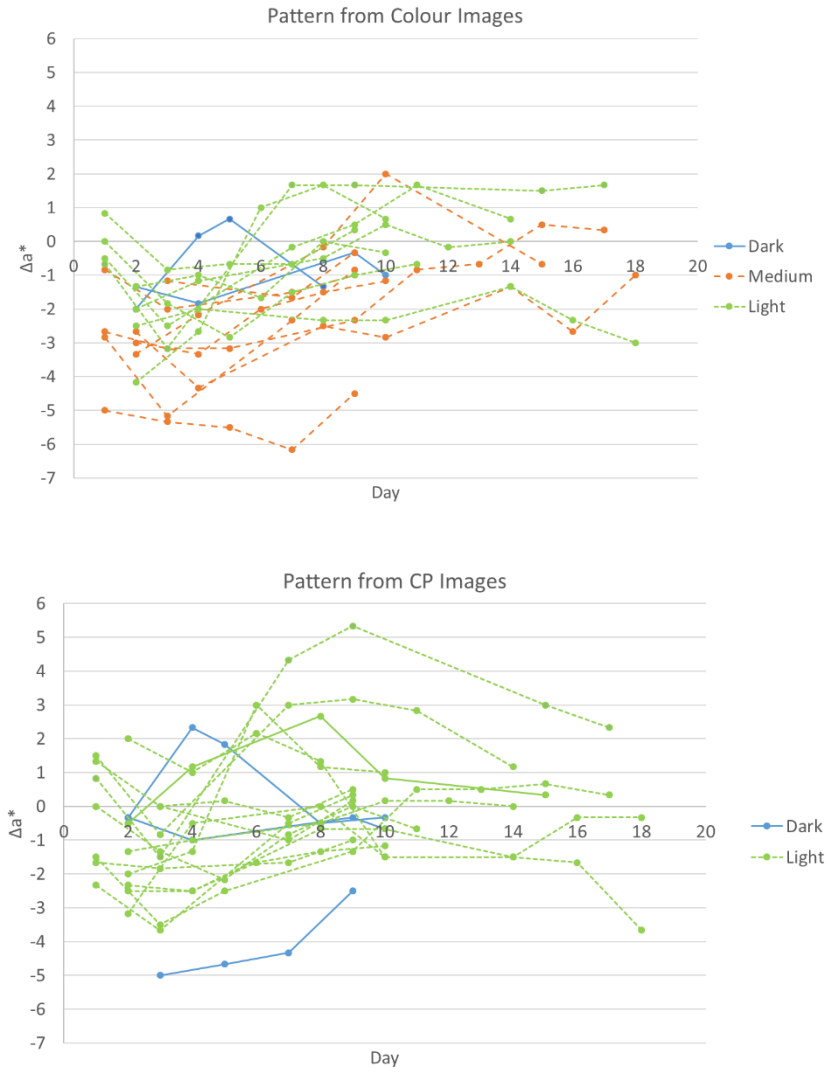

All a* patterns taken from both colour and CP images, grouped by dark, medium and light skin tones

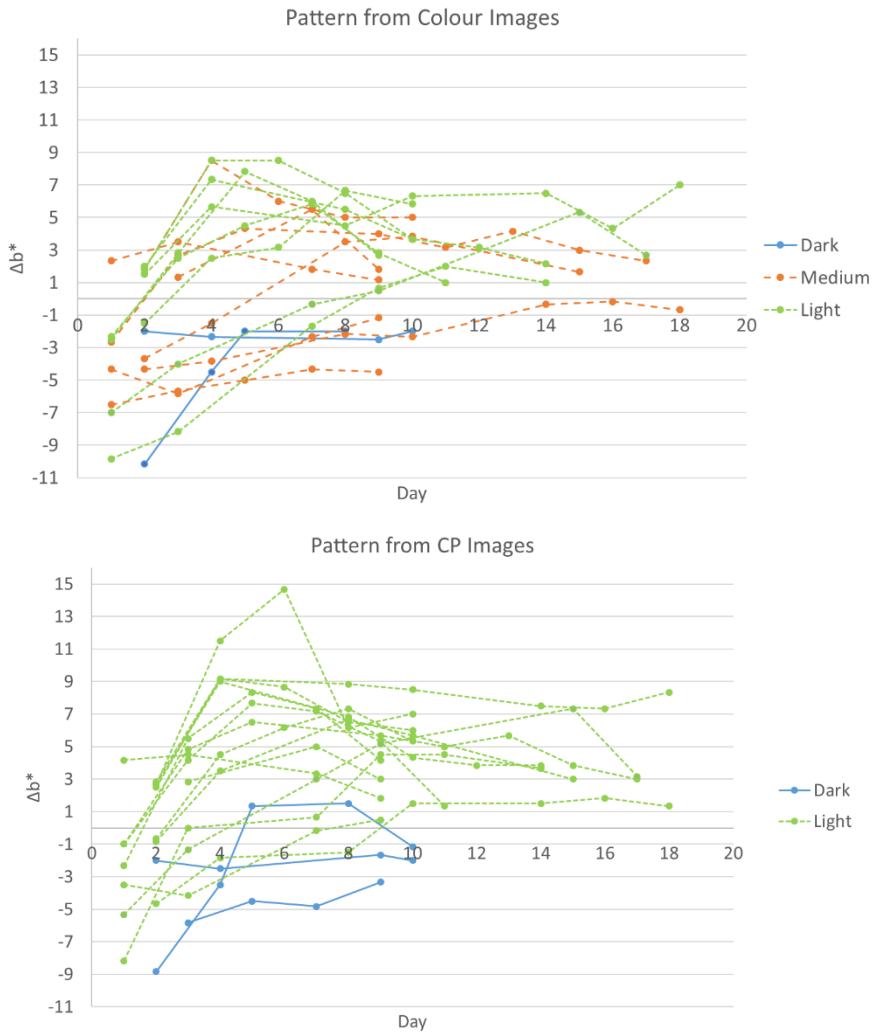

All b* patterns taken from both colour and CP images, grouped by dark, medium and light skin tones

Appendix K

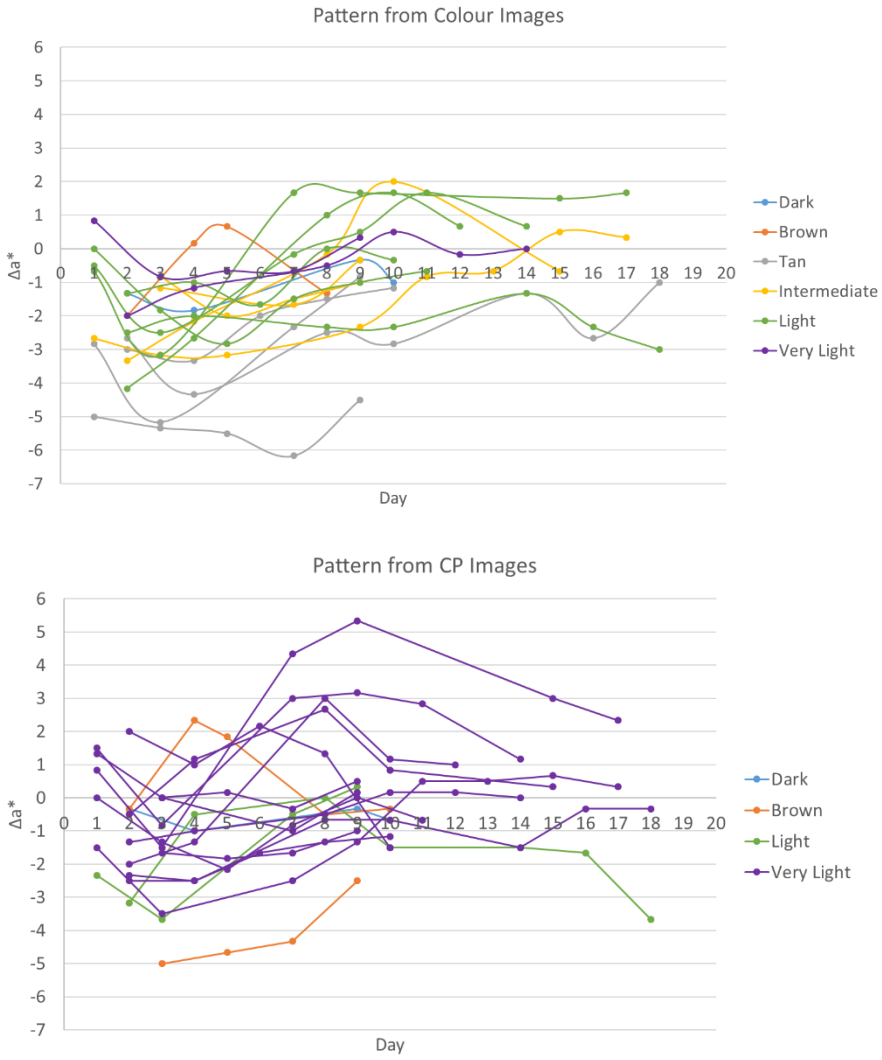

All a* patterns taken from both colour and CP images, grouped by dark, brown, tan, intermediate, light and very light skin tones

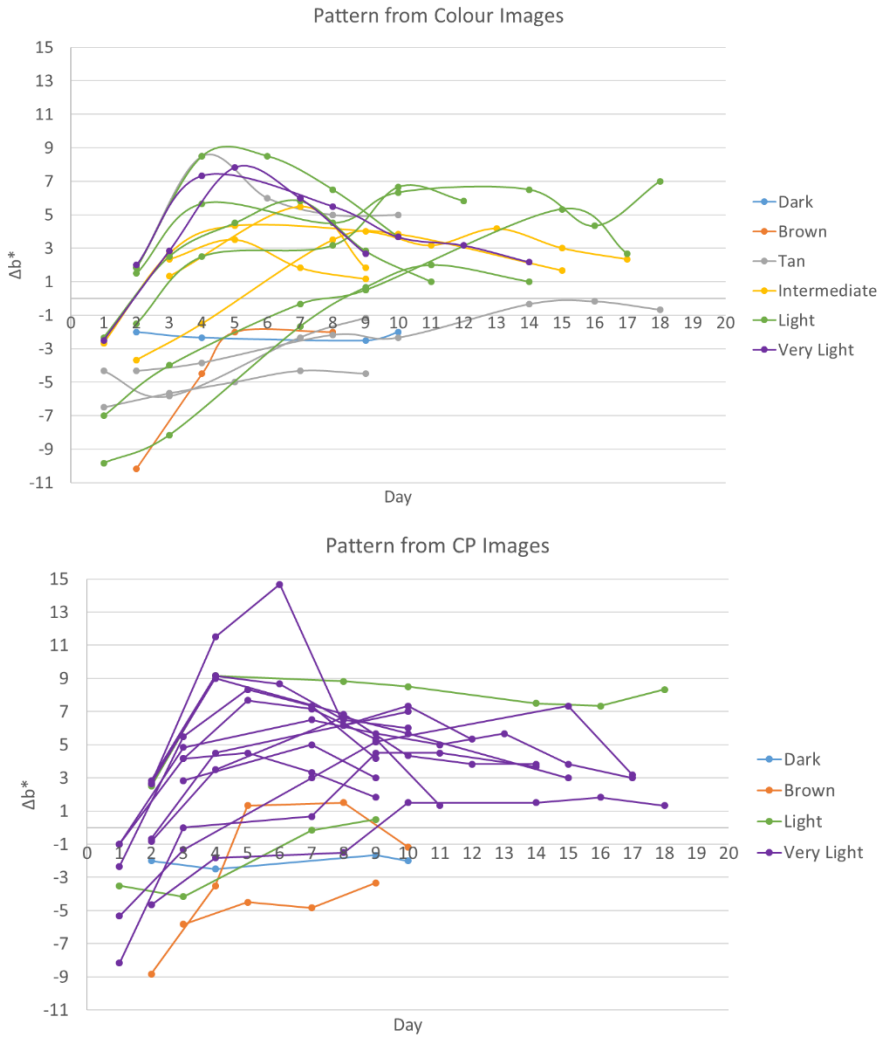

All b* patterns taken from both colour and CP images, grouped by dark, brown, tan, intermediate, light and very light skin tones

Appendix L

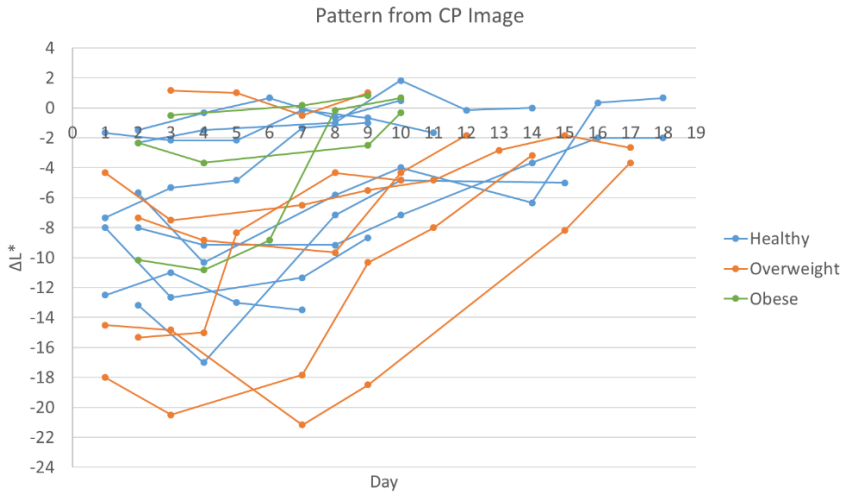

All L* patterns taken from the CP images, categorised by BMI

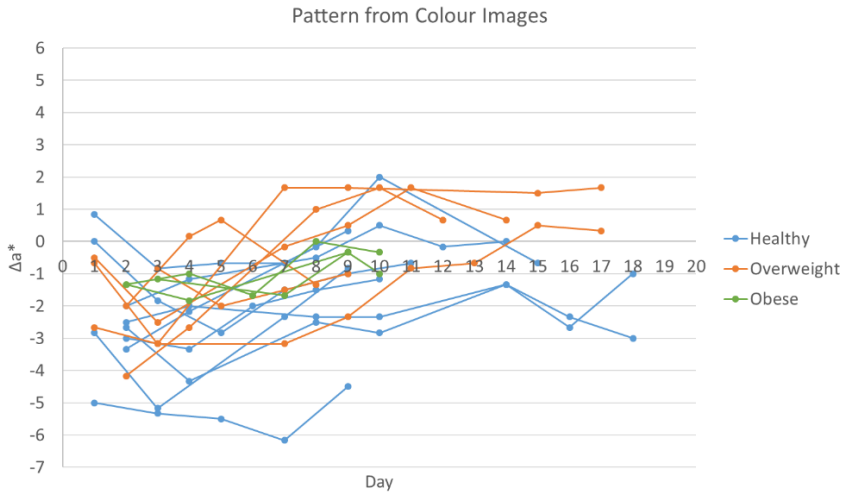

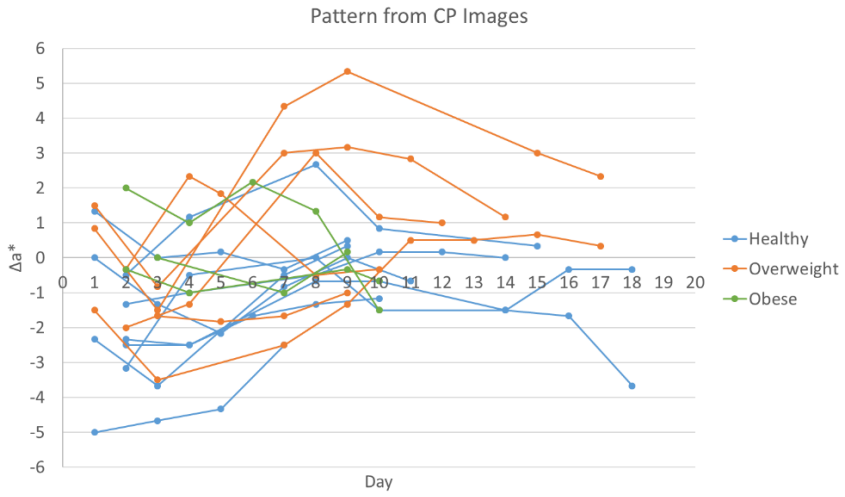

All a* patterns taken from both colour and CP images, categorised by BMI

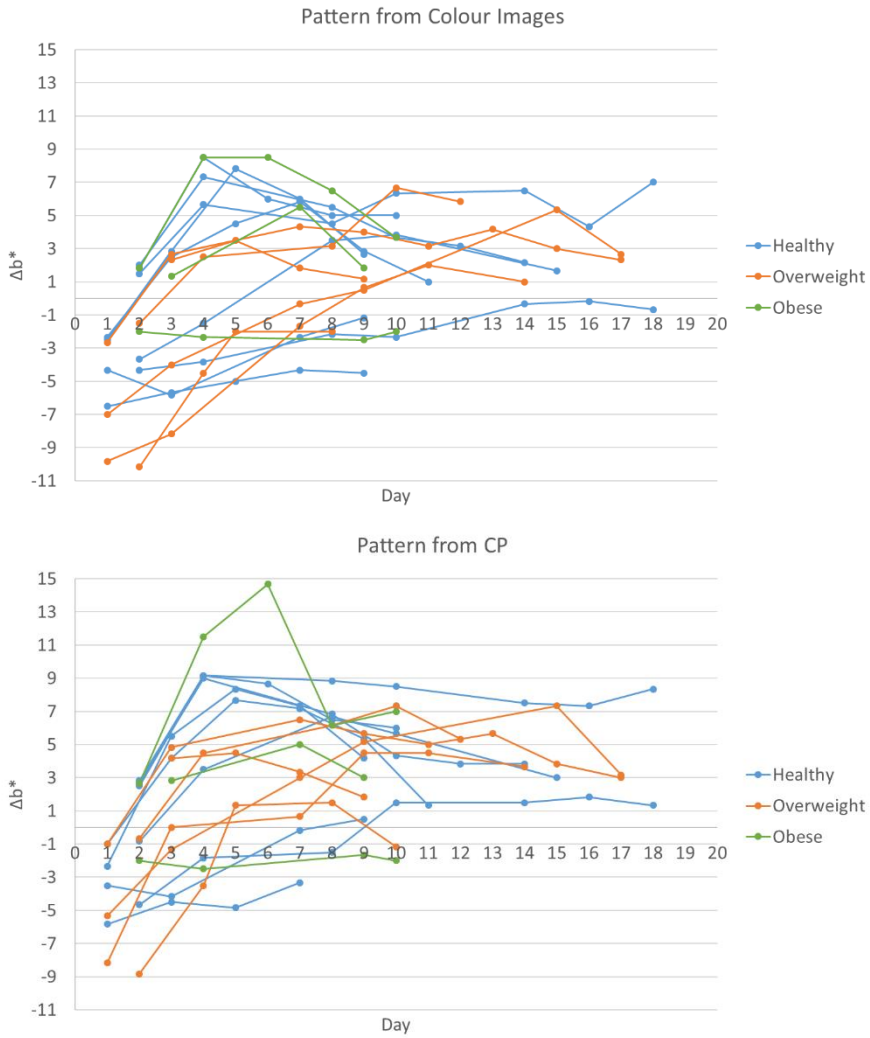

All b* patterns taken from both colour and CP images, categorised by BMI

Appendix M

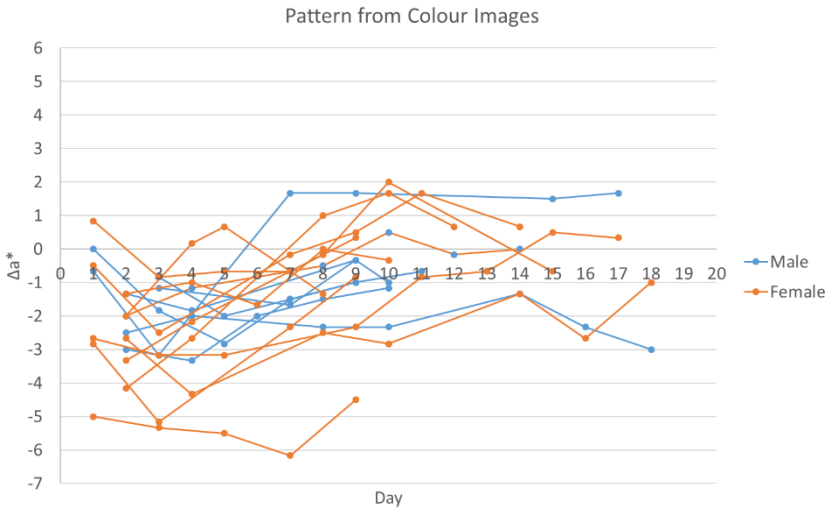

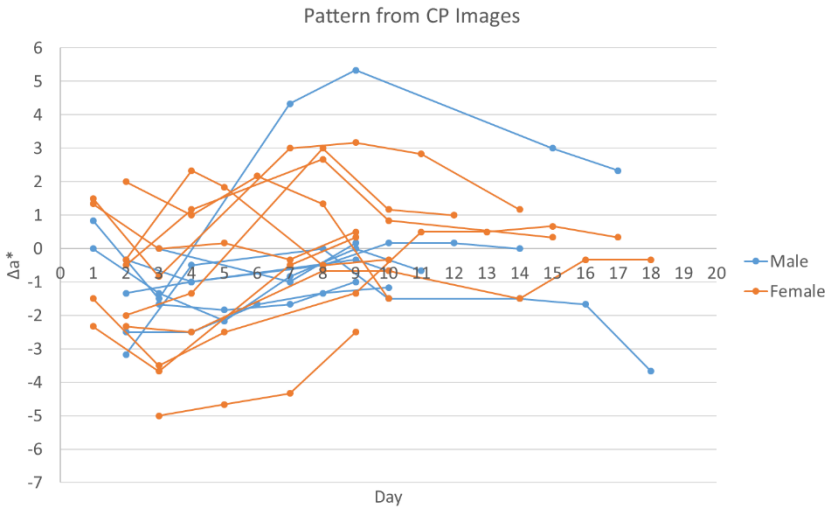

All a* patterns taken from both colour and CP images, categorised by gender

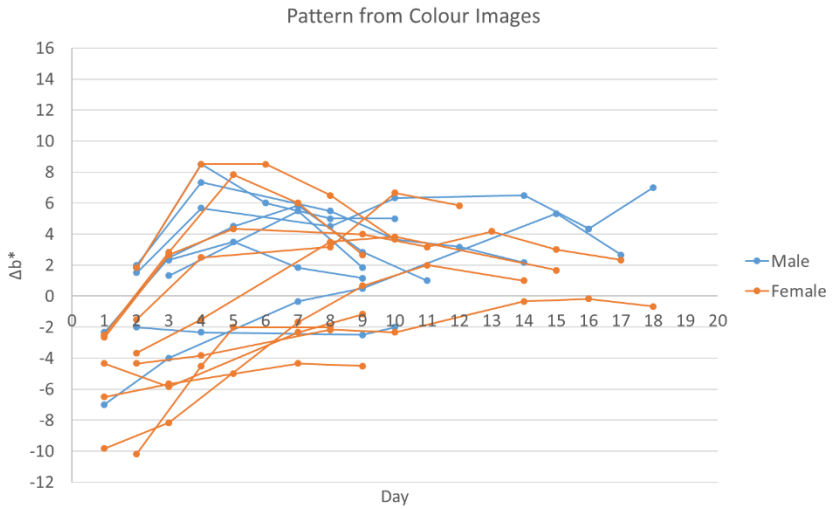

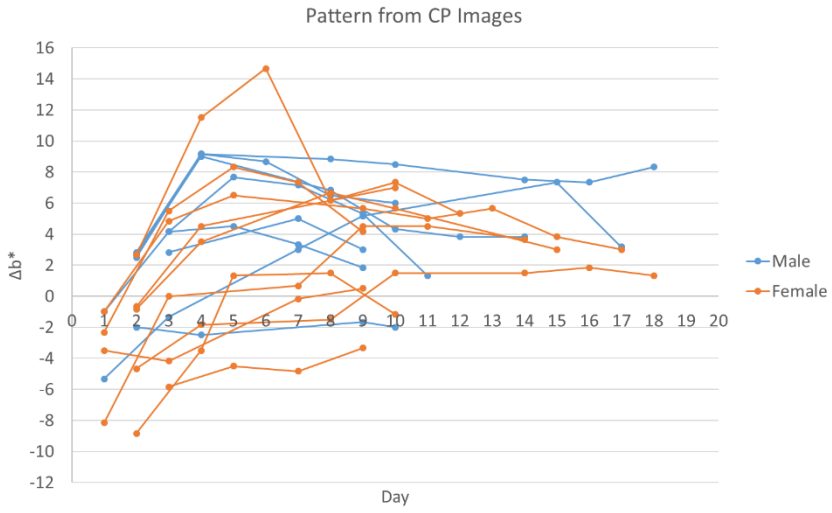

All b* patterns taken from both colour and CP images, categorised by gender

Appendix N

Image timelines for each participant's bruise (not included within main text)

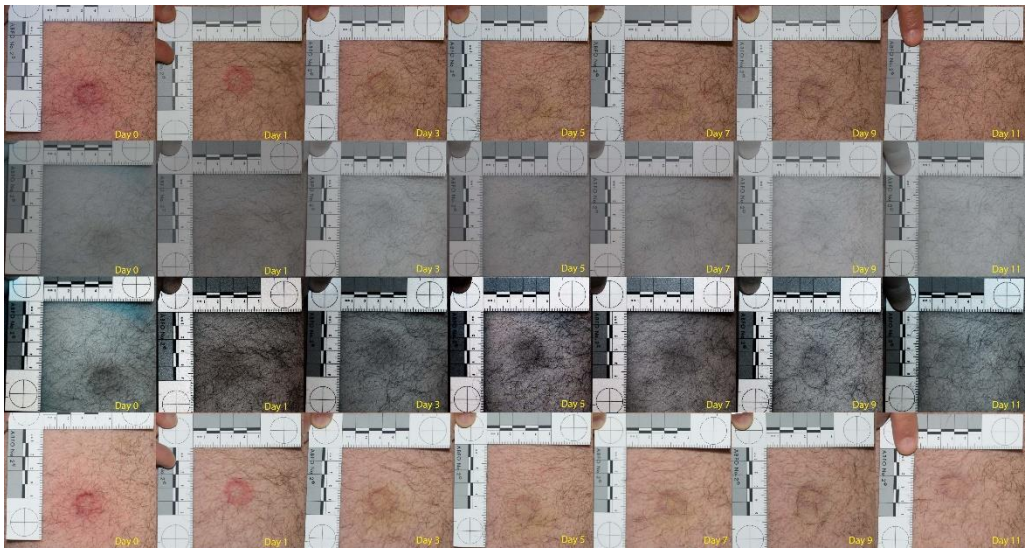

Participant 07G4B

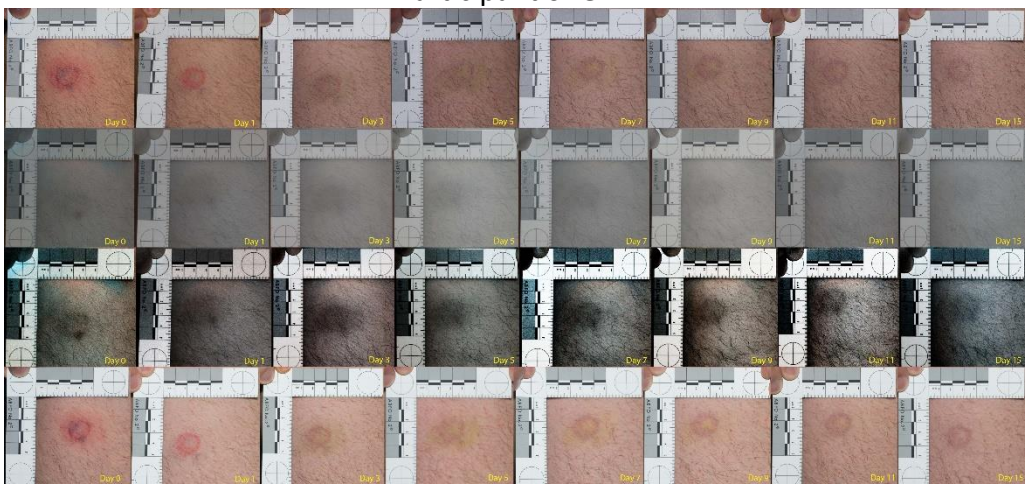

Participant AF04C

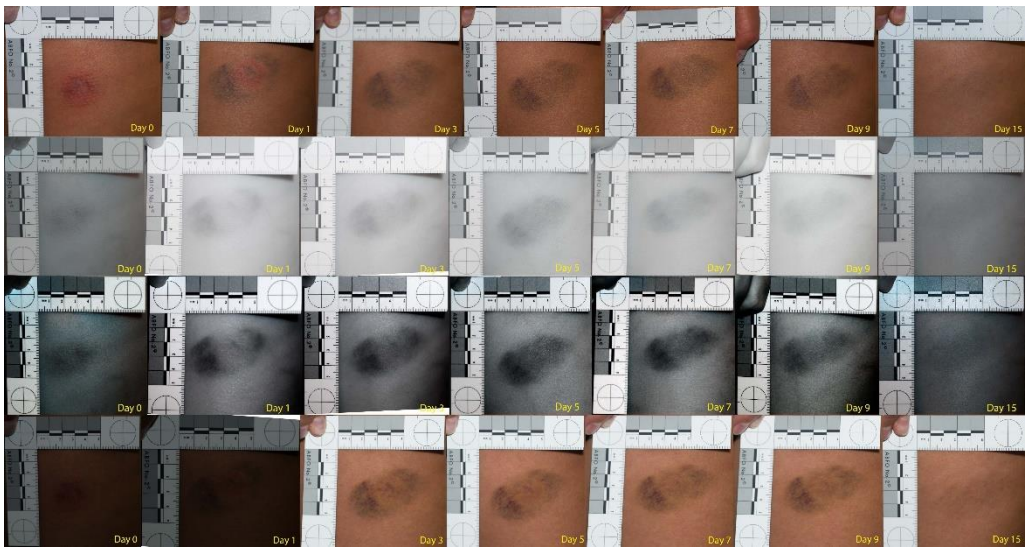

Participant AL07T

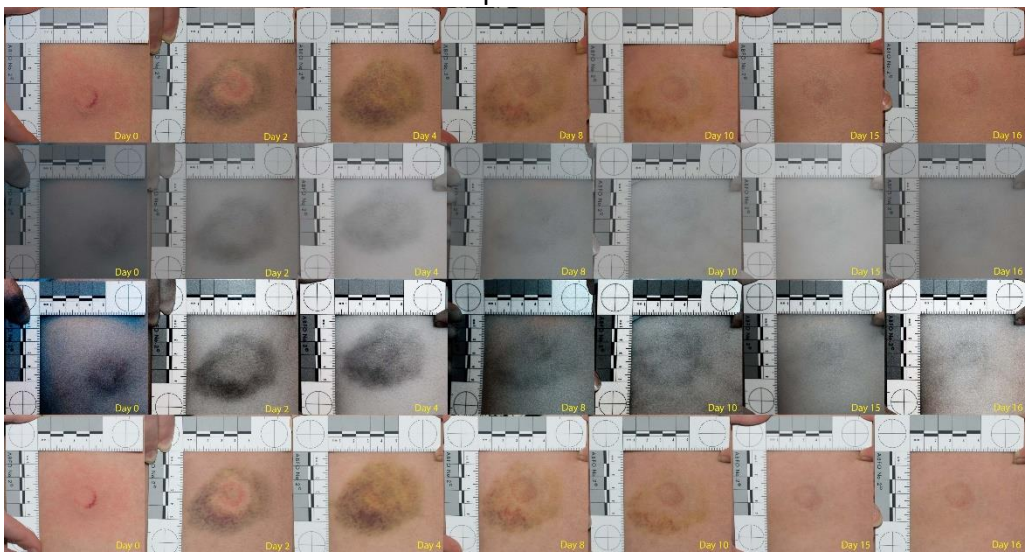

Participant AU02C

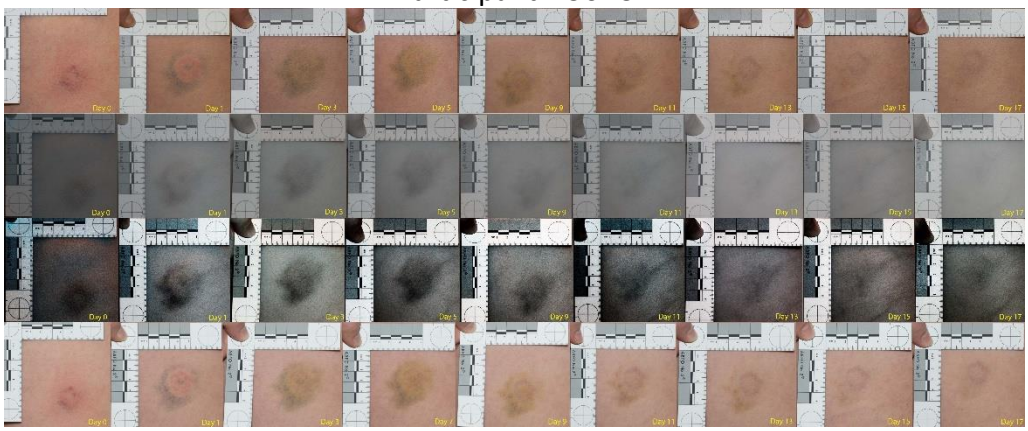

Participant BJ02C

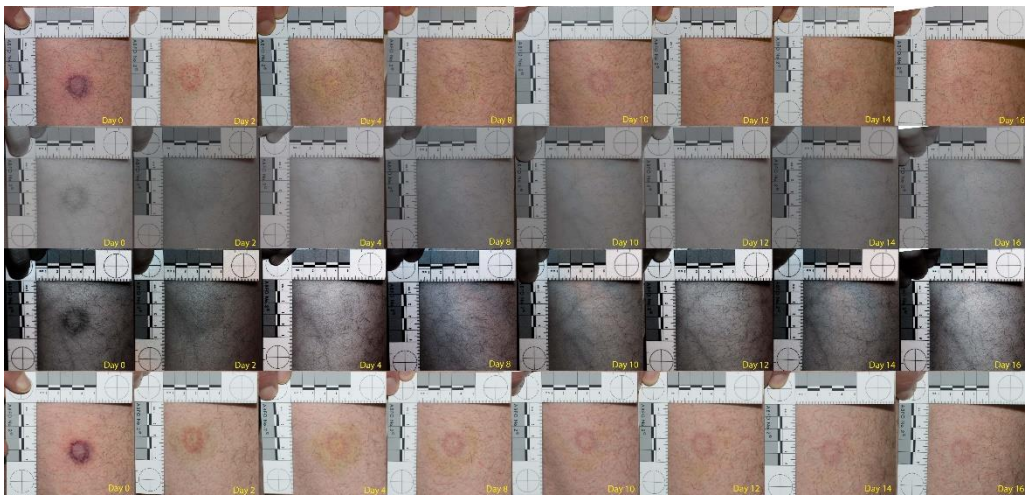

Participant DR09S

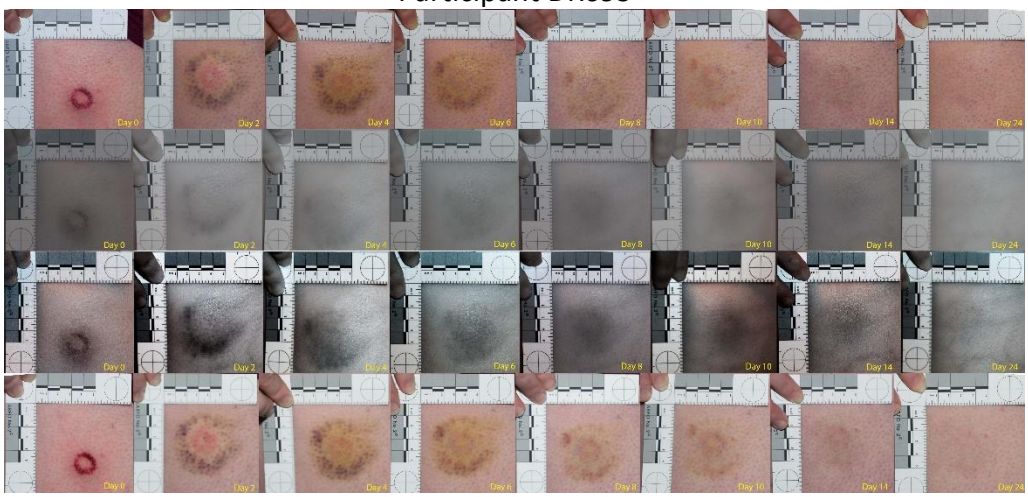

Participant EF02B

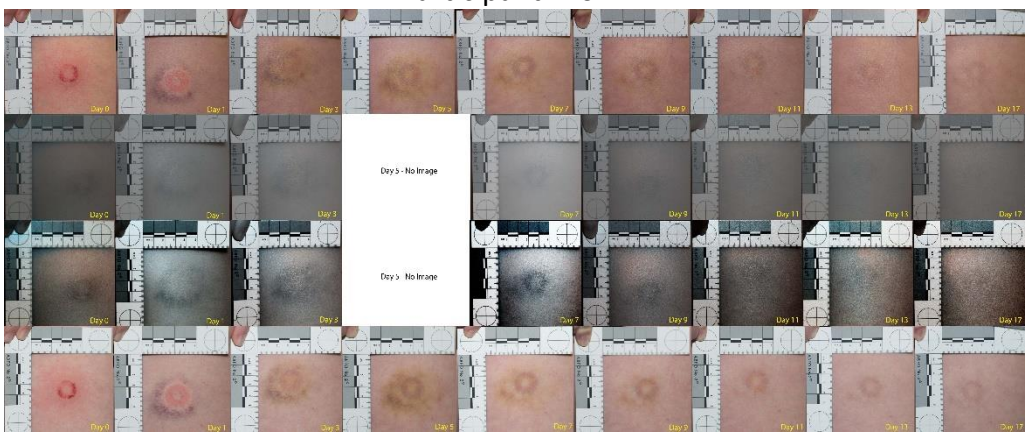

Participant FF08M

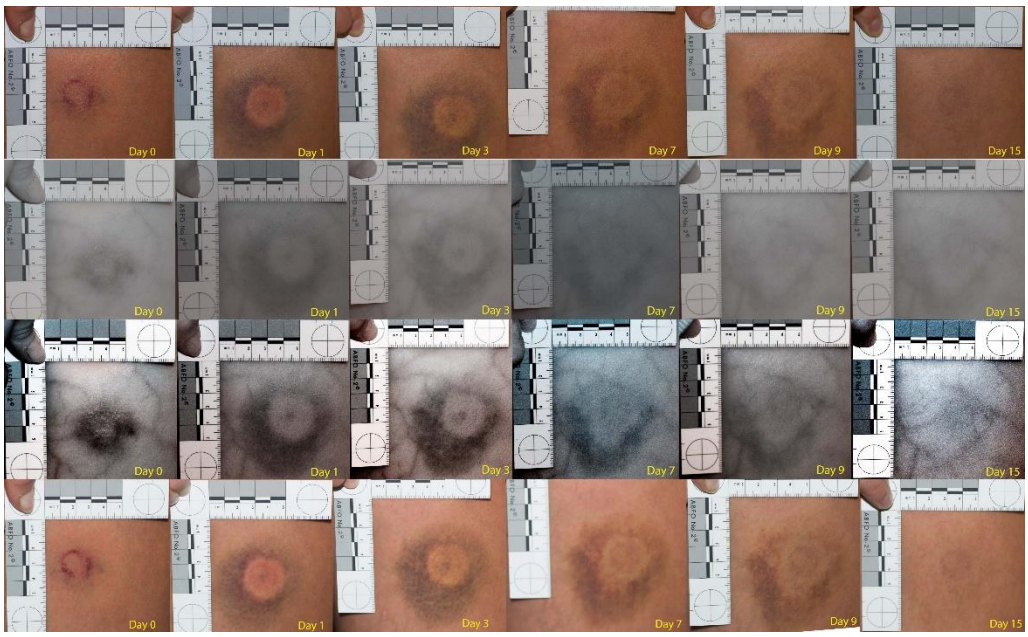

Participant O728C

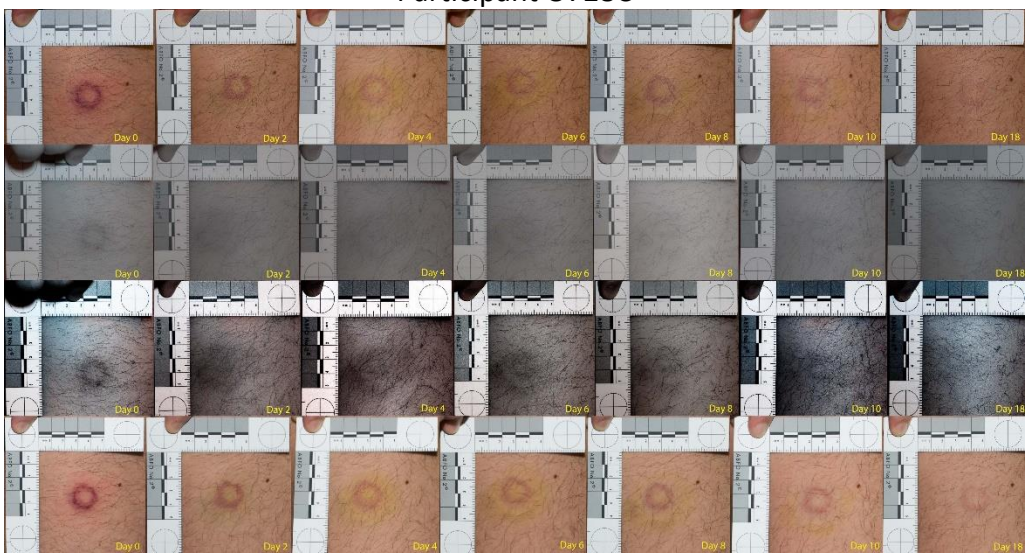

Participant PS03B

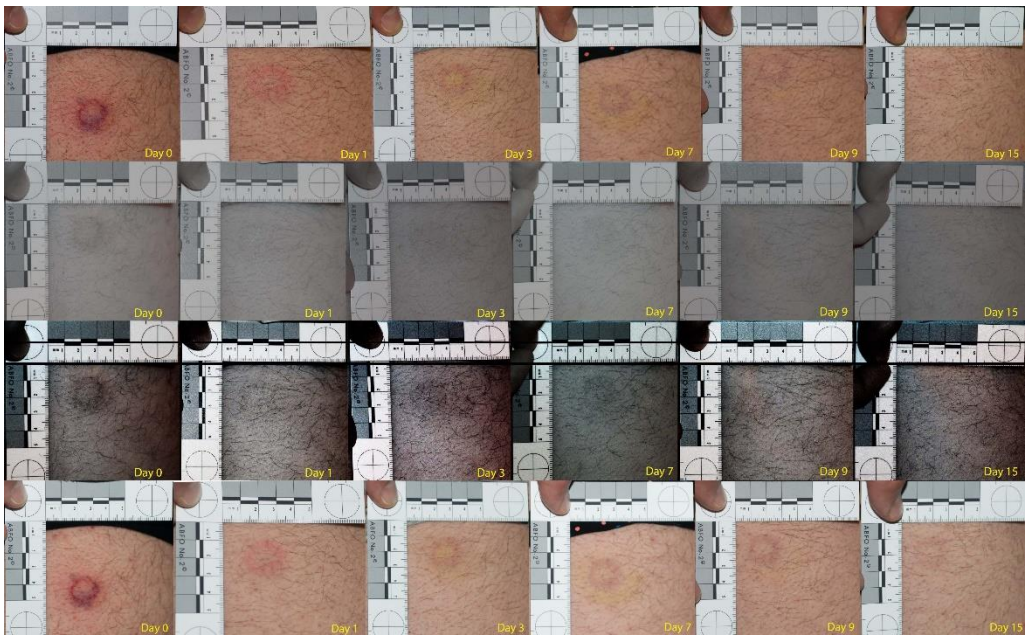

Participant PX02I

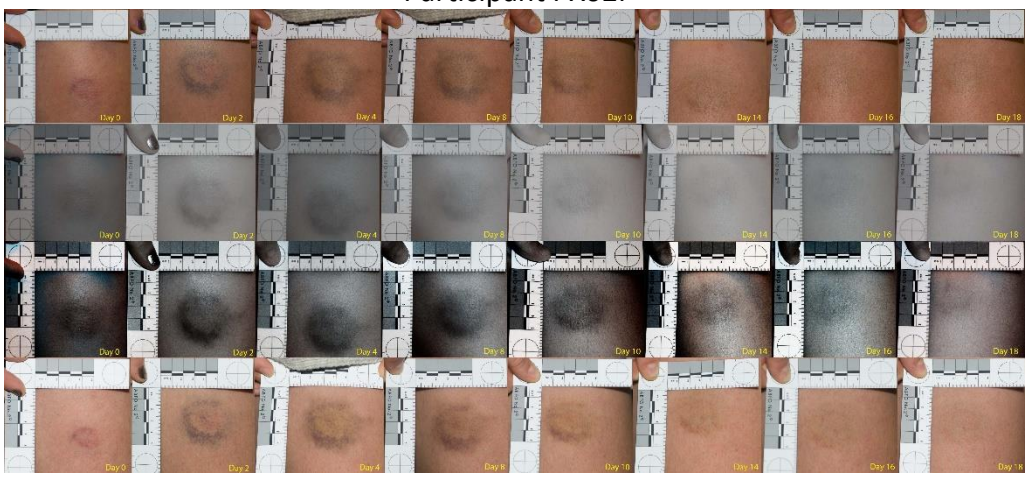

Participant QS05A

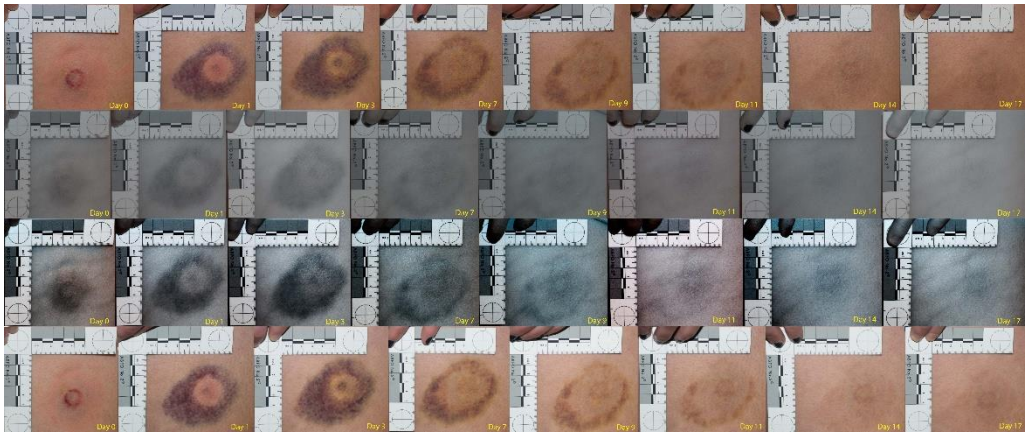

Participant RA06F

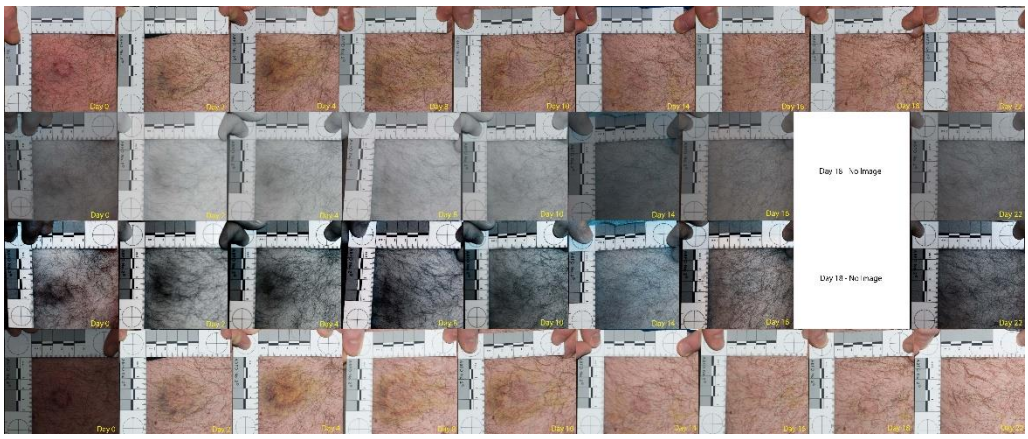

Participant RX02F

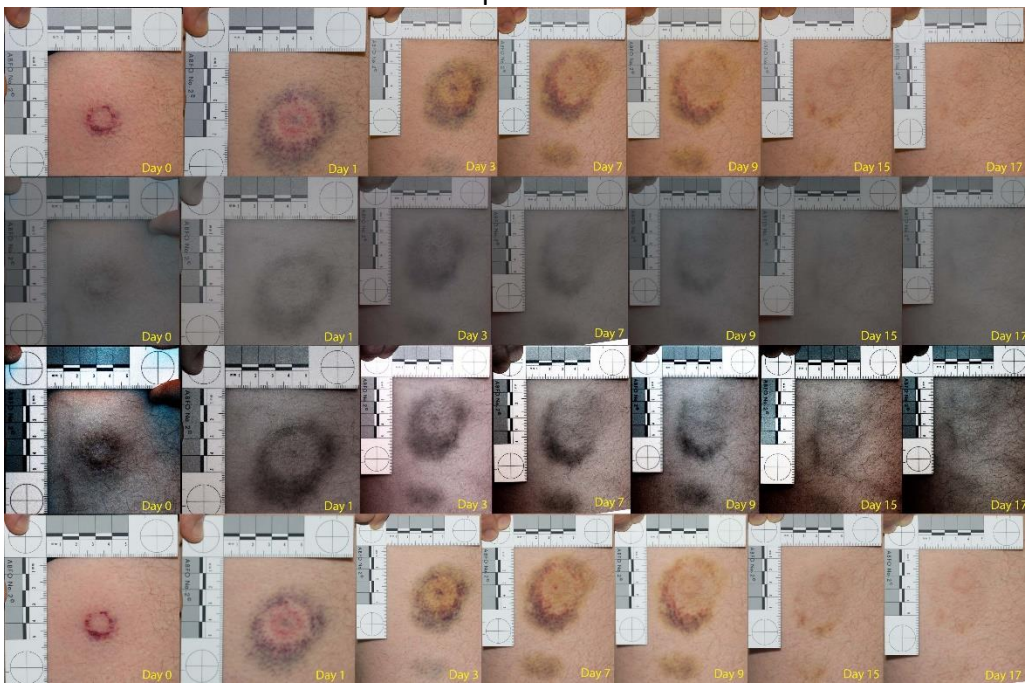

Participant ST05K

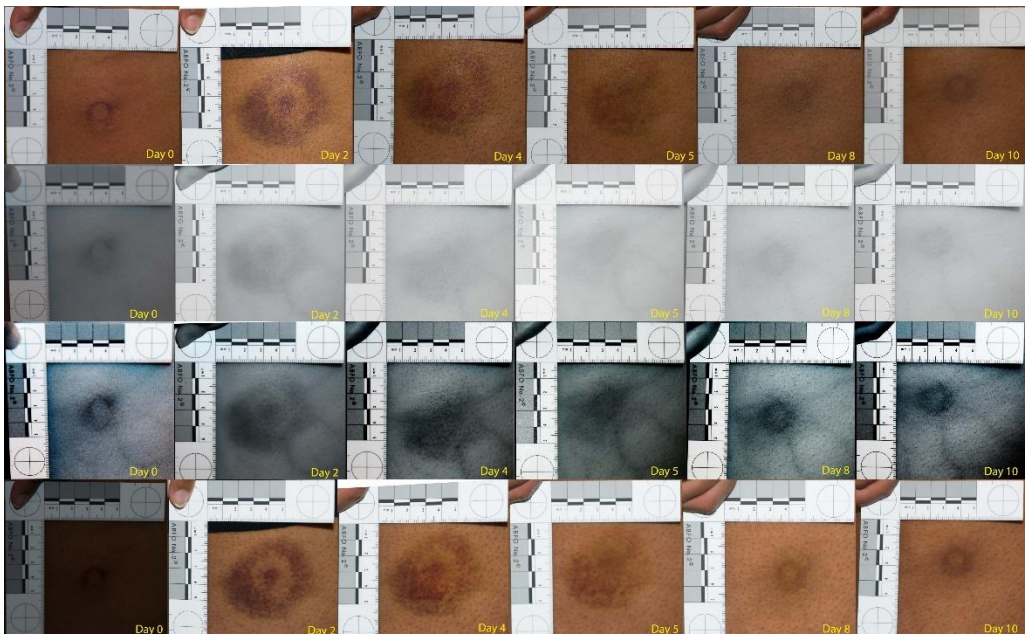

Participant TA11P

Appendix O

Electronic – Impact videos